RESOURCE ALLOCATION AND PERFORMANCE OPTIMIZATION IN FULL-DUPLEX MIMO/OFDMA SYSTEMS

YUNXIANG JIANG

Ph.D

The Hong Kong Polytechnic University

2016

The Hong Kong Polytechnic University

Department of Electronic and Information Engineering

Resource Allocation and Performance Optimization in Full-Duplex MIMO/OFDMA Systems

Yunxiang Jiang

A thesis submitted in partial fulfilment of the requirements for the degree of Doctor of Philosophy

June 2016

CERTIFICATE OF ORIGINALITY

I hereby declare that this thesis is my own work and that, to the best of my knowledge and belief, it reproduces no material previously published or written, nor material that has been accepted for the award of any other degree or diploma, except where due acknowledgement has been made in the text.

_____ (Signed)

Yunxiang Jiang (Name of student)

To my family

Abstract

With the development of self-interference (SI) cancellation, full-duplex (FD) radios, i.e., using the same frequency channel for transmit and receive, have recently gained significant attention owing to the potential to further improve or even double the capacity of conventional half-duplex (HD) systems. Although the gains of full-duplex systems can be easily foreseen, practical implementations of such full-duplex systems pose many challenges and a lot of technical problems still need to be solved. Moreover, many wireless systems are starting to use orthogonal frequency division multiple access (OFDMA) and multiple-input multiple-output (MIMO) as the core transmission techniques. In addition, the cooperative relaying technique is being considered to further increase the capacity of mobile cellular systems. Applying the full-duplex technology in MIMO/OFDM and/or cooperative systems will bring more degrees of freedom in system design and resource allocation, and therefore needs more insightful investigations.

In this thesis, we will explore the potential of full-duplex technology at the base station (BS) in MIMO/OFDM mobile cellular systems with/without relays while the user terminals are operating in the half-duplex mode. Firstly, we consider an OFDMA multi-user cellular system with one full-duplex base station communicating with multiple half-duplex users in a bidirectional way. The uplink and downlink transmissions are coupled together due to the existence of the self-interference (SI) at the base station and the inter-user interference (IUI) from the uplink users to the downlink users. We aim to maximize the system sum-rate of uplink and downlink transmissions by optimally pairing the uplink and downlink users, and allocating the subcarriers and powers to these users. We formulate the problem as a mixed integer nonlinear programming problem. A two-layer iterative solution based on the dual

method and the sequential parametric convex approximation (SPCA) method is proposed. It is referred to as the Dual-SPCA algorithm. The Dual-SPCA algorithm requires the IUI channel state information (CSI) to be available at the base station and hence a significant overhead is generated. To reduce the amount of overhead required, we assume that the IUI channel model is known at the BS and we design a location-aware resource allocation algorithm with limited CSI that maximizes the system sum-rate. Simulation results show that when SI is low, uplink and downlink user-pairing can provide significant improvement on the system sum-rate compared to the conventional unidirectional half-duplex transmission. In addition, by considering two different network deployments, i.e., urban macro cell scenario and small cell scenario, we show that the improvement of full-duplex transmission over half-duplex transmission highly depends on the channel parameters.

Secondly, we jointly consider three different transmission modes in cooperative OFDMA systems, i.e., direct transmission mode, half-duplex relay cooperative transmission mode and full-duplex relay transmission mode. The joint optimization problem of transmission mode selection, subcarrier assignment, relay selection, subcarrier-pairing as well as power allocation is investigated. We transform the binary assignment problem into a maximum weighted bipartite matching problem. Based on the dual method, we solve the joint power allocation and binary assignment problem iteratively. Specifically, since the direct link is considered to be interference in the full-duplex relay transmission mode, the power allocation problem in full-duplex relay transmission mode is non-trivial. Thus, we provide a novel hierarchical dual method to solve the power allocation problem in full-duplex relay transmission mode. In addition, in half-duplex relay cooperative transmission mode, the joint transmission of both source and relay is taken into account, and we provide a simple and insightful power allocation scheme. Results show that the system throughput enhances significantly compared to previous works.

Thirdly, we investigate a max-min weighted SINR problem in a full-duplex multi-user MIMO system, where a full-duplex-capable base station equipped with multiple antennas communicates with multiple half-duplex downlink and uplink users under the same system resources. Instead of optimizing the joint uplink and downlink max-min weighted SINR, we consider a more practical scenario where the

downlink minimum weighted SINR is maximized under specific SINR constraints for uplink users. Moreover, the optimization is conducted by jointly considering the base station transmit power, uplink transmit power, and base station transmit and receive beamforming. This optimization problem is therefore subject to multiple uplink SINR constraints and multiple transmit power constraints. Due to the SINR constraints, negative matrix components arise and hence the optimization problem cannot be solved by the Perron–Frobenius theory directly. With fixed base station transmit and receive beamforming, we first optimize the max-min weighted SINR problem under multiple uplink SINR constraints and a single power constraint, and show how the subgradient projection-based method can be applied to optimize the problem under multiple-power-constraint conditions. Then we derive the network duality of the same problem, i.e., fixed base station transmit/receive beamforming with multiple uplink SINR constraints and a single power constraint. To solve the original problem, we propose an optimization algorithm that iteratively updates (i) the transmit power vector and receive beamforming in the primal domain, and (ii) the dual transmit power vector and transmit beamforming in the dual domain. Moreover, the algorithm, which is also based on the subgradient projection-based method, is proven to converge under appropriate initialization parameters. With network duality, we avoid optimizing coupled transmit beamforming in the primal domain and instead are able to optimize individual transmit beamformers easily in the dual domain. Simulation results show that our proposed algorithm has a fast convergence rate and leads to a better performance compared to other optimization techniques that do not jointly considered all parameters.

Finally, energy efficiency of a full-duplex relay system under the total power constraint and fixed circuitry power consumption is studied. An optimization problem is formulated towards maximizing the system energy efficiency. Unfortunately, this problem is non-trivial and cannot be solved by conventional fractional programming methods, such as the Dinbelbach's method. To resolve this issue, an algorithm called sequential parametric convex approximation-Dinbelbach is proposed. Simulation results show that the proposed algorithm can converge to the global optimum very quickly.

Publications

1. Y. Jiang, F. C. M. Lau, Ivan W. H. Ho, and Y. Gong, "Resource Allocation for Multi-User OFDMA Hybrid Full-/Half-Duplex Relaying Systems With Direct Links" *IEEE Transactions on Vehicular Technology*, Article first published online: 09 Sep. 2015.

2. Y. Jiang, H. Chen, F. C. M. Lau, P. Wang, and Y. Li. "Full-Duplex OFDMA Multi-user Cellular Systems: Resource Allocation and User Pairing," *Transactions on Emerging Telecommunications Technologies*, Article first published online: 14 Dec. 2015, DOI: 10.1002/ett.3005

3. Y. Jiang, F. C. M. Lau, H. Chen, and F. Zhao, "Energy Efficiency Optimisation in Full-Duplex Relay System". *Transactions on Emerging Telecommunications Technologies*, Article first published online: 17 Feb. 2015, DOI: 10.1002/ett.2926.

4. Y. Jiang, F. C. M. Lau, Ivan W. H. Ho, H. Chen, and Y. Huang, "Max-Min Weighted Downlink SINR with Uplink SINR Constraints for Full-Duplex MIMO Systems" Submitted to *IEEE Transactions on Signal Processing*.

Acknowledgements

Since graduated from Beijing Jiaotong University, China, in 2011, I had been seizing every opportunity to pursue a PhD degree. The path had been winded and filled with pitfalls and difficulties. Without the help and support from many others, it would not be possible for me to get through and complete my PhD degree.

First of all, I am cordially grateful to my supervisor, Prof. Francis C. M. Lau for his unwavering support and encouragement, which had made my PhD study also a joyful journey. Whenever I knocked on his office door, he would put aside what he was working on and would eagerly discuss with me about my work. He also granted me the freedom of choosing a research topic that interested me, guided me throughout the whole study and provided me with his unconditional support. Moreover, he was tolerant of my on-and-off ignorant and arrogant characters. He further helped me enhancing the mathematical derivations and my English writing skills with great patience.

Next, I would like to express my gratitude to Prof. Yonghui Li and Dr. He (Henry) Chen of the School of Electrical and Information Engineering, University of Sydney, Australia. During the six-month visit to their Telecommunications Laboratory in 2013, I had been generously furnished with invaluable comments and advices. Moreover, the collaboration with Prof. Li and Dr. Chen had greatly improved my capability in performing research. I should also thank the colleagues in the Laboratory for their assistance on research and my stay in Sydney. Even though we had spent a short time together, the friendship that built among us would last forever.

My grateful acknowledgement is also made to the leader of our Applied Nonlinear Circuits and Systems Research Group, Prof. Chi. K. Tse. He always shared

with us his views on career development, research directions and even lifestyle in various seminars and social gatherings. In addition, thanks are expressed to groupmates and colleagues, such as Prof. Qingfeng Zhou, Dr. Ivan Wang-Hei Ho, Dr. Zhenyu Shan, Dr. Zhen Li, Dr. Jiajing Wu, Dr. Ben C. T. Cheng (just to name a few in an arbitrary order), for encouraging me and decorating my PhD study with happiness and friendship.

Last but not least, I am deeply indebted to my wife, my parents and my parents-in-law. I do not believe that I could have overcome all the hard times during these years without the lasting support from them. I also owe my deep appreciation to my wife for taking such a good care of our newborn baby, and for her enduring support and patience that made this PhD thesis possible.

Contents

List of Tables

List of Figures

Acronyms

AF	Amplify-and-forward
BPSK	Binary phase-shift-keying
AWGN	Additive white Gaussian noise
BER	Bit error rate
BS	Base station
CDMA	Code division multiple access
CP	Cyclic prefix
CSI	Channel state information
dB	Decibel
dBm	Decibel-milliwatts
DF	Decode-and-forward
DL	Downlink
DT	Direct transmission
EGC	Equal gain combining
EPA	Equal Power Allocation
FD	Full-duplex
FDD	Frequency division duplex

FFT	Fast Fourier transformation
HD	Half-duplex
HD-SUS	Half-Duplex Single User Selection
INRT	Interference-to-noise ratio temperature
IUI	Inter-user interference
KKT	Karush-Kuhn-Tucker
LDPC	Low density parity check
LTE	Long-Term Evolution
LOS	Line-of-sight
MAC	Medium access control
MIMO	Multiple-input multiple-output
MINLP	Mixed integer nonlinear programming problem
MISO	Multiple-input single-output
MMSE	Minimum mean square error
MRC	Maximal ratio combining
NLOS	Non line-of-sight
OFDMA	Orthogonal frequency division multiple access
QAM	Quadrature amplitude modulation
QPSK	Quadrature phase-shift-keying
RUPS	Random User-Pair Selection
SNR	Signal-to-noise ratio
SI	Self-interference
SISO	Single-input single-output
SIC	Self-interference cancellation

SINR	Signal-to-interference-plus-noise ratio
SMUMD	Separately Maximizing UL transmissions and Maximizing DL transmissions
SPCA	Sequential parametric convex approximation
TDD	Time division duplex
UL	Uplink
UMa	Urban macro
WiMAX	Worldwide interoperability for microwave access

Notations

Set

$\mathcal{R}$	Real number
$\mathcal{C}$	Complex number
$\mathcal{R}^n$	Real column vector
$\mathcal{C}^n$	Complex column vector
$\mathcal{R}^{n\times m}$	Real $n \times m$ matrix
$\mathcal{C}^{n\times m}$	Complex $n \times m$ matrix

Vector and matrix

x	Scalar value $x \in \mathbb{R}$ or $x \in \mathbb{C}$
$\mathbf{x}$	Column vector of $\mathcal{R}^{n\times 1}$ or $\mathcal{C}^{n\times 1}$
$\mathbf{I}$	Identity matrix
$\mathbf{X}$	Matrix $[x_{ij}]$ of $\mathcal{R}^{n\times m}$ or $\mathcal{C}^{n\times m}$
$\mathbf{X}^\dagger$	Transpose and complex conjugate of matrix $\mathbf{X}$
$\mathbf{X}^T$	Transpose of matrix $\mathbf{X}$
$\|x\|$	Absolute value of scalar x, or amplitude of complex x
$\det(\boldsymbol{X})$	Determinant of square matrix $\mathbf{X}$
$\mathrm{diag}(\mathbf{x})$	Diagonal matrix with diagonal entries $x_1, x_2, \cdots, x_n$

Operation and function

$\binom{m}{n}$	Binomial coefficient
$\exp(x)$	Exponential function
$\ln(x)$	Natural logarithm, base e
$\log(x)$	Logarithm on base 2
$\max\{x_1, \ldots, x_n\}$	Maximum of the elements $x_1, \ldots, x_n$
$\min\{x_1, \ldots, x_n\}$	Minimum of the elements of $x_1, \ldots, x_n$
$\mathcal{O}(x^3)$	Big O notation
$n!$	Factorial of n
$\Re(z)$	Real part of complex variable z

Probability

$\mathcal{CN}(\mu, \sigma^2)$	Complex circularly symmetric Gaussian distribution with mean μ and variance σ^2
$\Pr(\mathcal{A})$	Probability of an event $\mathcal{A}$
$E(\mathcal{A})$	Expectation of an event $\mathcal{A}$
$p(x)$	Probability density function of a random variable X

Chapter 1

Background and Motivations

Wireless communication systems have brought huge convenience to humans. The recent proliferation of "smart" mobile devices has allowed users to surf the Internet, download applications, and upload/download pictures/videos anytime and anywhere. Consequently, there has been a tremendous increase in mobile data usage. In the foreseeable future, the number of smart devices will continue to increase and the demand of high-speed wireless access will keep on rising. While many advanced technologies have been put together to enhance the wireless transmission rates, the improvement may not be able to cope with the rapid increase in demand.

The challenges in wireless communication originate from the shared, broadcast nature of the wireless medium. A shared medium implies that communication devices need to contend amongst themselves, requiring specific sharing mechanisms to use the medium efficiently. The wireless medium also exhibits rapid attenuation of signals. With such attenuation, different devices in a network can have very different and inconsistent views of the wireless channel. A typical example is that a device

cannot use the same frequency to send and receive data simultaneously. The main reason is that the transmitted signal from the wireless device will interfere severely with the useful received signal. This phenomenon is named as self-interference (SI) [1]. When the useful received signal is overwhelmed, it becomes useless. Thus, half-duplex (HD) mode is widely applied in current wireless systems. There are two classical duplexing techniques called Time-Division Duplexing and Frequency-Division Duplexing, which allow the transmitter and receiver operate at different time- and frequency-resources, respectively.

If each device can use the same frequency for transmit and receive at the same time, the capacity of the wireless systems can be enhanced considerably. This is the so called full-duplex (FD) transmission. Due to the existence of self-interference, the practical rate of FD transmission cannot reach twice of transmission rate of HD transmission. Yet recent research has shown that SI can be reduced practically [2–19] and hence it is envisaged in the near future that SI can be reduced significantly. There are other major technical challenges to be overcome before we can fully utilize the extra capacity. For example, when the same frequency is used in the uplink (UL) and in the downlink (DL), the signal from the UL user will interfere with the DL signal arriving at the DL user. In order to minimize such interferences, there is a need to investigate strategies for assigning channels to UL and DL users. Moreover, existing base stations (BSs) and mobile devices may be equipped with multiple antennas that can enhance the signal quality and hence channel capacity. We need to devise ways to continue fully utilizing such features in future cellular systems. Optimizing the resources in FD systems is therefore the main focus of this thesis.

1.1 Motivations

Resource allocation is a general strategy to control interferences and enhance the performance of wireless networks [20–22]. The basic idea for resource allocation is to utilize the channels more efficiently by sharing the spectrum through optimizing parameters such as transmit power, transmission rate, subcarrier, coding scheme, or combinations of these parameters. Moreover, the network performance can be further improved by introducing more diversity and cross-layer considerations. Various DL and UL resource allocation algorithms have been proposed and investigated for Orthogonal Frequency Division Multiple Access (OFDMA) systems [23–28]. Most literatures studying resource allocation focus on either DL or UL transmissions, and they model all subchannels (i.e., subcarriers) as interference-free channels. It means that the transmission rate is only affected by the signal-to-noise ratio (SNR) and therefore, water-filling algorithms can be applied to solve the power allocation problem. As more advanced self-interference cancellation (SIC) techniques are being developed, FD technology is becoming very promising in improving spectral efficiency and system throughput. OFDMA systems consisting of FD-capable BS have not been thoroughly investigated yet. In addition, the optimization approach provided in multi-user HD OFDMA systems may not be applicable to analyzing multi-user FD OFDMA systems due to the residual self-interference of FD equipment. Thus, there is a need to provide solutions for the resource allocation problems in FD OFDMA multi-user systems.

In addition, adding the cooperative relaying nodes in OFDMA-based networks has brought more degrees of freedom in system design and resource allocation, and has become a hot research topic [29–44]. Much of the previous research focuses

on the HD relaying system due to the limitation of FD transmission. In particular, the authors in [35] have provided an in-depth analysis and algorithm in joint FD and HD relaying system for resource allocation. However, the direct link has been neglected in [35]. Since cooperative relay transmission mode may not always achieve higher data rate than direct transmission mode [36, 45], it is necessary to jointly consider direct transmission mode and cooperative relay transmission mode. More importantly, unlike the HD relaying transmission where the direct link can be treated as an improvement, the signal from the direct link is inevitable and should be considered as interference in FD relaying transmission [16, 46]. This fact would definitely decrease the system performance when the mobile users are near the BS. Advanced resource allocation schemes are therefore required to further improve the system performance. Another important property of OFDMA-based relaying that is missing in [35] is the so-called *subcarrier-pairing*, where the first-hop subcarrier and the second-hop subcarrier at the relay need to be carefully "matched" [37–42]. In [47], an excellent idea has been provided for solving the interference problem between direct link and relay link by jointly processing the sum of signals from the source and the relay. The authors have designed a fast construct-and-forward full-duplex relay which can utilize the direct link as an additional path to the relay path, resulting in strengthening the received signal at the destination. It has been shown that this fast construct-and-forward full-duplex relay can be well applied in a TDMA system, e.g., WiFi system. However, the processing is performed in the time domain which means that all subcarriers would be given the same amplification. Since the amplifications are identical for all subcarriers, the relay cannot apply different power allocations to different subcarriers. In other words, power allocation and subcarrier allocation are not feasible in this fast construct-and-forward full-duplex

relay. Hence, the performance of the fast construct-and-forward full-duplex relay in OFDMA systems is still an open problem. More importantly, only one relay and one user are considered in [47] such that the signals from the relay link and direct link can be designed to arrive at the user with the same phase. However, when multiple relays and multiple users are considered, the signal design becomes much more complex and the problem is yet to be solved. Thus, the joint optimization problem of transmission mode selection (including direct transmission (DT) mode, HD relay cooperative transmission (HDRCT) mode and FD relay transmission (FDRT) mode), subcarrier assignment, relay selection, subcarrier-pairing as well as power allocation has not been systematically investigated yet.

FD techniques have been investigated under multi-user MIMO cellular systems where the base station (BS) is allowed to transmit and receive signals in the same time-frequency block while the uplink and downlink users work in a half-duplex way [48–50]. The target of these open literatures are to optimize the system sum-rate. In additional to the system sum-rate, the signal-to-interference-plus-noise-ratio (SINR) balancing problem, which is also named as max-min weighted SINR problem [51], is another important performance metric in wireless networks. The earliest work on the max-min weighted SINR problem appeared in [51]. The single-input-single-output (SISO) problem with a single power constraint was solved by applying the Perron-Frobenius theory [52]. The approach was subsequently extended to solving multiple-input-single-output (MISO) and single-input-multiple-output (MISO) problems [53–59]. Specifically, due to the coupled structure of the transmitted signals in MISO cases, the max-min weighted SINR problem with joint beamforming and power control is usually non-convex and thus cannot be solved directly. The

key technique used to overcome this difficulty is to transform the non-convex downlink joint optimization problem into a convex dual uplink problem via a so-called network duality relationship. In the equivalent dual uplink problem, beamforming vectors can be derived in closed-form expressions with respect to the powers. A unified analysis of max-min weighted SINR problem in MIMO systems has been further proposed [60] based on the network duality and nonlinear Perron-Frobenius theory [61, 62].

The max-min weighted SINR problem has also been extended to study cooperative transmissions in multiple cells [63–65]. Multiple power constraints, e.g., per-BS power constraints, therefore have to be considered in such an environment. However, it is not straightforward to extend the network duality with a single power constraint to the case with multiple power constraints. Thus, instead of using network duality in the max-min weighted SINR problem directly, the authors in [64, 65] have addressed the MISO max-min weighted SINR problem by iteratively solving the sum-power minimization problem and looking for a maximum feasible SINR. In [66], assuming all the weights are equal to one, i.e., all user priorities are the same, an analytical expression for the network duality has been derived and a more efficient solution for the MISO max-min SINR problem is provided. The SIMO max-min weighted SINR problem with multiple power constraints is first analyzed in [67] by decoupling the original problem into subproblems each involving a single power constraint. The proposed algorithm in [67] involves finding the solution to each subproblem separately, and choosing the solution which gives the smallest value for the objective function. The strategy in [67] has been applied to tackle MISO max-min weighted SINR problem with multiple linear transmit covariance constraints [68].

However, the results cannot be extended due to the lack of a convex reformulation of the relaxed problem. In [69], an explicit solution for the MISO max-min weighted SINR problem with multiple linear sum-power constraints has been provided based on network duality and nonlinear Perron-Frobenius theory. It has also been claimed in [69] that the solution can be extended to the MIMO problem when both the transmit and receive beamformers are optimized. This motivates us to investigate the max-min weighted SINR problem under a FD multi-user MIMO scenario, which has not been evaluated in the open literature yet.

Energy efficiency (EE), defined as bits/Joule delivered to the receivers, has also attracted much interest in the telecommunications community [70–80]. Increasing EE has become an important and urgent task. In relay communications, recent research efforts have focused on EE in half-duplex relay systems [71, 77–79, 81–83]. In this thesis, we also investigate EE of FD relay systems.

1.2 Thesis Organization

The rest of this thesis is divided into five chapters.

In Chapter 2, we consider an OFDMA multi-user cellular system with one FD base station (BS) communicating with multiple HD users in a bidirectional way. The UL and DL transmissions are coupled together due to the existence of the SI at the BS and the inter-user interference (IUI) from the UL users to the DL users. We aim to maximize the system sum-rate of UL and DL transmissions by optimally pairing the UL and DL users, and allocating the subcarriers and powers to these users. We formulate the problem as a mixed integer nonlinear programming prob-

lem. A two-layer iterative solution based on the dual method and the sequential parametric convex approximation (SPCA) method is proposed. It is referred to as the Dual-SPCA algorithm. The Dual-SPCA algorithm requires the IUI channel state information (CSI) to be available at the BS and hence a significant overhead is generated. To reduce the amount of overhead required, we assume that the IUI channel model is known at the BS and we design a location-aware resource allocation algorithm with limited CSI that maximizes the system sum-rate. Simulation results show that when SI is low, UL and DL user-pairing can provide significant improvement on the system sum-rate compared to the conventional unidirectional HD transmission. In addition, by considering two different network deployments, i.e., urban macro cell scenario and small cell scenario, we show that the improvement of FD transmission over HD transmission highly depends on the channel parameters.

In Chapter 3, we jointly consider three different transmission modes in cooperative relay OFDMA systems, i.e., direct transmission mode, HD relay cooperative transmission mode and FD relay transmission mode. The joint optimization problem of transmission mode selection, subcarrier assignment, relay selection, subcarrier-pairing as well as power allocation is investigated. We transform the binary assignment problem into a maximum weighted bipartite matching problem. Based on the dual method, we solve the joint power allocation and binary assignment problem iteratively. Specifically, since the direct link is considered to be interference in the HD relay transmission mode, the power allocation problem in HD relay transmission mode is non-trivial. Thus, we provide a novel hierarchical dual method to solve the power allocation problem in FD relay transmission mode. In addition, in HD relay cooperative transmission mode, the joint transmission of both source and

relay is taken into account, and we provide a simple and insightful power allocation scheme. Results show that the overall system throughput can be significantly enhanced compared to previous works.

In Chapter 4, we investigate a max-min weighted SINR problem in a FD multi-user MIMO system, where a FD-capable base station equipped with multiple antennas communicates with multiple HD DL and UL users under the same system resources. Instead of optimizing the joint UL and DL max-min weighted SINR, we consider a more practical scenario where the DL minimum weighted SINR is maximized under specific SINR constraints for uplink users. Moreover, the optimization is conducted by jointly considering the base station transmit power, uplink transmit power, and base station transmit and receive beamforming. This optimization problem is therefore subject to multiple uplink SINR constraints and multiple transmit power constraints. Due to the SINR constraints, negative matrix components arise and hence the optimization problem cannot be solved by the Perron-Frobenius theory directly. With fixed base station transmit and receive beamforming, we first optimize the max-min weighted SINR problem under multiple uplink SINR constraints and a single power constraint, and show how the subgradient projection-based method can be applied to optimize the problem under multiple-power-constraint conditions. Then we derive the network duality of the same problem, i.e., fixed base station transmit/receive beamforming with multiple uplink SINR constraints and a single power constraint. To solve the original problem, we propose an optimization algorithm that iteratively updates (i) the transmit power vector and receive beamforming in the primal domain, and (ii) the dual transmit power vector and transmit beamforming in the dual domain. Moreover,

the algorithm, which is also based on the subgradient projection-based method, is proven to converge under appropriate initialization parameters. With network duality, we avoid optimizing coupled transmit beamforming in the primal domain and instead are able to optimize individual transmit beamformers easily in the dual domain. Simulation results show that our proposed algorithm has a fast convergence rate and leads to a better performance compared to other optimization techniques that do not jointly considered all parameters.

In Chapter 5, energy efficiency of a FD relay system under the total power constraint and fixed circuitry power consumption is studied. An optimization problem is formulated towards maximizing the system energy efficiency. Unfortunately, this problem is non-trivial and cannot be solved by conventional fractional programming methods, such as the Dinbelbach's method. To resolve this issue, an algorithm called sequential parametric convex approximation-Dinbelbach is proposed. Simulation results show that the proposed algorithm can converge to the global optimum very quickly.

Finally, Chapter 6 concludes this thesis and outlines some possible future directions.

Chapter 2

Full-Duplex OFDMA Multi-user Cellular Systems: Resource Allocation and User Pairing

In this chapter, we investigate a FD multi-user OFDMA system consisting of one FD BS, multiple UL users and multiple DL users. As the SI cancellation technologies required for implementing the FD transmission are highly complex, we assume that FD is only implemented at BS but not at UL and DL users. In other words, the UL and DL transmissions of all users are performed in a HD mode. Since BS operates in the FD mode, it can communicate with a pair of HD UL and DL users using the same subcarrier. In order to maximize the system sum-rate, we consider the joint optimization of subcarrier allocation, power allocation, and UL and DL user-pairing by taking into account the SI at the BS and IUI from the UL users to the DL users. We aim to maximize the system sum-rate of all UL and DL transmissions.

In a FD OFDMA system, the channels are considered as interference-limited channels due to the existence of SI and IUI. Hence, UL transmissions and DL transmissions over the same subcarrier are coupled together. As a result, conventional OFDMA resource allocation algorithms and power allocation algorithms applicable to individual UL or DL transmissions cannot be applied here. While the paired UL and DL transmissions can be modeled as an interference channel and the power control scheme in an interference channel has been solved by some previous works [84, 85], the problem in our model is highly sophisticated. For instance, the allocated power over each subcarrier for each UL user is not only limited by the individual power constraint but is also dependent on IUI and SI. In our model, subcarrier allocation, power allocation and user-pairing are being tangled and coupled together, leading to a mixed integer nonlinear programming problem (MINLP).

To tackle the aforementioned problem, we apply the dual method [86] and the sequential parametric convex approximation (SPCA) method [87]. Specifically, we propose a two-layer iterative algorithm called *Dual-SPCA algorithm* to solve the MINLP problem. The Dual-SPCA algorithm requires full IUI channel state information (CSI) to be available at the BS and hence generates a significant amount of overhead. To overcome this issue, we further propose an algorithm that does not require full IUI CSI — a location-aware resource allocation algorithm with limited CSI (we abbreviate it as *location-aware algorithm with limited CSI*). The algorithm makes use of the user locations to estimate the IUI, and formulates and solves the scenario as a chance-constrained problem.

The rest of this chapter is organized as follows. Section 2.1 describes the system model and problem formulation. Section 2.2 presents the Dual-SPCA algorithm with

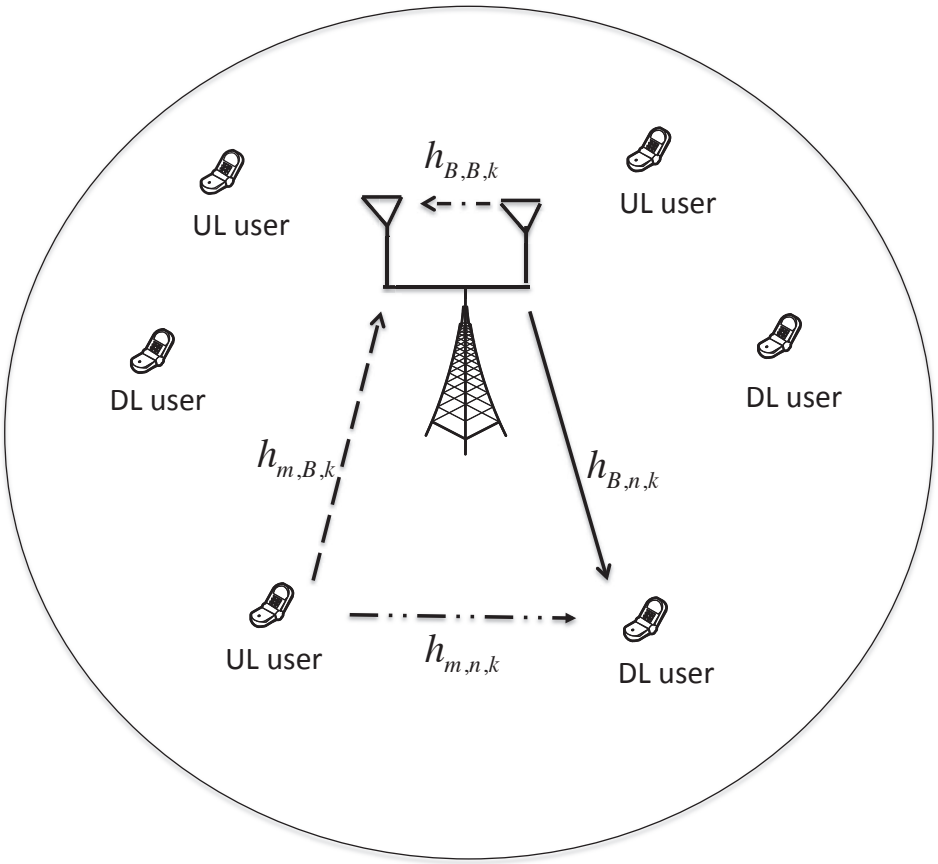

Figure 2.1: A single cell OFDMA system model with FD BS.

full CSI and Section 2.3 describes the location-aware algorithm. Section 2.4 provides and discusses the numerical results and Section 2.5 gives a summary.

2.1 System Model and Problem Formulation

We consider the multi-user OFDMA system shown in Fig. 2.1, where each subcarrier experiences independent flat fading. The system consists of a BS, multiple UL and DL users. The BS operates in the FD mode while all the users operate in the HD mode. We assume that the channel coefficients experience both path loss and short-

term fading. The path loss is a function of distance d and is denoted by $\mathrm{pl}(d)$ while the short-term fading of all channels is assumed to be Rayleigh independent and identically distributed (i.i.d.) with unit parameter. We further define the following symbols.

- B: base station
- U_m: m-th UL user
- D_n: n-th DL user
- K: number of subcarriers
- M: number of UL users
- N: number of DL users
- $\mathcal{K} = \{1, \ldots, K\}$
- $\mathcal{M} = \{1, \ldots, M\}$
- $\mathcal{N} = \{1, \ldots, N\}$
- $k \in \mathcal{K}$: subcarrier index
- $m \in \mathcal{M}$: UL-user index
- $n \in \mathcal{N}$: DL-user index
- σ_B^2: noise power at BS over each subcarrier
- $\sigma_{D,n}^2$: noise power at n-th DL user over each subcarrier

- $h_{B,n,k}$: complex channel coefficient of the link between B and D_n over subcarrier k
- $h_{m,B,k}$: complex channel coefficient of the link between U_m and B over subcarrier k
- $h_{m,n,k}$: complex channel coefficient of the link between U_m and D_n over subcarrier k
- $h_{B,B,k}$: SI channel coefficient at the BS over subcarrier k and is modeled as $h_{SI}/\sqrt{\tau}$, where τ is the SI attenuation and $h_{SI} \sim \mathcal{CN}(0,1)$[1]
- $p_{m,B,k}$: transmit power level of U_m to B over subcarrier k
- $p_{B,n,k}$: transmit power level of B to U_n over subcarrier k
- $\alpha_{B,n,k} = |h_{B,n,k}|^2/\sigma^2_{D,n}$: effective channel gain between B and D_n over subcarrier k
- $\alpha_{m,B,k} = |h_{m,B,k}|^2/\sigma^2_{B}$: effective channel gain between U_m and B over subcarrier k
- $\alpha_{m,n,k} = |h_{m,n,k}|^2/\sigma^2_{D,n}$: effective channel gain between U_m and D_n over subcarrier k
- $\alpha_{B,B,k} = |h_{B,B,k}|^2/\sigma^2_{B}$: effective SI channel gain at the BS over subcarrier k

In this system, we consider the following policy for subcarrier allocation and user-pairing.

[1]Before analog domain cancellation, the SI channel has a strong line-of-sight (LOS) component, and can be modeled as Ricean distribution with a large K-factor. It is shown experimentally in [10] that after applying an analog domain cancellation, the strong LOS component is attenuated, resulting in a Ricean distribution with a small K-factor or a Rayleigh distribution.

Policy: *Since BS operates in the FD mode, it can communicate with a UL user and a DL user over each subcarrier simultaneously. Therefore, UL users can form pairs with DL users. Then the UL user and DL user in each pair form a FD link and communicate with BS simultaneously. In our OFDMA system, each subcarrier can only be assigned to exactly one UL user and/or one DL user. However, each UL user or DL user can be assigned with multiple subcarriers.*

Let us assume that the UL user U_m and the DL user D_n are paired over subcarrier k. the corresponding UL rate and DL rate (in bits/s/Hz) of the OFDM transmission, denoted by $R_{m,B,k}$ and $R_{B,n,k}$, respectively, can be expressed as

$$R_{m,B,k} = \log(1 + \frac{\alpha_{m,B,k} p_{m,B,k}}{\alpha_{B,B,k} p_{B,n,k} + 1}), \tag{2.1}$$

$$R_{B,n,k} = \log(1 + \frac{\alpha_{B,n,k} p_{B,n,k}}{\alpha_{m,n,k} p_{m,B,k} + 1}). \tag{2.2}$$

(Unless otherwise stated, the log function has a base of 2.) Our objective is to maximize the total system transmission sum-rate subject to a set of constraints.

We assume that the BS and UL users are power-limited. Denoting P_B and $P_{U,m}$ as the maximum transmission powers of the BS and UL user U_m, respectively, we then have the following power constraints.

BS power constraint

$$\sum_{k=1}^{K} \sum_{n=1}^{N} p_{B,n,k} \leq P_B \tag{2.3}$$

UL user power constraint

$$\sum_{k=1}^{K} p_{m,B,k} \leq P_{U,m} \quad \forall m \in \mathcal{M} \tag{2.4}$$

To represent the Policy as a mathematical equation, we denote $t_{m,n,k} \in \{0,1\}$ as the subcarrier and user-pairing assignment. If the subcarrier k is assigned to the user pair (m,n), then $t_{m,n,k} = 1$; otherwise $t_{m,n,k} = 0$. Then the policy can be formulated as the following constraint.

Joint subcarrier-and-user-pairing-assignment constraint

$$\sum_{n=1}^{N}\sum_{m=1}^{M} t_{m,n,k} = 1 \quad \forall k \in \mathcal{K} \tag{2.5}$$

The above constraint indicates that each subcarrier should be allocated to one and only one user-pair. However, the UL/DL user may or may not use the assigned subcarrier, depending on the allocated power being positive or zero. In other words, each subcarrier may practically be used by (i) one UL user and one DL user; (ii) only one UL user; (iii) only one DL user; and (iv) none of the UL/DL users. Thus, the allocated powers and $t_{m,n,k}$ jointly indicate the transmission status of the UL/DL users over each subcarrier k. Table 2.1 summarizes the detailed UL/DL transmission status over each subcarrier by jointly considering allocated powers, and subcarrier and user-pairing assignments[2].

Lemma 2.1. Given $M \geq K$ in the optimal subcarrier allocation scheme that max-

[2]Note also that $t_{m,n,k} = 0$ means subcarrier k has not been assigned to UL user U_m AND DL user D_n simultaneously. It only guarantees that the transmit powers of UL user U_m and DL user D_n cannot be both non-zero, i.e., $p_{m,B,k} \neq 0$ AND $p_{B,n,k} \neq 0$ is not allowed. For example, it is still possible that $p_{m,B,k} \neq 0$ AND $p_{B,n,k} = 0$ because the m-th UL user may have paired up with the n'-th DL user over the k-th subcarrier for $n' \neq n$.

imizes the system sum-rate, there always exists an UL transmission or a DL transmission or both over each subcarrier.

Proof. We prove by contradiction. Assume that there is neither UL nor DL transmissions in a certain subcarrier k^*, i.e. $p_{m,B,k^*} = 0 \ \forall m \in \mathcal{M}$ and $p_{B,n,k^*} = 0 \ \forall n \in \mathcal{N}$. As each subcarrier can be allocated to at most one UL user, there exists at least one UL user U_m which is not assigned with any subcarrier (because $M \geq K$). Since there is no transmission in subcarrier k^*, U_m can use the subcarrier k^* for UL transmission and hence to increase the system sum-rate. Such a scenario is contradictory to the assumption and Lemma 2.1 is hence proved. □

To maximize the system sum-rate, we need to optimize the power allocation among subcarriers $(p_{m,B,k}, p_{B,n,k}) \ \forall m, n, k$ subject to the constraints (2.3) and (2.4); and to optimize the joint subcarrier and user-pairing assignments $t_{m,n,k} \ \forall m, n, k$ subject to the constraint (2.5). Such an optimization problem will be solved by the BS and the resulting allocation information will be sent to each user.

Defining $\boldsymbol{p}$ as $\{p_{m,B,k}, p_{B,n,k} | n \in \mathcal{N}, m \in \mathcal{M}, k \in \mathcal{K}\}$ and $\boldsymbol{t}$ as $\{t_{m,n,k} | m \in \mathcal{M}, n \in \mathcal{N}, k \in \mathcal{K}\}$, we seek the joint optimization of $\boldsymbol{p}$ and $\boldsymbol{t}$ to maximize the system transmission rate subject to the power and subcarrier assignment constraints, i.e.,

$$\mathbf{P1}: \max_{\boldsymbol{p},\boldsymbol{t}} \quad \sum_{k=1}^{K} \sum_{n=1}^{N} \sum_{m=1}^{M} t_{m,n,k} (R_{m,B,k} + R_{B,n,k}) \tag{2.6}$$

$$\text{s.t.} \quad (2.3), (2.4) \text{ and } (2.5).$$

Note that we only consider the instantaneous sum-rate as the performance metric. In other words, messages are transmitted separately over each channel realization.

Table 2.1: The Transmission Status of U_m and D_n over subcarrier k when $t_{m,n,k} = 1$ or 0.

$p_{m,B,k}$	$p_{B,n,k}$	U_m Status	D_n Status	$t_{m,n,k} = 1$	$t_{m,n,k} = 0$
non-zero	non-zero	on	on	Possible (when SI is low and IUI is low)	Not possible
non-zero	0	on	off	Possible (when SI is very high or DL rate is very low after BS transmit power is turned on)	Possible (when subcarrier k is assigned to UL user m and DL user n' where $n \neq n'$)
0	non-zero	off	on	Possible (when IUI is very high or UL rate is very low after UL user U_m transmit power is turned on)	Possible (when subcarrier k is assigned to UL user m' and DL user n where $m \neq m'$)
zero	zero	off	off	Possible only when $M < K$ in our system and all transmit powers have been used on other subcarriers; and not possible when $M \geq K$	Possible (when subcarrier k is assigned to UL user m' and DL user n' where $m \neq m'$ and $n \neq n'$)

The ergodic sum-rate, of which the messages are encoded over a very long period of channel realizations, is beyond the scope of this chapter. For ease of notation, we use sum-rate instead of instantaneous sum-rate in the rest of the chapter.

2.2 Dual-SPCA Algorithm with Full CSI

We first consider the scenario when BS has the access to all global CSI, including UL-CSI, DL-CSI, SI-CSI and IUI-CSI[3]. The optimal solution $\{\boldsymbol{p}, \boldsymbol{t}\}$ to (2.6) requires solving a MINLP problem. The total $(MN)^K$ possibilities of subcarrier and user-pairing assignment significantly complicate the problem when K, M and N are large. Fortunately, our optimization problem is a multiple subcarriers allocation problem and can be solved by using the dual method [86]. Moreover, the duality gap of the non-convex resource allocation problem is negligible when the number of subcarriers becomes sufficiently large, i.e., the solution is asymptotically optimal when K is large. We propose a two-layer iterative algorithm called *Dual-SPCA algorithm*, which includes three main steps: (i) problem transformation; (ii) optimizing the dual function at given primal variables; (iii) optimizing primal variables at a given dual point. Details of the proposed Dual-SPCA algorithm are described as follows.

2.2.1 Problem Transformation

The problem under consideration is a mixed combinatorial and non-convex optimization problem. The combinatorial nature comes from the integer constraint for the subcarrier and user-pairing assignment strategy. In general, a brute force approach is needed to obtain the global optimal solution. In this chapter, we propose to tackle the integer constraint in (2.5) with the following lemma.

Lemma 2.2. (Optimality of the time-sharing relaxation): If we relax the subcarrier

[3]Usually, the system performance under global CSI assumption is treated as the baseline. Note that BS can directly estimate UL-CSI and SI-CSI. However, the DL CSI and IUI-CSI have to be fed back by DL users.

and user-pairing variable $t_{m,n,k}$ in (2.5) to be a real value between zero and one, i.e., $0 \leq t_{m,n,k} \leq 1$, instead of a Boolean value, then the relaxed problem has the same solution as the original optimization problem in (2.6).

Proof. The above lemma can be proved by using a similar approach as in [86, 88]. □

To facilitate time-sharing the subcarrier and user-pairing variable $t_{m,n,k}$, we introduce two "virtual powers" variables $p^{(n)}_{m,B,k}$ and $p^{(m)}_{B,n,k}$. They are paired together and are defined as

$$\begin{aligned} p^{(n)}_{m,B,k} &= t_{m,n,k} p_{m,B,k} \\ p^{(m)}_{B,n,k} &= t_{m,n,k} p_{B,n,k}. \end{aligned} \tag{2.7}$$

The reason for proposing the concept of the virtual powers is to eliminate the integer factor $t_{m,n,k}$ and to decompose the optimization problem **P1** into a solvable dual problem. The actual transmit powers are still $p_{B,n,k}$ and $p_{m,B,k}$, which can directly derived after the virtual powers $p^{(m)}_{B,n,k}$ and $p^{(n)}_{m,B,k}$ and the user-pairing variable $t_{m,n,k}$ are obtained in the Dual-SPCA algorithm. Thus using the virtual powers $p^{(n)}_{m,B,k}$ and $p^{(m)}_{B,n,k}$, the UL rate and the DL rate of the OFDM transmission over subcarrier k can be re-defined as $R^{(n)}_{m,B,k}$ and $R^{(m)}_{B,n,k}$, which are re-expressed as

$$R^{(n)}_{m,B,k} = \log(1 + \frac{\alpha_{m,B,k} p^{(n)}_{m,B,k}}{\alpha_{B,B,k} p^{(m)}_{B,n,k} + 1}), \tag{2.8}$$

$$R^{(m)}_{B,n,k} = \log(1 + \frac{\alpha_{B,n,k} p^{(m)}_{B,n,k}}{\alpha_{m,n,k} p^{(n)}_{m,B,k} + 1}). \tag{2.9}$$

Then the BS and UL power constraints can be rewritten as follows.

BS power constraint

$$\sum_{k=1}^{K}\sum_{n=1}^{N}\sum_{m=1}^{M} p_{B,n,k}^{(m)} \leq P_B \tag{2.10}$$

UL user power constraint

$$\sum_{k=1}^{K}\sum_{n=1}^{N} p_{m,B,k}^{(n)} \leq P_{U,m}, \quad \forall m \in \mathcal{M} \tag{2.11}$$

Hence the problem **P1** can be transformed equivalently to

$$\mathbf{P2}: \max_{\hat{\boldsymbol{p}},\boldsymbol{t}} \quad \sum_{k=1}^{K}\sum_{n=1}^{N}\sum_{m=1}^{M} (R_{m,B,k}^{(n)} + R_{B,n,k}^{(m)}) \tag{2.12}$$

$$\text{s.t.} \quad (2.5),\ (2.10)\ \text{and}\ (2.11)$$

where $\hat{\boldsymbol{p}}$ is defined as $\{(p_{m,B,k}^{(n)}, p_{B,n,k}^{(m)}) | m \in \mathcal{M}, n \in \mathcal{N}, k \in \mathcal{K}\}$. It can be seen that the integer constraint for $t_{m,n,k}$ is eliminated.

2.2.2 Optimizing the dual function

We define $\mathcal{T}$ as the set of possible subcarrier and user-pairing assignments $\boldsymbol{t}$ satisfying (2.5). In addition, we define $\mathcal{P}(\boldsymbol{t})$ as the set of possible power allocations $\hat{\boldsymbol{p}}$ under the given $\boldsymbol{t}$. Then, the Lagrange dual problem **P2** can be readily written as [89]

$$\min_{\boldsymbol{\lambda}\geq\mathbf{0}} g(\boldsymbol{\lambda}) \triangleq \min_{\boldsymbol{\lambda}\geq\mathbf{0}} \max_{\hat{\boldsymbol{p}}\in\mathcal{P}(\boldsymbol{t}),\boldsymbol{t}\in\mathcal{T}} \quad L(\hat{\boldsymbol{p}}, \boldsymbol{t}, \boldsymbol{\lambda}), \tag{2.13}$$

where the Lagrangian is

$$
\begin{aligned}
L(\hat{\boldsymbol{p}}, \boldsymbol{t}, \boldsymbol{\lambda}) = & \sum_{k=1}^{K} \sum_{N=1}^{N} \sum_{m=1}^{M} \left(\log \left(1 + \frac{\alpha_{m,B,k} p_{m,B,k}^{(n)}}{\alpha_{B,B,k} p_{B,n,k}^{(m)} + 1} \right) \right. \\
& \left. + \log \left(1 + \frac{\alpha_{B,n,k} p_{B,n,k}^{(m)}}{\alpha_{m,n,k} p_{m,B,k}^{(n)} + 1} \right) \right) \\
& + \lambda_B \left(P_B - \sum_{k=1}^{K} \sum_{n=1}^{N} \sum_{m=1}^{M} p_{B,n,k}^{(m)} \right) \\
& + \sum_{m=1}^{M} \lambda_{U,m} \left(P_{U,m} - \sum_{k=1}^{K} \sum_{n=1}^{N} p_{m,B,k}^{(n)} \right)
\end{aligned} \tag{2.14}
$$

and $\boldsymbol{\lambda} = \{\lambda_B, \lambda_{U,1}, \cdots, \lambda_{U,M}\}$ represents the vector of the dual variables associated with the individual power constraints $\{P_B, P_{U,1}, \cdots, P_{U,M}\}$.

Since a dual function is always convex by definition [89], gradient or subgradient-based methods can be used to minimize $g(\boldsymbol{\lambda})$ with a guaranteed convergence. We let $\hat{\boldsymbol{p}}^*(\boldsymbol{\lambda})$ be the optimal power allocation at a dual point (to be discussed in the next subsection). Then a subgradient of $g(\boldsymbol{\lambda})$ can be derived using a similar method as in [86] and the dual variables $\boldsymbol{\lambda}$ can be updated as

$$
\lambda_B^{(l+1)} = \left[\lambda_B^{(l)} - \pi^{(l)} \left(P_B - \sum_{k=1}^{K} \sum_{n=1}^{N} \sum_{m=1}^{M} p_{B,n,k}^{(m)*} \right) \right]^+ \tag{2.15}
$$

$$
\lambda_{U,m}^{(l+1)} = \left[\lambda_{U,m}^{(l)} - \pi^{(l)} \left(P_{U,m} - \sum_{k=1}^{K} \sum_{n=1}^{N} p_{m,B,k}^{(n)*} \right) \right]^+ \tag{2.16}
$$

where $[\star]^+$ denotes $\max(0, \star)$, the superscript $^{(l)}$ denotes the iteration number, and $\pi^{(l)}$ represents the step size. When the step size $\pi^{(l)}$ follows the diminishing policy in [90], the subgradient method above is guaranteed to converge to the optimal dual variables. Here, we just take the simple diminishing step, i.e., $\pi^{(l)} = \pi^{(0)}/\sqrt{l}$, where

$\pi^{(0)} > 0$ is the initial step size. The computational complexity of such an updating method is polynomial in the number of dual variables $M + 1$ [86].

2.2.3 Optimizing Primal Variables at a Given Dual Point

Computing the dual function $g(\boldsymbol{\lambda})$ involves determining the optimal $(\boldsymbol{p}^*, \boldsymbol{t}^*)$ at the given dual point $\boldsymbol{\lambda}$. In this subsection, we present the detailed derivation of the optimal primal variables in three phases. Before that, we rewrite (2.13) as

$$g(\boldsymbol{\lambda}) = \max \left(\sum_{k=1}^{K} \sum_{n=1}^{N} \sum_{m=1}^{M} L_{m,n,k} + \lambda_B P_B + \sum_{m=1}^{M} \lambda_{U,m} P_{U,m} \right) \tag{2.17}$$

where

$$\begin{aligned} L_{m,n,k} =& \log \left(1 + \frac{\alpha_{m,B,k} p_{m,B,k}^{(n)}}{\alpha_{B,B,k} p_{B,n,k}^{(m)} + 1} \right) \\ &+ \log \left(1 + \frac{\alpha_{B,n,k} p_{B,n,k}^{(m)}}{\alpha_{m,n,k} p_{m,B,k}^{(n)} + 1} \right) \\ &- \lambda_B p_{B,n,k}^{(m)} - \lambda_{U,m} p_{m,B,k}^{(n)}. \end{aligned} \tag{2.18}$$

2.2.3.1 Optimal Power Allocation for a Given Subcarrier and User-pair Assignment

Here we analyze the optimal power allocation $\boldsymbol{p}^*$ for a given subcarrier and user-pairing assignment $\boldsymbol{t}$. We suppose that a user-pair (m, n) is assigned with the subcarrier k, i.e., $t_{m,n,k} = 1$. Then the optimal power allocation over this combination

(m, n, k) can be determined by solving the following problem:

$$\max_{\{p^{(n)}_{m,B,k}, p^{(m)}_{B,n,k}\}} \quad L_{m,n,k} \tag{2.19}$$

$$\text{s.t.} \quad p^{(n)}_{m,B,k} \geq 0,\, p^{(m)}_{B,n,k} \geq 0. \tag{2.20}$$

Since $L_{m,n,k}$ is non-convex, it is very hard to obtain a closed-from expression of $p^{(n)}_{m,B,k}$ and $p^{(m)}_{B,n,k}$ based on the Karush-Kuhn-Tucker (KKT) conditions [89]. Since the power control algorithm is not our main concern, we simply utilize a local optimization method. The method performs a successive parametric convex approximation (SPCA) of $L_{m,n,k}$ and solves the problem iteratively. The solution process of the SPCA method that maximizes $L_{m,n,k}$ is shown in Appendix 2.A. The SPCA method has been proved to satisfy the KKT conditions [87], which form a sufficient condition to apply the dual method [86]. Finally, the optimal value of the Lagrangian function for a given subcarrier and user-pairing assignment $t_{m,n,k}$ is set as $L^o_{m,n,k}$.

2.2.3.2 Optimal Subcarrier and User-pairing Assignment

For a given subcarrier k, we select a user-pair as $(m_k, n_k) = \arg\max_{\forall m,n} L^o_{m,n,k}$ through exhaustive search of all possible (MN) combinations. Then we set $t_{m_k,n_k,k} = 1$ and $t_{m',n',k} = 0$ for $m' \neq m_k$ or $n' \neq n_k$. It is not hard to verify that (2.5) is satisfied subsequently. Finally, the virtual powers $p^{(n')}_{m',B,k}$ and $p^{(m')}_{B,n',k}$ are set as zeros.

2.2.4 Optimality Analysis

In the outer iteration of our proposed Dual-SPCA algorithm, the dual method is used to optimize the dual variables based on a gradient-based method. In addition, in the inner iteration of our proposed Dual-SPCA algorithm, the SPCA method is guaranteed to converge to a KKT point [87]. Since a multiple subcarriers allocation problem solved by using the dual method is asymptotically optimal given the inner problem reaches a KKT point [86], we can conclude that our proposed Dual-SPCA algorithm is near-optimal.

2.3 Location-Aware Resource Allocation Algorithm with Limited CSI

In the previous section, we have assumed that the BS collects and processes all the instantaneous CSI information, including the UL-CSI, SI-CSI, DL-CSI and IUI-CSI. The UL-CSI and SI-CSI can be estimated by the BS directly. However, the DL-CSI and IUI-CSI are measured by the DL users and then fed back to the BS. Each of the N DL users is required to measure K DL-CSI and MK IUI-CSI. Since $M >> 1$, measuring the IUI-CSI and sending the information back to the BS requires considerable overhead. To overcome this problem, in this section we propose and investigate a sub-optimal IUI estimation algorithm. Instead of estimating and uploading the instantaneous IUI-CSI, each user only has to report its location — based on the global positioning system (GPS) or some other means — to the BS periodically. We further assume that the BS has the prior knowledge of the prob-

ability density function (PDF) of the channel fading model between users. Then, the BS can make use of the user-locations information to estimate the IUIs and to allocate resources.

2.3.1 Problem Relaxation

According to the decomposition theory [91] and inspired by [92], we introduce a set of slack variables $\Gamma_{B,k}$ denoting the constraint of the self-interference of BS over subcarrier k, and $\Gamma_{n,k}$ denoting the constraint of the interference suffered by D_n over subcarrier k. The vector $\mathbf{\Gamma} = \{\Gamma_{B,k}, \Gamma_{n,k} | n \in \mathcal{N}, k \in \mathcal{K}\}$ is similar to the concept of interference temperature in cognitive radios and here we refer to it as the *interference-to-noise temperature* (INRT) vector. Compared to the problem **P1**, the following problem decouples the subcarrier and user-pairing assignment into separable UL and DL user scheduling problem with the use of the INRT vector $\mathbf{\Gamma}$:

$$\max_{\boldsymbol{p},\boldsymbol{s},\mathbf{\Gamma}} \sum_{k=1}^{K}\sum_{m=1}^{M} s_{m,B,k} R'_{m,B,k} + \sum_{k=1}^{K}\sum_{n=1}^{N} s_{B,n,k} R'_{B,n,k} \tag{2.21}$$

s.t. (2.10) and (2.11)

$$\sum_{n=1}^{N} s_{B,n,k} = 1 \text{ and } \sum_{m=1}^{M} s_{m,B,k} = 1 \ \ \forall k \tag{2.22}$$

$$\sum_{n=1}^{N} \alpha_{B,B,k} p_{B,n,k} \leq \Gamma_{B,k} \ \ \forall k \tag{2.23}$$

$$\sum_{m=1}^{M} s_{B,n,k} s_{m,B,k} \alpha_{m,n,k} p_{m,B,k} \leq \Gamma_{n,k} \ \ \forall n, k \tag{2.24}$$

where

$$R'_{m,B,k} = \log\left(1 + \frac{\alpha_{m,B,k} p_{m,B,k}}{\Gamma_{B,k} + 1}\right), \tag{2.25}$$

$$R'_{B,n,k} = \log\left(1 + \frac{\alpha_{B,n,k} p_{B,n,k}}{\Gamma_{n,k} + 1}\right), \tag{2.26}$$

and $s_{B,n,k}$ and $s_{m,B,k}$ are, respectively, Boolean variables indicating scheduling of UL user and DL user over subcarrier k. Specifically, $s_{B,n,k} = 1$ indicates that the DL user D_n is scheduled over subcarrier k; otherwise $s_{B,n,k} = 0$. $s_{m,B,k}$ is also defined in a similar way. Here, the constraint (2.22) ensures that the subcarrier assignment and user scheduling satisfy the **Policy**; the constraint (2.23) guarantees that the actual self-interference-to-noise ratio over each subcarrier k is below the INRT level $\Gamma_{B,k}$; and the constraint (2.24) indicates that for any DL user who is scheduled over each subcarrier k, the corresponding interference-to-noise ratio should be below the INRT $\Gamma_{n,k}$.

Since there is no instantaneous IUI-CSI available at the BS side, the constraint (2.24) may not be satisfied all the time. Hence, we consider a more realistic interference constraint called chance-constrained IUI, which specifies the minimum probability that the IUI interference constraint in (2.24) is satisfied. We introduce the concept of chance-constrained resource allocation which has been recently proposed in [93, 94]. The constraint (2.24) is then re-written as

$$\Pr\left\{\sum_{m=1}^{M} s_{B,n,k} s_{m,B,k} \alpha_{m,n,k} p_{m,B,k} \leq \Gamma_{n,k}\right\} \geq 1 - \epsilon. \tag{2.27}$$

The above inequality enforces that if DL user D_n is scheduled over subcarrier k, the probability of the interference suffered by the DL user being smaller than INRT $\Gamma_{n,k}$

is no less than $1-\epsilon$. As a result, $\epsilon \in (0,1)$ denotes the maximum probability that the INRT $\Gamma_{n,k}$ is exceeded.

Lemma 2.3. Assuming that the long-term fading and the PDF of short-term fading of the IUI channel are known, the constraint (2.27) can be re-written as

$$\sum_{m=1}^{M} s_{B,n,k} s_{m,B,k} \tilde{\alpha}_{m,n,k} p_{m,B,k} \leq \Gamma_{n,k} \quad \forall n,k \tag{2.28}$$

where $\tilde{\alpha}_{m,n,k} = \log(\frac{1}{\varepsilon})/\mathrm{pl}(d_{m,n})\sigma_{D_n}^2$.

Proof. Please refer to Appendix 2.B. □

Subsequently for a given $\boldsymbol{\Gamma}$, the problem of (2.21) with the additional constraint (2.28) can be formulated as follows.

$$\mathbf{P3}(\boldsymbol{\Gamma}): \max_{\boldsymbol{p},\boldsymbol{s}} \sum_{k=1}^{K}\sum_{m=1}^{M} s_{m,B,k} R'_{m,B,k} + \sum_{k=1}^{K}\sum_{n=1}^{N} s_{B,n,k} R'_{B,n,k}$$
$$\text{s.t.} \quad (2.10),\ (2.11),\ (2.22),\ (2.23) \text{ and } (2.28)$$

Note that without knowing full IUI-CSI, we cannot solve the optimization problem **P1**. Instead, we can estimate the chance-constrained interference based on limited CSI, i.e., IUI channel model and user locations, and transform problem **P1** to problem **P3**. Obtaining the optimal solution $(\boldsymbol{p},\boldsymbol{s})$ of problem $\mathbf{P3}(\boldsymbol{\Gamma})$ requires solving a mixed integer programming problem. In Sections 2.3.2 and 2.3.3, we will show that by using the dual method, the problem can be solved iteratively with a fixed $\boldsymbol{\Gamma}$. Then, in Section 2.3.4, we will show that having solved the problem $\mathbf{P3}(\boldsymbol{\Gamma})$, we can solve the master problem in (2.21) by updating the INRT vector $\boldsymbol{\Gamma}$.

2.3.2 Optimizing Dual Function

We define $\mathcal{S}$ as the set of possible subcarrier and user scheduling $(s_{m,B,k}, s_{B,n,k})$ satisfying (2.22). In addition, we define $\mathcal{P}(\boldsymbol{s})$ as the set of all power allocations $\boldsymbol{p}$ that satisfy (i) $p_{m,B,k} > 0$ for $s_{m,B,k} = 1$, (ii) $p_{B,n,k} > 0$ for $s_{B,n,k} = 1$, (iii) $p_{m,B,k} = 0$ for $s_{m,B,k} = 0$, and (iv) $p_{B,n,k} = 0$ for $s_{B,n,k} = 0$[4]. Then, the dual problem $\mathbf{P3}(\boldsymbol{\Gamma})$ can be readily written as

$$\min_{\boldsymbol{\lambda},\boldsymbol{\mu},\boldsymbol{\nu}\geq 0} g(\boldsymbol{\lambda},\boldsymbol{\mu},\boldsymbol{\nu}) \triangleq \min_{\boldsymbol{\lambda},\boldsymbol{\mu},\boldsymbol{\nu}\geq 0} \max_{\boldsymbol{p}\in\mathcal{P}(\boldsymbol{s}),\boldsymbol{s}\in\mathcal{S}} \quad L(\boldsymbol{p},\boldsymbol{s},\boldsymbol{\lambda},\boldsymbol{\mu},\boldsymbol{\nu}) \tag{2.29}$$

where the Lagrangian is

$$\begin{aligned}
L(\boldsymbol{p},\boldsymbol{s},\boldsymbol{\lambda},\boldsymbol{\mu},\boldsymbol{\nu}) &= \sum_{k=1}^{K}\sum_{m=1}^{M} \log\left(1+\frac{\alpha_{m,B,k}p_{m,B,k}}{\Gamma_{B,k}+1}\right) \\
&+ \sum_{k=1}^{K}\sum_{n=1}^{N} \log\left(1+\frac{\alpha_{B,n,k}p_{B,n,k}}{\Gamma_{n,k}+1}\right) \\
&+ \lambda_B\left(P_B - \sum_{k=1}^{K}\sum_{n=1}^{N} p_{B,n,k}\right) \\
&+ \sum_{m=1}^{M} \lambda_{U,m}\left(P_{U,m} - \sum_{k=1}^{K} p_{m,B,k}\right) \\
&+ \sum_{k=1}^{K} \mu_{B,k}\left(\Gamma_{B,k} - \sum_{n=1}^{N} \alpha_{B,B,k}p_{B,n,k}\right) \\
&+ \sum_{k=1}^{K}\sum_{n=1}^{N} \nu_{n,k}\left(\Gamma_{n,k} - \sum_{n=1}^{N}\sum_{m=1}^{M} s_{B,n,k}\tilde{\alpha}_{m,n,k}p_{m,B,k}\right);
\end{aligned} \tag{2.30}$$

[4]In fact, we can directly use a mapping between allocated power and user scheduling instead of utilizing additional "virtual powers" introduced in the near-optimal algorithm.

$\boldsymbol{\lambda} = \{\lambda_B, \lambda_{U,1}, \cdots, \lambda_{U,M}\}$ represents the vector of the dual variables associated with the individual power constraints $\{P_B, P_{U,1}, \cdots, P_{U,M}\}$; $\boldsymbol{\mu} = \{\mu_{B,k} | k \in \mathcal{K}\}$ represents the vector of the dual variables associated with the individual INRT constraints $\{\Gamma_{B,k} | k \in \mathcal{K}\}$; and $\boldsymbol{\nu} = \{\mu_{n,k} | n \in \mathcal{N}, k \in \mathcal{K}\}$ represents the vector of the dual variables corresponding to the individual INRT constraints $\{\Gamma_{n,k} | n \in \mathcal{N}, k \in \mathcal{K}\}$.

As in Section 2.2.2, the updating rules of these dual variables are based on the subgradient method, i.e.,

$$\lambda_B^{(l+1)} = \left[\lambda_B^{(l)} - \pi_1^{(l)} \left(P_B - \sum_{k=1}^{K}\sum_{n=1}^{N} p_{B,n,k}^*\right)\right]^+ \tag{2.31}$$

$$\lambda_{U,m}^{(l+1)} = \left[\lambda_{U,m}^{(l)} - \pi_2^{(l)} \left(P_{U,m} - \sum_{k=1}^{K} p_{m,B,k}^*\right)\right]^+, \tag{2.32}$$

$$\mu_{B,k}^{(l+1)} = \left[\mu_{B,k}^{(l)} - \pi_3^{(l)} \left(\Gamma_{B,k} - \sum_{n=1}^{N} \alpha_{B,B,k} p_{B,n,k}^*\right)\right]^+, \tag{2.33}$$

$$\nu_{n,k}^{(l+1)} = \left[\nu_{n,k}^{(l)} - \pi_4^{(l)} \left(\Gamma_{n,k} - \sum_{m=1}^{M} s_{B,n,k} \tilde{\alpha}_{m,n,k} p_{m,B,k}^*\right)\right]^+, \tag{2.34}$$

where the step size $\pi_i^{(l)} (i \in \{1, 2, 3, 4\})$ follows the same diminishing policy described in Section 2.2.2. Note that the subgradient of $\nu_{n,k}$ highly depends on $s_{B,n,k}$. The physical implication is that if the subcarrier k is assigned to DL user D_n, the UL transmit power would affect the estimated INRT and reduce the convergence speed of $\nu_{n,k}$. However, if the subcarrier k is not assigned to DL user D_n, the corresponding constraint is always satisfied and the update process of $\nu_{n,k}$ can quickly converge to the optimal value.

2.3.3 Optimizing the Primal Variables at a Given Dual Point

By dual decomposition, the dual problem is decomposed into $(K \times M + K \times N)$ sub-problems, i.e.,

$$g(\boldsymbol{\lambda}, \boldsymbol{\mu}, \boldsymbol{\nu}) = \max \left(\sum_{k=1}^{K} \sum_{m=1}^{M} L_{m,k} + \sum_{k=1}^{K} \sum_{n=1}^{N} L_{n,k} + \sum_{k=1}^{K} \mu_{B,k} \Gamma_{B,k} + \sum_{k=1}^{K} \sum_{n=1}^{N} \nu_{n,k} \Gamma_{n,k} + \lambda_B P_B + \sum_{m=1}^{M} \lambda_{U,m} P_{U,m} \right) \tag{2.35}$$

where

$$L_{m,k} = \log \left(1 + \frac{\alpha_{m,B,k} p_{m,B,k}}{\Gamma_{B,k} + 1} \right) - \left(\lambda_{U,m} + \sum_{n=1}^{N} \nu_{n,k} s_{B,n,k} \tilde{\alpha}_{m,n,k} \right) p_{m,B,k} \tag{2.36}$$

$$L_{n,k} = \log \left(1 + \frac{\alpha_{B,n,k} p_{B,n,k}}{\Gamma_{n,k} + 1} \right) - (\lambda_B + \mu_{B,k} \alpha_{B,B,k}) p_{B,n,k}. \tag{2.37}$$

From (2.36), we can see that the sub-problem $L_{m,k}$ highly depends on the DL user scheduling $s_{B,n,k}$. However, the subproblem $L_{n,k}$ is independent of UL user scheduling. Hence, we can first optimize the power allocation and user scheduling of DL users and then optimize the power allocation and user scheduling of UL users. The optimal solution is further described in Lemma 2.4.

Lemma 2.4. The optimal power allocation and user scheduling for DL users and

UL users over any subcarrier k are given as follows.

$$s^*_{B,n,k} = \begin{cases} 1, & \text{if } n = \arg\max_{\forall n} L^o_{n,k} \\ 0, & \text{otherwise} \end{cases} \tag{2.38}$$

$$p^*_{B,n,k} = \begin{cases} \left[\frac{1}{\lambda_B + \mu_{B,k}\alpha_{B,B,k}} - \frac{\Gamma_{n,k}+1}{\alpha_{B,n,k}}\right]^+, & \text{if } s^*_{B,n,k} = 1 \\ 0, & \text{if } s^*_{B,n,k} = 0 \end{cases} \tag{2.39}$$

$$s^*_{m,B,k} = \begin{cases} 1, & \text{if } m = \arg\max_{\forall m} L^o_{m,k} \\ 0, & \text{otherwise} \end{cases} \tag{2.40}$$

$$p^*_{m,B,k} = \begin{cases} \left[\frac{1}{\lambda_{U,m} + \nu_{n_k,k}\tilde{\alpha}_{m,n_k,k}} - \frac{\Gamma_{B,k}+1}{\alpha_{m,B,k}}\right]^+, & \text{if } s^*_{m,B,k} = 1 \\ 0, & \text{if } s^*_{m,B,k} = 0 \end{cases} \tag{2.41}$$

$L^o_{m,k}$ and $L^o_{n,k}$ are defined as the optimal values of $L_{m,k}$ and $L_{n,k}$ with respect to the powers $p_{m,B,k}$ and $p_{B,n,k}$, respectively. n_k is the optimal DL user over subcarrier k.

Proof. Please refer to Appendix 2.C. □

2.3.4 Optimizing Interference-to-Noise Ratio Temperature

Having solved the problem $\mathbf{P3}(\mathbf{\Gamma})$, we then define the master problem as the function of updating the INRT vector $\mathbf{\Gamma}$, i.e.,

$$\mathbf{P3}^{\text{mas}} : \max_{\mathbf{\Gamma}} \quad \mathbf{P3}(\mathbf{\Gamma}) \tag{2.42}$$

$$\text{s.t.} \quad \mathbf{\Gamma} \geq 0. \tag{2.43}$$

The master problem can be solved iteratively using a subgradient method and the following lemma suggests the subgradients for each $\Gamma_{B,k}$ and $\Gamma_{n,k}$.

Lemma 2.5. The subgradient of $\Gamma_{B,k}$ and $\Gamma_{n,k}$ in the master problem are given by, respectively,

$$\Delta\Gamma_{B,k} = -\frac{\alpha_{m_k,B,k}p^*_{m_k,B,k}/(1+\Gamma_{B,k})}{\mathrm{In}2(1+\Gamma_{B,k}+\alpha_{m_k,B,k}p^*_{m_k,B,k})} + \mu^*_{B,k} \quad \forall k, \tag{2.44}$$

$$\Delta\Gamma_{n,k} = -\frac{\alpha_{B,n,k}p^*_{B,n,k}/(1+\Gamma_{n,k})}{\mathrm{In}2(1+\Gamma_{n,k}+\alpha_{B,n,k}p^*_{B,n,k})} + \nu^*_{n,k} \quad \forall n,k, \tag{2.45}$$

where m_k is the selected UL user over subcarrier k; $p^*_{m,B,k}$ and $p^*_{B,n,k}$ are given by (2.41) and (2.39), respectively; $\mu^*_{B,k}$ and $\nu^*_{n,k}$ are the optimal dual multipliers corresponding to the constraints (2.23) and (2.24), respectively.

Proof. Please refer to Appendix 2.D. □

According to Lemma 2.5, the BS has to update $K(N+1)$ INRTs after solving the relaxed $\mathbf{P3}(\mathbf{\Gamma})$. $\Gamma_{B,k}$ and $\Gamma_{n,k}$ are updated, respectively, using

$$\Gamma^{(l+1)}_{B,k} = \left[\Gamma^{(l)}_{B,k} + \varrho^{(l)}_1 \Delta\Gamma_{B,k}\right]^+ \quad \forall k \tag{2.46}$$

$$\Gamma^{(l+1)}_{n,k} = \left[\Gamma^{(l)}_{n,k} + \varrho^{(l)}_2 \Delta\Gamma_{n,k}\right]^+ \quad \forall n,k \tag{2.47}$$

where $\varrho^{(l)}_i (i \in \{1,2\})$ is a positive step size. The updating process is stopped when $|\Gamma^{(l+1)}_{B,k} - \Gamma^{(l)}_{B,k}|/\Gamma^{(l)}_{B,k} \leq \zeta$ and $|\Gamma^{(l+1)}_{n,k} - \Gamma^{(l)}_{n,k}|/\Gamma^{(l)}_{n,k} \leq \zeta$, where ζ is a sufficiently small convergence tolerance.

Remark: In the Dual-SPCA algorithm, all CSI information is available. The BS can therefore exhaustively consider all possible combinations of paired UL-DL users and determines the best user-pair over each subcarrier in order to achieve near-optimal performance. Compared with the Dual-SPCA algorithm with full CSI, the

location-aware algorithm with limited CSI does not need the exact IUI-CSI of each subcarrier but requires the long-term fading and short-term fading PDF of the IUI channel. Only UL users of which the interference to the DL users are under the interference threshold with a certain probability are treated as potential candidates for pairing. Then, the best paired UL and DL users over each subcarrier are selected under the given interference threshold. Subsequently, by updating the interference threshold iteratively, we can find the ultimate paired users over each subcarrier. In summary, by introducing the interference threshold in the location-aware algorithm, we can first select a DL user over a given subcarrier and then find a UL user that can maximize the sum-rate over the subcarrier. This fact also leads to another advantage of the proposed location-aware algorithm, i.e., we can easily adopt a semi-distributed way to implement the location-aware algorithm.

2.4 Simulation Results

To quantify the potential benefit of the full-duplex transmission considered in this chapter, we evaluate the performance of the proposed algorithms under the 3GPP LTE specifications for both urban macro (UMa) cell and small cell deployments. The simulation parameters of an UMa cell and a small cell are taken from [95, 96] and listed in Table 2.2. The cell coverage area is assumed to be circular, as shown in Fig. 2.1. For an UMa cell, the radius is set to 2 km and all the channels are considered to be under the non-line-of-sight (NLOS) environment. By setting the heights of BS and users to 31 m and 1.5 m, respectively, above ground [96, Section.1.2.1.3], we

Table 2.2: System simulation parameters.

Basic Parameters	
Cellular Layout	Isolated Cell, 1-sector
Noise spectral density	-174 dBm/Hz
Bandwidth	10 MHz
Number of subcarriers	32
Center frequency	2 GHz
Noise figure	9 dB
Short-term fading	Standard Rayleigh fading
Parameters for UMa Cell	
Cell area	The radius is 2km
Path-loss of UL and DL channels	$122.5+35\log_{10}(d)$
Path-loss of IUI channels	$146.2+39.8\log_{10}(d_{\mathrm{IUI}})$
$P_{BS} - P_U$	20dB
Parameters for Small Cell	
Cell area	The radius is 100m
Path-loss of UL and DL channels	$103.8+20.9\log_{10}(d)$
Path-loss of IUI channels	$145.4+37.5\log_{10}(d_{\mathrm{IUI}})$
$P_{BS} - P_U$	3dB

obtain the path-loss models of the UL channels, DL channels, and the IUI channels[5]. Also, according to the suggestion in [95], the peak power constraints for UL users are the same and set to be 20 dB below the peak power constraint of BS. For a small cell, the radius is set to 100 m. Moreover, the DL and UL channels are assumed to experience a path-loss model for line-of-sight (LOS) communications while IUI channels are assumed to encounter a path-loss model for NLOS transmissions [97]. Furthermore, the peak power constraint for UL users are the same and set to be 3 dB below the peak power constraint of BS [95].

[5]According to [96], the height of BS can be from 0 to 50 m above ground. We therefore set the height of BS to 31 m in the UL and DL channel models. However, the path-loss model of IUI channels has not been given specifically. Here we set the height of users to 1.5 m above ground in the IUI channel models as well as UL and DL channel models.

In addition to our proposed algorithms, the following four approaches are simulated.

- Half-Duplex Single User Selection (HD-SUS): For each subcarrier, only one UL or DL user is selected optimally based on the water-filling algorithm [98, 99]. In this approach, even if the total number of users is larger than the number of subcarriers, at most K users are allowed to access to the network simultaneously.

- Equal Power Allocation (EPA): In this approach, we firstly set equal power for all subcarriers and select the best user-pair over each subcarrier. Supposing the m-th UL user U_m is assigned with a total of K_m subcarriers, we then divide the total transmit power $P_{U,m}$ equally among these subcarriers, i.e., we set $p_{m,B,k} = P_{U,m}/K_m$ if $t_{m,n,k} = 1$.

- Random User-Pair Selection (RUPS): For each subcarrier, a random UL and DL user-pair is selected. Then power allocation is optimized at the given subcarrier and user-pairing assignment.

- Separately Maximizing UL transmissions and Maximizing DL transmissions (SMUMD): For each subcarrier, one UL user and one DL user are selected based on the water-filling algorithm. Then the UL transmissions and DL transmissions are maximized separately without taking IUI into account. In other words, SMUMD optimizes subcarrier assignment and power allocation without taking IUI into account.

A total of 5000 different channel realizations have been used. The number of subcarriers is set to $K = 32$. The number of UL and DL users are set to $M = N = 32$,

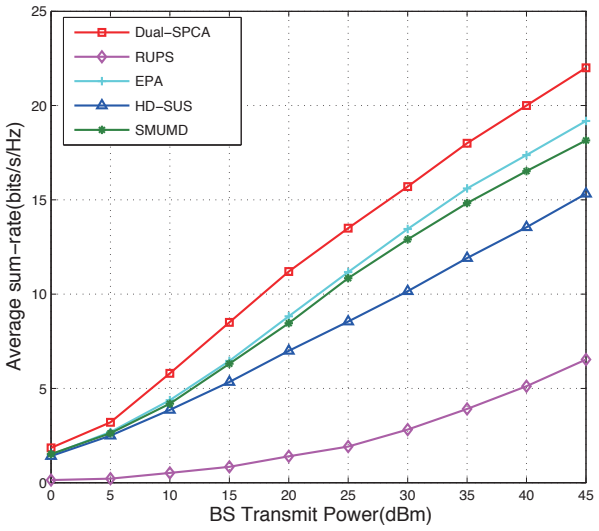

(a) $\tau = 120$ dB

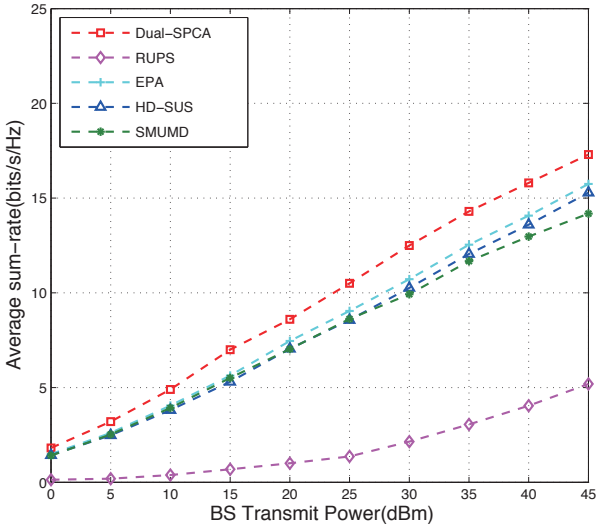

(b) $\tau = 100$ dB

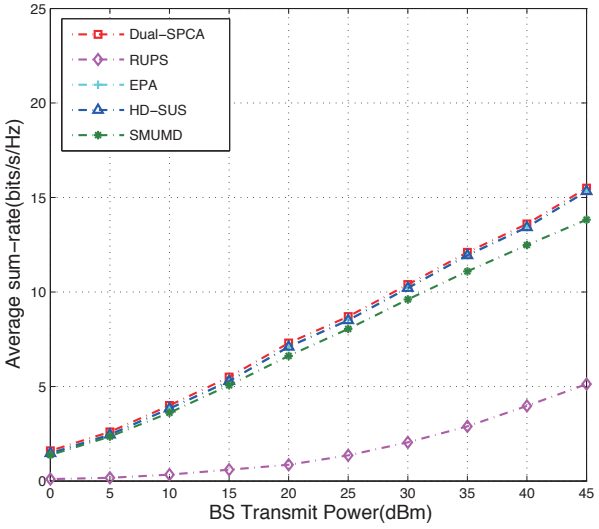

(c) $\tau = 80$ dB

Figure 2.2: Average sum-rate versus BS transmit power with different SI attenuations (τ) under a UMa cell scenario.

which are the same as the number of subcarriers.

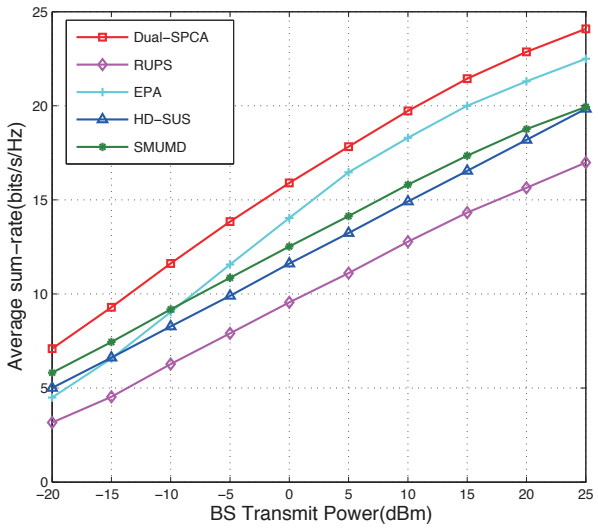

(a) $\tau = 120$ dB

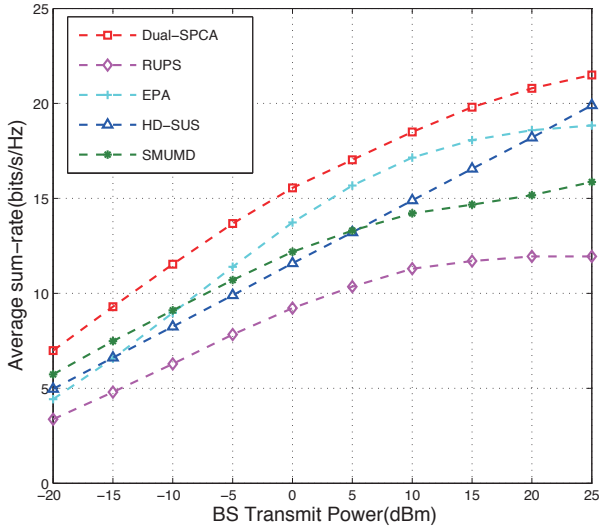

(b) $\tau = 100$ dB

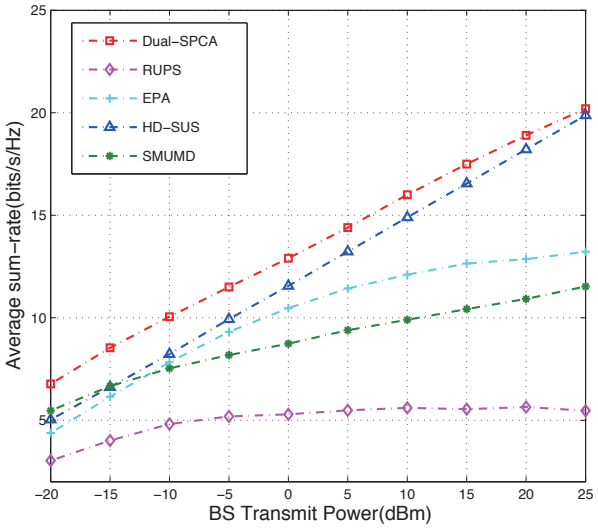

(c) $\tau = 80$ dB

Figure 2.3: Average sum-rate versus BS transmit power with different SI attenuations (τ) under a small cell scenario.

2.4.1 Average Sum-rate Performance of the Proposed Dual-SPCA Algorithm with Full CSI at BS

We first study the average sum-rates achieved by different schemes with different SI attenuations τ under both UMa cell scenario and small cell scenario. The results

under the UMa cell scenario and the small cell scenario are plotted in Figs. 2.2 and 2.3, respectively. Based on the curves, we have the following observations.

- The average sum-rates of all algorithms increase with the BS transmit power.
- As expected, the average sum-rate of HD-SUS algorithm is independent of SI attenuation.
- Under FD transmissions, the average sum-rates of Dual-SPCA, EPA, RUPS and SMUMD algorithms increase with SI attenuation.
- Dual-SPCA algorithm outperforms the other four baseline approaches, i.e., HD-SUS, EPA, RUPS and SMUMD algorithms. Among the four FD transmission algorithms, their relative performance in decreasing order is as follows: Dual-SPCA, EPA, SMUMD, RUPS.
- When SI is large (e.g. 120 dB), Dual-SPCA algorithm can outperform HD-SUS algorithm substantially. In particular, with 25 dBm BS transmit power and 120 dB SI attenuation, the proposed Dual-SPCA algorithm achieves about 60% average sum-rate improvement compared with the HD-SUS approach under an UMa cell environment and about 20% improvement under a small cell environment. The results also show that besides SI attenuation, other parameters such as cell environment are affecting the performance of FD transmissions.
- When SI attenuation is not large (e.g. 80 dB), Dual-SPCA algorithm only slightly outperforms HD-SUS algorithm. When the SI attenuation is not large, the transmit DL signal at BS creates a substantial interference to the receive signal in the UL channel. Under such circumstances, the effectiveness of FD

transmissions is reduced and using FD transmissions becomes not much beneficial.

- Among the four FD transmission algorithms, our proposed Dual-SPCA is the best. Moreover, EPA and SMUMD are the second best and third best, respectively. The results show that ignoring IUI in the optimization process (as in SMUMD) produces a larger degradation (compared with Dual-SPCA) than not optimizing the power allocation (as in EPA). Thus, pairing up UL and DL users appropriately by considering IUI is an important step in FD transmissions. Furthermore, depending on the BS transmit power, SI attenuation and channel environment, EPA and SMUMD may or may not outperform HD-SUS.

- For a given SI attenuation, RUPS algorithm always provides the lowest average sum-rate among the five algorithms. The results indicate that randomly pairing UL and DL users followed by optimized power allocation gives the worst performance — even worse than HD-SUS — and hence should never be used in practice.

Based on the above observations, we can conclude that without both appropriate user-pairing and optimized power allocation, FD transmissions may be worse than HD transmissions in an OFDMA multi-user cellular system. To gain further insights out of the system under study, we plot the percentage sum-rate gain of our proposed Dual-SPCA algorithm over the HD-SUS approach in Fig. 2.4. The results show that when SI attenuation is low (below 80 dB), there is not much gain when using Dual-SPCA compared with HD-SUS. It means that SI is causing much interference to the UL transmissions and FD transmissions cannot be utilized effectively. When SI attenuation increases from 90 dB to 120 dB, we can observe a

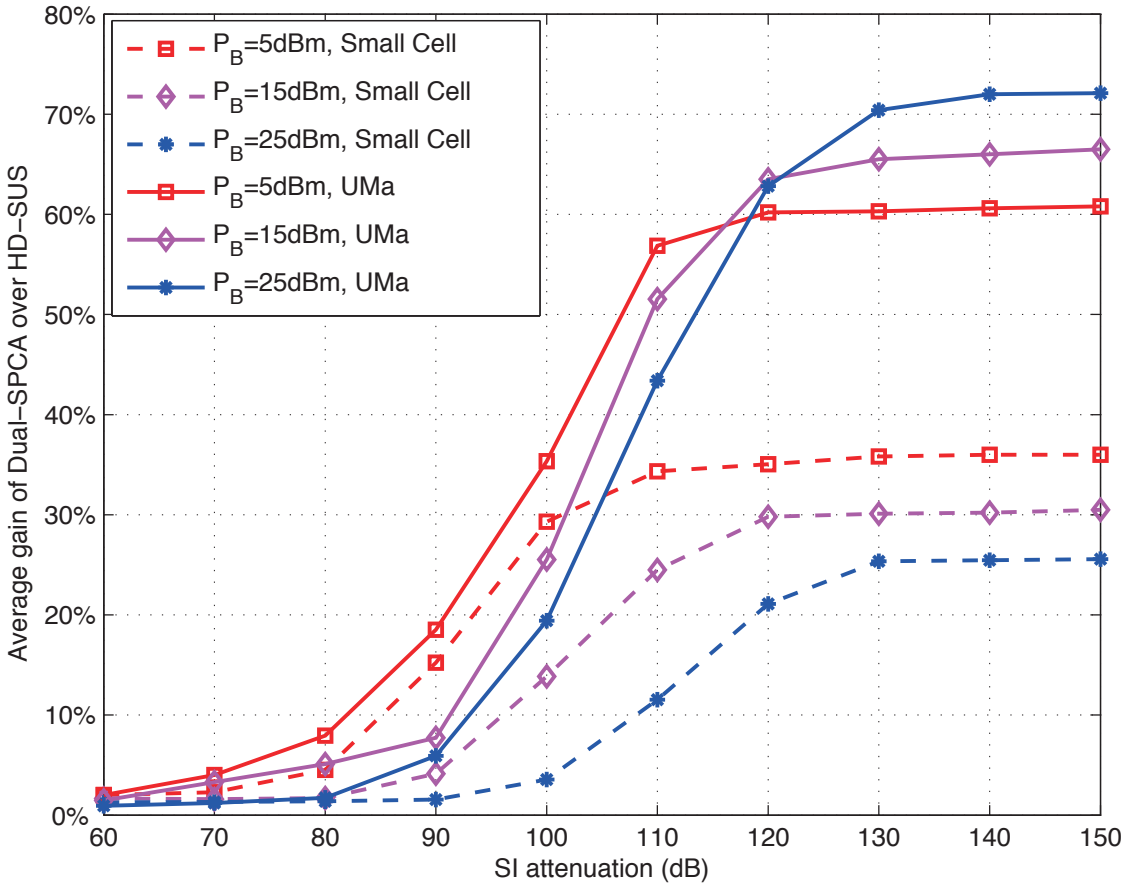

Figure 2.4: Average sum-rate gain of our proposed Dual-SPCA algorithm over HD-SUS approach versus SI attenuation for different BS transmit powers under both UMa cell and small cell scenarios.

steep rise in the gain. It indicates that more and more FD transmissions are being utilized and our proposed Dual-SPCA algorithm are providing substantial sum-rate improvements over HD-SUS. When SI attenuation is beyond 130 dB, the gain becomes flat but less than 100%. It shows that SI has become minimal, and all FD transmissions as well as the advantage of the Dual-SPCA algorithm have been fully realized. Moreover, due to the effect of IUI, the improvement of Dual-SPCA over HD-SUS cannot reach 100%. In other words, if there were no IUI, FD transmissions can be fully utilized in the system and the average sum-rates should be twice that of

HD transmissions. For the same BS transmit power, we observe that the gain of our proposed Dual-SPCA algorithm under an UMa scenario is always higher than that under a small cell scenario. It is due to the larger sum-rates achieved by HD-SUS under a small cell scenario than under an UMa scenario (see Figs. 2.2 and 2.3). For the same reason, the ultimate gain (i.e., when SI attenuation is very large) increases with BS transmit power under an UMa scenario but decreases under a small cell scenario. The above results indicate that the improvement of sum-rates achieved by Dual-SPCA not only on depends SI attenuation, but is also related to the network deployment environment. It is because other factors such as cell radius, path-loss models and maximum transmit powers are influencing the IUI which in turn affects the DL transmission rate and hence the sum-rate.

In Figs. 2.5 and 2.6, we plot the average sum-rate of our proposed Dual-SPCA algorithm and SMUMD approach under a UMa scenario and a small cell scenario, respectively. Given a BS transmit power, we observe that the average sum-rate increases with SI attenuation and reaches a maximum after the SI attenuation is above a certain threshold. When SI attenuation increases, FD transmissions become more effective and hence the sum-rate increases. Above a certain SI attenuation, the effect of SI becomes very minimal and the change in sum-rate is negligible. Figs. 2.5 and 2.6 also show that the Dual-SPCA algorithm always outperforms the SMUMD approach under the same conditions. The main reason is that IUI has been considered in the Dual-SPCA algorithm but ignored in the SMUMD algorithm. Thus, we can conclude that IUI plays a major role in determining the performance of a FD multiuser OFDMA cellular system.

Fig. 2.7 plots the average sum-rate versus number of UL/DL users ($M = N$)

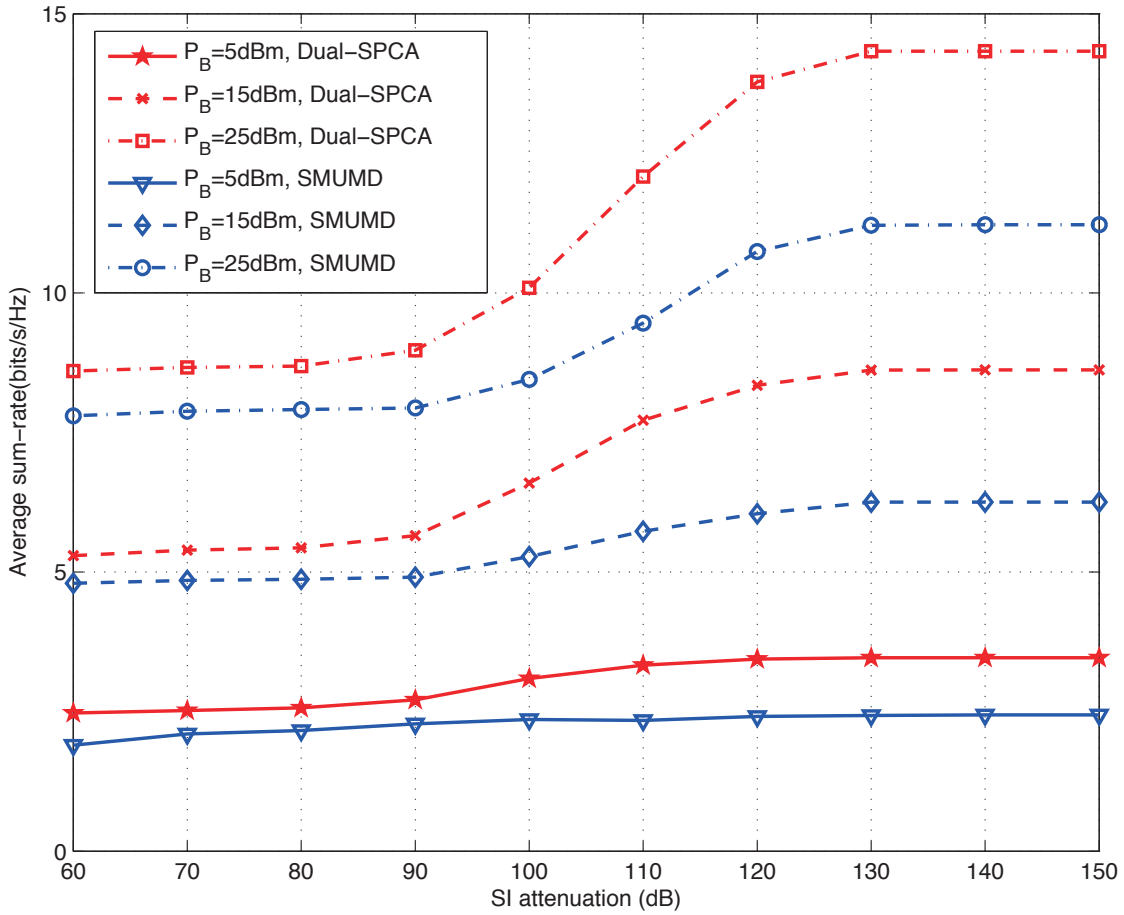

Figure 2.5: Average sum-rate of our proposed Dual-SPCA algorithm and SMUMD approach versus SI attenuation for different BS transmit powers under a UMa cell scenario.

when the number of subcarriers is 32. We find that our proposed Dual-SPCA algorithm outperforms all other algorithms. We can also observe that all algorithms except RUPS generate increasing average sum-rate as the number of UL/DL users ($M = N$) increases. When there are more users to select from during the pairing process, it is obvious that a better solution (except RUPS) can be found so as to generate a higher sum-rate. As for RUPS which pairs users up randomly, its average sum-rate is the lowest among all algorithms. Moreover, its sum-rate quickly becomes

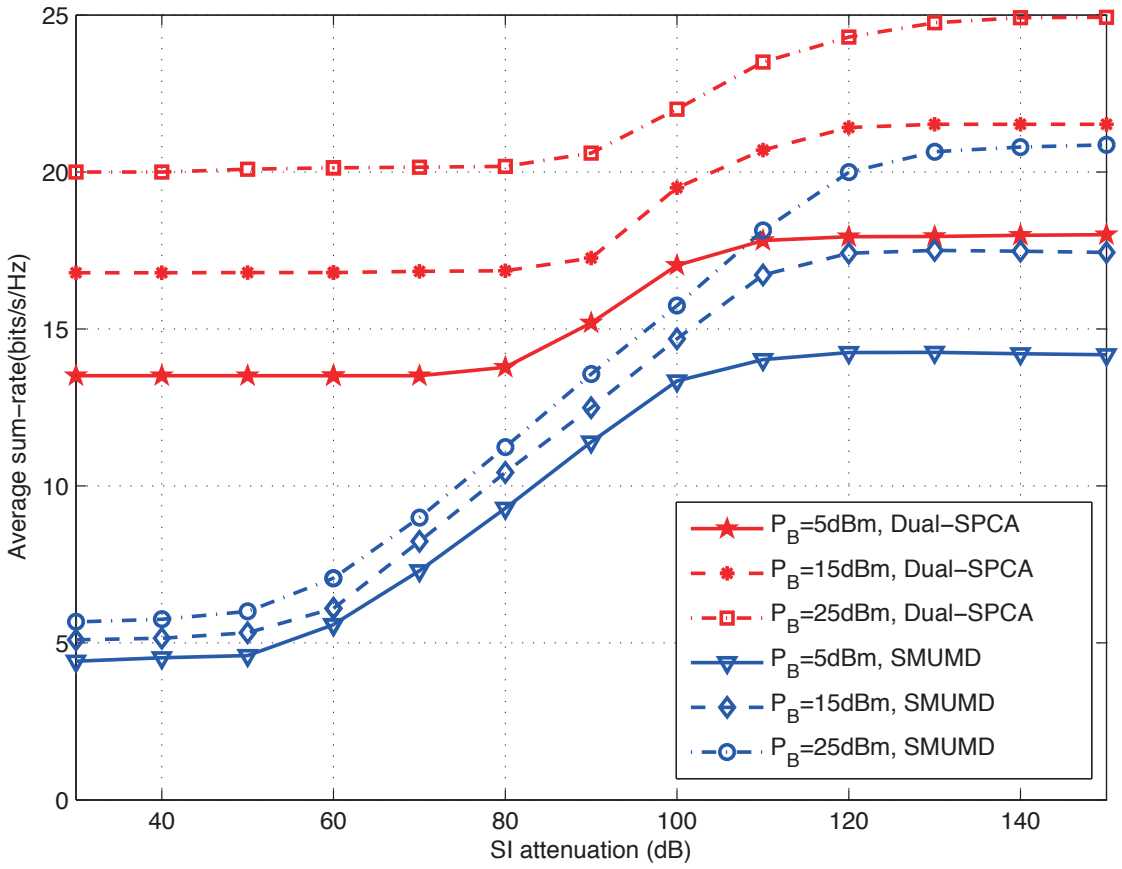

Figure 2.6: Average sum-rate of our proposed Dual-SPCA algorithm and SMUMD approach versus SI attenuation for different BS transmit powers under a small cell scenario.

flat when the number of UL/DL users reaches 40. It is because when the number of UL/DL users reaches a certain threshold (40 in this case), the pool of users become sufficiently large and the selection process becomes "random" enough. Increasing the number of users further will no longer increase the randomness and the sum-rate becomes almost constant.

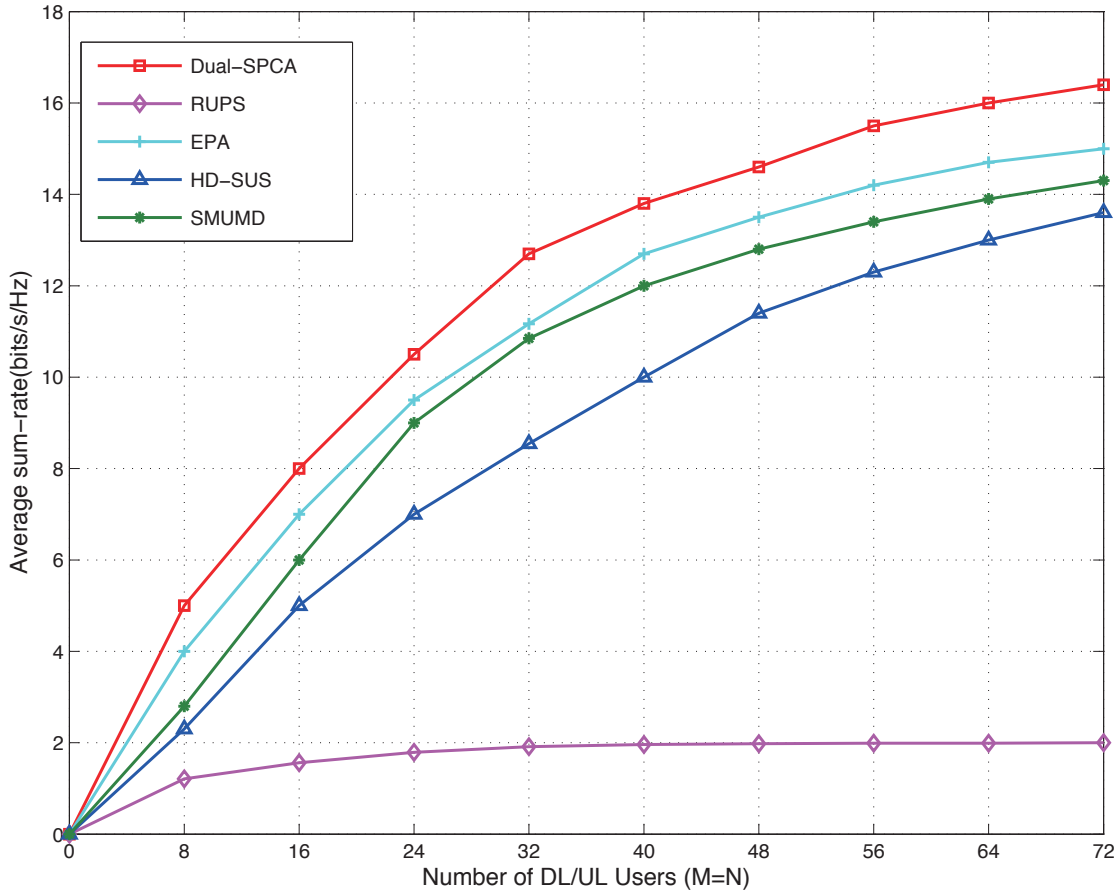

Figure 2.7: Average sum-rate versus number of UL/DL users ($M = N$) under a UMa cell scenario when the BS transmit power is 25 dBm and the number of subcarriers is 32. SI attenuation $\tau = 120$ dB.

2.4.2 Performance Comparison of the Proposed Dual-SPCA Algorithm and Location-Aware Algorithm

In this section, we further consider the case when the BS does not receive any IUI-CSI information from the users. Instead, the BS makes use of the location-aware sub-optimal algorithm to estimate the IUIs and to assign the subcarriers to users. Furthermore, the IUI for each user over each subcarrier should lie below the INRT threshold with a chance-constrained probability of $1 - \epsilon$. The value of $1 - \epsilon$ in fact

determines the confidence level of the system sum-rate. A larger value increases the confidence probability but at the same time reduces the system sum-rate. Thus, the effect of the value of ϵ needs to be investigated.

Since we focus on the effect of IUI in this section, we evaluate the system performance at a SI attenuation of 120 dB such that the effect of SI becomes negligible. We also use the "goodput", which is defined as bits/s/Hz successfully received [100, 101], as the performance metric when comparing the location-aware algorithm with limited CSI and the Dual-SPCA algorithm with full CSI. Figs. 2.8 and 2.9 plot the goodput of the two algorithms under an UMa cell scenario and a small cell scenario, respectively. From the results, we observe that the location-aware sub-optimal algorithm can achieve close performance as the Dual-SPCA near-optimal algorithm when the value of ϵ in the location-aware algorithm is around -20 dB$(= 0.01)$. In Tables 2.3 and 2.4, we further plot the performance loss when $\epsilon = -20$ dB. Results show that the performance losses under all scenarios range between 4.7% and 8.4%. Thus we conclude that our proposed location-aware algorithm, which does not require precise IUI-CSI but estimates IUI-CSI based on user locations, suffers from a small degradation in goodput compared with the Dual-SPCA near-optimal algorithm. Note that when the estimated IUI in a certain pair of UL and DL users for the location-aware algorithm is higher than the actual IUI, it is easy to derive that the goodput of the location-aware algorithm is lower than the goodput of Dual-SPCA algorithm. In addition, when the estimated IUI in a certain pair of UL and DL users for the location-aware algorithm is lower than the actual IUI, the goodput of the location-aware algorithm would be in outage such that the goodput of the location-aware algorithm is lower than the goodput of Dual-SPCA algorithm. That

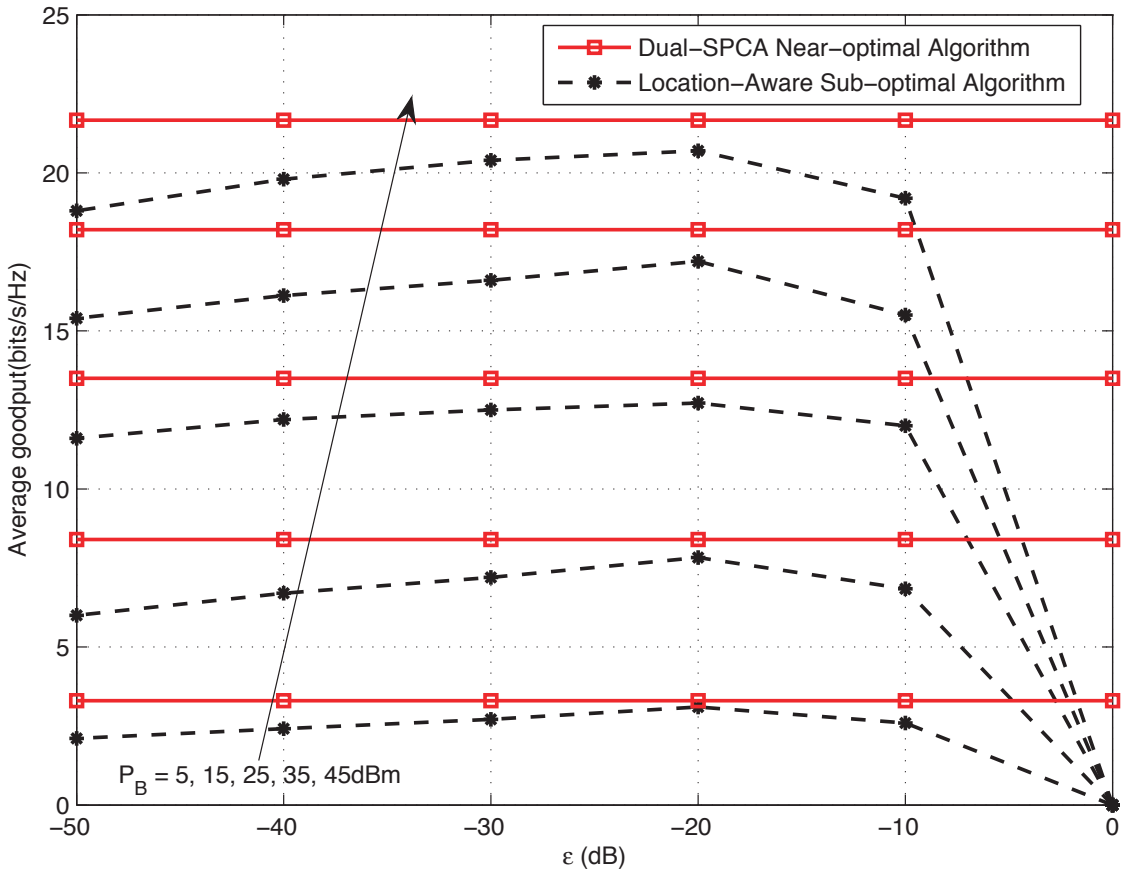

Figure 2.8: Goodput versus ϵ for Dual-SPCA near-optimal algorithm and location-aware sub-optimal algorithm under a UMa cell scenario.

is why the goodput of the location-aware algorithm is lower than that of Dual-SPCA algorithm.

2.4.3 Feedback Overhead and Computational Complexity Analysis

We now give a brief analysis of the overhead complexity of the proposed Dual-SPCA algorithm with full CSI and location-aware algorithm with limited CSI. We

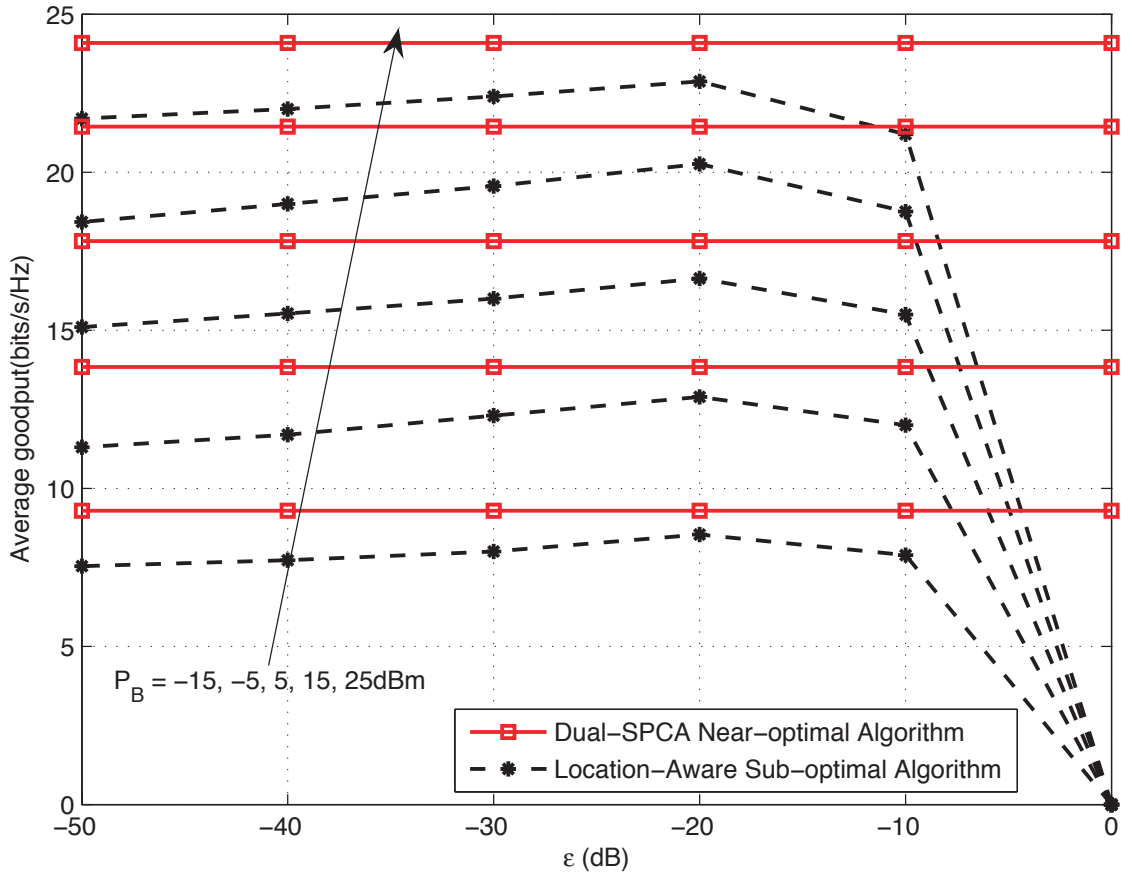

Figure 2.9: Goodput versus ϵ for Dual-SPCA near-optimal algorithm and location-aware sub-optimal algorithm under a small cell scenario.

first analyze the system feedback requirement. The Dual-SPCA algorithm with full CSI requires $\mathcal{O}(KMN + KN)$ measurements fed back from the DL users in order to obtain the global CSI while the location-aware algorithm with limited CSI only requires KN such measurements. Thus the sub-optimal algorithm requires much less feedback overhead than the near-optimal algorithm.

In Table 2.5, we further list the system feedback requirement of all algorithms, i.e., Dual-SPCA/location-aware/HD-SUS/EPA/RUPS/SMUND algorithms. The results indicate that (i) Dual-SPCA and EPA algorithms require the same and

Table 2.3: Goodput of Dual-SPCA algorithm and location-aware algorithm under an UMa cell scenario.

P_B (dBm)	Average goodput (bits/s/Hz)		Loss
	Dual-SPCA	Location-Aware	
5	3.44	3.15	8.4%
15	8.40	7.83	6.8%
25	13.53	12.72	6%
35	18.20	17.21	5.5%
45	21.66	20.65	4.7%

Table 2.4: Goodput of Dual-SPCA algorithm and location-aware algorithm under a small cell scenario.

P_B (dBm)	Average goodput (bits/s/Hz)		Loss
	Dual-SPCA	Location-Aware	
-15	9.29	8.54	8.1%
-5	13.84	12.89	6.9%
5	17.82	16.68	6.3%
15	21.44	20.26	5.5%
25	24.09	22.88	5.1%

largest amount of feedback measurements; (ii) location-aware, HD-SUS and SMUND algorithms require the same and moderate amount of feedback measurements; and (iii) RUPS algorithm requires the least feedback.

Next we analyze the computational complexity of all algorithms.

- In the Dual-SPCA algorithm with full CSI, the computational complexity for the outer iteration is $\mathcal{O}((M+1)T_o)$ where T_o is the number of outer iterations; and the computational complexity for the inner iteration is $\mathcal{O}(KMNT_i)$ where T_i is the number of inner iterations. Hence, the overall computational complexity of the Dual-SPCA algorithm with full CSI is $\mathcal{O}(KMNT_i((M+1))T_o) \approx$

Table 2.5: System Feedback Requirement of Different Algorithms

Algorithm	Feedback Requirement
Dual-SPCA	$\mathcal{O}(KMN + KN)$
Location-Aware	$\mathcal{O}(KN)$
HD-SUS	$\mathcal{O}(KN)$
EPA	$\mathcal{O}(KMN + KN)$
RUPS	$\mathcal{O}(K)$
SMUND	$\mathcal{O}(KN)$

$\mathcal{O}(KM^2N)$.

- In the location-aware algorithm with limited CSI, the computational complexity for updating INRT in the outer iteration is $\mathcal{O}(K(N+1)T_o')$ where T_o' is the number of outer iterations. The computational complexity for solving the sub-problem in the inner iteration is $\mathcal{O}(K(N+1)T_i' + (M+1)T_i' + 2(M+N)K)$ where $K(N+1)T_i'$ is the number of updated dual variables corresponding to the INRT constraint, $(M+1)T_i'$ is the number of updated dual variables corresponding to the power constraint, $2(M+N)K$ is the number of water-filling calculations and user scheduling, and T_i' is the number of inner iterations. Finally, the overall computational complexity of the sub-optimal algorithm is $\mathcal{O}((K(N+1)T_i' + (M+1)T_i' + 2K(M+N))K(N+1)T_o') \approx \mathcal{O}(2K^2(M+N))$.

- In the HD-SUS algorithm, the computational complexity is proportional to the number of water-filling calculations and user scheduling, i.e., $\mathcal{O}(K(M+N))$.

- In the EPA algorithm, the computational complexity is proportional to the number of user pairing without power allocations, i.e., $\mathcal{O}(KMN)$.

- In the RUPS algorithm, the computational complexity is proportional to the

Table 2.6: Computational Complexity of Different Algorithms

Algorithm	Computational Complexity
Dual-SPCA	$\mathcal{O}(KM^2N)$
Location-Aware	$\mathcal{O}(2K^2(M+N))$
HD-SUS	$\mathcal{O}(K(M+N))$
EPA	$\mathcal{O}(KMN)$
RUPS	$\mathcal{O}(K)$
SMUND	$\mathcal{O}(K(M+N))$

number of power allocation calculations in all subcarriers, i.e., $\mathcal{O}(K)$.

- In the SMUND algorithm, the computational complexity is proportional to the number of water-filling calculations and user scheduling, i.e., $\mathcal{O}(K(M+N))$

The complexities of the algorithms are further summarized in Table 2.6. We can observe that the location-aware algorithm with limited CSI has a lower computational complexity than the Dual-SPCA algorithm with full CSI when M and N are very large. Moreover, the Location-Aware algorithm and Dual SPCA algorithm, which can achieve higher sum-rates compared with HD-SUS/EPA/RUPS/SMUND algorithms, require higher computational complexities.

2.5 Summary

In this chapter, we have investigated a full-duplex multiuser OFDMA cellular system. We have optimized the system sum-rate with respect to subcarrier allocation, power allocation, and UL and DL user-pairing. By integrating the dual method and the SPCA method, we have solved the optimization problem in a two-layer iterative way. We have shown that when the self-interference attenuation is high (i.e.,

self-interference is low), using full duplex can substantially increase the system sum-rate. We have also found that user-pairing can substantially reduce the inter-user interference and hence improve the system sum-rate. In addition, by considering two different network deployments, i.e., urban macro cell scenario and small cell scenario, we show that the improvement of full-duplex transmission over half-duplex transmission also depends on the cell size and channel parameters. Furthermore, we have presented a location-aware algorithm which requires less channel state information and has a lower computational complexity than the dual-SPCA algorithm.

Appendix 2.A SPCA solution to maximize $L_{m,n,k}$

To solve the non-convex optimization problem, we apply the SPCA method in [87]. The basic principle of the SPCA method is to replace the non-convex function by its convex upper bound and to iteratively solve the resulting problem by judiciously updating the variables in the convex approximation until convergence. This convex upper bound should also have two properties [87].

Lemma 2.6. *Consider a non-convex function $g(\boldsymbol{x})$. If the function $G(\boldsymbol{x}, \boldsymbol{y})$ replaces $g(\boldsymbol{x})$ in the SPCA method, $G(\boldsymbol{x}, \boldsymbol{y})$ should have the following two properties:*

i) for any $\boldsymbol{x}$, $g(\boldsymbol{x}) \leq G(\boldsymbol{x}, \boldsymbol{y}) \quad \forall \boldsymbol{y} > 0$;

ii) for a given feasible point $\boldsymbol{x_0}$, there exists $\boldsymbol{y} = \psi(\boldsymbol{x_0})$ satisfying $g(\boldsymbol{x}) = G(\boldsymbol{x}, \boldsymbol{y})$ and $\nabla g(\boldsymbol{x}) = \nabla G(\boldsymbol{x}, \boldsymbol{y})$.

Proof. Refer to [87]. □

Additionally, it has been proven that the convergence of the SPCA method

always exists and the convergent point satisfies the KKT conditions theoretically [87].

Now, we describe the solution process to maximize $L_{m,n,k}$. For simplicity, $p_{m,B,k}^{(n)}$ and $p_{B,n,k}^{(m)}$ are replaced by p_1 and p_2, respectively. Similarly $\alpha_{m,B,k}$, $\alpha_{m,n,k}$, $\alpha_{B,n,k}$ and $\alpha_{B,B,k}$ are replaced by α_1, α_1', α_2 and α_2', respectively. $\lambda_{U,m}$ and λ_B are replaced by λ_1 and λ_2, respectively. We use the first-order inequality $\log(1+x) \leq \log(1+y)+(x-y)/(1+y)$ for $x \geq 0$ where y is an arbitrary operating point. Then, $L_{m,n,k}$ in (2.18) is lower bounded by

$$\begin{aligned} L(p_1,p_2) \geq & \log(1+\alpha_1 p_1+\alpha_2' p_2)+\log(1+\alpha_1' p_1+\alpha_2 p_2) \\ & -\log(1+\alpha_2' y_2)-\frac{\alpha_2'(p_2-y_2)}{1+\alpha_2' y_2} \\ & -\log(1+\alpha_1' y_1)-\frac{\alpha_1'(p_1-y_1)}{1+\alpha_1' y_1} \\ & -\lambda_2 p_2-\lambda_1 p_1 = L_{LB}. \end{aligned} \tag{2.48}$$

It is not hard to verify that this inequality satisfies the two properties defined in Lemma 2.6. Also the right hand side of this inequality is a convex function [89]. According to the SPCA method, in each iteration, $y_1^{(l+1)}$ and $y_2^{(l+1)}$ is updated by $p_1^{(l)}$ and $p_2^{(l)}$, respectively, where l represents the l-th iteration. One can use the interior-point method (or other convex optimization method) to obtain the optimal values $p_1^{(l)}$ and $p_2^{(l)}$ that maximize $L_{LB}^{(l)}$ in each iteration. However, we can give a closed-form solution of the lower-bounded optimization problem alternatively. For simplicity, we omit the superscript in the following derivation.

The partial derivative of L_{LB} over p_1 and p_2 are given by, respectively,

$$\frac{\partial L_{LB}}{\partial p_1} = \alpha_1 Q + \alpha_1' T - \frac{\alpha_1'}{1+\alpha_1' y_1} - \lambda_1 \tag{2.49}$$

$$\frac{\partial L_{LB}}{\partial p_2} = \alpha_2' Q + \alpha_2 T - \frac{\alpha_2'}{1+\alpha_2' y_2} - \lambda_2 \tag{2.50}$$

where $Q = 1/((1+\alpha_1 p_1 + \alpha_2' p_2)\log_e 2)$ and $T = 1/((1+\alpha_1' p_1 + \alpha_2 p_2)\log_e 2)$.

Defining $\tilde{\lambda}_1 = (\frac{\alpha_1'}{1+\alpha_1' y_1} + \lambda_1)\log_e 2$ and $\tilde{\lambda}_2 = (\frac{\alpha_2'}{1+\alpha_2' y_2} + \lambda_2)\log_e 2$, we divide the original problem that maximizes L_{LB} with respect to p_1 and p_2 into four cases.

Case A : When $\tilde{\lambda}_1 \geq \alpha_1 + \alpha_1'$ and $\tilde{\lambda}_2 \geq \alpha_2 + \alpha_2'$, L_{LB} is a decreasing function of both p_1 and p_2. Thus, we have $p_1 = p_2 = 0$.

Case B : When $\tilde{\lambda}_1 \geq \alpha_1 + \alpha_1'$ and $\tilde{\lambda}_2 < \alpha_2 + \alpha_2'$, L_{LB} (i) is a decreasing function of p_1, and (ii) increases then decreases as p_2 increases. Thus, we obtain (i) $p_1 = 0$ and (ii) a unique solution for p_2 by letting $\partial L_{LB}/\partial p_2 = 0$, i.e.,

$$p_2 = \frac{1}{2\tilde{\lambda}_2 \alpha_2 \alpha_2'}\left(-\tilde{\lambda}_2(\alpha_2+\alpha_2') + 2\alpha_2\alpha_2' + \sqrt{(\tilde{\lambda}_2(\alpha_2+\alpha_2') + 2\alpha_2\alpha_2')^2 + 4\tilde{\lambda}_2^2\alpha_2\alpha_2'}\right). \tag{2.51}$$

Case C : When $\tilde{\lambda}_1 < \alpha_1 + \alpha_1'$ and $\tilde{\lambda}_2 \geq \alpha_2 + \alpha_2'$, L_{LB} is a decreasing function of p_2. Using a similar analysis as in Case B, we obtain (i) $p_2 = 0$ and (ii) p_1 as

$$p_1 = \frac{1}{2\tilde{\lambda}_1 \alpha_1 \alpha_1'}\left(-\tilde{\lambda}_1(\alpha_1+\alpha_1') + 2\alpha_1\alpha_1' + \sqrt{(\tilde{\lambda}_1(\alpha_1+\alpha_1') + 2\alpha_1\alpha_1')^2 + 4\tilde{\lambda}_1^2\alpha_1\alpha_1'}\right). \tag{2.52}$$

Case D : When $\tilde{\lambda}_1 < \alpha_1 + \alpha_1'$ and $\tilde{\lambda}_2 < \alpha_2 + \alpha_2'$, L_{LB} increases then decreases

as both p_1 and p_2 increase. However, deriving the closed-form solution in this case is not straightforward. Hence, we give an iterative solution in this case. By letting $\partial L_{LB}/\partial p_1 = \partial L_{LB}/\partial p_2 = 0$, we obtain

$$p_1 = [\frac{1}{\tilde{\lambda}_1 - \alpha_1' T} - \frac{\alpha_2' p_2^{\text{pre}}}{\alpha_1}]^+ \tag{2.53}$$

$$p_2 = [\frac{1}{\tilde{\lambda}_2 - \alpha_2' Q} - \frac{\alpha_1' p_1^{\text{pre}}}{\alpha_2}]^+ \tag{2.54}$$

where p_1^{pre} and p_2^{pre} are the values obtained in the previous iteration. In practice, we do not have to wait for full convergence and a single ascent step is sufficient before updating.

To sum up, the entire algorithm is listed in Algorithm 1.

Appendix 2.B Proof of Lemma 2.3

According to the constraint (2.22), only one UL user and one DL user can be scheduled over subcarrier k. Assuming that the scheduled UL user is U_{m_k} and the scheduled UL user is D_{n_k}, we have $s_{m_k,B,k} = s_{n_k,B,k} = 1$ and $s_{m',B,k} = s_{n',B,k} = 0$ for $m' \neq m_k, n' \neq n_k$. In this case, the constraint (2.27) can be simplified to

$$\Pr\{\alpha_{m_k,n,k} p_{m_k,B,k} \leq \Gamma_{n,k}\} \geq 1 - \epsilon, \text{for } n = n_k \text{ and } \forall k \tag{2.55}$$

$$\Pr\{0 \leq \Gamma_{n',k}\} \geq 1 - \epsilon, \text{for } n \neq n_k \text{ and } \forall k. \tag{2.56}$$

It is obvious that the inequality (2.56) is always satisfied. Since the long-term fading between U_m and D_n is given by $\text{pl}(d_{m,n})$ and the short-term fading from U_m

Algorithm 1 Solution of $L_{m,n,k}$

Set $I_{\max}$ (maximum number of iterations)
    $\epsilon_i > 0$ (convergence tolerance)
Set arbitrary positive values for $\boldsymbol{y}^{(1)}$.
$l \leftarrow 1$.
while $||\boldsymbol{y}^{(l)} - \boldsymbol{y}^{(l-1)}|| > \epsilon_i$ and $l < I_{\max}$ **do**
  if $\tilde{\lambda}_1 \geq \alpha_1 + \alpha_1'$ and $\tilde{\lambda}_2 \geq \alpha_2 + \alpha_2'$ **then**
    $p_1^{(l)} = p_2^{(l)} = 0$.
  else if $\tilde{\lambda}_1 \geq \alpha_1 + \alpha_1'$ and $\tilde{\lambda}_2 < \alpha_2 + \alpha_2'$ **then**
    $p_1^{(l)} = 0$ and $p_2^{(l)}$ is given in (2.51).
  else if $\tilde{\lambda}_1 < \alpha_1 + \alpha_1'$ and $\tilde{\lambda}_2 \geq \alpha_2 + \alpha_2'$ **then**
    $p_2^{(l)} = 0$ and $p_1^{(l)}$ is given in (2.52).
  else
    use (2.53) and (2.54) to obtain $p_1^{(l)}$ and $p_2^{(l)}$, respectively.
  end if
  $\boldsymbol{y}^{(l+1)} \leftarrow (p_1^{(l)}, p_2^{(l)})$.
  $l \leftarrow l + 1$.
end while
The optimal solution of maximizing $L_{m,n,k}$ is $(p_1^*, p_2^*) = \boldsymbol{y}^{(l)}$. The optimal value of $L_{m,n,k}$ is obtained as $L_{LB}^{(l-1)}$.
return

to D_n is assumed to be the standard Rayleigh fading, the inequality (2.55) can be expressed as

$$\int_0^{\Gamma_{n,k}} \frac{1}{\zeta} \mathrm{e}^{-x/\zeta} dx \geq 1 - \varepsilon \quad \text{for } n = n_k \text{ and } \forall k \tag{2.57}$$

where $\zeta = 1/\mathrm{pl}(d_{m_k,n})\sigma_{D_n}^2$. Then, (2.57) can be further simplified to

$$\tilde{\alpha}_{m_k,n,k} p_{m_k,B,k} \leq \Gamma_{n,k} \quad \text{for } n = n_k \text{ and } \forall k \tag{2.58}$$

where $\tilde{\alpha}_{m_k,n,k} = \log(\frac{1}{\varepsilon})/\mathrm{pl}(d_{m_k,n})\sigma_{D_n}^2$. Combining (2.55), (2.56) and (2.58), we readily have Lemma 3.

Appendix 2.C Proof of Lemma 2.4

By applying KKT conditions of the sub-problem (2.37), the partial derivative of $L_{n,k}$ over $p_{B,n,k}$ is given by

$$\frac{\partial L_{n,k}}{\partial p_{B,n,k}} = \frac{\alpha_{B,n,k}}{\mathrm{In2}(\Gamma_{n,k} + 1 + \alpha_{B,n,k} p_{B,n,k})} - \lambda_B - \mu_{B,k}\alpha_{B,B,k}. \tag{2.59}$$

Equating (2.59) to zero and applying the positive power constraint, we obtain the optimal power for the n-th DL user over subcarrier k as

$$p^*_{B,n,k} = \left[\frac{1}{(\lambda_B + \mu_{B,k}\alpha_{B,B,k})\log_e 2} - \frac{\Gamma_{n,k}+1}{\alpha_{B,n,k}}\right]^+. \tag{2.60}$$

The corresponding optimal value of the Lagrangian function $L_{n,k}$ for the n-th DL user over subcarrier k is set as $L^o_{n,k}$. Then, we select the optimal DL user over subcarrier k as $n_k = \arg\max_{\forall n} L^o_{n,k}$ and set $s_{n_k,k} = 1$. Moreover, we set $s_{n',k} = 0$ for $n' \neq n_k$ and the power $p^*_{B,n',k}$ to zero accordingly. Hence, (2.38) and (2.39) are proved.

Similarly, by applying KKT conditions of the sub-problem (2.36), the partial derivative of $L_{m,k}$ over $p_{m,B,k}$ is given by

$$\frac{\partial L_{m,k}}{\partial p_{m,B,k}} = \frac{\alpha_{m,B,k}}{(\Gamma_{B,k} + 1 + \alpha_{m,B,k} p_{m,B,k})\log_e 2} - \lambda_{U,m} - \sum_{n=1}^{N} \nu_{n,k} s_{B,n,k} \tilde{\alpha}_{m,n,k}. \tag{2.61}$$

Since $s_{B,n_k,k} = 1$ and $s_{B,n',k} = 0$ for $n' \neq n_k$, (2.61) can be simplified to

$$\frac{\partial L_{m,k}}{\partial p_{m,B,k}} = \frac{\alpha_{m,B,k}}{(\Gamma_{B,k} + 1 + \alpha_{m,B,k} p_{m,B,k})\log_e 2} - \lambda_{U,m} - \nu_{n_k,k}\tilde{\alpha}_{m,n_k,k}. \tag{2.62}$$

Equating (2.62) to zero and applying the positive power constraint, we obtain the optimal power for the m-th UL user over subcarrier k as

$$p^*_{m,B,k} = \left[\frac{1}{(\lambda_{U,m} + \nu_{n_k,k}\tilde{\alpha}_{m,n_k,k})\log_e 2} - \frac{\Gamma_{B,k}+1}{\alpha_{m,B,k}}\right]^+. \tag{2.63}$$

The corresponding optimal value of the Lagrangian function $L_{m,k}$ for the m-th UL user over subcarrier k is set as $L^o_{m,k}$. We select the optimal UL user over subcarrier k as $m_k = \arg\max_{\forall m} L^o_{m,k}$ and set $s_{m_k,k} = 1$. Moreover, we set $s_{m',k} = 0$ for $m' \neq m_k$ and the power $p^*_{m',B,k}$ to zero accordingly.

Finally, we have completely proved Lemma 2.4.

Appendix 2.D Proof of Lemma 2.5

We compute the subgradient for $\mathbf{\Gamma}$ from the Lagrangian dual function of the problem $\mathbf{P3}(\mathbf{\Gamma})$ which is given by (2.29). The partial derivatives of $g(\boldsymbol{\lambda}, \boldsymbol{\mu}, \boldsymbol{\nu}, \mathbf{\Gamma})$ in (2.29) (considering $\mathbf{\Gamma}$ as a variable in (2.29)) with respect to $\Gamma_{B,k}$ and $\Gamma_{n,k}$ are given by

$$\frac{\partial g}{\partial \Gamma_{B,k}} = \max_{\boldsymbol{p},\boldsymbol{s}} \left(\mu_{B,k} - \sum_{m=1}^{M} \frac{\alpha_{m,B,k} p_{m,B,k}}{(1+\Gamma_{B,k}+\alpha_{m,B,k}p_{m,B,k})(1+\Gamma_{B,k})\log_e 2}\right) \tag{2.64}$$

$$\frac{\partial g}{\partial \Gamma_{n,k}} = \max_{\boldsymbol{p},\boldsymbol{s}} \left(\nu_{n,k} s_{B,n,k} - \frac{\alpha_{B,n,k} p_{B,n,k}}{(1+\Gamma_{n,k}+\alpha_{B,n,k}p_{B,n,k})(1+\Gamma_{n,k})\log_e 2}\right) \tag{2.65}$$

Combining (2.41) and (2.64), we can prove (2.44). Similarly, Combining (2.39) and (2.65), (2.45) is readily obtained.

Chapter 3

Resource Allocation for Multi-User OFDMA Hybrid Full-/Half-Duplex Relaying Systems With Direct Links

In this chapter, we aim to investigate the joint optimization problem of transmission mode selection (including direct transmission (DT) mode, HD relay cooperative transmission (HDRCT) mode and FD relay transmission (FDRT) mode), subcarrier assignment, relay selection, subcarrier-pairing as well as power allocation in the DL of a cooperative OFDMA system.

This joint optimization problem is sophisticated because all these factors are highly coupled with one another, leading to a mixed integer non-linear programming problem. In this chapter, we first show that the binary assignment problem of trans-

mission mode selection, subcarrier assignment, relay selection and subcarrier-pairing with fixed power allocation can be transformed into a maximum weighted bipartite matching problem which is solved by the classical Hungarian method. Then, based on the dual method, we divide the joint power allocation and binary assignment problem into multiple sub-problems. In each sub-problem, the power allocation schemes in FDRT mode, HDRCT mode and DT mode are all provided. Specifically, we design a hierarchical dual method to solve the power allocation problem in FDRT mode. In addition, unlike most previous works [37–41], we consider the joint transmission of both source and relay in HDRCT mode so as to fully utilize the transmit power of the source. (Details of this HDRCT mode will be presented in the following.)

The rest of this chapter is organized as follows. Section 3.1 describes the system model and problem formulation. Section 3.2 presents the optimal solution for the binary assignment problem with fixed power allocation, and Section 3.3 shows the solution of the joint power allocation and binary assignment problem. Section 3.4 presents the numerical results and finally Section 3.5 provides a summary.

3.1 System Model and Problem Formulation

3.1.1 System Description

We consider the single-cell multi-user DL OFDMA system shown in Fig. 3.1. The system consists of a BS, multiple decode-and-forward relays[1] and multiple users.

[1]In this chapter, the decode-and-forward relaying protocol is adopted because the relay has to decode the signals in order to perform self-interference digital cancellation. Recently, a fast and constructive full duplex relay using an amplify-and-forward technique has been proposed [47].

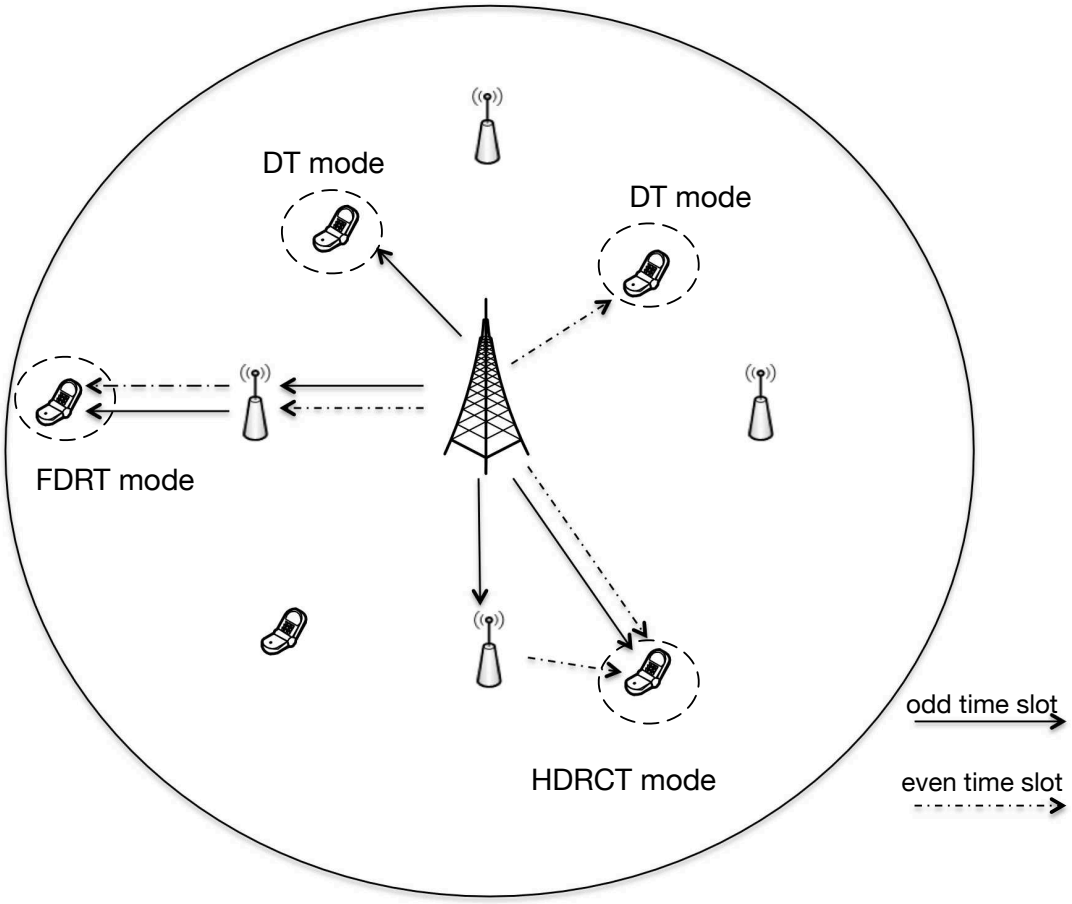

Figure 3.1: System Model. Illustration of three different transmission modes.

Each node (BS, relay or user) is equipped with a single antenna. In particular, each relay uses the same single antenna for simultaneous transmission and signal reception in FDRT mode. All links are assumed to be frequency selective and each is assigned with a subcarrier undergoing flat fading. For each symbol in each link, the transmission is in either FDRT mode, HDRCT mode, or DT mode. We also assume that each user decodes each subcarrier signal independently from other subcarrier signals. We further define the following symbols.

Since the relay has the ability to perform digital computations, we do not treat it as a traditional amplify-and-forward relay.

- B: BS (base station)
- R_m: m-th relay
- U_n: n-th user
- K: numbers of subcarriers
- M: numbers of relays
- N: numbers of users
- $\mathcal{K} = \{1, \ldots, K\}$
- $\mathcal{M} = \{1, \ldots, M\}$
- $\mathcal{N} = \{1, \ldots, N\}$
- σ_0^2: noise power at the relays and users over each subcarrier
- $k \in \mathcal{K}$: subcarrier index
- $h_{b,m,k}$: complex channel coefficient of the link between B and R_m over subcarrier k
- $h_{b,n,k}$: complex channel coefficient of the link between B and U_n over subcarrier k
- $h_{m,n,k}$: complex channel coefficient of the link between R_m and U_n over subcarrier k
- $p_{b,n,k}$: BS transmit power for U_n over subcarrier k
- $p_{m,n,k}$: R_m transmit power for U_n over subcarrier k

- σ_e^2: self-interference (SI) power at the relay and is modeled as an additive white Gaussian noise (AWGN) [2]

- $\alpha_{b,m,k} = |h_{b,m,k}|^2/(\sigma_0^2 + \sigma_e^2)$: effective channel gain between B and R_m over subcarrier k (we assume all subcarriers at the relays would suffer from an extra noise due to SI cancellation operations)

- $\alpha_{b,n,k} = |h_{b,n,k}|^2/\sigma_0^2$: effective channel gain between B and U_n over subcarrier k

- $\alpha_{m,n,k} = |h_{m,n,k}|^2/\sigma_0^2$: effective channel gain between R_m and U_n over subcarrier k

Note that we assume that the additive white noises at all nodes are independent circular symmetric complex Gaussian random variables, each having zero mean and σ_0^2 variance. Moreover, all subcarrier signals received by the relays suffer from an extra noise due to relays performing SI cancellation operations.

The DL transmission from the BS to the users is on a time-frame basis with each frame consisting of multiple OFDM symbols. Each frame is further divided into $2L$ equal time slots, where $2L$ represents the number of coherent time slots[3]. We consider three different transmission modes which are FDRT mode, HDRCT mode

[2]The authors in [15, 16, 102] have considered the issue of residual self-interference (SI) due to the imperfect FD realization. In their model, the SI is proportional to the transmit power. However, the latest FD techniques used by the Stanford team [13, 103] have offered some astonishing results. Their FD systems are able to keep the SNR loss uncorrelated with the transmit power and to maintain the residual self-interference of the same order as noise power. The results can greatly simplify the modeling of a FD transmission because the residual SI can be treated as a constant. Here we assume that each FD relay uses a single antenna for simultaneous transmission and signal reception. Our work can be readily extended to the case when the FD relays use multiple antennas for simultaneous transmission and signal reception.

[3]In practice, the coherence time for each frame depends on the mobility of the users. For example, the coherence time is roughly 200 ms with a central carrier frequency of 2.5 GHz and a user mobility of 2 km/h [104, 105].

and DT mode. We use i to be the transmission mode index, i.e., $i = 1$ represents FDRT mode, $i = 2$ represents HDRCT mode, and $i = 3$ represents DT mode. The subcarriers allocated in odd and even time slots are represented as k_1 and k_2, respectively. We denote the transmit power levels in the BS transmission and in the relay R_m transmission for the user U_n over subcarrier k_1 in the odd time slot by p_{b,n,k_1} and p_{m,n,k_1}, respectively $(\forall m, n, k_1)$. Similarly, we denote those over subcarrier k_2 in even time slot by p_{b,n,k_2} and p_{m,n,k_2}, respectively $(\forall m, n, k_2)$. Without loss of generality, the end-to-end transmission rate in any transmission mode is expressed in nats/s/Hz. In the following, we describe the three different transmission modes.

3.1.1.1 FD relay transmission (FDRT) mode

In both odd and even time slots, the BS transmits DL signals containing independent messages to the relays while the relays decode and re-transmit the signals, received from the BS in the previous time slot, to different users. For the same user, the BS and the relay transmit their signals over the same subcarrier in both odd and even time slots, i.e., $k_1 = k_2 = k$.

In this chapter, we treat the signals from the BS as the interference to the links between the relays and users[4]. Hence, the transmission rate for U_n through

[4]If the signal from the relay is considered to be interference, FDRT becomes meaningless. Note that there are advanced encoding strategies, namely block Markov encoding, which enable the direct link to help rather than to interfere with the relay link [45, 106]. Yet the block Markov encoding needs some advanced decoding algorithms, such as joint decoding [45], successive decoding, sliding-window decoding and backward decoding [107]. However, joint decoding has a much higher computation complexity and decoding delay, and successive decoding/sliding-window decoding/backward decoding could increase the probability of error propagation in practical systems. Thus, we do not consider block Markov encoding strategies in this work.

R_m within one frame in FDRT mode is expressed as,

$$R_{n,m}^{k_1,k_2,1} = \frac{1}{2}\min\left\{\log(1+p_{b,n,k_2}\alpha_{b,m,k_2}), \log(1+\frac{p_{m,n,k_1}\alpha_{m,n,k_1}}{p_{b,n,k_1}\alpha_{b,n,k_1}+1})\right\} + \frac{1}{2}\min\left\{\log(1+p_{b,n,k_1}\alpha_{b,m,k_1}), \log(1+\frac{p_{m,n,k_2}\alpha_{m,n,k_2}}{p_{b,n,k_2}\alpha_{b,n,k_2}+1})\right\} \quad (3.1)$$

where $k_1 = k_2$.

Note that we do not consider subcarrier-pairing in FDRT mode. In other words, we do not consider the case where $k_1 \neq k_2$. Hence, the transmission rate for U_n through R_m within one frame in FDRT mode is given by

$$R_{n,m}^{k_1,k_2,1} = 0, \quad \text{if } k_1 \neq k_2. \quad (3.2)$$

3.1.1.2 HD relay cooperative transmission (HDRCT) mode

In an odd time slot, the BS transmits the DL signals containing independent messages for different users, while all the users and the HD relays keep silent. In an even time slot, the HD relays forward the signals received in the odd time slot to the users operating in the HDRCT mode. At the same time, the BS transmits the same information as the relay to the target user. The users then combine the signals (i) received from the BS in the odd time slot and (ii) received from the BS and the relay in the even time slot using maximal-ratio-combining (MRC) technique. The subcarrier used in the link between BS and relay can be different from the subcarrier used in the link between the relay and the user. The pairing of the subcarriers is the so-called *subcarrier-pairing*. More explicitly, subcarrier pairing means that the signals received by the relay on subcarrier k_1 will be forwarded on subcarrier k_2 to the destinated user, where k_1 and k_2 are not necessarily the same and they form a

subcarrier pair denoted as (k_1, k_2). When the decode-and forward relaying strategy is used, the transmission rate for U_n through R_m within one frame is given by

$$R_{n,m}^{k_1,k_2,2} = \frac{1}{2}\min\{\log(1+p_{b,n,k_1}\alpha_{b,m,k_1}), \log(1+p_{b,n,k_1}\alpha_{b,n,k_1}+(\sqrt{p_{b,n,k_2}\alpha_{b,n,k_2}}+\sqrt{p_{m,n,k_2}\alpha_{m,n,k_2}})^2)\} \tag{3.3}$$

3.1.1.3 Direct Transmission (DT) Mode

In both odd and even time slots, the BS transmits DL signals containing independent messages for different users while no relay transmits signals. The BS can use two different subcarriers in the odd and even time slots, i.e., subcarrier k_1 is for the transmission in the odd time slots and k_2 is for the transmission in the even time slots. Then, the achievable rates of user U_n over subcarrier k_1 and k_2 for DT mode within one frame are given by, respectively,

$$R_n^{k_1} = \frac{1}{2}\log(1+p_{b,n,k_1}\alpha_{b,n,k_1}) \tag{3.4}$$

$$R_n^{k_2} = \frac{1}{2}\log(1+p_{b,n,k_2}\alpha_{b,n,k_2}). \tag{3.5}$$

Remark 1: In HDRCT mode, the subcarrier in the first hop can be different from the subcarrier in the second hop. In addition, in DT mode, the subcarriers in the first hop and second hop are not necessarily the same. However, in FDRT mode, we restrict that the subcarriers assigned in the first hop and second hop are the same, i.e., $k_1 = k_2 = k$. The reason is that if subcarriers in the first hop and the second hop are not assigned to the same relay, inter-relay interference will appear.

For example, we suppose the subcarrier k is assigned in the first hop to the relay R_1 and also assigned in the second hop to the relay R_2. While R_1 is receiving signals from the BS, it will be interfered by R_2 over subcarrier k.

Remark 2: In summary, each given relay decodes signals from subcarriers selected for FDRT or HDRCT mode during the odd time slots, and re-transmit them in the even time slots. Similarly, the relay decodes signals from subcarriers ONLY selected for FDRT during the even time slots and re-transmit them in the odd time slots. Thus, once the subcarriers selected for FD or HD relay transmission are known, the relay can perform the decode-and retransmission accordingly. Hence, our system model can be implemented in practice.

3.1.2 Subcarrier and Power Constraints

3.1.2.1 Subcarrier Constraints

We now introduce four sets of binary assignment variables for subcarriers as follows.

- $\rho_n^{k_1,1}$ indicates whether subcarrier k_1 in the odd (first) time slot is assigned to user U_n in DT mode.
- $\rho_n^{k_2,2}$ indicates whether subcarrier k_2 in the even (second) time slot is assigned to user U_n in DT mode.
- $\rho_{n,m}^{k_1,k_2,1}$ indicates whether subcarrier pair (k_1, k_2) is assigned to relay R_m to assist user U_n in FDRT mode, where $\rho_{n,m}^{k_1,k_2,1} = 0$ for $k_1 \neq k_2$.
- $\rho_{n,m}^{k_1,k_2,2}$ indicates whether subcarrier pair (k_1, k_2) is assigned to relay R_m to assist user U_n in HDRCT mode.

In this chapter, we assume that each subcarrier in each time slot can be assigned to one and only one transmission mode in order to avoid interference. Therefore, these binary variables must satisfy the following constraints:

$$\sum_{n=1}^{N} \rho_n^{k_1,1} + \sum_{i=1}^{2} \sum_{n=1}^{N} \sum_{m=1}^{M} \sum_{k_2=1}^{K} \rho_{n,m}^{k_1,k_2,i} = 1, \forall k_1 \in \mathcal{K} \tag{3.6}$$

$$\sum_{n=1}^{N} \rho_n^{k_2,2} + \sum_{i=1}^{2} \sum_{n=1}^{N} \sum_{m=1}^{M} \sum_{k_1=1}^{K} \rho_{n,m}^{k_1,k_2,i} = 1, \forall k_2 \in \mathcal{K} \tag{3.7}$$

$$\rho_{n,m}^{k_1,k_2,1} = 0, \quad \forall k_1, k_2 \in \mathcal{K}, k_1 \neq k_2 \tag{3.8}$$

Note that each user can use FDRT, HDRCT or DT over different sets of subcarriers. Moreover, each user can be assisted by multiple relays over multiple subcarriers.

3.1.2.2 Individual Peak Power Constraints

Total peak power constraints have been widely assumed in the literatures [36, 43, 108]. Based on the total peak power constraints, power allocation schemes can be greatly simplified by deriving the equivalent channel gains [36, 43, 108]. However, power constraints are usually affected by the individual electronic power amplifier in a practical system. In other words, individual peak power constraints become more meaningful than total peak power constraints. Hence, in this chapter, we consider individual peak power constraints of the BS and the relays in each time

slot[5]. Consequently, individual power constraints are given as follows.

$$\sum_{n=1}^{N}\sum_{k_1=1}^{K} p_{b,n,k_1} \leq P_b, \quad \sum_{n=1}^{N}\sum_{k_2=1}^{K} p_{b,n,k_2} \leq P_b \tag{3.9}$$

$$\sum_{n=1}^{N}\sum_{k_1=1}^{K} p_{m,n,k_1} \leq P_m, \quad \sum_{n=1}^{N}\sum_{k_2=1}^{K} p_{m,n,k_2} \leq P_m, \forall m \in \mathcal{M} \tag{3.10}$$

where P_b and P_m denote the peak power constraints for BS and the m-th relay, respectively.

3.1.3 Problem Formulation

To avoid allocating all the resources to users closest to the BS or relays and leading to an unfair resource allocation, users who have been assigned more resource over previous time frames will be given a lower priority in the next time frame. Specifically, we denote $\tilde{r}_n$ as the long-term average rate for the n-th user, i.e., average number of transmitted bits over previous time frames. Then, a weight of $\omega_n = 1/\tilde{r}_n$ will be given to the rate r_n of the n-th user in the next time frame. Our objective is therefore to maximize the *weighted* sum-rate by optimally selecting transmission mode, allocating subcarriers, pairing subcarriers, selecting the best relays and allocating powers. Mathematically, this can be formulated as (**P1**):

$$\mathbf{P1}: \max_{\boldsymbol{\rho},\boldsymbol{p}} \quad R_{tot} = \sum_{n=1}^{N} \omega_n r_n \tag{3.11}$$

$$s.t. \quad (3.6), (3.7), (3.8), (3.9) \text{ and } (3.10)$$

[5]Strictly speaking, energy constraints are considered in [37] though they have been named as individual peak power constraints.

where

$$r_n = \sum_{k_1=1}^{K} \rho_n^{k_1,1} R_n^{k_1} + \sum_{k_2=1}^{K} \rho_n^{k_2,2} R_n^{k_2} + \sum_{i=1}^{2} \sum_{m=1}^{M} \sum_{k_1=1}^{K} \sum_{k_2=1}^{K} \rho_{n,m}^{k_1,k_2,i} R_{n,m}^{k_1,k_2,i}$$

$$\boldsymbol{\rho} = \{\rho_n^{k_1,1}, \rho_n^{k_2,2}, \rho_{n,m}^{k_1,k_2,1}, \rho_{n,m}^{k_1,k_2,2}\}$$

$$\boldsymbol{p} = \{p_{b,n,k_1}, p_{b,n,k_2}, p_{m,n,k_1}, p_{m,n,k_2}\}, \forall k_1, k_2, m, n.$$

Note that (3.6), (3.7) and (3.8) indicate the mode selection, relay selection, user selection and subcarrier-pairing constraints; while (3.9) and (3.10) indicate the individual power constraints of the BS and the relays.

We assume that the BS collects all the channel state information and performs the scheduling. In particular, the relay transmits the channel state information of the relay-to-user link to the BS, and the BS informs all the relays the scheduling results[6]. Hence, our approach is a centralized one.

3.2 Optimal Binary Assignment

In this section, we fix the power allocation, and propose a solution for joint optimal subcarrier assignment, relay selection, subcarrier pairing and transmission mode

[6]We assume that the time taken to (i) collect all channel state information by the BS, and (ii) compute and disseminate the scheduling results to the relays, is very short compared to a time frame. Moreover, one time frame is limited to the coherence time.

selection[7]. For a given power allocation, **P1** can be transformed into (**P2**):

$$\mathbf{P2}: \max_{\boldsymbol{\rho}} \quad R_{tot} \tag{3.12}$$
$$s.t. \quad (3.6) \text{ to } (3.8)$$

where R_{tot} is given in (3.11). Problem **P2** is a combinatorial optimization problem and the optimal solution can be obtained by exhaustive search. However, the complexity is exponential and thus prohibitive when K, M, and N are large. Here, we propose a graph-based approach to solve the problem optimally in polynomial time. While we can easily prove that the problem **P2** is a minimum cost network flow problem by using a method similar to that in [37], we alternatively transform problem **P2** into a maximum weighted bipartite matching problem. It is because the maximum weighted bipartite matching solution requires a lower computational complexity than the minimum cost network flow one.

Referring to the first summation term of (3.11), i.e., $\sum_{n=1}^{N} \omega_n \sum_{k_1=1}^{K} \rho_n^{k_1,1} R_n^{k_1}$, there is at most one non-zero element for a given subcarrier k_1 because of constraint (3.6). It implies that among the N users, at most one user can utilize the subcarrier k_1 for DT in the odd time slot. Similarly, in the second summation term of (3.11), there is at most one non-zero element for a given subcarrier k_2 because of constraint (3.7). It means that at most one user can utilize the subcarrier k_2 for DT mode in the even time slot. In the third summation term of (3.11), there is also at most one non-zero element for a given subcarrier pair (k_1, k_2) because of constraints (3.6), (3.7) and

[7]In most previous works focusing on resource allocation without subcarrier pairing [86, 109], the binary assignment optimization problem can be solved by the greedy algorithm directly. However, if subcarrier pairing is taken into account, the joint optimization problem of subcarrier assignment, relay selection, subcarrier pairing and transmission mode selection is non-trivial and cannot be solved by the greedy algorithm.

(3.8). In summary, the subcarrier pair (k_1, k_2) can only be assigned to assist one user in (i) FDRT mode, (ii) HDRCT mode with one relay, or (iii) DT mode without relay.

Based on the above observations, in FDRT mode, we define

$$\mathcal{R}^1(k_1, k_2) = \max_{n\in\mathcal{N}, m\in\mathcal{M}} \omega_n R_{n,m}^{k_1,k_2,1} \tag{3.13}$$

for each possible subcarrier pair (k_1, k_2). In HDRCT mode, we define

$$\mathcal{R}^2(k_1, k_2) = \max_{n\in\mathcal{N}, m\in\mathcal{M}} \omega_n R_{n,m}^{k_1,k_2,2} \tag{3.14}$$

for each possible subcarrier pair (k_1, k_2). In DT mode, we define

$$\mathcal{R}^3(k_1) = \max_{n\in\mathcal{N}} \omega_n R_n^{k_1} \tag{3.15}$$

$$\mathcal{R}^3(k_2) = \max_{n\in\mathcal{N}} \omega_n R_n^{k_2} \tag{3.16}$$

which are the maximal weighted transmission rates over subcarrier k_1 in the odd time slot and k_2 in the even time slot, respectively. Then, we define

$$\mathcal{R}^3(k_1, k_2) = \mathcal{R}^3(k_1) + \mathcal{R}^3(k_2) \tag{3.17}$$

which is the maximal weighted transmission rate for DT mode over subcarrier-pair (k_1, k_2). As a result, the maximal transmission rate for a given subcarrier-pair (k_1, k_2) is given by

$$\mathcal{R}(k_1, k_2) = \max_{i=1,2,3} \mathcal{R}^i(k_1, k_2). \tag{3.18}$$

We further denote the associated user nodes, relay node, and selected transmission mode that take the maximum in (3.18) for the subcarrier pair (k_1, k_2) as (n_1^*, n_2^*), m^* and i^*, respectively. Specifically, n_1^* and n_2^* are defined as the selected users in the odd time slot and even time slot, respectively. If either FDRT mode or HDRCT mode has been adopted, the selected users will be identical, i.e., $n_1^* = n_2^*$. When DT mode is adopted, $m^* = 0$ (no relay used) and n_1^* is not necessarily the same as n_2^*. We therefore introduce a new binary variable $\rho_{n_1,n_2,m}^{k_1,k_2,3}$. When $m = 0$, the value of $\rho_{n_1,n_2,m}^{k_1,k_2,3}$ indicates whether k_1 in the first time slot is assigned to user n_1 AND k_2 in the second time slot is assigned to user n_2 for DT mode. Thus, if $\rho_{n_1}^{k_1,1} = 1$ AND $\rho_{n_2}^{k_2,2} = 1$, then $\rho_{n_1,n_2,0}^{k_1,k_2,3} = 1$; otherwise $\rho_{n_1,n_2,0}^{k_1,k_2,3} = 0$. Consequently, using $\rho_{n_1^*,n_2^*,m^*}^{k_1,k_2,i^*}$ to indicate that the subcarrier pair (k_1, k_2) is assigned with the associated user nodes (n_1^*, n_2^*), relay node m^*, and selected transmission mode i^*, we can transform the problem **P2** to the following simplified problem **P3** without loss of optimality:

$$\begin{aligned} \mathbf{P3}: \max \quad & \sum_{k_1=1}^{K}\sum_{k_2=1}^{K} \mathcal{R}(k_1,k_2)\rho_{n_1^*,n_2^*,m^*}^{k_1,k_2,i^*} \\ s.t. \quad & \sum_{k_1=1}^{K} \rho_{n_1^*,n_2^*,m^*}^{k_1,k_2,i^*} = 1, \forall k_1 \in \mathcal{K} \\ & \sum_{k_2=1}^{K} \rho_{n_1^*,n_2^*,m^*}^{k_1,k_2,i^*} = 1, \forall k_2 \in \mathcal{K}. \end{aligned} \tag{3.19}$$

In the following, we show that the simplified problem **P3** is equivalent to a standard maximum weighted bipartite matching problem [110].

A balanced bipartite graph $\mathcal{G} = (\mathcal{V}_1 \times \mathcal{V}_2, \xi, \mathcal{W})$ is constructed, where the two set of vertices, $\mathcal{V}_1$ and $\mathcal{V}_2$ are the set of subcarriers $\mathcal{K}$ in the odd time slot and the

even time slot, respectively. ξ is the set of edges that connect all possible pairs of vertices in the two set of vertices. Note that $\mathcal{K}$ is shared in both odd and even time slots, and thus $|\mathcal{V}_1| = |\mathcal{V}_2| = |\mathcal{K}| = K$, where $|\cdot|$ is the cardinality of a set. $\mathcal{W}$ is the weighting function such that $\xi \to \mathbb{R}_+$. Specifically, each edge is assigned a weight, representing the maximum achievable rate over the two connected vertices (i.e., subcarriers), namely,

$$\mathcal{W}_{(k_1,k_2)} = \mathcal{R}(k_1, k_2) \tag{3.20}$$

where $\mathcal{R}(k_1, k_2)$ is defined in (3.18). The weighting process is done across all edges. According to (3.13)–(3.18), the complexity of the weighting process is $\mathcal{O}(MNK + MNK^2 + 2NK + 4K^2)$, which is polynomial.

Consequently, the binary assignment problem of subcarrier-pairing based subcarrier assignment, relay selection, user selection and transmission mode selection for the weighted sum-rate maximization is equivalent to finding a perfect matching $\xi^* \subseteq \xi$ in $\mathcal{G}$ so that the sum weights of ξ^* is maximum. This is the so-called maximum weighted bipartite matching problem **P4**:

$$\mathbf{P4}: \quad \max_{\xi^* \subseteq \xi} \quad \sum_{(k_1,k_2)\in\xi^*} \mathcal{W}_{(k_1,k_2)}. \tag{3.21}$$

The key of the proposed algorithm is the mapping from the original problem **P2** to the simplified problem **P3** and then to the maximum weighted bipartite matching problem **P4** without loss of optimality. Once the mapping is done, the classic Hungarian method can be adopted to solve **P4** optimally with a computational complexity of $\mathcal{O}(K^3)$ [111]. By combining the two aforementioned complexities, the total complexity of our proposed algorithm is $\mathcal{O}(MNK+MNK^2+2NK+4K^2+K^3)$,

which is polynomial and lower than that for solving the minimum cost network flow problem [37].

3.3 Joint Power Allocation and Binary Assignment

In the previous section, we have proposed a solution for the binary assignment problem, i.e., joint optimal subcarrier assignment, relay selection, subcarrier pairing and transmission mode selection with a given power allocation scheme. In this section, we further take power allocation into account, and solve the joint power allocation and binary assignment problem which is a mixed integer non-linear programming problem. The large number of binary assignment possibilities ($(3MN)^K$) significantly complicates the problem when K, M, and N are large. Recently, it has been shown in [86] that in multicarrier systems, the duality gap of a non-convex resource allocation problem is negligible when the number of subcarriers becomes sufficiently large. Since our optimization problem is obviously a multiple subcarriers allocation problem, it can be solved by using the dual method and the solution is asymptotically optimal when K is large. The solution procedure includes three main steps: (i) problem transformation; (ii) optimizing the dual function at given primal variables; and (iii) optimizing primal variables at a given dual point.

3.3.1 Problem Transformation

The problem **P1** under consideration is a mixed combinatorial and non-convex optimization problem. The combinatorial nature comes from the binary integer constraints. In general, a brute force approach is needed to obtain the global optimal solution. Here, we propose handling the integer constraints in (3.6), (3.7), and (3.8) using the following process.

To facilitate binary assignment variables $\rho_n^{k_1,1}$, $\rho_n^{k_2,2}$, and $\rho_{n,m}^{k_1,k_2,i}$, we introduce a series of "virtual power" variables:

$$p_{b,n,k_1}^{m,k_2,i} = \rho_{n,m}^{k_1,k_2,i} p_{b,n,k_1}, \tag{3.22a}$$

$$p_{m,n,k_2}^{k_1,i} = \rho_{n,m}^{k_1,k_2,i} p_{m,n,k_2}, \tag{3.22b}$$

$$p_{b,n,k_2}^{m,k_1,i} = \rho_{n,m}^{k_1,k_2,i} p_{b,n,k_2}, \tag{3.22c}$$

$$p_{m,n,k_1}^{k_2,1} = \rho_{n,m}^{k_1,k_2,1} p_{m,n,k_1}, \tag{3.22d}$$

$$p_{b,n,k_1}^{3} = \rho_{n}^{k_1,1} p_{b,n,k_1},\ p_{b,n,k_2}^{3} = \rho_{n}^{k_2,2} p_{b,n,k_2} \tag{3.22e}$$

for $i = \{1, 2\}$, $\forall k_1, k_2 \in \mathcal{K}$, $\forall m \in \mathcal{M}$, and $\forall n \in \mathcal{N}$.

- $p_{b,n,k_1}^{m,k_2,i}$ in (3.22a) indicates the transmit power of the BS assigned to the user U_n through the relay R_m over subcarrier k_1 paired with subcarrier k_2 in transmission mode i.

- $p_{m,n,k_2}^{k_1,i}$ in (3.22b) indicates the transmit power of the relay R_m assigned to the user U_n over subcarrier k_2 paired with subcarrier k_1 in transmission mode i.

- $p_{b,n,k_2}^{m,k_1,i}$ in (3.22c) indicates the transmit power of the BS assigned to the user U_n through the relay R_m over subcarrier k_2 paired with subcarrier k_1 in trans-

$$\mathbf{P5}: \max_{\boldsymbol{\rho},\hat{\boldsymbol{p}}} \quad \hat{R}_{tot} = \sum_{n=1}^{N} \omega_n \left(\sum_{k_1=1}^{K} \hat{R}_n^{k_1} + \sum_{k_2=1}^{K} \hat{R}_n^{k_2} + \sum_{i=1}^{2} \sum_{m=1}^{M} \sum_{k_1=1}^{K} \sum_{k_2=2}^{K} \hat{R}_{n,m}^{k_1,k_2,i} \right) \quad (3.27)$$
$$s.t. \quad (3.6) - (3.8), \text{ and } (3.23) - (3.26)$$

mission mode i.

- $p_{m,n,k_1}^{k_2,1}$ in (3.22d) indicates the transmit power of the relay R_m assigned to the user U_n over subcarrier k_1 paired with subcarrier k_2 in FDRT mode.

- p_{b,n,k_1}^{3} and p_{b,n,k_2}^{3} in (3.22e) indicate the transmit power of the BS assigned to the user U_n over subcarrier k_1 and k_2, respectively, in DT mode.

As a result, the power constraints in (3.9) and (3.10) should be transformed into

$$\sum_{n=1}^{N} \sum_{k_1=1}^{K} p_{b,n,k_1}^{3} + \sum_{i=1}^{2} \sum_{n=1}^{N} \sum_{m=1}^{M} \sum_{k_2=1}^{K} \sum_{k_1=1}^{K} p_{b,n,k_1}^{m,k_2,i} \leq P_b \quad (3.23)$$

$$\sum_{n=1}^{N} \sum_{k_2=1}^{K} p_{b,n,k_2}^{3} + \sum_{i=1}^{2} \sum_{n=1}^{N} \sum_{m=1}^{M} \sum_{k_2=1}^{K} \sum_{k_1=2}^{K} p_{b,n,k_2}^{m,k_1,1} \leq P_b \quad (3.24)$$

$$\sum_{n=1}^{N} \sum_{m=1}^{M} \sum_{k_2=1}^{K} \sum_{k_1=1}^{K} p_{m,n,k_1}^{k_2,1} \leq P_m, \forall m \in \mathcal{M} \quad (3.25)$$

$$\sum_{i=1}^{2} \sum_{n=1}^{N} \sum_{m=1}^{M} \sum_{k_2=1}^{K} \sum_{k_1=1}^{K} p_{m,n,k_2}^{k_1,i} \leq P_m, \forall m \in \mathcal{M}. \quad (3.26)$$

Thus, the problem **P1** is transformed into the problem **P5** where $\hat{R}_{n,m}^{k_1,k_2,1}$, $\hat{R}_{n,m}^{k_1,k_2,2}$,

$\hat{R}_n^{k_1}$ and $\hat{R}_n^{k_2}$ are given in (3.28), (3.29) and (3.30), respectively.

$$\hat{R}_{n,m}^{k_1,k_2,1} = \frac{1}{2}\min\left\{\log\left(1+p_{b,n,k_2}^{m,k_1,1}\alpha_{b,m,k_2}\right), \log\left(1+\frac{p_{m,n,k_1}^{k_2,1}\alpha_{m,n,k_1}}{p_{b,n,k_1}^{m,k_2,1}\alpha_{b,n,k_1}+1}\right)\right\} + \frac{1}{2}\min\left\{\log\left(1+p_{b,n,k_1}^{m,k_2,1}\alpha_{b,m,k_1}\right), \log\left(1+\frac{p_{m,n,k_2}^{k_1,1}\alpha_{m,n,k_2}}{p_{b,n,k_2}^{m,k_1,1}\alpha_{b,n,k_2}+1}\right)\right\} \quad (3.28)$$

$$\hat{R}_{n,m}^{k_1,k_2,2} = \frac{1}{2}\min\left\{\log\left(1+p_{b,n,k_1}^{m,k_2,2}\alpha_{b,m,k_1}\right), \log\left(1+p_{b,n,k_1}^{m,k_2,2}\alpha_{b,n,k_1}+\left(\sqrt{p_{b,n,k_2}^{m,k_1,2}\alpha_{b,n,k_2}}+\sqrt{p_{m,n,k_2}^{k_1,2}\alpha_{m,n,k_2}}\right)^2\right)\right\} \quad (3.29)$$

$$\hat{R}_n^{k_1} = \frac{1}{2}\log(1+p_{b,n,k_1}^3\alpha_{b,n,k_1}), \qquad \hat{R}_n^{k_2} = \frac{1}{2}\log(1+p_{b,n,k_2}^3\alpha_{b,n,k_2}). \quad (3.30)$$

In addition, $\hat{\boldsymbol{p}} = \{p_{b,n,k_1}^{m,k_2,i}, p_{m,n,k_2}^{k_1,i}, p_{b,n,k_2}^{m,k_1,i}, p_{m,n,k_1}^{k_2,1}, p_{b,n,k_1}^3, p_{b,n,k_2}^3\}$. The binary assignment can be obtained after allocating the powers based on the objective function $\hat{R}_{tot}$. In other words, with known power allocations, the problem **P5** is evolved into a binary assignment problem. Thus, we can firstly optimize the power allocation, and then optimize the binary assignment problem by using a similar method provided in Section 3.2.

We introduce a Lagrangian multiplier vector $\boldsymbol{\lambda} = \{\lambda_{b,i}, \lambda_{1,i}, \lambda_{2,i}, \cdots, \lambda_{m,i}, \ldots, \lambda_{M,i}\}$ $(i = 1, 2)$ associated with the individual power constraints. We also define $\mathcal{I}$ as the set of possible binary assignments $\boldsymbol{\rho}$ satisfying (3.6)–(3.8). In addition, we define $\mathcal{P}(\boldsymbol{\rho})$ as the set of possible power allocations $\hat{\boldsymbol{p}}$ under the given $\boldsymbol{\rho}$. Then, the dual problem of problem **P5** can be readily written as

$$g(\boldsymbol{\lambda}) \triangleq \max_{\hat{\boldsymbol{p}}\in\mathcal{P}(\boldsymbol{\rho}),\boldsymbol{\rho}\in\mathcal{I}} \quad L(\hat{\boldsymbol{p}}, \boldsymbol{\rho}, \boldsymbol{\lambda}), \quad (3.31)$$

where the Lagrangian is given in (3.32). In (3.32), the first term (3.32a) represents the *profit expression* of FDRT mode in the dual domain; the second term (3.32b) is the profit expression of HDRCT mode; and the third and fourth terms together (3.32c) represent the profit expression of DT mode. Computing the dual function $g(\boldsymbol{\lambda})$ requires determining the optimal $(\hat{\boldsymbol{p}}^*, \boldsymbol{\rho}^*)$ for the given dual vector $\boldsymbol{\lambda}$. In the following we present the derivations in detail. It is worth mentioning that we set $\boldsymbol{\lambda}$ to be sufficiently large and $\hat{\boldsymbol{p}}$ to be zeros in the initialization process.

3.3.2 Optimizing Dual Function at Given Primal Variables

The dual optimization problem is given by

$$\begin{aligned} \min_{\boldsymbol{\lambda} \succeq \mathbf{0}} \quad & g(\boldsymbol{\lambda}) \\ s.t. \quad & \boldsymbol{\lambda} \succeq \mathbf{0}. \end{aligned} \tag{3.34}$$

Since a dual function is always convex by definition [89], gradient- or subgradient-based methods can be used to minimize $g(\boldsymbol{\lambda})$ with guaranteed convergence. We denote $(\hat{\boldsymbol{p}}^*, \boldsymbol{\rho}^*)$ as the optimal power allocation and binary assignment pair at a given dual point (to be discussed in the next subsection). Then a subgradient of $g(\boldsymbol{\lambda})$ can be derived using a similar method as in [86] such that the dual variables $\boldsymbol{\lambda}$ are updated as in (3.33), where $[\star]^+$ denotes $\max(0, \star)$, the superscript $^{(l)}$ denotes the iteration number, and $\pi^{(l)}$ represents the step size. When the step size $\pi^{(l)}$ follows the diminishing policy in [90], the subgradient method above is guaranteed to converge to the optimal dual variables. Here, we just take the simple diminishing

$$L(\hat{\boldsymbol{p}},\boldsymbol{\rho},\boldsymbol{\lambda}) = \sum_{n=1}^{N}\omega_n\sum_{m=1}^{M}\sum_{k_1=1}^{K}\sum_{k_2=2}^{K}\left(\hat{R}_{n,m}^{k_1,k_2,1} - \lambda_{b,1}p_{b,n,k_1}^{m,k_2,1} - \lambda_{b,2}p_{b,n,k_2}^{m,k_1,1} - \lambda_{m,1}p_{m,n,k_1}^{k_2,1} - \lambda_{m,2}p_{m,n,k_2}^{k_1,1}\right) \tag{3.32a}$$

$$+\sum_{n=1}^{N}\omega_n\sum_{m=1}^{M}\sum_{k_1=1}^{K}\sum_{k_2=2}^{K}\left(\hat{R}_{n,m}^{k_1,k_2,2} - \lambda_{b,1}p_{b,n,k_1}^{m,k_2,2} - \lambda_{b,2}p_{b,n,k_2}^{m,k_1,2} - \lambda_{m,2}p_{m,n,k_2}^{k_1,2}\right) \tag{3.32b}$$

$$+\sum_{n=1}^{N}\omega_n\sum_{k_1=1}^{K}\left(\hat{R}_{n}^{k_1} - \lambda_{b,1}p_{b,n,k_1}^{3}\right) + \sum_{n=1}^{N}\omega_n\sum_{k_2=1}^{K}\left(\hat{R}_{n}^{k_2} - \lambda_{b,2}p_{b,n,k_2}^{3}\right) \tag{3.32c}$$

$$+(\lambda_{b,1}+\lambda_{b,2})P_b + \sum_{m=1}^{M}(\lambda_{m,1}+\lambda_{m,2})P_m \tag{3.32d}$$

$$\lambda_{b,1}^{(l+1)} = \left[\lambda_{b,1}^{(l)} - \pi^{(l)}\left(P_b - \sum_{n=1}^{N}\sum_{k_1=1}^{K}p_{b,n,k_2}^{3} - \sum_{n=1}^{N}\sum_{m=1}^{M}\sum_{k_2=1}^{K}\sum_{k_1=1}^{K}p_{b,n,k_1}^{m,k_2,1}\right)\right]^{+} \tag{3.33a}$$

$$\lambda_{b,2}^{(l+1)} = \left[\lambda_{b,2}^{(l)} - \pi^{(l)}\left(P_b - \sum_{n=1}^{N}\sum_{k_1=1}^{K}p_{b,n,k_2}^{3} - \sum_{n=1}^{N}\sum_{m=1}^{M}\sum_{k_2=1}^{K}\sum_{k_1=1}^{K}p_{b,n,k_1}^{m,k_2,1}\right)\right]^{+} \tag{3.33b}$$

$$\lambda_{m,1}^{(l+1)} = \left[\lambda_{m,1}^{(l)} - \pi^{(l)}\left(P_m - \sum_{n=1}^{N}\sum_{m=1}^{M}\sum_{k_2=1}^{K}\sum_{k_1=1}^{K}p_{m,n,k_1}^{k_2,1}\right)\right]^{+} \tag{3.33c}$$

$$\lambda_{m,2}^{(l+1)} = \left[\lambda_{m,2}^{(l)} - \pi^{(l)}\left(P_m - \sum_{i=1}^{2}\sum_{n=1}^{N}\sum_{m=1}^{M}\sum_{k_2=1}^{K}\sum_{k_1=1}^{K}p_{m,n,k_2}^{k_1,i}\right)\right]^{+} \tag{3.33d}$$

step, i.e., $\pi^{(l)} = \pi^{(0)}/\sqrt{l}$, where $\pi^{(0)} > 0$ is the initial step size[8]. The computational complexity of such an updating method is polynomial in the number of dual variables $2(M+1)$ [86].

[8]Since optimizing the step size is not the main theme of our work, we apply only a simple diminishing step. This simple diminishing step is not in an optimized way but is guaranteed to converge.

3.3.3 Optimizing Primal Variables at a Given Dual Point

Computing the dual function $g(\boldsymbol{\lambda})$ involves determining the optimal $(\hat{\boldsymbol{p}}^*, \boldsymbol{\rho}^*)$ at the given dual point $\boldsymbol{\lambda}$. In this subsection, we present the detailed derivation of the optimal primal variables in two phases. We first find the optimal power variables $\hat{\boldsymbol{p}}$ by fixing the integer variables $\boldsymbol{\rho}$. Then we search the optimal $\boldsymbol{\rho}$ by eliminating $\hat{\boldsymbol{p}}$ in the objective function. Also, we optimize the power in the three different transmission modes sequentially.

3.3.3.1 Optimizing Power Allocation in FDRT Mode

In FDRT mode, i.e., $i = 1$, the corresponding objective function is in (3.32a). Based on (3.32a), the problem can be decomposed into MNK^2 subproblems. With given dual variables, the power allocation can be performed by solving the corresponding sub-primal problem. The optimal power allocation that maximizes (3.32a) does not have a closed-form solution in general, and we introduce a *hierarchical dual method* to solve the power allocation problem. Details can be found in Appendix 3.A.

3.3.3.2 Optimizing Power Allocation in HDRCT Mode

In HDRCT mode, i.e., $i = 2$, the corresponding objective function is in (3.32b). Given m, n, k_1 and k_2, a slight change of (3.32b) gives

$$\begin{aligned} L_{m,n}^{k_1,k_2,2} =& \frac{1}{2}\log(1+\gamma_{m,n}^{k_1,k_2}) + \nu(p_{b,n,k_1}^{m,k_2,2}\alpha_{b,m,k_1} - \gamma_{m,n}^{k_1,k_2}) \\ & - \lambda_{b,1}p_{b,n,k_1}^{m,k_2,2} - \lambda_{b,2}p_{b,n,k_2}^{m,k_1,2} - \lambda_{m,2}p_{m,n,k_2}^{k_1,2} \end{aligned} \tag{3.35}$$

where

$$\gamma_{m,n}^{k_1,k_2} = p_{b,n,k_1}^{m,k_2,2}\alpha_{b,n,k_1} + (\sqrt{p_{b,n,k_2}^{m,k_1,2}\alpha_{b,n,k_2}} + \sqrt{p_{m,n,k_2}^{k_1,2}\alpha_{m,n,k_2}})^2. \tag{3.36}$$

The second term on the right hand side of (3.35) is associated with the Lagrange multiplier $\nu \geq 0$, corresponding to the condition

$$p_{b,n,k_1}^{m,k_2,2}\alpha_{b,m,k_1} \geq \gamma_{m,n}^{k_1,k_2} \tag{3.37}$$

for relay transmission mode rather than DT mode [43]. If (3.37) is not valid, the power of the given relay can be reallocated, without reducing its rate to other subcarriers, or simply be conserved. We aim at maximizing the Lagrange function (3.35) subject to the individual powers for given m, n, k_1 and k_2. The referred problem is obviously a convex optimization problem. To derive the convex optimization problem, one may formulate and solve a set of equations based on the KKT conditions and the method in [43]. The method, however, is effective only when the objective function (3.35) and all the constraints are differentiable at the optimum solution. However, $\gamma_{m,n}^{k_1,k_2}$ is not differentiable at $p_{b,n,k_2}^{m,k_1,2} = 0$ or $p_{m,n,k_2}^{k_1,2} = 0$. As a result, the KKT-conditions-based method cannot be applied to finding the optimum solution. In this chapter, we provide a much simpler analysis to solve this problem.

We define the optimal powers as $p_{b,n,k_1}^{m,k_2,2*}$, $p_{b,n,k_2}^{m,k_1,2*}$ and $p_{m,n,k_2}^{k_1,2*}$. Then the power allocation scheme can be analyzed under the following three cases.

- Case 1 $p_{m,n,k_2}^{k_1,2*} = 0$: It means that the relay does not transmit any information. As a result, $p_{b,n,k_1}^{m,k_2,2*} = 0$ and $p_{b,n,k_2}^{m,k_1,2*} = 0$. Note that (3.35) may not be optimal under $p_{b,n,k_1}^{m,k_2,2*} = p_{b,n,k_2}^{m,k_1,2*} = 0$ and $p_{m,n,k_2}^{k_1,2*} = 0$. However, in this chapter, we also

have taken into account the DT mode. In DT mode, we can have a better achievable rate than that of HDRCT mode when $p_{m,n,k_2}^{k_1,2*} = 0$. Thus, we directly give the results following the definition of HDRCT mode.

- Case 2 $p_{m,n,k_2}^{k_1,2*} > 0$ and $p_{b,n,k_2}^{m,k_1,2*} = 0$: By substituting $p_{b,n,k_2}^{m,k_1,2*} = 0$ into (3.35), and equating the partial derivatives of $L_{m,n}^{k_1,k_2,2}$ in (3.35) over $p_{b,n,k_1}^{m,k_2,2}$ and $p_{m,n,k_2}^{k_1,2}$ to zeros, the closed-forms of the optimal power allocations $p_{b,n,k_1}^{m,k_2,2*}$ and $p_{m,n,k_2}^{k_1,2*}$ can be readily obtained as follows.

  If $\alpha_{b,m,k_1} > \alpha_{b,n,k_1}$, *and* $1/2(\beta_{k_1,k_2}\lambda_{b,1} + \lambda_{m,2}) - 1/\alpha_{b,m,k_1}\beta_{k_1,k_2} > 0$, *where* $\beta_{k_1,k_2} = \alpha_{m,n,k_2}/(\alpha_{b,m,k_1} - \alpha_{b,n,k_1})$, *then*

$$p_{b,n,k_1}^{m,k_2,2*} = \frac{1}{2(\lambda_{b,1} + \lambda_{m,2}/\beta_{k_1,k_2})} - \frac{1}{\alpha_{b,m,k_1}} \tag{3.38}$$

$$p_{m,n,k_2}^{k_1,2*} = \frac{1}{2(\beta_{k_1,k_2}\lambda_{b,1} + \lambda_{m,2})} - \frac{1}{\alpha_{b,m,k_1}\beta_{k_1,k_2}}; \tag{3.39}$$

  otherwise, Case 2 is not feasible.

  Note that the condition $\alpha_{b,m,k_1} > \alpha_{b,n,k_1}$ for selecting HDRCT mode is based on the fact that in this situation, the relay will receive more information than the destination. Otherwise, there is no need to use the relay and we should go back to Case 1. The other condition $1/2(\beta_{k_1,k_2}\lambda_{b,1} + \lambda_{m,2}) - 1/\alpha_{b,m,k_1}\beta_{k_1,k_2} > 0$ is used to guarantee $p_{m,n,k_2}^{k_1,2*} > 0$ and hence to satisfy the condition of Case 2.

- Case 3 $p_{m,n,k_2}^{k_1,2*} > 0$ and $p_{b,n,k_2}^{m,k_1,2*} > 0$: By equating the partial derivatives of $L_{m,n}^{k_1,k_2,2}$ in (3.35) over $p_{b,n,k_1}^{m,k_2,2}$, $p_{b,n,k_2}^{m,k_1,2}$ and $p_{m,n,k_2}^{k_1,2}$ to zeros and after some manipulations, the closed-forms of the optimal power allocations $p_{b,n,k_1}^{m,k_2,2*}$, $p_{b,n,k_2}^{m,k_1,2*}$ and $p_{m,n,k_2}^{k_1,2*}$ can be readily obtained as follows. *If* $\alpha_{b,m,k_1} - \alpha_{b,n,k_1} > 0$ *and*

$\gamma_{m,n}^{k_1,k_2*} > 0$, *then*

$$p_{b,n,k_1}^{m,k_2,2*} = \gamma_{m,n}^{k_1,k_2*}/\alpha_{b,m,k_1} \tag{3.40}$$

$$p_{b,n,k_2}^{m,k_1,2*} = \frac{\gamma_{m,n}^{k_1,k_2*}\eta^*(\alpha_{b,m,k_1} - \alpha_{b,n,k_1})}{\alpha_{b,m,k_1}(\alpha_{b,n,k_2} + \eta^*\alpha_c)^2} \tag{3.41}$$

$$p_{m,n,k_2}^{k_1,2*} = \frac{\gamma_{m,n}^{k_1,k_2*}\alpha_{b,m,k_1} - \alpha_{b,n,k_1}}{\alpha_{b,m,k_1}(\alpha_{b,n,k_2} + \eta^*\alpha_c)^2} \tag{3.42}$$

where

$$\eta^* = \frac{1}{2\lambda_{m,2}\alpha_c}\left(-(\lambda_{m,2}\alpha_{b,n,k_2} - \lambda_{b,2}\alpha_{m,n,k_2}) + \sqrt{(\lambda_{m,2}\alpha_{b,n,k_2} - \lambda_{b,2}\alpha_{m,n,k_2})^2 + \lambda_{m,2}\lambda_{b,2}\alpha_c^2}\right), \tag{3.43}$$

$$\gamma_{m,n}^{k_1,k_2*} = \frac{(\alpha_{b,n,k_2} + \eta\alpha_c)/2}{\lambda_{b,2}(\alpha_{b,n,k_1} - \alpha_{b,m,k_1}) - \lambda_{b,1}(\alpha_{b,n,k_2} + \eta^*\alpha_c)} - 1, \tag{3.44}$$

$$\alpha_c = \sqrt{\alpha_{b,n,k_2}\alpha_{m,n,k_2}}; \tag{3.45}$$

otherwise, Case 3 is not feasible. Details of the proof are shown in Appendix 3.B.

Subsequently, we evaluate the Lagrangian function (3.35) under the above three power allocation schemes. Then we select the power allocation scheme corresponding to the largest Lagrangian function as the optimal one[9].

[9]In [112], a more general solution has been proposed for the scenario where multiple relays jointly assist the source to transmit information. However, the general solution is inefficient and not easy to understand under a single-relay case scenario. Our proposed method here is a kind of exhaustive search algorithm that searches all the possible cases and find the optimal one. Yet, the method is very efficient because the number of power variables is limited and only three cases need to be analyzed.

3.3.3.3 Optimizing Power Allocation in DT Mode

In DT mode, i.e., $i = 3$, the corresponding objective function is in (3.32c). By applying KKT conditions, the closed-forms of optimal power allocations p^3_{b,n,k_1} and p^3_{b,n,k_2} for a given set of n, k_1 and k_2 can be easily obtained

$$p^3_{b,n,k_1} = \left[\frac{1}{2\lambda_{b,1}} - \frac{1}{\alpha_{b,n,k_1}}\right]^+, \tag{3.46}$$

$$p^3_{b,n,k_2} = \left[\frac{1}{2\lambda_{b,2}} - \frac{1}{\alpha_{b,n,k_2}}\right]^+. \tag{3.47}$$

3.3.3.4 Optimizing binary assignment

Following a similar procedure as in [37], our proposed algorithm in Section 3.2 can be applied to solve the problem in (3.31) by replacing the rate expressions with the profit expressions. Specifically, we have

$$\bar{\mathcal{R}}^1(k_1,k_2) = \max_{n\in\mathcal{N},m\in\mathcal{M}} \omega_n(\hat{R}^{k_1,k_2,1}_{n,m} - \lambda_{b,1}p^{m,k_2,1}_{b,n,k_1} - \lambda_{b,2}p^{m,k_1,1}_{b,n,k_2} - \lambda_{m,1}p^{k_2,1}_{m,n,k_1} - \lambda_{m,2}p^{k_1,1}_{m,n,k_2}) \tag{3.48}$$

$$\bar{\mathcal{R}}^2(k_1,k_2) = \max_{n\in\mathcal{N},m\in\mathcal{M}} \omega_n(\hat{R}^{k_1,k_2,2}_{n,m} - \lambda_{b,1}p^{m,k_2,2}_{b,n,k_1} - \lambda_{m,2}p^{k_1,2}_{m,n,k_2}) \tag{3.49}$$

$$\bar{\mathcal{R}}^3(k_1) = \max_{n\in\mathcal{N}} \omega_n(\hat{R}^{k_1}_{n} - \lambda_{b,1}p^3_{b,n,k_1}) \tag{3.50}$$

$$\bar{\mathcal{R}}^3(k_2) = \max_{n\in\mathcal{N}} \omega_n(\hat{R}^{k_2}_{n} - \lambda_{b,2}p^3_{b,n,k_2}) \tag{3.51}$$

$$\bar{\mathcal{R}}^3(k_1,k_2) = \bar{\mathcal{R}}^3(k_1) + \bar{\mathcal{R}}^3(k_2). \tag{3.52}$$

Then, the maximal transmission rate for a given subcarrier-pair is given by

$$\bar{\mathcal{R}}(k_1,k_2) = \max_{i=1,2,3} \bar{\mathcal{R}}^i(k_1,k_2). \tag{3.53}$$

Replacing $\mathcal{R}(k_1, k_2)$ in (3.19) by $\bar{\mathcal{R}}(k_1, k_2)$, the problem becomes a maximum weighted bipartite matching problem and can be solved by the classic Hungarian algorithm.

3.3.4 Computation Complexity

In our joint power allocation and binary assignment problem, the computation complexity is determined by the complexity of the dual method, power allocation and binary assignment jointly. It has been shown in Section 3.3.2 that the computational complexity of updating the dual variables is $\mathcal{O}(2(M+1))$. In each dual problem, the computational complexity of the binary assignment problem has been shown in Section 3.2 to be $\mathcal{O}(MNK + MNK^2 + 2NK + 4K^2 + K^3)$. For each binary assignment, the power allocation scheme in DT mode has a closed form solution, and thus its computational complexity is $\mathcal{O}(1)$; that in the HD relay cooperative transmission mode has three cases of which each has a closed form solution, and thus its computational complexity is $\mathcal{O}(3)$; that in FD relay transmission mode has four cases among which the first three have closed form solutions and the fourth case needs a further dual-based computation, and thus its computational complexity is $\mathcal{O}(3 + 2 * (2 + 1)) = \mathcal{O}(9)$. Thus, the overall computation complexity of our joint optimization problem is $\mathcal{O}(26(M+1)(MNK + MNK^2 + 2NK + 4K^2 + K^3))$.

3.4 Simulation Results

In this section, we evaluate the system performance of our proposed algorithm by simulations. We consider the 3GPP ITU-R urban macro (UMa) cell in Fig. 3.1 where the BS locates at the center of the cell [96]. We assume a cell radius of 2 km

and a total of $N = 32$ users. We adopt the path loss model from [96], i.e., path loss equals $122.5 + 35 \log_{10} d$ (in dB), where d denotes the distance in km and the path loss exponent is set to be 3.5 for the height of BS as 31 meters over the ground. The small-scale fading is modeled as a multipath time-delay model following ITU-R M.1225 PedA [96]. The center frequency is 2 GHz and the bandwidth is 10 MHz, within which there are 64 subcarriers. The noise spectral density is -174 dBm/Hz and the noise figure is set to 9 dB. The number of the relays is $M = 4$ and they are located at [0, 1], [0, -1], [1, 0] and [-1, 0] (km). A total of 50000 different channel realizations are conducted in the simulation. For each channel realization, the locations of the users are randomly and uniformly distributed. The peak power constraints for all relay nodes are the same and set to be 5 dB lower than the peak power constraint of the BS. In addition to our proposed algorithm, the following benchmark approaches are simulated for comparison[10].

1) No Subcarrier Pairing (NSP) : The operation is in either DT mode, FDRT mode or HDRCT mode. When operating in the HDRCT mode, however, the same subcarrier is used in the two time slots of the cooperative transmission. The joint optimization is performed with respect to power allocation, subcarrier assignment, relay selection, and transmission mode selection; and can be solved by per-subcarrier basis using the greedy policy.

2) DT only: The operation is in DT mode only. All users transmit directly without the assistance of the relays. In this case, the greedy policy is optimal for throughput maximization. The joint optimization is performed with respect to power allocation

[10]The prior work [35] considers the scenario that the users are located at the cell edge such that the direct link can be neglected. The algorithm proposed in [35] becomes ineffective when the users are uniformly distributed in the cell because the direct link could not be neglected. In our system model, the users are uniformly distributed in the cell. Thus, it is not appropriate to compare the work [35] with our work.

and subcarrier assignment.

3) No DT (NDT): In the NDT mode, the operation is in either FDRT mode or HDRCT mode, and all users require the assistance of the relays. The joint optimization is performed with respect to power allocation, relay selection, subcarrier pairing and assignment.

4) FDRT: The operation is in FDRT mode only and all users require the assistance of the relays. The joint optimization is performed with respect to power allocation, relay selection and subcarrier assignment.

5) HDRCT: The operation is in HDRCT mode only and all users require the assistance of the relays. The joint optimization is performed with respect to power allocation, relay selection, subcarrier pairing and assignment.

For the ease of notation, we define the interference-to-noise ratio (INR) as the self-interference power over noise power, i.e., σ_e^2/σ_0^2.

3.4.1 Convergence of the Proposed Algorithm

Fig. 3.2 plots the average sum-rate of the primal problem and the dual problem versus the number of iterations when the maximum BS transmit power equals 20 dBm and INR = 3 dB. The results in Fig. 3.2 show that the proposed hybrid FD transmission algorithm converges very fast and becomes very close to the optimal value in 5 iterations. In other words, the duality gap between the solutions of the primal and the dual of the joint optimization problem is negligible. The main reason is that the number of subcarriers (i.e., 64) is sufficiently large.

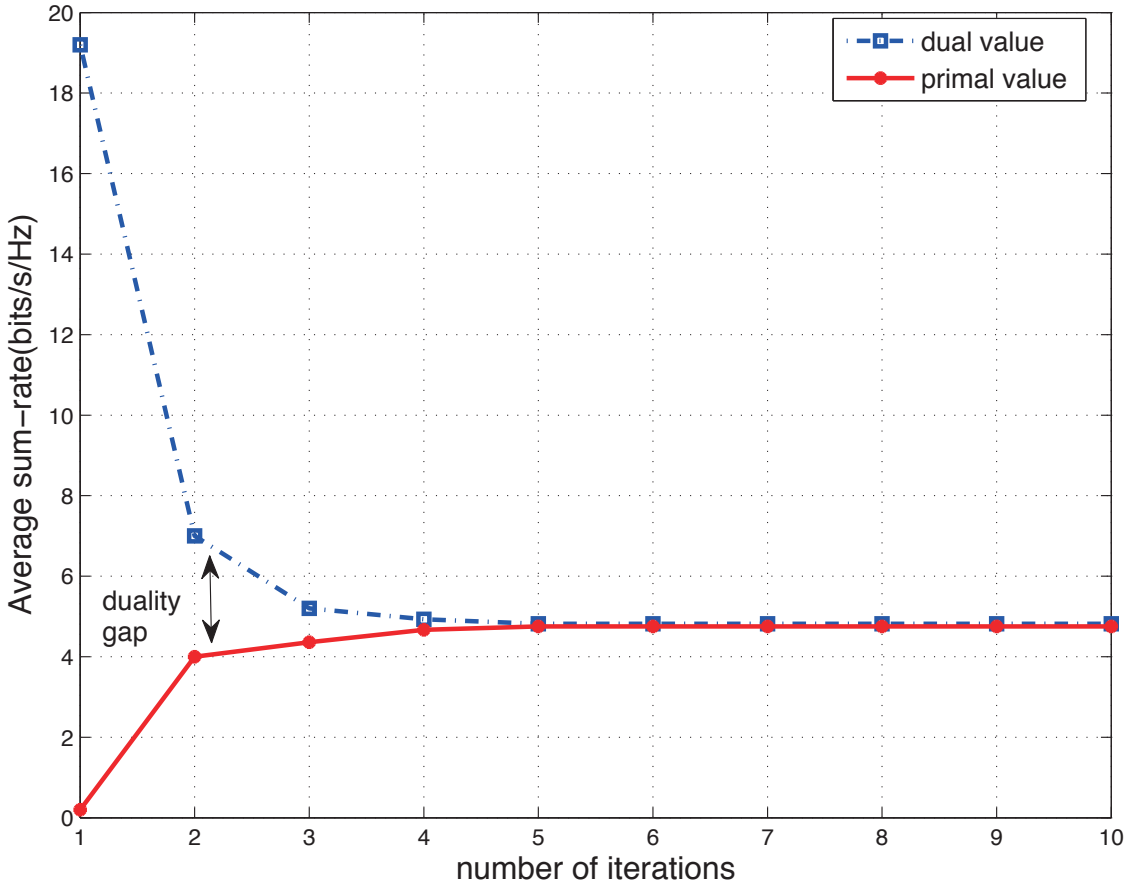

Figure 3.2: Average sum-rate for primal problem and dual problem versus number of iterations when the maximum BS transmit power equals 20 dBm and INR = 3 dB.

3.4.2 Comparison with Benchmark Approaches

In this subsection, we evaluate the performance of our proposed algorithm and compare it with those of the benchmark approaches. In Fig. 3.3(a) and Fig. 3.3(b), we plot the average sum-rates of the different approaches under INR = 3 dB and INR = 10 dB, respectively. Firstly, among all the algorithms, our proposed algorithm achieves the highest average sum-rate. Compared with the NSP scheme, our proposed algorithm can provide about 8% and 10% throughput improvements at

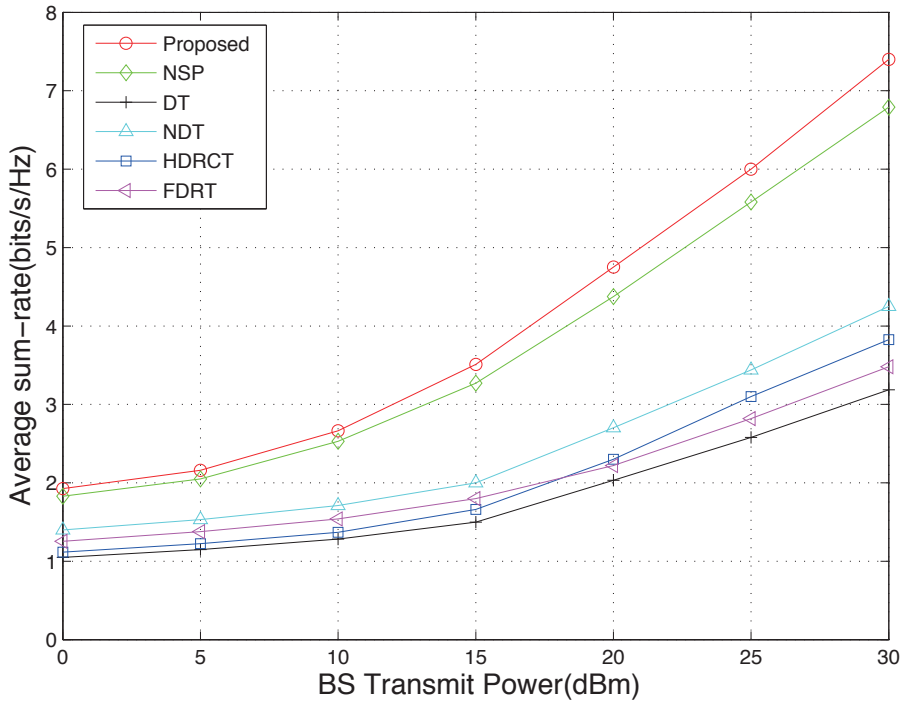

(a) INR = 3 dB

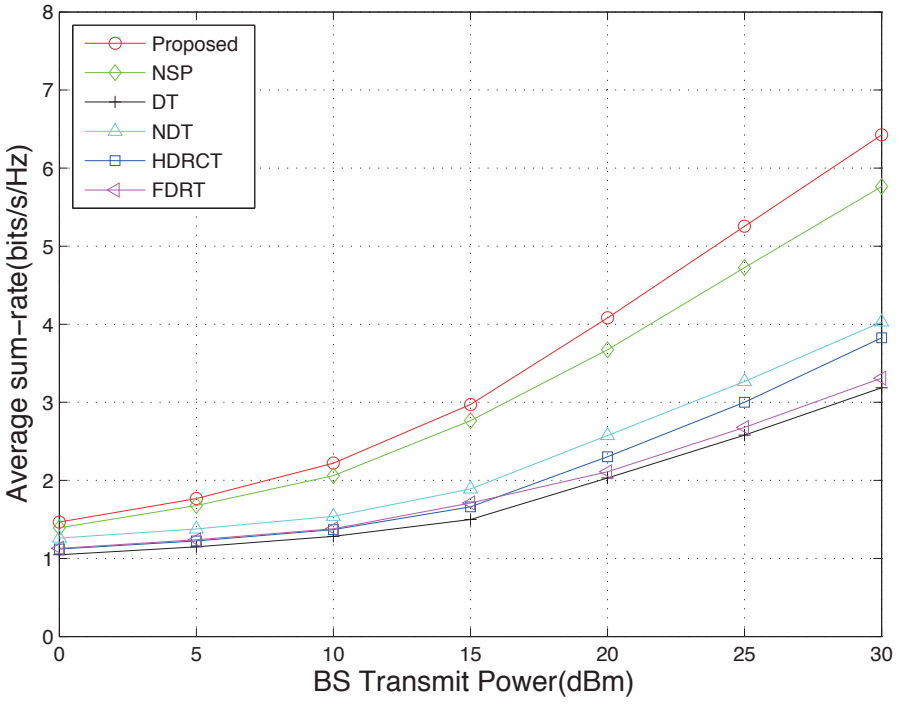

(b) INR = 10 dB

Figure 3.3: Performance comparison between our proposed algorithm and five other benchmark approaches. (a) INR = 3 dB; (b) INR = 10 dB.

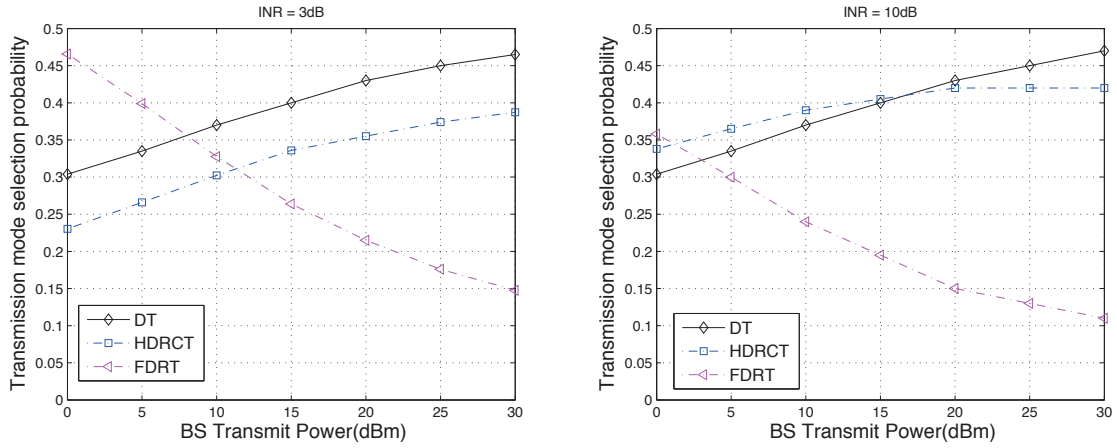

Figure 3.4: Transmission mode selection probability versus BS transmit power for INR = 3 dB and INR = 10dB.

INR = 3 dB and INR = 10 dB, respectively, when the BS transmit power equals 30 dBm. The results reveal that the use of subcarrier pairing can indeed increase the throughput. Moreover, we observe that our proposed algorithm can improve the system sum-rate significantly (even above 100%) compared with the FDRT, HDRCT, NDT and DT schemes. From Fig. 3.3(a) and Fig. 3.3(b), we also find that the HDRCT scheme achieves better performance than the FDRT scheme when the BS transmit power is high, and vice versa. The reason is that when the BS transmit power increases, the users under the FDRT scheme suffer from a higher interference from the BS. While the overall sum-rate of the FDRT scheme still improves with the BS transmit power, the improvement is relatively smaller compared with that achieved by the HDRCT scheme, in which the users are benefited by the stronger signals from the BS.

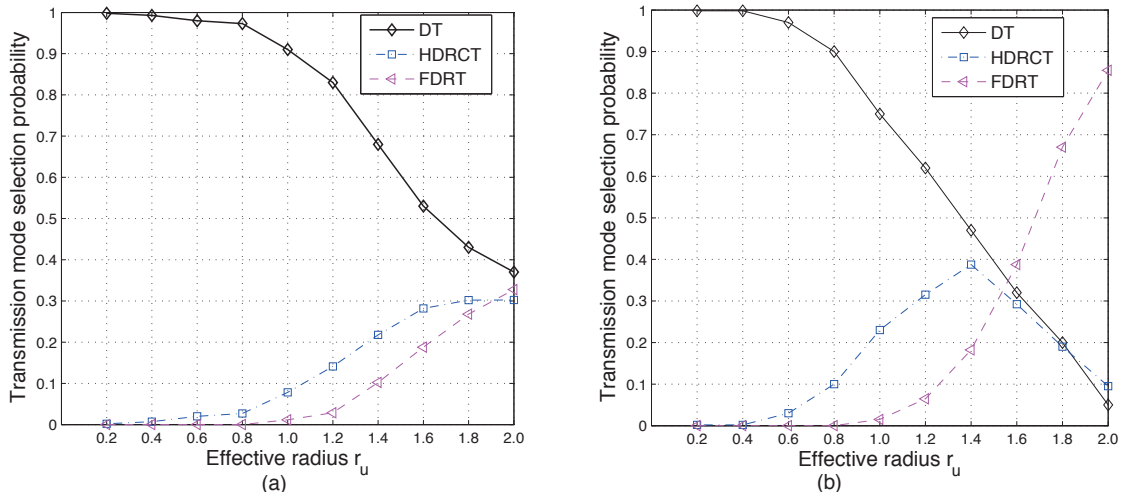

Figure 3.5: Transmission mode selection probability versus the effective radius r_u with given transmit power $P_B = 10$ dBm and INR = 3 dB, in which the users in the circle area $0 < d < r_u$ and the two concentric ring-shaped discs area $r_u - 0.1 < d < r_u$ are considered as effective users in (a) and (b), respectively.

3.4.3 Transmission Mode Selection Probability

To gain more insightful results, we analyze the different transmission mode selection probabilities under our proposed hybrid transmission protocol. In Fig. 3.4, we plot the selection probability of DT, HDRCT and FDRT modes versus BS transmit power under INR = 3 dB and INR = 10 dB. Firstly, the results show that the DT mode selection probability and the HDRCT mode selection probability increase whereas the FDRT mode selection probability decreases with the BS transmit power. The phenomenon is reasonable because a stronger BS transmit power (a) introduces a higher interference to the user in FDRT mode and (ii) provides a stronger signal to users in HDRCT or DT mode. Hence, both HDRCT and DT modes will be selected with an increasing probability as BS transmit power increases; and consequently, the probability of selecting FDRT mode will be reduced. Secondly, FDRT mode selection probability decreases with self-interference power, which is expected.

Next, we study the transmission mode selection probability of users in different locations. Fig. 3.5 illustrates the transmission mode selection probability versus the effective radius r_u under a BS transmit power $P_B = 10$ dBm and INR = 3 dB. Users located within a distance of r_u from the BS are considered as effective users in Fig. 3.5(a); while users located further than $r_u - 0.1$ but within r_u from the BS are considered as effective users in Fig. 3.5(b).

Referring to Fig. 3.5(b), when users are located very near the BS (up to $r_u = 0.6$), they can receive very strong signals from the BS and almost all of them select DT mode. Under this condition, DT mode can provide significant gain compared to HDRCT mode because DT uses only one time slot to transmit information. It also performs better than FDRT mode in this scenario since the strong direct link is considered as interference. As users move away from the BS ($0.8 \leq r_u \leq 1.4$) and become close to the relays (located at [0, 1], [0, -1], [1, 0] and [-1, 0]), users begin to receive not-so-strong signals from the BS but stronger ones from the relays. The advantage of DT diminishes and DT becomes less likely to be selected. The combined signals from the BS and the relay favor the selection of the HDRCT mode within this range. The probability of FDRT mode being selected is still small because of the relatively strong interference signal from the BS. When users move further away from both the BS and relays ($1.6 \leq r_u \leq 2.0$), the signal from the BS becomes very weak. The selection probability of DT mode continues to decline. HDRCT mode also begins to lose its advantage compare to FDRT mode. It is because FDRT mode uses only one time slot to transmit information and the users far from the BS receive very little interference from it.

3.4.4 Effect of Power Allocation

Next, we evaluate the effectiveness of the power allocation (PA) algorithm in our proposed scheme. In the top-left sub-figure of Fig. 3.6, we plot the sum-rate versus BS transmit power when INR = 3 dB. The upper bound obtained by searching the optimal power allocation exhaustively in the dual domain under a given binary assignment is provided as a comparison. We also plot the results for the equal power allocation (EPA) scheme in which the transmit powers of BS and relays are equally shared among all subcarriers. In particular, the proposed EPA scheme optimizes the binary assignment problem by using the Hungarian algorithm directly with EPA.

The results show that our proposed algorithm approaches the upper bound very closely. It verifies that the duality gap is negligible when the number of subcarriers is large. Moreover, the performance improvement of our proposed algorithm compared to the proposed EPA scheme is larger in low and moderate BS transmit power regimes but limited when the BS transmit power is high.

In a previous work [37], it has been shown the EPA scheme has nearly the same performance as the optimal power allocation at the high signal-to-noise-ratio (SNR) region (i.e., high BS transmit power) in a HD relaying system. In this work, we show that a similar conclusion can be obtained in the hybrid relaying system. In other sub-figures of Fig. 3.6, we plot the sum-rates of using DT mode, HDRCT mode and FDRT mode under optimized PA scheme and equal PA scheme. The results indicate that PA scheme has a small effect on the sum-rates of DT mode and HDRCT mode, and it has a large effect on the sum-rates of FDRT mode. A first glance at the very large difference of the sum-rate achieved by FDRT mode (lower-right sub-figure of Fig. 3.6) at the high SNR regime under the optimized PA scheme

and the EPA scheme would suggest that there should also be a large difference of our proposed hybrid scheme under the optimized PA scheme and the EPA scheme in the same regime (top-left sub-figure of Fig. 3.6). However, as the results in Fig. 3.4 have shown, the probability of FDRT mode being selected is relatively small at the high SNR region. Thus the difference in the sum-rate achieved by the optimized PA scheme and the EPA scheme under FDRT mode at the high SNR region has a small effect on the our proposed hybrid scheme.

3.4.5 Fairness to Users

Finally, we look at the average transmission rate of each user under our proposed scheme (i.e., maximizing *weighted* sum-rate). For comparison, we also show the average transmission rate when all weights are equal, i.e., $\omega_n = 1$ and the sum-rate is maximized. Fig. 3.7 plots the average individual user transmission rate in a descending order when the maximum BS transmit power equals 20 dBm and INR = 3 dB. The results indicate that our proposed algorithm can provide a more balanced transmission rate (ranging from 3 bits/s/Hz to 6 bits/s/Hz) to all users while the maximizing sum-rate scheme gives a very diverse transmission rate (ranging from 1 bits/s/Hz to 11.7 bits/s/Hz) to users. In other words, our proposed scheme is fairer to all users in terms of resource allocation.

3.5 Summary

In this chapter, we have investigated resource allocation in OFDMA DL cooperative networks. We have formulated the combinatorial binary assignment optimization

problem of optimizing the subcarrier pairing, subcarrier assignment, relay selection, and transmission mode selection. We have transformed the binary assignment problem into an equivalent maximum weighted bipartite matching problem which can be solved by the classic Hungarian algorithm. Subsequently, we have considered the joint power allocation and binary assignment problem which is solved by the dual-based iterative algorithm. Specifically, the power allocation schemes of FD relay transmission mode and HD relay cooperative transmission mode are solved in semi-closed forms. Simulation results have shown that our proposed algorithm can achieve significant throughput gain compared to the other benchmark approaches.

Appendix 3.A Power Allocation in FDRT Mode

For simplicity, $p_{b,n,k_1}^{m,k_2,1}$, $p_{b,n,k_2}^{m,k_1,1}$, $p_{m,n,k_1}^{k_2,1}$, and $p_{m,n,k_2}^{k_1,1}$ are replaced by $p_{b,1}$, $p_{b,2}$, $p_{m,1}$, and $p_{m,2}$, respectively. In addition, α_{b,m,k_1}, α_{b,m,k_2}, α_{m,n,k_1}, α_{m,n,k_2}, α_{b,n,k_1}, and α_{b,n,k_2} are replaced by $\alpha_{b,1}$, $\alpha_{b,2}$, $\alpha_{m,1}$, $\alpha_{m,2}$, $\alpha'_{b,1}$, and $\alpha'_{b,2}$, respectively. Then, for a given set of (m, n, k_1, k_2), we transform the problem of maximizing (3.32a) into the following equivalent problem

$$\max_{\bar{\boldsymbol{p}}} \quad R_1 + R_2 - \Psi \tag{3.54}$$

$$s.t. \quad R_1 \leq \frac{1}{2}\log(1 + p_{b,2}\alpha_{b,2}) \tag{3.55}$$

$$R_1 \leq \frac{1}{2}\log(1 + \frac{p_{m,1}\alpha_{m,1}}{p_{b,1}\alpha'_{b,1} + 1}) \tag{3.56}$$

$$R_2 \leq \frac{1}{2}\log(1 + p_{b,1}\alpha_{b,1}) \tag{3.57}$$

$$R_2 \leq \frac{1}{2}\log(1 + \frac{p_{m,2}\alpha_{m,2}}{p_{b,2}\alpha'_{b,2} + 1}) \tag{3.58}$$

where $\bar{\boldsymbol{p}} = \{p_{b,1}, p_{b,2}, p_{m,1}, p_{m,2}\} \succeq 0$, and $\Psi = \lambda_{b,1}p_{b,1} + \lambda_{b,2}p_{b,2} + \lambda_{m,1}p_{m,1} + \lambda_{m,2}p_{m,2}$.

We first introduce non-negative Lagrangian multipliers $\mu_{1,1}$, $\mu_{1,2}$, $\mu_{2,1}$, and $\mu_{2,2}$ associated with the rate constraints (3.55), (3.56), (3.57), and (3.58), respectively. All of them are denoted as $\boldsymbol{\mu} \succeq \mathbf{0}$. Then the dual function of problem (3.54) can be defined as

$$\bar{g}(\boldsymbol{\mu}) \stackrel{\Delta}{=} \max_{\bar{\boldsymbol{p}}} \quad L(\bar{\boldsymbol{p}}), \tag{3.59}$$

where the Lagrangian is given by

$$\begin{aligned} L(\bar{\boldsymbol{p}}) &= R_1(1-\mu_{1,1}-\mu_{1,2}) + R_2(1-\mu_{2,1}-\mu_{2,2}) - \Psi \\ &+ \frac{\mu_{1,1}}{2}\log(1+p_{b,2}\alpha_{b,2}) + \frac{\mu_{1,2}}{2}\log(1+\frac{p_{m,1}\alpha_{m,1}}{p_{b,1}\alpha'_{b,1}+1}) \\ &+ \frac{\mu_{2,1}}{2}\log(1+p_{b,1}\alpha_{b,1}) + \frac{\mu_{2,2}}{2}\log(1+\frac{p_{m,2}\alpha_{m,2}}{p_{b,2}\alpha'_{b,2}+1}). \end{aligned} \tag{3.60}$$

To make sure the dual function is bounded, we have $\mu_{1,1}+\mu_{1,2} = 1$ and $\mu_{2,1}+\mu_{2,2} = 1$. By substituting these results into (3.60), the Lagrangian can be rewritten as

$$\begin{aligned} L(\bar{\boldsymbol{p}}) =& \frac{\mu_{1,1}}{2}\log(1+p_{b,2}\alpha_{b,2}) + \frac{\mu_{2,1}}{2}\log(1+p_{b,1}\alpha_{b,1}) - \Psi \\ &+ \frac{1-\mu_{1,1}}{2}\log(1+\frac{p_{m,1}\alpha_{m,1}}{p_{b,1}\alpha'_{b,1}+1}) + \frac{1-\mu_{2,1}}{2}\log(1+\frac{p_{m,2}\alpha_{m,2}}{p_{b,2}\alpha'_{b,2}+1}). \end{aligned} \tag{3.61}$$

By applying Karush-Kuhn-Tucker (KKT) conditions [89], i.e., equating the partial

derivatives of (3.60) over all the power variables $\bar{\boldsymbol{p}}$ to zeros, we can obtain

$$\frac{\partial L}{\partial p_{b,1}} = \frac{\mu_{2,1}\alpha_{b,1}}{2(1+p_{b,1}\alpha_{b,1})} + \frac{(1-\mu_{1,1})\alpha'_{b,1}}{2(1+p_{b,1}\alpha'_{b,1}+p_{m,1}\alpha_{m,1})}\frac{(1-\mu_{1,1})\alpha'_{b,1}}{2(1+p_{b,1}\alpha'_{b,1})} - \lambda_{b,1} = 0 \tag{3.62}$$

$$\frac{\partial L}{\partial p_{m,1}} = \frac{(1-\mu_{1,1})\alpha_{m,1}}{2(1+p_{b,1}\alpha'_{b,1}+p_{m,1}\alpha_{m,1})} - \lambda_{m,1} = 0 \tag{3.63}$$

$$\frac{\partial L}{\partial p_{b,2}} = \frac{\mu_{1,1}\alpha_{b,2}}{2(1+p_{b,2}\alpha_{b,2})} + \frac{(1-\mu_{2,1})\alpha'_{b,2}}{2(1+p_{b,2}\alpha'_{b,2}+p_{m,2}\alpha_{m,2})} - \frac{(1-\mu_{2,1})\alpha'_{b,2}}{2(1+p_{b,2}\alpha'_{b,2})} - \lambda_{b,2} = 0 \tag{3.64}$$

$$\frac{\partial L}{\partial p_{m,2}} = \frac{(1-\mu_{2,1})\alpha_{m,2}}{2(1+p_{b,2}\alpha'_{b,2}+p_{m,2}\alpha_{m,2})} - \lambda_{m,2} = 0. \tag{3.65}$$

To derive the power allocation scheme, one may formulate and solve a set of equations based on the KKT conditions, i.e., (3.62) to (3.65). This method is effective only when the objective function (3.61) and all the constraints are differentiable at all the feasible regions. However, the differentiations of the constraints are not unique in zero value. It means that the KKT-conditions-based method is not capable of finding the optimum solution in general.

We denote the optimal powers as $p^*_{b,1}$, $p^*_{b,2}$, $p^*_{m,1}$, and $p^*_{m,2}$. In order to derive the allocated powers, we firstly give the following lemma.

Lemma 3.1. *If $p^*_{m,1} = 0$, then $p^*_{b,2} = 0$. Similarly, $p^*_{b,1} = 0$ when $p^*_{m,2} = 0$.*

Proof. According to the expression of rate for FDRT mode in (3.1), it is easy to verify that the rate would be maximized when $p^*_{b,2} = 0$ if $p^*_{m,1} = 0$. Similar result can be applied into the fact that $p^*_{b,1} = 0$ when $p^*_{m,2} = 0$. □

Then, we give the explicit analysis of the power allocation scheme in four different cases:

- Case 1: $p^*_{m,1} = 0$ and $p^*_{m,2} = 0$. According to lemma 3.1, we can obtain $p^*_{b,1} = p^*_{b,2} = 0$.

- Case 2: $p^*_{m,1} > 0$ and $p^*_{m,2} = 0$. According to lemma 3.1, $p_{b,1} = 0$. Then, we examine the feasibility of Case 2. By substituting $p^*_{b,1} = 0$ into (3.63) and combining the fact that $p^*_{m,1} > 0$, we can conclude that Case 2 is feasible if $\frac{1-\mu_{1,1}}{2\lambda_{m,1}} - \frac{1}{\alpha_{m,1}} > 0$ and vice versa. If Case 2 is feasible, the exact value of $p^*_{m,1}$ is given by

$$p^*_{m,1} = \frac{1-\mu_{1,1}}{2\lambda_{m,1}} - \frac{1}{\alpha_{m,1}}. \tag{3.66}$$

  By substituting $p^*_{m,2} = 0$ into (3.64), $p^*_{b,2}$ can be derived as

$$p^*_{b,2} = \left[\frac{\mu_{1,1}}{2\lambda_{b,2}} - \frac{1}{\alpha_{b,2}}\right]^+. \tag{3.67}$$

- Case 3: $p^*_{m,1} = 0$ and $p^*_{m,2} > 0$. Similar to Case 2, we have $p^*_{b,2} = 0$. By substituting $p_{b,2} = 0$ into (3.65) and combining the fact that $p_{m,2} > 0$, we can conclude that Case 3 is feasible if $\frac{1-\mu_{2,1}}{2\lambda_{m,2}} - \frac{1}{\alpha_{m,2}} > 0$ and vice versa. If Case 3 is feasible, the exact value of $p_{m,2}$ is given by

$$p^*_{m,2} = \frac{1-\mu_{2,1}}{2\lambda_{m,2}} - \frac{1}{\alpha_{m,2}}. \tag{3.68}$$

  By substituting $p^*_{m,1} = 0$ into (3.62), $p^*_{b,1}$ can be derived as

$$p^*_{b,1} = \left[\frac{\mu_{2,1}}{2\lambda_{b,1}} - \frac{1}{\alpha_{b,1}}\right]^+. \tag{3.69}$$

- Case 4: $p^*_{m,1} > 0$ and $p^*_{m,2} > 0$. Since $p^*_{m,1} > 0$ and $p^*_{m,2} > 0$, (3.63) and (3.65) are satisfied. Then (3.62) and (3.64) can be simplified to (3.70) and (3.71), where $\chi_1 = 2\lambda_{m,1}\alpha'_{b,1}/\alpha_{m,1} - 2\lambda_{b,1}$ and $\chi_2 = 2\lambda_{m,2}\alpha'_{b,2}/\alpha_{m,2} - 2\lambda_{b,2}$. Thus, the allocated powers $p^*_{b,1}$ and $p^*_{b,2}$ are the non-negative real roots of equations (3.70) and (3.71), respectively. After obtaining the allocated BS powers, according to (3.63) and (3.65), we can allocate the relay powers as follows

$$p^*_{m,1} = \frac{1-\mu_{1,1}}{2\lambda_{m,1}} - \frac{1+p_{b,1}\alpha'_{b,1}}{\alpha_{m,1}} \tag{3.72}$$

$$p^*_{m,2} = \frac{1-\mu_{2,1}}{2\lambda_{m,2}} - \frac{1+p_{b,2}\alpha'_{b,2}}{\alpha_{m,2}}. \tag{3.73}$$

  It is also necessary to check the feasibility of Case 4. If both (3.70) and (3.71) have non-negative real roots, and $\frac{1-\mu_{1,1}}{2\lambda_{m,1}} - \frac{1+p^*_{b,1}\alpha'_{b,1}}{\alpha_{m,1}} > 0$ and $\frac{1-\mu_{2,1}}{2\lambda_{m,2}} - \frac{1+p^*_{b,2}\alpha'_{b,2}}{\alpha_{m,2}} > 0$ under the given source powers $p^*_{b,1}$ and $p^*_{b,2}$, Case 4 is feasible; otherwise, Case 4 is not feasible.

We compare the Lagrangian function (3.61) with different power allocation schemes in four cases, and choose the one with largest value of the Lagrangian function as the optimal power allocation scheme.

The allocated powers depend on the dual variables $\boldsymbol{\mu}$. The dual optimization problem is given by

$$\begin{aligned} \min_{\boldsymbol{\mu} \succeq \mathbf{0}} \quad & \bar{g}(\boldsymbol{\mu}) \\ s.t. \quad & \boldsymbol{\mu} \succeq \mathbf{0} \end{aligned} \tag{3.74}$$

As described in Section 3.3.2, a dual function is always convex. Hence, subgradient-

Algorithm 2 Algorithm for Power Allocation in FDRT mode

1: Initialize $\boldsymbol{\mu}$
   $\epsilon_\mu > 0$ (convergence tolerance of iterations)
2: **while** $\boldsymbol{\mu}^{(l)} - \boldsymbol{\mu}^{(l-1)} \leq \epsilon_\mu$ **do**
3: Compare the Lagrangian function (3.61) with different power allocation schemes in four cases. Choose the ones with largest value of the Lagrangian function as the optimal powers $p_{b,1}^{(l)}$, $p_{b,2}^{(l)}$, $p_{m,1}^{(l)}$, and $p_{m,2}^{(l)}$.
4: Update $\boldsymbol{\mu}$ using ellipsoid method with gradient of the constraints (3.75) and (3.76).
5: $l \leftarrow l + 1$.
6: **end while**
7: The optimal powers are given by $p_{b,1}^{(l-1)}$, $p_{b,2}^{(l-1)}$, $p_{m,1}^{(l-1)}$, and $p_{m,2}^{(l-1)}$.
8: **return**

based methods, e.g., ellipsoid method, can be used to minimize $\bar{g}(\boldsymbol{\mu})$ with guaranteed convergence [89]. In this chapter, we use ellipsoid method to update $\boldsymbol{\mu}$ based on the following subgradient vectors:

$$\Delta\mu_{1,1} = \log(1 + p_{b,2}\alpha_{b,2}) - \log(1 + \frac{p_{m,1}\alpha_{m,1}}{p_{b,1}\alpha'_{b,1} + 1}) \tag{3.75}$$

$$\Delta\mu_{2,1} = \log(1 + p_{b,1}\alpha_{b,1}) - \log(1 + \frac{p_{m,2}\alpha_{m,2}}{p_{b,2}\alpha'_{b,2} + 1}). \tag{3.76}$$

We note that the duality gap between the dual problem (3.59) and primary problem (3.54) is non-zero due to the non-convexity of rate constraints (3.56) and (3.58). However, according to the results in [86], the duality gap goes to zero as the number of subcarrier tends to infinity. It is also worth to mention that for given dual variables $\boldsymbol{\lambda}$, we introduce new dual variables $\boldsymbol{\mu}$ to decompose the problem (3.54) into a solvable problem. Hence, we named this method as *hierarchical dual method*. To sum up, the entire algorithm for power allocation in FDRT mode is given in Algorithm 1.

Appendix 3.B Derivations for (3.40) to (3.42)

By equating the partial derivative of $L_{m,n}^{k_1,k_2,2}$ in (3.35) over $p_{b,n,k_1}^{m,k_2,2}$, $p_{b,n,k_2}^{m,k_1,2}$ and $p_{m,n,k_2}^{k_1,2}$ to zeros, and after some manipulations, the closed-forms of optimal power allocations $p_{b,n,k_1}^{m,k_2,2*}$, $p_{b,n,k_2}^{m,k_1,2*}$ and $p_{m,n,k_2}^{k_1,2*}$ can be readily obtained as

$$\frac{\alpha_{b,n,k_1}}{2(1+\gamma_{m,n}^{k_1,k_2})} = \lambda_{b,1} + \nu(\alpha_{b,n,k_1} - \alpha_{b,m,k_1}) \tag{3.77}$$

$$\frac{(\alpha_{b,n,k_2} + \eta\alpha_c)}{2(1+\gamma_{m,n}^{k_1,k_2})} = \lambda_{b,2} + \nu(\alpha_{b,n,k_2} + \eta\alpha_c) \tag{3.78}$$

$$\frac{(\alpha_{m,n,k_2} + \alpha_c/\eta)}{2(1+\gamma_{m,n}^{k_1,k_2})} = \lambda_{m,2} + \nu(\alpha_{m,n,k_2} + \alpha_c/\eta) \tag{3.79}$$

where

$$\eta = p_{b,n,k_2}^{m,k_1,2}/p_{m,n,k_2}^{k_1,2} \tag{3.80}$$

$$\alpha_c = \sqrt{\alpha_{b,n,k_2}\alpha_{m,n,k_2}}. \tag{3.81}$$

Eliminating $\gamma_{m,n}^{k_1,k_2}$ and ν by using (3.77) to (3.79), we obtain

$$\lambda_{m,2}\alpha_c\eta^2 + (\lambda_{m,2}\alpha_{b,n,k_2} - \lambda_{b,2}\alpha_{m,n,k_2})\eta - \lambda_{b,2}\alpha_c = 0. \tag{3.82}$$

Based on the solution for a quadratic equation, it is easy to obtain that (3.82) has one and only one positive root, which is

$$\begin{aligned}\eta^* =& \frac{1}{2\lambda_{m,2}\alpha_c}\left(-(\lambda_{m,2}\alpha_{b,n,k_2} - \lambda_{b,2}\alpha_{m,n,k_2})\right. \\ &\left. + \sqrt{(\lambda_{m,2}\alpha_{b,n,k_2} - \lambda_{b,2}\alpha_{m,n,k_2})^2 + \lambda_{m,2}\lambda_{b,2}\alpha_c^2}\right).\end{aligned} \tag{3.83}$$

By substituting (3.83) into (3.77) and (3.78) and eliminating ν, $\gamma_{m,n}^{k_1,k_2}$ can be derived as

$$\gamma_{m,n}^{k_1,k_2*} = \frac{(\alpha_{b,n,k_2} + \eta\alpha_c)/2}{\lambda_{b,2}(\alpha_{b,n,k_1} - \alpha_{b,m,k_1}) - \lambda_{b,1}(\alpha_{b,n,k_2} + \eta\alpha_c)} - 1. \tag{3.84}$$

Since ν is the Lagrange multiplier of (3.37), based on the KKT conditions, we have to guarantee

$$\nu(p_{b,n,k_1}^{m,k_2,2*}\alpha_{b,m,k_1} - \gamma_{m,n}^{k_1,k_2*}) = 0. \tag{3.85}$$

Since ν cannot be guaranteed to be zero, we have

$$p_{b,n,k_1}^{m,k_2,2*}\alpha_{b,m,k_1} - \gamma_{m,n}^{k_1,k_2*} = 0. \tag{3.86}$$

As a result, we obtain $p_{b,n,k_1}^{m,k_2,2*}$ in (3.40). Then, according to (3.40), (3.84) and (3.80), $p_{b,n,k_2}^{m,k_1,2*}$ and $p_{m,n,k_2}^{k_1,2*}$ are given in (3.41) and (3.42), respectively. We also have to evaluate the feasible region. In order to ensure that all the powers be positive, we have $\gamma_{m,n}^{k_1,k_2*} > 0$ and $\alpha_{b,m,k_1} - \alpha_{b,n,k_1} > 0$. Thus, we readily have the results.

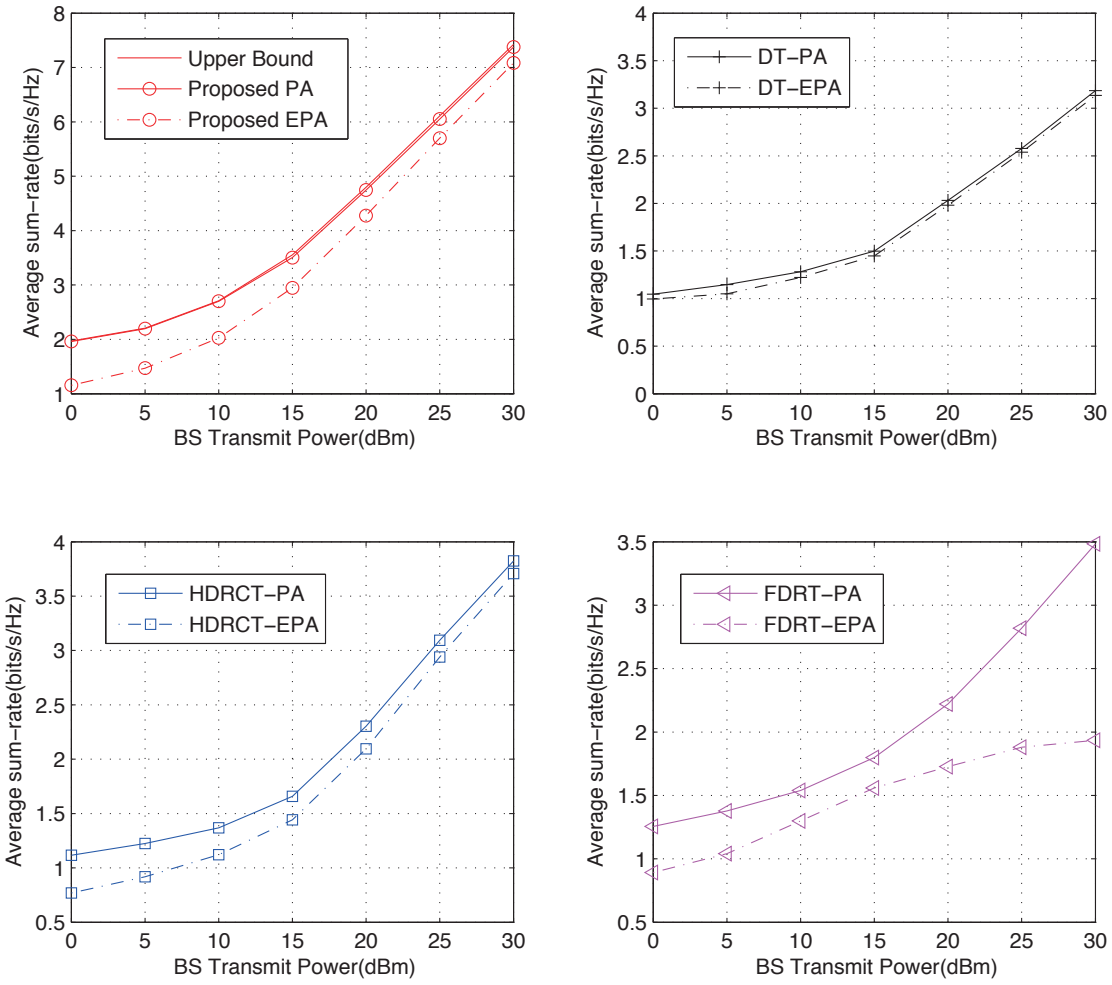

Figure 3.6: Average sum-rate versus BS transmit power of the proposed PA scheme compared with EPA scheme for INR = 3 dB.

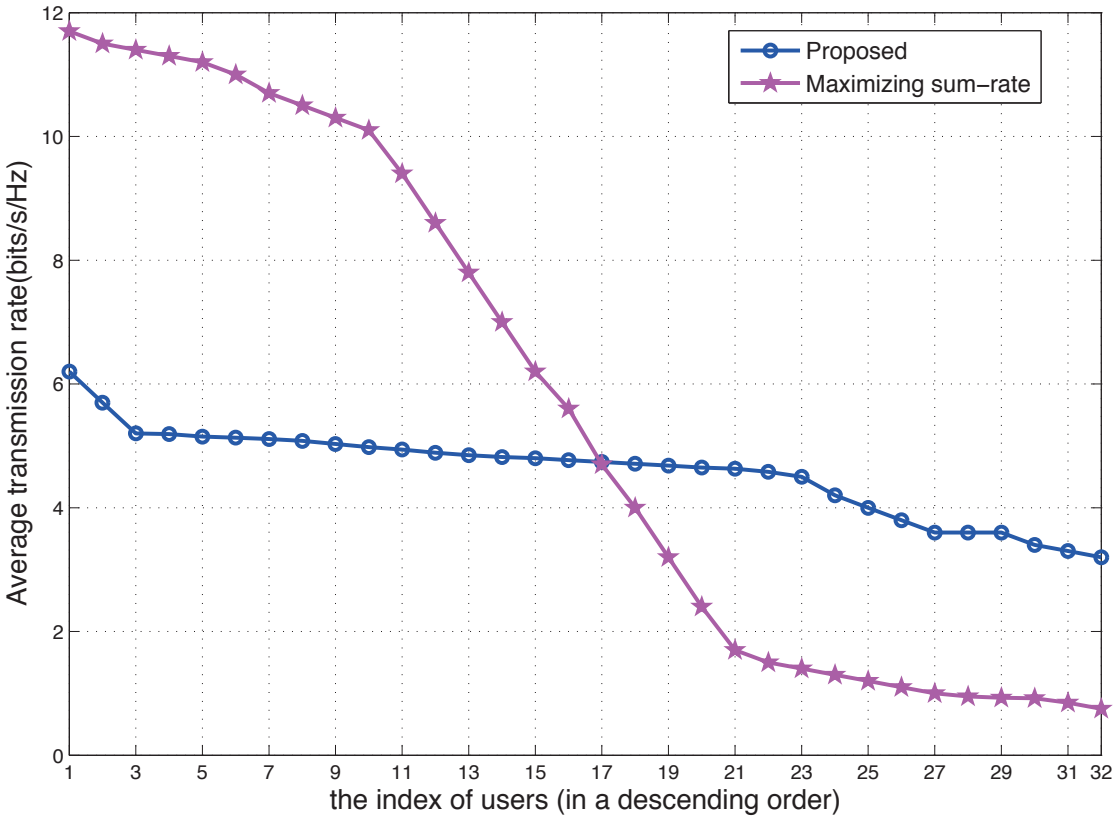

Figure 3.7: Average individual user transmission rate in a descending order when the maximum BS transmit power equals 20 dBm and INR = 3 dB.

$$\chi_1\alpha_{b,1}\alpha'_{b,1}p_{b,1}^2 + (\chi_1(\alpha_{b,1}+\alpha'_{b,1}) + (\mu_{2,1}+\mu_{1,1}-1)\alpha_{b,1}\alpha'_{b,1})p_{b,1} + \chi_1 + \mu_{2,1}\alpha_{b,1} + (1-\mu_{1,1})\alpha'_{b,1} = 0 \tag{3.70}$$

$$\chi_2\alpha_{b,2}\alpha'_{b,2}p_{b,2}^2 + (\chi_2(\alpha_{b,2}+\alpha'_{b,2}) + (\mu_{1,1}+\mu_{2,1}-1)\alpha_{b,2}\alpha'_{b,2})p_{b,2} + \chi_2 + \mu_{1,1}\alpha_{b,2} + (1-\mu_{2,1})\alpha'_{b,2} = 0 \tag{3.71}$$

Chapter 4

Max-Min Weighted downlink SINR with uplink SINR Constraints for full-duplex MIMO Systems

In this chapter, we investigate the max-min weighted SINR problem in a FD multi-user MIMO system, where each user is equipped with a single antenna. Instead of optimizing the joint UL and DL max-min weighted SINR, we consider a more practical scenario in which the DL minimum weighted SINR is maximized under some target SINR constraints for UL users. Specifically, the system should first guarantee the quality of service (QoS) of UL users before sharing the spectrum resources to the DL users. We consider jointly (i) the transmit beamforming at the BS, (ii) the receive beamforming at the BS, (iii) the transmit powers at the

BS, and (iv) the transmit powers at the UL users, such that the UL users can be provided with specific SINRs and the SINRs of the DL users should be balanced and maximized. Since the additional SINR constraints are not non-negative power constraints, the problem cannot be solved directly or with trivial transformations by the Perron-Frobenius theory or other existing algorithms.

To tackle the aforementioned problem, we propose an iterative optimization algorithm which is proved to be convergent. The proposed algorithm iteratively optimizes (i) the power control and receive beamforming, and then (ii) the power control and transmit beamforming. By fixing the transmit and receive beamforming at the BS, we first transform the original problem into a standard SISO max-min weighted SINR problem with multiple SINR constraints and multiple power constraints. Under the single power constraint scenario, we also derive the network duality of the optimization problem. Based on the network duality principle, we show that the optimization problem with multiple power constraints can be decoupled into subproblems each with a single power constraint. Subsequently, we apply the Perron-Frobenius theory and subgradient projection-based method to solve the transformed SISO max-min weighted SINR problem with multiple power constraints and multiple SINR constraints. By using network duality and minimum-mean-squared-error (MMSE) criterion, the transmit and receive beamforming can be iteratively derived accordingly.

The remaining chapter is organized as follows. In Section 4.1, we describe the system model and problem formulation. In Section 4.2, we derive the optimization algorithm when the transmit and receive beamforming are fixed. In Section 4.3, we propose optimization algorithms for the max-min weighted SINR problem by consid-

ering both power and beamforming and prove their convergence. The performance of the proposed algorithm is compared with that of other optimization techniques in Section 4.4. Finally, a summary is given in Section 4.5.

4.1 System Model and Problem Formulation

Referring to Fig. 4.1, we consider a single-cell FD wireless communication system in which a FD BS is designed to communicate with K_d single-antenna users in the DL transmission and K_u single-antenna users in the UL transmission at the same time and frequency band. The total number of users is denoted as $K = K_d + K_u$. Furthermore, there is a total of $N_T + N_R$ antennas at the BS, where N_T represents the number of transmit antennas for DL data transmissions and N_R represents the number of receive antennas for UL data receptions.

We generalize the FD system into a MIMO network where K independent data streams are transmitted over a common frequency band. We denote the transmitter and receiver of the k-th stream by t_k and r_k, respectively. We also define the following sets: $\mathcal{K} = \{1, \ldots, K\}$, $\mathcal{K}_d = \{1, \ldots, K_d\}$ and $\mathcal{K}_u = \{K_d + 1, \ldots, K\}$. When $k \in \mathcal{K}_d$, (i) t_k represents the transmitter at the BS for the k-th DL user and $N_{t_k} = N_T$; and (ii) r_k represents the DL user and $N_{r_k} = 1$. However, when $k \in \mathcal{K}_u$, (i) t_k represents the transmitter of the k-th UL user and $N_{t_k} = 1$; and (ii) r_k represents the receiver at the BS for the k-th user and $N_{r_k} = N_R$. We further assume that the channels suffer from flat fading but channel state information (CSI) is perfectly known at both the BS and users.

We model the equivalent MIMO network as a Gaussian broadcast channel

which is given by

$$\mathbf{y}_k = \sum_{l=1}^{K} \mathbf{H}_{kl}\mathbf{x}_l + \mathbf{z}_k, \quad k \in \mathcal{K} \tag{4.1}$$

where $\mathbf{y}_k \in \mathbb{C}^{N_{r_k}}$ is the received signal vector at r_k, $\mathbf{x}_l \in \mathbb{C}^{N_{t_l}}$ is the transmitted signal vector of the transmitter t_l, i.e., l-th stream, $\mathbf{H}_{kl} \in \mathbb{C}^{N_{r_k} \times N_{t_l}}$ is the channel vector between t_l and r_k, $\mathbf{z}_k \sim \mathcal{CN}(\mathbf{0}, n_k\mathbf{I})$ is the circularly symmetric Gaussian noise vector at r_k with covariance $n_k\mathbf{I}$ and $n_k \in \mathbb{R}_{>0}$. Specifically, when $l \in \mathcal{K}_d$ and $k \in \mathcal{K}_u$, $\mathbf{H}_{kl}$ represents the SI channel between the transmit antennas and the receive antennas at the FD BS, and its entries are determined by the capability of the SI cancellation techniques. When $l \in \mathcal{K}_u$ and $k \in \mathcal{K}_d$, $\mathbf{H}_{kl}$ represents the IUI channel between the UL t_l and the DL r_k.

We assume linear transmit and receive beamforming. The transmitted signal vector of the l-th stream ($l \in \mathcal{K}$) can be written as $\mathbf{x}_l = \sqrt{p_l}\mathbf{w}_l s_l$, where $\mathbf{w}_l \in \mathbb{C}^{N_{t_l} \times 1}$ is the normalized transmit beamformer, and s_l and p_l are the information signal and transmit power, respectively. The k-th received stream $\mathbf{y}_k$ ($k \in \mathcal{K}$) is decoded using a normalized receive beamformer $\mathbf{v}_k \in \mathbb{C}^{N_{r_k} \times 1}$. We denote $\mathbf{p} = [p_1, \ldots, p_K]^T$ as the power vector and $\mathbf{n} = [n_1, \ldots, n_K]^T$ as the noise covariance vector. We also denote $\mathbb{W} = (\mathbf{w}_1, \ldots, \mathbf{w}_K)$ as the tuples of transmit beamformers and $\mathbb{V} = (\mathbf{v}_1, \ldots, \mathbf{v}_K)$ as the tuples of receive beamformers. Recall that each user is equipped with a single antenna. Therefore, we have

$$\mathbf{w}_k \in \mathbb{C}^{N_T \times 1} \quad \text{and} \quad \mathbf{v}_k = 1, \qquad \forall k \in \mathcal{K}_d; \tag{4.2}$$

$$\mathbf{w}_k = 1 \quad \text{and} \quad \mathbf{v}_k \in \mathbb{C}^{N_R \times 1}, \qquad \forall k \in \mathcal{K}_u. \tag{4.3}$$

We define a matrix $\mathbf{G} \in \mathbb{R}_{\geq \mathbf{0}}^{\mathbf{K} \times \mathbf{K}}$ in which the (k, l)-th element G_{kl} represents

the effective link gain between t_l and r_k, i.e.,

$$G_{kl} = |\mathbf{v}_k^\dagger \mathbf{H}_{kl} \mathbf{w}_l|^2. \tag{4.4}$$

Applying (4.2) and (4.3) to (4.4), we obtain

$$G_{kl} = \begin{cases} |\mathbf{H}_{kl}\mathbf{w}_l|^2 & \text{if } k,l \in \mathcal{K}_d \\ |\mathbf{v}_k^\dagger \mathbf{H}_{kl}|^2 & \text{if } k,l \in \mathcal{K}_u \\ |\mathbf{H}_{kl}|^2 & \text{if } k \in \mathcal{K}_d \text{ and } l \in \mathcal{K}_u \\ |\mathbf{v}_k^\dagger \mathbf{H}_{kl}\mathbf{w}_l|^2 & \text{if } k \in \mathcal{K}_u \text{ and } l \in \mathcal{K}_d. \end{cases} \tag{4.5}$$

The SINR of the k-th received stream can hence be expressed as

$$\mathrm{SINR}_k(\mathbf{p}, \mathbb{W}, \mathbb{V}) = \frac{p_k G_{kk}}{\left(\sum_{l \in \mathcal{K}, l \neq k} p_l G_{kl}\right) + n_k}, \quad \forall k \in \mathcal{K} \tag{4.6}$$

$$= \begin{cases} \frac{p_k |\mathbf{H}_{kk}\mathbf{w}_k|^2}{\left(\sum_{l \in \mathcal{K}, l \neq k} p_l |\mathbf{H}_{kl}\mathbf{w}_l|^2\right) + n_k} \triangleq \mathrm{SINR}_k^{\mathrm{DL}}(\mathbf{p}, \mathbb{W}) & \text{if } k \in \mathcal{K}_d \\ \frac{p_k |\mathbf{v}_k^\dagger \mathbf{H}_{kk}|^2}{\left(\sum_{l \in \mathcal{K}, l \neq k} p_l |\mathbf{v}_k^\dagger \mathbf{H}_{kl}\mathbf{w}_l|^2\right) + n_k} \triangleq \mathrm{SINR}_k^{\mathrm{UL}}(\mathbf{p}, \mathbb{W}, \mathbb{V}) & \text{if } k \in \mathcal{K}_u \end{cases} \tag{4.7}$$

where (4.2)–(4.5) have been applied in arriving at the second equality, and $\mathrm{SINR}_k^{\mathrm{DL}}(\mathbf{p}, \mathbb{W})$ and $\mathrm{SINR}_k^{\mathrm{UL}}(\mathbf{p}, \mathbb{W}, \mathbb{V})$ are defined as the DL (DL) and UL (UL) SINR, respectively. Applying (4.5) again, we can re-write $\mathrm{SINR}_k^{\mathrm{DL}}(\mathbf{p}, \mathbb{W})$ and $\mathrm{SINR}_k^{\mathrm{UL}}(\mathbf{p}, \mathbb{W}, \mathbb{V})$ as fol-

lows.

$$\mathrm{SINR}_k^{\mathrm{DL}}(\mathbf{p},\mathbb{W}) = \frac{p_k|\mathbf{H}_{kk}\mathbf{w}_k|^2}{\left(\sum_{l\in\mathcal{K}_d,l\neq k} p_l|\mathbf{H}_{kl}\mathbf{w}_l|^2\right)+\left(\sum_{l\in\mathcal{K}_u} p_l|\mathbf{H}_{kl}|^2\right)+n_k} \quad \forall k\in\mathcal{K}_d \tag{4.8}$$

$$\mathrm{SINR}_k^{\mathrm{UL}}(\mathbf{p},\mathbb{W},\mathbb{V}) = \frac{p_k|\mathbf{v}_k^\dagger\mathbf{H}_{kk}|^2}{\left(\sum_{l\in\mathcal{K}_d} p_l|\mathbf{v}_k^\dagger\mathbf{H}_{kl}\mathbf{w}_l|^2\right)+\left(\sum_{l\in\mathcal{K}_u,l\neq k} p_l|\mathbf{v}_k^\dagger\mathbf{H}_{kl}|^2\right)+n_k} \quad \forall k\in\mathcal{K}_u \tag{4.9}$$

Our target is to maximize the minimum weighted SINR of the DL streams when the UL streams have to satisfy certain SINR constraints. We therefore formulate the problem as

$$\mathcal{P}: \max_{\mathbf{p},\mathbb{W},\mathbb{V}} \quad \min_{k_d\in\mathcal{K}_d} \frac{\mathrm{SINR}_{k_d}^{\mathrm{DL}}(\mathbf{p},\mathbb{W})}{\beta_{k_d}} \tag{4.10a}$$

$$s.t. \quad \mathrm{SINR}_{k_u}^{\mathrm{UL}}(\mathbf{p},\mathbb{W},\mathbb{V}) \geq \beta_{k_u}, \quad \forall k_u\in\mathcal{K}_u \tag{4.10b}$$

$$\mathbf{t}_i^T\mathbf{p}\leq P_i, \quad \mathbf{p}\geq\mathbf{0}, \quad \forall i=0,1,\ldots,K_u \tag{4.10c}$$

$$||\mathbf{w}_k||=1, \quad ||\mathbf{v}_k||=1, \quad \forall k\in\mathcal{K} \tag{4.10d}$$

where $1/\beta_{k_d}$ is the weight assigned to the k_d-th DL user; β_{k_u} is the pre-assigned SINR constraint for the UL user corresponding to k_u (i.e., the (k_u-K_d)-th UL user); $\mathbf{t}_0=[\overbrace{1,\ldots,1}^{K_d},\overbrace{0,\ldots,0}^{K_u}]^T$, $\mathbf{t}_i=[\overbrace{0,\ldots,0}^{K_d},\overbrace{\underbrace{0,\ldots,0}_{i-1},1,\underbrace{0,\ldots,0}_{K_u-i}}^{K_u}]^T$ for $i=1,\ldots,K_u$; P_0 is the total power constraint at the BS; P_i is the individual power constraint of the i-th UL user ($i=1,\ldots,K_u$); and $\mathbf{0}$ is an all-zero vector of appropriate size. We also define $\boldsymbol{\beta}=[\beta_1,\ldots,\beta_K]$ in which the k-th element is related to the weight or constraint assigned to the SINR of the k-th stream.

4.2 Power optimization with Fixed Beamforming

In this section, we fix the transmit and receive beamforming vectors and aim to optimize the power vector $\mathbf{p}$. The problem $\mathcal{T}$, under the problem $\mathcal{P}$ with fixed beamforming vectors, is defined as

$$\mathcal{T}: \max_{\mathbf{p}} \quad \min_{k_d \in \mathcal{K}_d} \frac{\mathrm{SINR}_{k_d}^{\mathrm{DL}}(\mathbf{p})}{\beta_{k_d}} \tag{4.11a}$$

$$s.t. \quad \mathrm{SINR}_{k_u}^{\mathrm{UL}}(\mathbf{p}) \geq \beta_{k_u}, \quad \forall k_u \in \mathcal{K}_u \tag{4.11b}$$

$$\mathbf{t}_i^T \mathbf{p} \leq P_i, \quad \mathbf{p} \geq \mathbf{0}, \quad \forall i = 0, 1, \ldots, K_u \tag{4.11c}$$

where $\mathrm{SINR}_k(\mathbf{p}) = \mathrm{SINR}_k(\mathbf{p}, \mathbb{W}, \mathbb{V})$ with fixed $\mathbb{W}$ and $\mathbb{V}$. It can be seen that $\mathcal{T}$ is a max-min power optimization problem (refer to (4.11a) with multiple power constraints ($P_0, P_1, \ldots, P_{K_u}$ in (4.11c) and multiple SINR constraints ($\beta_{K_d+1}, \beta_{K_d+2}, \ldots, \beta_{K_d+K_u}$ in (4.11b). Next, we consider $\mathcal{T}$ under a certain i and formulate the new problem as

$$\mathcal{T}^i: \max_{\mathbf{p}} \quad \min_{k_d \in \mathcal{K}_d} \frac{\mathrm{SINR}_{k_d}^{\mathrm{DL}}(\mathbf{p})}{\beta_{k_d}} \tag{4.12a}$$

$$s.t. \quad \mathrm{SINR}_{k_u}^{\mathrm{UL}}(\mathbf{p}) \geq \beta_{k_u}, \quad \forall k_u \in \mathcal{K}_u \tag{4.12b}$$

$$\mathbf{t}_i^T \mathbf{p} \leq P_i, \quad \mathbf{p} \geq \mathbf{0}. \tag{4.12c}$$

Due to the fixed i, $\mathcal{T}^i$ is a problem with a single power constraint (P_i in (4.12c) and multiple SINR constraints ($\beta_{K_d+1}, \beta_{K_d+2}, \ldots, \beta_{K_d+K_u}$ in (4.12b)). $\mathcal{T}^i$ can also be re-formulated as

$$\mathcal{T}^i: \max_{\tau^i, \mathbf{p}} \quad \tau^i \tag{4.13a}$$

$$s.t. \quad \tau^i \leq \frac{\mathrm{SINR}_{k_d}^{\mathrm{DL}}(\mathbf{p})}{\beta_{k_d}}, \quad \forall k_d \in \mathcal{K}_d \tag{4.13b}$$

$$\mathrm{SINR}_{k_u}^{\mathrm{UL}}(\mathbf{p}) \geq \beta_{k_u}, \quad \forall k_u \in \mathcal{K}_u \tag{4.13c}$$

$$\mathbf{t}_i^T \mathbf{p} \leq P_i, \quad \mathbf{p} \geq \mathbf{0} \tag{4.13d}$$

where τ^i is simply an auxiliary variable.

Lemma 4.1. *Under the optimal solutions of $\mathcal{T}^i$, the constraints in* (4.13b), (4.13c) *and* (4.13d) *must be satisfied with equality for all $k_d \in \mathcal{K}_d$ and $k_u \in \mathcal{K}_u$. That is to say,*

$$\hat{\tau}^i = \frac{\mathrm{SINR}_{k_d}^{\mathrm{DL}}(\hat{\mathbf{p}}^i)}{\beta_{k_d}}, \quad \forall k_d \in \mathcal{K}_d \tag{4.14a}$$

$$\mathrm{SINR}_{k_u}^{\mathrm{UL}}(\hat{\mathbf{p}}^i) = \beta_{k_u}, \quad \forall k_u \in \mathcal{K}_u \tag{4.14b}$$

$$\mathbf{t}_i^T \hat{\mathbf{p}}^i = P_i, \quad \hat{\mathbf{p}}^i \geq \mathbf{0} \tag{4.14c}$$

where $\hat{\tau}^i$ and $\hat{\mathbf{p}}^i$ are the optimal solutions.

Proof. Refer to Appendix 4.A. □

Theorem 4.1. *Let $\hat{\mathbf{p}}^i$ denote the unique solution and $\hat{\tau}^i$ be the optimal value of $\mathcal{T}^i$. Also, let $s = \arg\min_{i=0,\ldots,K_u} \hat{\tau}^i$. Then the optimal value and unique solution of the original problem $\mathcal{T}$ are given by $\hat{\tau} = \hat{\tau}^s$ and $\hat{\mathbf{p}} = \hat{\mathbf{p}}^s$, respectively.*

Proof. Refer to Appendix 4.B. □

4.2.1 Solving the Single-Power-and-Multiple-SINR-Constraint Problem

Theorem 4.1 shows that $\mathcal{T}$ can be solved by separately solving $K_u + 1$ single-power-and-multiple-SINR-constraint sub-problems $\mathcal{T}^i$. In the following, we describe the way to solving these sub-problems $\mathcal{T}^i$.

We define a cross-channel interference matrix $\mathbf{F} \in \mathbb{R}_{\geq 0}^{K \times K}$ and a weighted vector $\tilde{\boldsymbol{\beta}} \in \mathbb{R}_{\geq 0}^{1 \times K}$ as follows:

$$F_{kl} = \begin{cases} 0, & \text{if } l = k \\ G_{kl}, & \text{if } l \neq k \end{cases} \qquad l, k \in \mathcal{K} \tag{4.15}$$

$$\tilde{\boldsymbol{\beta}} = \left(\frac{\beta_1}{G_{11}}, \cdots, \frac{\beta_K}{G_{KK}} \right). \tag{4.16}$$

Then, the weighted SINR of the k-th stream can be rewritten as

$$\frac{\mathrm{SINR}_k(\hat{\mathbf{p}}^i)}{\beta_k} = \frac{p_k}{\left[\mathrm{diag}(\tilde{\boldsymbol{\beta}})(\mathbf{F}\hat{\mathbf{p}}^i + \mathbf{n}) \right]_k}, \quad k \in \mathcal{K} \tag{4.17}$$

where the subscript k in $\left[\mathrm{diag}(\tilde{\boldsymbol{\beta}})(\mathbf{F}\hat{\mathbf{p}}^i + \mathbf{n}) \right]_k$ denotes the k-th element of the vector $\left[\mathrm{diag}(\tilde{\boldsymbol{\beta}})(\mathbf{F}\hat{\mathbf{p}}^i + \mathbf{n}) \right]$. We further decompose the cross-channel interference matrix $\mathbf{F}$ into

$$\mathbf{F} = \begin{bmatrix} \mathbf{F}_{dd} & \mathbf{F}_{du} \\ \mathbf{F}_{ud} & \mathbf{F}_{uu} \end{bmatrix} \tag{4.18}$$

where $\mathbf{F}_{dd}$ is a matrix of size $K_d \times K_d$, $\mathbf{F}_{du}$ of size $K_d \times K_u$, $\mathbf{F}_{ud}$ of size $K_u \times K_d$,

and $\mathbf{F}_{uu}$ of size $K_u \times K_u$. We split $\tilde{\boldsymbol{\beta}}$ into

$$\tilde{\boldsymbol{\beta}} = [\boldsymbol{\beta}_d, \boldsymbol{\beta}_u] \tag{4.19}$$

where $\boldsymbol{\beta}_d$ is a vector of length K_d and $\boldsymbol{\beta}_u$ is of length K_u. Then $\text{diag}(\tilde{\boldsymbol{\beta}})$ can be written as

$$\text{diag}(\tilde{\boldsymbol{\beta}}) = \begin{bmatrix} \mathbf{B_d} & \mathbf{0} \\ \mathbf{0} & \mathbf{B_u} \end{bmatrix} \tag{4.20}$$

where $\mathbf{B_d} = \text{diag}(\tilde{\boldsymbol{\beta}}_\mathbf{d})$ and $\mathbf{B_u} = \text{diag}(\tilde{\boldsymbol{\beta}}_\mathbf{u})$.

In Lemma 4.1, we have proved that under the optimal solutions of $\mathcal{T}^i$, (4.14a), (4.14b) and (4.14c) become valid. We divide $\hat{\mathbf{p}}^i$, $\mathbf{n}$ and $\mathbf{t}_i$ into

$$\hat{\mathbf{p}}^i = \begin{bmatrix} \hat{\mathbf{p}}^i_d \\ \hat{\mathbf{p}}^i_u \end{bmatrix} \tag{4.21}$$

$$\mathbf{n} = \begin{bmatrix} \mathbf{n}_d \\ \mathbf{n}_u \end{bmatrix} \tag{4.22}$$

$$\mathbf{t}_i = \begin{bmatrix} \mathbf{t}_{i,d} \\ \mathbf{t}_{i,u} \end{bmatrix} \tag{4.23}$$

where $\hat{\mathbf{p}}^i_d$, $\mathbf{n}_d$ and $\mathbf{t}_{i,d}$ are vectors of size K_d; and $\hat{\mathbf{p}}^i_u$, $\mathbf{n}_u$ and $\mathbf{t}_{i,u}$ are of size K_u. We then re-write (4.14a), (4.14b) and (4.14c) as follows.

$$\frac{1}{\hat{\tau}^i}\hat{\mathbf{p}}^i_d = \mathbf{B}_d\mathbf{F}_{dd}\hat{\mathbf{p}}^i_d + \mathbf{B}_d\mathbf{n}_d + \mathbf{B}_d\mathbf{F}_{du}\hat{\mathbf{p}}^i_u \tag{4.24}$$

$$\hat{\mathbf{p}}^i_u = \mathbf{B}_u\mathbf{F}_{uu}\hat{\mathbf{p}}^i_u + \mathbf{B}_u\mathbf{n}_u + \mathbf{B}_u\mathbf{F}_{ud}\hat{\mathbf{p}}^i_d \tag{4.25}$$

$$P_i = \mathbf{t}^T_{i,d}\hat{\mathbf{p}}^i_d + \mathbf{t}^T_{i,u}\hat{\mathbf{p}}^i_u \tag{4.26}$$

Using (4.25) and assuming that $(\mathbf{I} - \mathbf{B}_u\mathbf{F}_{uu})$ is invertible, we have

$$\hat{\mathbf{p}}_u^i = (\mathbf{I} - \mathbf{B}_u\mathbf{F}_{uu})^{-1}\mathbf{B}_u\mathbf{n}_u + (\mathbf{I} - \mathbf{B}_u\mathbf{F}_{uu})^{-1}\mathbf{B}_u\mathbf{F}_{ud}\hat{\mathbf{p}}_d^i. \tag{4.27}$$

By substituting (4.27) into (4.24), we further obtain

$$\frac{1}{\hat{\tau}^i}\hat{\mathbf{p}}_d^i = \mathbf{E}\hat{\mathbf{p}}_d^i + \mathbf{e} \tag{4.28}$$

where

$$\mathbf{E} = \mathbf{B}_d\mathbf{F}_{dd} + \mathbf{B}_d\mathbf{F}_{du}(\mathbf{I} - \mathbf{B}_u\mathbf{F}_{uu})^{-1}\mathbf{B}_u\mathbf{F}_{ud} \tag{4.29}$$

$$\mathbf{e} = \mathbf{B}_d\mathbf{n}_d + \mathbf{B}_d\mathbf{F}_{du}(\mathbf{I} - \mathbf{B}_u\mathbf{F}_{uu})^{-1}\mathbf{B}_u\mathbf{n}_u. \tag{4.30}$$

Similarly, we substitute (4.27) into (4.26) and obtain

$$P_i' = \mathbf{g}_i\hat{\mathbf{p}}_d^i \tag{4.31}$$

where

$$P_i' = P_i - \mathbf{t}_{i,u}^T(\mathbf{I} - \mathbf{B}_u\mathbf{F}_{uu})^{-1}\mathbf{B}_u\mathbf{n}_u \tag{4.32}$$

$$\mathbf{g}_i = \mathbf{t}_{i,d}^T + \mathbf{t}_{i,u}^T(\mathbf{I} - \mathbf{B}_u\mathbf{F}_{uu})^{-1}\mathbf{B}_u\mathbf{F}_{ud}. \tag{4.33}$$

Combining (4.28) and (4.31), we have

$$\frac{1}{\hat{\tau}^i} = \frac{1}{P_i'}\mathbf{g}_i\mathbf{E}\hat{\mathbf{p}}_d^i + \frac{1}{P_i'}\mathbf{g}_i\mathbf{e}. \tag{4.34}$$

We can therefore conclude that the sub-problem $\mathcal{T}^i$ can be converted into the determination of power allocation for only the DL transmission, i.e., (4.28) and (4.34). These two equations can also be formulated into the following eigensystem

$$\frac{1}{\hat{\tau}^i}\acute{\mathbf{p}}_d^i = \boldsymbol{\Upsilon}^i \acute{\mathbf{p}}_d^i \tag{4.35}$$

where

$$\acute{\mathbf{p}}_d^i = \begin{bmatrix} \hat{\mathbf{p}}_d^i \\ 1 \end{bmatrix} \tag{4.36}$$

$$\boldsymbol{\Upsilon}^i = \begin{bmatrix} \mathbf{E} & \mathbf{e} \\ \frac{1}{P_i'}\mathbf{g}_i\mathbf{E} & \frac{1}{P_i'}\mathbf{g}_i\mathbf{e} \end{bmatrix}. \tag{4.37}$$

The optimal DL power allocation then corresponds to the unique positive eigenvector of the matrix $\boldsymbol{\Upsilon}^i$ [55]. In order to solve the eigensystem (4.35), we apply the Perron-Frobenious theory which requires the matrix of the eigensystem to be non-negative [55]. If the requirement is satisfied, the eigenvector corresponding to the largest eigenvalue of the non-negative matrix is always non-negative and unique. To this end, the following Lemma is sufficient and necessary to ensure the matrix $\boldsymbol{\Upsilon}^i$ in (4.37) is non-negative.

Lemma 4.2. *The matrix $\boldsymbol{\Upsilon}^i$ in* (4.37) *is a non-negative matrix if and only if*

$$\rho(\mathbf{B}_u\mathbf{F}_{uu}) < 1 \tag{4.38}$$

$$\mathbf{t}_{i,u}^T(\mathbf{I} - \mathbf{B}_u\mathbf{F}_{uu})^{-1}\mathbf{B}_u\mathbf{n}_u < P_i \tag{4.39}$$

where $\rho(\mathbf{B}_u\mathbf{F}_{uu})$ is the Perron-Frobenius eigenvalue of the non-negative matrix $\mathbf{B}_u\mathbf{F}_{uu}$.

Proof. Refer to Appendix 4.C. □

Result 1: The optimal value of the sub-problem $\mathcal{T}^i$ is given by

$$\hat{\tau}^i = \frac{1}{\lambda_{\max}(\boldsymbol{\Upsilon}^i)} \tag{4.40}$$

where $\lambda_{\max}(\boldsymbol{\Upsilon}^i)$ is the maximal eigenvalue of $\boldsymbol{\Upsilon}^i$. By scaling the dominant eigenvector of $\boldsymbol{\Upsilon}^i$ such that the last element equals unity, the first K_d elements of the dominant eigenvector become the optimal power vector $\hat{\mathbf{p}}_d^i$ for the DL transmission. Subsequently, the optimal power vector $\hat{\mathbf{p}}_u^i$ for the UL transmission can be computed using (4.27).

By solving the $K_u + 1$ sub-problems $\mathcal{T}^i$ $(i = 0, 1, \ldots, K_u)$ using the aforementioned procedures, the problem $\mathcal{T}$ can be solved based on Theorem 4.1.

4.2.2 Solving $\mathcal{T}$ with subgradient projection-based method

Corollary 4.1. *We define a function $\mathcal{T}(\boldsymbol{\theta})$ as*

$$\mathcal{T}(\boldsymbol{\theta}): \max_{\mathbf{p}} \quad \min_{k_d \in \mathcal{K}_d} \frac{\mathrm{SINR}_{k_d}^{\mathrm{DL}}(\mathbf{p})}{\beta_{k_d}} \tag{4.41a}$$

$$s.t. \quad \mathrm{SINR}_{k_u}^{\mathrm{UL}}(\mathbf{p}) \geq \beta_{k_u}, \quad \forall k_u \in \mathcal{K}_u \tag{4.41b}$$

$$\sum\nolimits_i \theta_i \mathbf{t}_i^T \mathbf{p} \leq \sum\nolimits_i \theta_i P_i, \quad \mathbf{p} \geq \mathbf{0}. \tag{4.41c}$$

Then, the optimal solution $\hat{\tau}$ of $\mathcal{T}$ is equal to

$$\hat{\tau} = \min\{\mathcal{T}(\boldsymbol{\theta}) : \boldsymbol{\theta} \geq \mathbf{0}\}. \tag{4.42}$$

Proof. Refer to Appendix 4.D. □

Corollary 4.2. *$\mathcal{T}(\boldsymbol{\theta})$ is a quasi-convex function with respect to (w.r.t.) $\boldsymbol{\theta}$.*

Proof. Refer to Appendix 4.E. □

Result 2: By replacing (i) $\mathbf{t}_i^T$ in (4.12c) with $\sum_i \theta_i \mathbf{t}_i^T$ and (ii) P_i with $\sum_i \theta_i P_i$, we can obtain (4.41c). Thus the method described in Sect. 4.2.1 can also be applied to find the solution of $\mathcal{T}(\boldsymbol{\theta})$ for a given $\boldsymbol{\theta}$.

It is also well known that the optimal point of a quasi-convex function can be found by using subgradient projection-based method. Based on Corollaries 4.1 and 4.2, we can therefore solve the minimum of $\mathcal{T}(\boldsymbol{\theta})$ with the subgradient projection-based method and obtain the optimal solution $\hat{\tau}$ of $\mathcal{T}$. To this end, the explicit solution of the multiple-power-and-multiple-SINR-constraint problem is given explicitly in Algorithm 1.

4.3 Joint Power and Beamforming Optimization

In this section, we optimize the max-min weighted SINR problem by considering both power and beamforming, i.e., the problem $\mathcal{P}$ in (4.10a) to (4.10d). In general, the global optimization of $\mathcal{P}$ is an open problem because its non-convexity. Moreover, the mutual coupling between the transmit beamformers and receive beamformers make it very difficult to jointly optimize the beamformers. Here, we propose a suboptimal algorithm for solving the problem $\mathcal{P}$. The flowchart of the proposed

[1]When the step size α_n follows the diminishing policy in [89], the subgradient method above is guaranteed to converge to the optimal value. Here, we just take the simple diminishing step, i.e., $\alpha_n = \alpha_0/(n+1)$.

Algorithm 1 Solution of the multiple-power-and-multiple-SINR-constraint problem without beamforming

1: Define $I = K_u + 1$ and $\boldsymbol{\theta} \in \mathbb{R}^I_{\geq 0}$.
2: Initialization: Set stopping criterion $\varepsilon = 0.01$; $\boldsymbol{\theta}^{(0)} > \mathbf{0}$; subgradient-projection-method step size $\alpha_0 > 0$; $\Delta\tau = 1$; and $\hat{\tau}^{(0)} = -1000$.
3: $n \leftarrow 0$.
4: **while** $\Delta\tau > \varepsilon$ **do**
5: Solve $\mathcal{T}(\boldsymbol{\theta}^{(n+1)})$ by using **Result 2** and **Result 1**. The optimal value of $\mathcal{T}(\boldsymbol{\theta}^{(n+1)})$ is denoted as $\hat{\tau}^{(n+1)}$ and the optimal power allocation vector is denoted as $\hat{\mathbf{p}}^{(n+1)}$.
6: Update $\boldsymbol{\theta}^{(n+1)}$ using the subgradient projection method with $\alpha_n = \alpha_0/(n+1)^1$, i.e.,

$$\boldsymbol{\theta}^{(n+1)} = \boldsymbol{\theta}^{(n)} - \alpha_n \boldsymbol{f}(\hat{\mathbf{p}}^{(n+1)})$$

where $\boldsymbol{f}(\hat{\mathbf{p}}^{(n+1)}) = [P_0 - \mathbf{t}_0\hat{\mathbf{p}}^{(n+1)}, P_1 - \mathbf{t}_1^T\hat{\mathbf{p}}^{(n+1)}, \ldots, P_{K_u} - \mathbf{t}_{K_u}^T\hat{\mathbf{p}}^{(n+1)}]$.
7: Set $\Delta\tau = \hat{\tau}^{(n+1)} - \hat{\tau}^{(n)}$.
8: $n \leftarrow n + 1$.
9: **end while**
10: Set $\hat{\mathbf{p}} = \hat{\mathbf{p}}^{(n-1)}$ and the optimal value of the problem $\mathcal{T}$ as $\hat{\tau}^{(n-1)}$.

algorithm is shown in Fig. 4.2. As in the last section, we consider the power constraints individually and then jointly optimize power and beamforming. Finally, we select the optimized system that achieves the minimum objective function value.

In the following, we again focus on the single-power-and-multiple-SINR-constraint problem $\mathcal{T}^i$. We first prove the network duality for the problem, and then describe the solutions for (i) receive beamforming optimization with fixed power vector and transmit beamforming and (ii) transmit beamforming optimization with fixed power vector and receive beamforming. Afterwards, we describe the ways to obtain solutions for the problem $\mathcal{P}$.

4.3.1 Network Duality for the Single-Power-and-Multiple-SINR-Constraint Problem

In this section, we derive the network duality for the single-power-and-multiple-SINR-constraint problem. We re-write the single-power-and-multiple-SINR-constraint problem $\mathcal{T}^i$ in (4.13a) to (4.13d) as

$$\mathcal{T}^i : \max_{\tau^i, \mathbf{p}} \quad \tau^i \tag{4.43a}$$

$$s.t. \quad \tau^i \leq \frac{\mathrm{SINR}_{k_d}^{\mathrm{DL}}(\mathbf{p}^i)}{\beta_{k_d}}, \quad \forall k_d \in \mathcal{K}_d \tag{4.43b}$$

$$\mathrm{SINR}_{k_u}^{\mathrm{UL}}(\mathbf{p}^i) \geq \beta_{k_u}, \quad \forall k_u \in \mathcal{K}_u \tag{4.43c}$$

$$\mathbf{t}_i^T \mathbf{p}^i \leq P_i, \quad \mathbf{p}^i \geq \mathbf{0} \tag{4.43d}$$

Theorem 4.2. *The single-power-and-multiple-SINR-constraint problem* $\mathcal{T}^i$ *in* (4.43a) *to* (4.43d) *is equivalent to following power optimization problem* $\mathcal{S}^i$

$$\mathcal{S}^i : \max_{\tau^i, \mathbf{q}^i} \quad \tau^i \tag{4.44a}$$

$$s.t. \quad \tau^i \leq \frac{\mathrm{SINR}_{k_d}^{\mathrm{UL,D}}(\mathbf{q}^i)}{\beta_{k_d}}, \quad \forall k_d \in \mathcal{K}_d \tag{4.44b}$$

$$\mathrm{SINR}_{k_u}^{\mathrm{DL,D}}(\mathbf{q}^i) \geq \beta_{k_u}, \quad \forall k_u \in \mathcal{K}_u \tag{4.44c}$$

$$\mathbf{n}^T \mathbf{q}^i \leq P_i, \quad \mathbf{q}^i \geq \mathbf{0} \tag{4.44d}$$

where

$$\frac{\mathrm{SINR}_{k_d}^{\mathrm{UL,D}}(\mathbf{q}^i)}{\beta_{k_d}} = \frac{q_{k_d}G_{k_dk_d}}{\sum_{l\in\mathcal{K},l\neq k_d} q_l G_{k_dl} + t_{i,k_d}}, \quad \forall k_d \in \mathcal{K}_d \tag{4.45}$$

$$\frac{\mathrm{SINR}_{k_u}^{\mathrm{DL,D}}(\mathbf{q}^i)}{\beta_{k_u}} = \frac{q_{k_u}G_{k_uk_u}}{\sum_{l\in\mathcal{K},l\neq k_u} q_l G_{k_ul} + t_{i,k_u}}, \quad \forall k_u \in \mathcal{K}_u \tag{4.46}$$

are the dual weighted UL SINR and weighted DL SINR, respectively.

Proof. Making the logarithmic change of variables $\tilde{\tau}^i = \log \tau^i$ in (4.43a) and $\tilde{p}_k^i = \log p_k^i$ for the problem $\mathcal{T}^i$, and applying (4.15)–(4.17), we arrive at the following equivalent convex problem:

$$\begin{aligned}
\min_{\tilde{\tau}^i,\tilde{\mathbf{p}}^i} \quad & -\tilde{\tau}^i \\
s.t. \quad & \log\left(\frac{\left[(e^{\tilde{\tau}}\mathrm{diag}(\tilde{\boldsymbol{\beta}}))(\mathbf{F}\mathbf{p}^i+\mathbf{n})\right]_{k_d}}{e^{\tilde{p}_{k_d}^i}}\right) \leq 0, \quad \forall k_d \in \mathcal{K}_d \\
& \log\left(\frac{\left[(\mathrm{diag}(\tilde{\boldsymbol{\beta}}))(\mathbf{F}\mathbf{p}^i+\mathbf{n})\right]_{k_u}}{e^{\tilde{p}_{k_u}^i}}\right) \leq 0, \quad \forall k_u \in \mathcal{K}_u \\
& \log\left(\frac{1}{P_i}\mathbf{t}_i^T e^{\tilde{\mathbf{p}}^i}\right) \leq 0.
\end{aligned} \tag{4.47}$$

where $\mathbf{F}$ and $\tilde{\boldsymbol{\beta}}$ have defined in (4.15) and (4.16), respectively; and the subscript k in $[\cdot]_k$ denotes the k-the element of $[\cdot]$. Furthermore, the Lagrangian function

associated with (4.47) equals

$$
\begin{aligned}
L(\tilde{\tau}^i, \tilde{\mathbf{p}}^i, \mu, \boldsymbol{\lambda}) = & -\tilde{\tau}^i + \mu \log \left(\frac{1}{P_i} \mathbf{t}_i^T e^{\tilde{\mathbf{p}}^i} \right) \\
& + \sum_{k_d \in \mathcal{K}_d} \lambda_{k_d} \log \left(\frac{\left[(e^{\tilde{\tau}^i} \operatorname{diag}(\tilde{\boldsymbol{\beta}}))(\mathbf{F}\mathbf{p}^i + \mathbf{n}) \right]_{k_d}}{e^{\tilde{p}^i_{k_d}}} \right) \\
& + \sum_{k_u \in \mathcal{K}_u} \lambda_{k_u} \log \left(\frac{\left[(\operatorname{diag}(\tilde{\boldsymbol{\beta}}))(\mathbf{F}\mathbf{p}^i + \mathbf{n}) \right]_{k_u}}{e^{\tilde{p}^i_{k_u}}} \right)
\end{aligned} \tag{4.48}
$$

where μ and λ_k are the non-negative Lagrange dual variables. It is easy to check that the convex problem given by (4.47) satisfies Slater's condition. Hence, the Karush–Kuhn–Tucker (KKT) conditions are necessary and sufficient conditions for the optimality of (4.47). Adding the symbol "$\hat{}$" to the optimal solutions, the KKT

conditions are represented as follows.

$$\hat{\tau}^i = \frac{\hat{p}^i_{k_d}}{\left[(\mathrm{diag}(\tilde{\boldsymbol{\beta}}))(\mathbf{F}\hat{\mathbf{p}}^i + \mathbf{n})\right]_{k_d}} \quad , \quad \forall k_d \in \mathcal{K}_d \tag{4.49}$$

$$1 = \frac{\hat{p}^i_{k_u}}{\left[(\mathrm{diag}(\tilde{\boldsymbol{\beta}}))(\mathbf{F}\hat{\mathbf{p}}^i + \mathbf{n})\right]_{k_u}} \quad , \quad \forall k_u \in \mathcal{K}_u \tag{4.50}$$

$$\mathbf{t}_i^T \hat{\mathbf{p}}^i = P_i \tag{4.51}$$

$$\hat{\tau}^i = \frac{\hat{q}^i_{k_d}}{\left[(\mathrm{diag}(\tilde{\boldsymbol{\beta}}))(\mathbf{F}^T\hat{\mathbf{q}}^i + \mathbf{t}_i)\right]_{k_d}} \quad , \quad \forall k_d \in \mathcal{K}_d \tag{4.52}$$

$$1 = \frac{\hat{q}^i_{k_u}}{\left[(\mathrm{diag}(\tilde{\boldsymbol{\beta}}))(\mathbf{F}^T\hat{\mathbf{q}}^i + \mathbf{t}_i)\right]_{k_u}} \quad , \quad \forall k_u \in \mathcal{K}_u \tag{4.53}$$

$$\sum\nolimits_{k_d \in \mathcal{K}_d} \lambda_{k_d} = 1, \tag{4.54}$$

$$\hat{\mathbf{q}}^i = \frac{P_i}{\hat{\mu}} \cdot \left(\frac{\hat{\tau}^i \hat{\lambda}_1 \tilde{\beta}_1}{\hat{p}^i_1}, \cdots, \frac{\hat{\tau}^i \hat{\lambda}_{K_d} \tilde{\beta}_{K_d}}{\hat{p}^i_{K_d}}, \frac{\hat{\lambda}_{K_d+1} \tilde{\beta}_{K_d+1}}{\hat{p}^i_{K_d+1}}, \cdots, \frac{\hat{\lambda}_K \tilde{\beta}_K}{\hat{p}^i_K} \right)^T \tag{4.55}$$

$$\hat{\lambda}_k > 0, \quad \forall k \in \mathcal{K} \tag{4.56}$$

$$\hat{\mu} > 0 \tag{4.57}$$

Here, (4.49), (4.50) and (4.51) are the transformations of (4.14a), (4.14b) and (4.14c), respectively; (4.52) and (4.53) follow from $\partial L/\partial p_k = 0$; (4.54) follows from $\partial L/\partial \tau = 0$; and (4.56) and (4.57) follow from the fact that $\hat{\lambda}_k$ and $\hat{\mu}$ must be strictly positive to satisfy the constraints (4.49), (4.50) and (4.51). We can see that $\mathbf{F}^T$ becomes the channel matrix in the dual network. Hence, from (4.52) and (4.53), we conclude that $\hat{\mathbf{q}}^i$ is the optimal dual power vector and $\mathbf{t}_i$ is the noise covariance vector in the dual network [55]. To obtain the equivalent power constraint in the

dual network, we rewrite (4.52) and (4.53), respectively, in vector form as

$$\left[\mathbf{F}^T\hat{\mathbf{q}}^i + \mathbf{t}_i\right]_{k_d} = \left[\frac{1}{\hat{\tau}^i}\text{diag}(\tilde{\boldsymbol{\beta}})^{-1}\hat{\mathbf{q}}^i\right]_{k_d}, \quad \forall k_d \in \mathcal{K}_d \tag{4.58}$$

$$\left[\mathbf{F}^T\hat{\mathbf{q}}^i + \mathbf{t}_i\right]_{k_u} = \left[\text{diag}(\tilde{\boldsymbol{\beta}})^{-1}\hat{\mathbf{q}}^i\right]_{k_u}, \quad \forall k_u \in \mathcal{K}_u. \tag{4.59}$$

Substituting (4.49) and (4.50) into (4.58) and (4.59), respectively, we can obtain a unified equation, i.e.,

$$\left[\mathbf{F}^T\hat{\mathbf{q}}^i + \mathbf{t}_i\right]_k \hat{p}_k^i = \left[\mathbf{F}\hat{\mathbf{p}}^i + \mathbf{n}\right]_k \hat{q}_k^i, \quad \forall k \in \mathcal{K}. \tag{4.60}$$

Applying (4.51) and

$$(\mathbf{F}^T\hat{\mathbf{q}}^i)^T\hat{\mathbf{p}}^i = (\hat{\mathbf{q}}^i)^T\mathbf{F}\hat{\mathbf{p}}^i = (\hat{\mathbf{p}}^i)^T\mathbf{F}^T\hat{\mathbf{q}}^i = (\mathbf{F}\hat{\mathbf{p}}^i)^T\hat{\mathbf{q}}^i, \tag{4.61}$$

to (4.60), we have

$$\begin{aligned}
& \left[\mathbf{F}^T\hat{\mathbf{q}}^i + \mathbf{t}_i\right]_k \hat{p}_k^i && = \left[\mathbf{F}\hat{\mathbf{p}}^i + \mathbf{n}\right]_k \hat{q}_k^i, \quad \forall k \in \mathcal{K} \\
\Rightarrow \quad & \left[\mathbf{F}^T\hat{\mathbf{q}}^i + \mathbf{t}_i\right]^T \hat{\mathbf{p}}^i && = \left[\mathbf{F}\hat{\mathbf{p}}^i + \mathbf{n}\right]^T \hat{\mathbf{q}}^i \\
\Rightarrow \quad & \left[\mathbf{F}^T\hat{\mathbf{q}}^i\right]^T \hat{\mathbf{p}}^i + \mathbf{t}_i^T\hat{\mathbf{p}}^i && = \left[\mathbf{F}\hat{\mathbf{p}}^i\right]^T \hat{\mathbf{q}}^i + \mathbf{n}^T\hat{\mathbf{q}}^i \\
\Rightarrow \quad & \mathbf{n}^T\hat{\mathbf{q}}^i && = \mathbf{t}_i^T\hat{\mathbf{p}}^i = P_i
\end{aligned} \tag{4.62}$$

Therefore, (4.49)–(4.57) are equivalent to the following conditions.

$$\hat{\tau}^i = \frac{\hat{q}^i_{k_d}}{\left[(\mathrm{diag}(\tilde{\boldsymbol{\beta}}))(\mathbf{F}^T\hat{\mathbf{q}}^i + \mathbf{t}_i)\right]_{k_d}} \quad , \quad \forall k_d \in \mathcal{K}_d \tag{4.63}$$

$$1 = \frac{\hat{q}^i_{k_u}}{\left[(\mathrm{diag}(\tilde{\boldsymbol{\beta}}))(\mathbf{F}^T\hat{\mathbf{q}}^i + \mathbf{t}_i)\right]_{k_u}} \quad , \quad \forall k_u \in \mathcal{K}_u \tag{4.64}$$

$$\mathbf{n}^T\hat{\mathbf{q}}^i = P_i \tag{4.65}$$

$$\hat{\tau}^i = \frac{\hat{p}^i_{k_d}}{\left[(\mathrm{diag}(\tilde{\boldsymbol{\beta}}))(\mathbf{F}\hat{\mathbf{p}}^i + \mathbf{n})\right]_{k_d}} \quad , \quad \forall k_d \in \mathcal{K}_d \tag{4.66}$$

$$1 = \frac{\hat{p}^i_{k_u}}{\left[(\mathrm{diag}(\tilde{\boldsymbol{\beta}}))(\mathbf{F}\hat{\mathbf{p}}^i + \mathbf{n})\right]_{k_u}} \quad , \quad \forall k_u \in \mathcal{K}_u \tag{4.67}$$

$$\sum\nolimits_{k_d \in \mathcal{K}_d} \lambda_{k_d} = 1 \tag{4.68}$$

$$\hat{\mathbf{p}}^i = \frac{P_i}{\hat{\mu}} \cdot \left(\frac{\hat{\tau}^i\hat{\lambda}_1\tilde{\beta}_1}{\hat{q}_1}, \cdots, \frac{\hat{\tau}^i\hat{\lambda}_{K_d}\tilde{\beta}_{K_d}}{\hat{q}^i_{K_d}}, \frac{\hat{\lambda}_{K_d+1}\tilde{\beta}_{K_d+1}}{\hat{q}^i_{K_d+1}}, \cdots, \frac{\hat{\lambda}_K\tilde{\beta}_K}{\hat{q}^i_K} \right)^T \tag{4.69}$$

$$\hat{\lambda}_k > 0, \quad \forall k \in \mathcal{K} \tag{4.70}$$

$$\hat{\mu} > 0 \tag{4.71}$$

Here, we replace the power constraint (4.51) with the dual power constraint (4.65). We can also observe that (4.63)–(4.67) can be obtained from (4.49)–(4.53) via the following substitutions:

$$\begin{gathered} \mathbf{p}^i \leftrightarrow \mathbf{q}^i \\ \mathbf{t}^i \leftrightarrow \mathbf{n} \\ \mathbf{n} \leftrightarrow \mathbf{t}^i \\ \mathbf{F} \leftrightarrow \mathbf{F}^T \end{gathered} \tag{4.72}$$

Hence, (4.63)–(4.71) are necessary and sufficient conditions to achieve the optimal

solution of $\mathcal{S}^i$ where the parameters and variables in $\mathcal{S}^i$ are defined by the mappings in (4.72). Thus, Theorem 4.2 is proved. □

Theorem 4.2 shows the problem $\mathcal{T}^i$ has a network duality relationship with the problem $\mathcal{S}^i$. In the following, we also provide the solution to the problem $\mathcal{S}^i$.

Result 3: The optimal value of the problem $\mathcal{S}^i$ is given by

$$\hat{\tau}^i = \frac{1}{\lambda_{\max}(\bar{\mathbf{\Upsilon}}^i)} \tag{4.73}$$

where $\lambda_{\max}(\bar{\mathbf{\Upsilon}}^i)$ is the maximal eigenvalue of $\bar{\mathbf{\Upsilon}}^i$ and

$$\bar{\mathbf{\Upsilon}}^i = \begin{bmatrix} \bar{\mathbf{E}} & \bar{\mathbf{e}} \\ \frac{1}{P_i'}\bar{\mathbf{g}}_i\bar{\mathbf{E}} & \frac{1}{P_i'}\bar{\mathbf{g}}_i\bar{\mathbf{e}} \end{bmatrix} \tag{4.74}$$

$$\frac{1}{\hat{\tau}^i}\hat{\mathbf{q}}_d^i = \mathbf{B}_d\mathbf{F}_{dd}^T\hat{\mathbf{q}}_d^i + \mathbf{B}_d\mathbf{t}_{i,d} + \mathbf{B}_d\mathbf{F}_{ud}^T\hat{\mathbf{q}}_u^i \tag{4.75}$$

$$\hat{\mathbf{q}}_u^i = \mathbf{B}_u\mathbf{F}_{uu}^T\hat{\mathbf{q}}_u^i + \mathbf{B}_u\mathbf{t}_{i,u} + \mathbf{B}_u\mathbf{F}_{du}^T\hat{\mathbf{q}}_d^i \tag{4.76}$$

$$P_i = \mathbf{n}_d^T\hat{\mathbf{q}}_d^i + \mathbf{n}_u^T\hat{\mathbf{q}}_u^i \tag{4.77}$$

$$\bar{\mathbf{E}} = \mathbf{B}_d\mathbf{F}_{dd}^T + \mathbf{B}_d\mathbf{F}_{ud}^T(\mathbf{I} - \mathbf{B}_u\mathbf{F}_{uu}^T)^{-1}\mathbf{B}_u\mathbf{F}_{du}^T \tag{4.78}$$

$$\bar{\mathbf{e}} = \mathbf{B}_d\mathbf{t}_{i,d} + \mathbf{B}_d{\mathbf{F}_{ud}}^T(\mathbf{I} - \mathbf{B}_u\mathbf{F}_{uu}^T)^{-1}\mathbf{B}_u\mathbf{t}_{i,u}. \tag{4.79}$$

$$\bar{P}_i' = P_i - \mathbf{n}_u^T(\mathbf{I} - \mathbf{B}_u\mathbf{F}_{uu}^T)^{-1}\mathbf{B}_u\mathbf{t}_{i,u} \tag{4.80}$$

$$\bar{\mathbf{g}}_i = \mathbf{n}_d^T + \mathbf{n}_u^T(\mathbf{I} - \mathbf{B}_u\mathbf{F}_{uu}^T)^{-1}\mathbf{B}_u\mathbf{F}_{du}^T \tag{4.81}$$

$$\hat{\mathbf{q}}^i = \begin{bmatrix} \hat{\mathbf{q}}_d^i \\ \hat{\mathbf{q}}_u^i \end{bmatrix} \tag{4.82}$$

with $\hat{\mathbf{q}}_d^i$ and $\hat{\mathbf{q}}_u^i$ being vectors of size K_d and K_u, respectively. By scaling the dominant eigenvector of $\bar{\mathbf{\Upsilon}}^i$ such that the last element equals unity, the first K_d elements

of the dominant eigenvector become the optimal dual power vector $\hat{\mathbf{q}}_d^i$ for the DL transmission. Subsequently, the optimal dual power vector $\hat{\mathbf{q}}_u^i$ for the UL transmission can be computed using (4.76).

Note that the necessary and sufficient conditions to guarantee that $\bar{\boldsymbol{\Upsilon}}^i$ being a non-negative matrix are given by

$$\rho(\mathbf{B}_u \mathbf{F}_{uu}^T) < 1 \tag{4.83}$$

$$\mathbf{n}_u^T (\mathbf{I} - \mathbf{B}_u \mathbf{F}_{uu}^T)^{-1} \mathbf{B}_u \mathbf{t}_{i,u} < P_i. \tag{4.84}$$

The proof is similar to that of Lemma 4.2 and is thus omitted here.

By considering both transmit and receive beamforming, we can re-write the dual UL SINR $\mathrm{SINR}_k^{\mathrm{UL,D}}(\mathbf{q}^i, \mathbb{W}, \mathbb{V})$ and dual DL SINR $\mathrm{SINR}_k^{\mathrm{DL,D}}(\mathbf{q}^i, \mathbb{V})$ as follows.

$$\mathrm{SINR}_k^{\mathrm{UL,D}}(\mathbf{q}^i, \mathbb{W}, \mathbb{V}) = \frac{q_k^i |\mathbf{w}_k^\dagger \mathbf{H}_{kk}|^2}{\left(\sum_{l \in \mathcal{K}_d, l \neq k} q_l^i |\mathbf{w}_k^\dagger \mathbf{H}_{kl}|^2\right) + \left(\sum_{l \in \mathcal{K}_u, l \neq k} q_l^i |\mathbf{w}_k^\dagger \mathbf{H}_{kl} \mathbf{v}_l|^2\right) + t_{i,k}} \quad \forall k \in \mathcal{K}_u \tag{4.85}$$

$$\mathrm{SINR}_k^{\mathrm{DL,D}}(\mathbf{q}^i, \mathbb{V}) = \frac{q_k^i |\mathbf{H}_{kk} \mathbf{v}_k|^2}{\left(\sum_{l \in \mathcal{K}_d, l \neq k} q_l^i |\mathbf{H}_{kl}|^2\right) + \left(\sum_{l \in \mathcal{K}_u, l \neq k} q_l^i |\mathbf{H}_{kl} \mathbf{v}_l|^2\right) + t_{i,k}} \quad \forall k \in \mathcal{K}_d \tag{4.86}$$

4.3.2 Optimizing Receive Beamforming with Fixed Power and Transmit Beamforming

Assuming that the power vector $\mathbf{p}^i$ and transmit beamforming $\mathbb{W}$ are fixed, we optimize the receive beamforming $\mathbb{V}$ in the primal domain. For a given power constraint,

i.e., $\mathbf{t}_i^T\mathbf{p} \leq P_i$, the receive beamforming problem can be written as follows.

$$\begin{aligned}\mathcal{P}^i(\mathbb{V}):\ \max_{\mathbb{V}} \quad & \min_{k_d\in\mathcal{K}_d} \frac{\mathrm{SINR}_{k_d}^{\mathrm{DL}}(\mathbf{p}^i,\mathbb{W})}{\beta_{k_d}}, \\ s.t. \quad & \mathrm{SINR}_{k_u}^{\mathrm{UL}}(\mathbf{p}^i,\mathbb{W},\mathbb{V}) \geq \beta_{k_u}, \quad \forall k_u \in \mathcal{K}_u \\ & \mathbf{t}_i^T\mathbf{p}^i \leq P_i, \quad \mathbf{p}^i \geq \mathbf{0} \\ & ||\mathbf{v}_k|| = 1, \quad \forall k \in \mathcal{K}\end{aligned} \tag{4.87}$$

The receive beamforming only appears in the UL SINR constraints because $\mathbf{v}_k = 1$ when $k \in \mathcal{K}_d$. If the receive beamforming $\mathbb{V}$ is optimized, we will be able to reduce the UL transmit power vector $\mathbf{p}_u^i$ to meet the SINR constraints. Then the weighted DL SINRs can be increased subsequently. Therefore, for a given power vector $\mathbf{p}^i$ and transmit beamforming $\mathbb{W}$, we can optimize the receive beamforming $\mathbb{V}$ as follows.

$$\begin{aligned}\mathcal{P}^i(\mathbb{V}):\ \max_{\mathbb{V}} \quad & \min_{k_u\in\mathcal{K}_u} \mathrm{SINR}_{k_u}^{\mathrm{UL}}(\mathbb{V}), \\ s.t. \quad & ||\mathbf{v}_{k_u}|| = 1, \quad \forall k_u \in \mathcal{K}_u\end{aligned} \tag{4.88}$$

As a result, the receive beamforming should be designed to maximize its SINR, i.e.,

$$\hat{\mathbf{v}}_k = \arg\max_{\mathbf{v}_k} \frac{\mathbf{v}_k^T\mathbf{U}_{kk}\mathbf{v}_k}{\mathbf{v}_k^T\left(\sum_{l\in\mathcal{K},l\neq k}\hat{\mathbf{p}}_l^i\mathbf{U}_{kl}\mathbf{v}_l + n_k\mathbf{I}\right)\mathbf{v}_k}, \quad \forall k \in \mathcal{K}_u \tag{4.89}$$

$$s.t. \quad ||\mathbf{v}_k|| = 1, \quad \forall k \in \mathcal{K}_u$$

where $\mathbf{U}_{kl} = \mathbf{H}_{kl}\mathbf{w}_l, (l,k \in \mathcal{K})$. The solution can be obtained by finding the dominant generalized eigenvector of the matrix pairs $[\mathbf{U}_{kk}, \sum_{l\in\mathcal{K},l\neq k}\hat{\mathbf{p}}_l^i\mathbf{U}_{kl} + n_k\mathbf{I}]$.

4.3.3 Optimizing Transmit Beamforming with Fixed Power and Receive Beamforming

Assuming that the power vector $\mathbf{p}^i$ and receive beamforming $\mathbb{V}$ are fixed, we optimize the transmit beamforming $\mathbb{W}$ in the dual domain. For a given power constraint, i.e., $\mathbf{t}_i^T \mathbf{p}^i \leq P_i$, the transmit beamforming problem in the primal domain can be written as follows.

$$\begin{aligned} \mathcal{P}^i(\mathbb{W}): \max_{\mathbb{W}} \quad & \min_{k_d \in \mathcal{K}_d} \frac{\mathrm{SINR}_{k_d}^{\mathrm{DL}}(\mathbf{p}^i, \mathbb{W})}{\beta_{k_d}}, \\ s.t. \quad & \mathrm{SINR}_{k_u}^{\mathrm{UL}}(\mathbf{p}^i, \mathbb{W}, \mathbb{V}) \geq \beta_{k_u}, \quad \forall k_u \in \mathcal{K}_u \\ & \mathbf{t}_i^T \mathbf{p}^i \leq P_i, \quad \mathbf{p}^i \geq \mathbf{0} \\ & ||\mathbf{w}_k|| = 1, \quad \forall k \in \mathcal{K} \end{aligned} \tag{4.90}$$

We can observe that it is very difficult to solve the problem in the primal domain. However, the problem becomes much simpler in the dual domain. By using network duality, the dual problem of $\mathcal{P}^i(\mathbb{W})$ is given by

$$\begin{aligned} \mathcal{S}^i(\mathbb{W}): \max_{\mathbb{W}} \quad & \min_{k_d \in \mathcal{K}_d} \frac{\mathrm{SINR}_{k_d}^{\mathrm{UL,D}}(\mathbf{q}^i, \mathbb{W}, \mathbb{V})}{\beta_{k_d}}, \\ s.t. \quad & \mathrm{SINR}_{k_u}^{\mathrm{DL,D}}(\mathbf{q}^i, \mathbb{V}) \geq \beta_{k_u}, \quad \forall k_u \in \mathcal{K}_u \\ & \mathbf{n}^T \mathbf{q}^i \leq P_i, \quad \mathbf{q}^i \geq \mathbf{0} \\ & ||\mathbf{w}_k|| = 1, \quad \forall k \in \mathcal{K} \end{aligned} \tag{4.91}$$

where $\mathrm{SINR}_{k_d}^{\mathrm{UL,D}}(\mathbf{q}^i, \mathbb{W}, \mathbb{V})$ and $\mathrm{SINR}_{k_d}^{\mathrm{DL,D}}(\mathbf{q}^i, \mathbb{V})$ are given in (4.85) and (4.86), respectively. From the expression of $\mathrm{SINR}_{k_d}^{\mathrm{DL,D}}(\mathbf{q}, \mathbb{V})$, we can see that the transmit

beamforming $\mathbb{W}$ does not affect the SINR constraints of dual DL because $\mathbf{w}_k = 1$ when $k \in \mathcal{K}_u$. Therefore, for a given dual power vector $\mathbf{q}^i$ and receive beamforming $\mathbb{V}$, we can simplify the problem $\mathcal{S}^i(\mathbb{W})$ to

$$\mathcal{S}^i(\mathbb{W}): \max_{\mathbb{W}} \quad \min_{k_d \in \mathcal{K}_d} \frac{\mathrm{SINR}_{k_d}^{\mathrm{UL,D}}(\mathbb{W})}{\beta_{k_d}}, \qquad (4.92)$$
$$s.t. \quad ||\mathbf{w}_{k_d}|| = 1, \quad \forall k_d \in \mathcal{K}_d.$$

The optimal transmit beamforming $\mathbb{W}$ is exactly the same as the solution of the max-min weighted multiple-input-single-output (MISO) optimization problem and can be obtained by independently maximizing the SINR of each channel in the dual domain [55]. In other words, the optimal transmit beamforming $\mathbb{W}$ can be determined by solving the following optimization problem

$$\hat{\mathbf{w}}_k = \arg\max_{\mathbf{w}_k} \frac{\mathbf{w}_k^T \mathbf{R}_{kk} \mathbf{w}_k}{\mathbf{w}_k^T \left(\sum_{l \in \mathcal{K}, l \neq k} \hat{\mathbf{q}}_l^i \mathbf{R}_{kl} \mathbf{w}_l + t_{i,k} \mathbf{I} \right) \mathbf{w}_k}, \quad \forall k \in \mathcal{K}_d \qquad (4.93)$$
$$s.t. \quad ||\mathbf{w}_k|| = 1, \quad \forall k \in \mathcal{K}_d$$

where $\mathbf{R}_{kl} = \mathbf{H}_{kl} \mathbf{v}_l, (l, k \in \mathcal{K})$. The solution can be obtained by finding the dominant generalized eigenvector of the matrix pairs $[\mathbf{R}_{kk}, \sum_{l \in \mathcal{K}, l \neq k} \hat{\mathbf{q}}_l^i \mathbf{R}_{kl} + t_{i,k} \mathbf{I}]$.

4.3.4 Iterative Power and Transmit/Receive Beamforming Optimization based on multiple single-power-constraint problems

Referring to Fig. 4.2, we can solve the joint optimization problem $\mathcal{P}$ iteratively. In the primal domain we optimize the power and receive beamforming while in the dual domain, we optimize the dual power and transmit beamforming. We describe the steps of the suboptimal algorithm as follows.

1. Split the multiple-power-constraint problem $\mathcal{P}$ in (4.10a)–(4.10d) into (K_u+1) single-power-constraint problems, i.e.,

$$\begin{aligned} \mathcal{P}^i(\mathbf{p}^i, \mathbb{W}, \mathbb{V}): \max_{\mathbf{p}^i, \mathbb{W}, \mathbb{V}} \quad & \min_{k_d \in \mathcal{K}_d} \frac{\mathrm{SINR}_{k_d}^{\mathrm{DL}}(\mathbf{p}^i, \mathbb{W})}{\beta_{k_d}}, \\ s.t. \quad & \mathrm{SINR}_{k_u}^{\mathrm{UL}}(\mathbf{p}^i, \mathbb{W}, \mathbb{V}) \geq \beta_{k_u}, \quad \forall k_u \in \mathcal{K}_u \\ & \mathbf{t}_i^T \mathbf{p}^i \leq P_i, \quad \mathbf{p}^i \geq \mathbf{0} \\ & ||\mathbf{w}_k|| = 1, \quad ||\mathbf{v}_k|| = 1, \quad \forall k \in \mathcal{K} \end{aligned} \tag{4.94}$$

   where $i = 0, 1, \ldots, K_u$.

2. For $i = 0, 1, \ldots, K_u$, initialize the transmit and receive beamforming as $\mathbb{W}^i$ and $\mathbb{V}^i$.

3. For $i = 0, 1, \ldots, K_u$, update the power vector $\mathbf{p}^i$ in the primal domain and the corresponding solution $\hat{\tau}_i$ using **Result 1**.

4. For $i = 0, 1, \ldots, K_u$, update receive beamforming $\mathbb{V}^i$ in the primal domain using (4.89).

5. For $i = 0, 1, \ldots, K_u$, update the dual power vector $\mathbf{q}^i$ in the dual domain using **Result 3**.

6. For $i = 0, 1, \ldots, K_u$, update transmit beamforming $\mathbb{W}^i$ in the dual domain using (4.93).

7. If one or more $\hat{\tau}_i$ has not converged, repeat Steps 3 to 6.

8. Select s such that $\hat{\tau}_s$ is the minimum among all $\hat{\tau}_i$, i.e.,

$$s = \arg \min_{i=0,1,\ldots,K_u} \hat{\tau}_i. \tag{4.95}$$

   Then $\mathbf{p}^s, \mathbb{W}^s$ and $\mathbb{V}^s$ are the solutions for $\mathcal{P}$.

Lemma 4.3. *If the initial beamforming parameters $\mathbb{W}^i$ and $\mathbb{V}^i$ satisfy the conditions* (4.38) *and* (4.39)*, these conditions will continue to be satisfied in the iteration algorithm.*

Proof. Please refer to Appendix 4.F. □

4.3.5 Iterative Power and Transmit/Receive Beamforming Optimization with subgradient projection-based method

As in Sect 4.2.2, we can solve $\mathcal{P}$ iteratively using the subgradient projection-based method. It is more efficient compared with the previous algorithm that splits the multiple-power-constraint problem into many single-power-constraint problems. We show the iterative algorithm in Fig. 4.3 and describe the steps as follows.

1. Since the subgradient projection-based method is used, the multiple-power-constraint problem $\mathcal{P}$ is re-written as

$$\begin{aligned} \mathcal{P}(\mathbf{p}, \mathbb{W}, \mathbb{V}, \boldsymbol{\theta}) : \max_{\mathbf{p}, \mathbb{W}, \mathbb{V}} \quad & \min_{k_d \in \mathcal{K}_d} \frac{\mathrm{SINR}_{k_d}^{\mathrm{DL}}(\mathbf{p}, \mathbb{W})}{\beta_{k_d}} \\ s.t. \quad & \mathrm{SINR}_{k_u}^{\mathrm{UL}}(\mathbf{p}, \mathbb{W}, \mathbb{V}) \geq \beta_{k_u}, \quad \forall k_u \in \mathcal{K}_u \\ & \sum\nolimits_i \theta_i \mathbf{t}_i^T \mathbf{p} \leq \sum\nolimits_i \theta_i P_i, \quad \mathbf{p} \geq \mathbf{0} \\ & ||\mathbf{w}_k|| = 1, \quad ||\mathbf{v}_k|| = 1, \quad \forall k \in \mathcal{K}. \end{aligned} \tag{4.96}$$

2. Initialize $\boldsymbol{\theta}$ and subgradient-projection-method step size α.

3. Initialize the transmit and receive beamforming as $\mathbb{W}$ and $\mathbb{V}$.

4. [Outer Loop begins.]

5. (Inner Loop begins)

   (a) Update the power vector $\mathbf{p}$ in the primal domain and the corresponding solution $\hat{\tau}_{\mathrm{inner}}$ using **Result 2** and **Result 1** .

   (b) Update receive beamforming $\mathbb{V}$ in the primal domain using (4.89).

   (c) Update the dual power vector $\mathbf{q}$ in the dual domain using **Result 3**.

   (d) Update transmit beamforming $\mathbb{W}$ in the dual domain using (4.93).

   (e) If $\hat{\tau}_{\mathrm{inner}}$ has not converged, repeat Steps 5a to 5d.

6. (Inner loop ends.)

7. Set $\hat{\tau}_{\mathrm{outer}} = \hat{\tau}_{\mathrm{inner}}$.

8. If $\hat{\tau}_{\text{outer}}$ has not converged, update $\boldsymbol{\theta}$ using the subgradient projection method and go to Step 4.

9. [Outer loop ends.]

10. $\mathbf{p}, \mathbb{W}$ and $\mathbb{V}$ are the solutions for $\mathcal{P}$ and the optimal value equals $\hat{\tau}_{\text{outer}}$.

Lemma 4.4. *If the initial beamforming parameters* $\mathbb{W}$ *and* $\mathbb{V}$ *for the inner loop satisfy the conditions* (4.38) *and* (4.39)*, these conditions will continue to be satisfied in the iteration algorithm.*

Proof. Same as that of Lemma 4.3. □

Lemma 4.5. *If the initial beamforming parameters* $\mathbb{W}$ *and* $\mathbb{V}$ *satisfy the conditions* (4.38) *and* (4.39)*, the algorithm will converge.*

Proof. Please refer to Appendix 4.G. □

Note that the convergence point of the proposed solution is dependent on the appropriate choice of initial conditions. We consider a random initialization to satisfy the feasible conditions conditions (4.38) and (4.39). If a selected random initialization does not satisfy the feasible conditions conditions (4.38) and (4.39), we drop it and select a new one until it satisfies the feasible conditions conditions (4.38) and (4.39). Here, we do not consider any other advanced initializations, e.g., minimizing SI and maximizing UL transmission rate.

4.4 Results

To quantify the potential benefit of the FD transmission considered in this chapter, we evaluate the performance of the proposed algorithms under the 3GPP LTE specifications for urban macro (UMa) cell deployments. The simulation parameters of an UMa cell are taken from [95, 96]. The cell coverage area is assumed to be circular. For an UMa cell, the radius is set to 2 km and all the channels are considered to be under the non-line-of-sight (NLOS) environment. By setting the heights of BS and users to 31 m and 1.5 m, respectively, above ground [96, Section.1.2.1.3], we obtain the path-loss models of the UL channels, DL channels, and the IUI channels[2]. Then, the path-loss model of DL and UL channels is $122.5+35\log_{10}(d)$ and the path-loss model of inter-user-interference channels is $146.2+39.8\log_{10}(d_{\text{IUI}})$ where d and d_{IUI} are distances in km. Also, according to the suggestion in [95], the peak power constraints for UL users are the same and set to be 20 dB below the peak power constraint of BS. The noise spectral density is -174 dBm/Hz and the noise figure is set to 9 dB. The number of UL and DL users are both set as 8. The number of transmit and receive antennas are both set as 8. The small-scale fading is modeled as a multi-path time delay model following ITU-R M.1225 PedA [96]. The center frequency is 2 GHz and system bandwidth is 10 MHz. For simplicity, the UL SINR requirements are the same for all users, i.e., $\beta_{k_u} = \gamma$ $(\forall k_u \in \mathcal{K}_u)$ and the weights for the DL SINR are also the same, i.e., $\beta_{k_d} = \omega$ $(\forall k_d \in \mathcal{K}_d)$.

An accurate model for the SI channel plays an important role in evaluating the

[2]According to [96], the height of BS can be from 0 to 50 m above ground. We therefore set the height of BS to 31 m in the UL and DL channel models. However, the path-loss model of IUI channels has not been given specifically. Here we set the height of users to 1.5 m above ground in the IUI channel models as well as UL and DL channel models.

system performance of FD systems. A pioneer practical experiment on SI channel model has been carried out in [10]. The main conclusion of [10] is that the Rician probability distribution with a small Rician factor should be used to characterize the residual SI. Hence, in this chapter, the SI channel matrix $\boldsymbol{H}_{SI}$ is generated as $\mathcal{CN}(\sqrt{\frac{L\sigma_{SI}^2}{1+L}}\bar{\boldsymbol{H}}_{SI}, \frac{\sigma_{SI}^2}{1+K}\boldsymbol{I}_{N_R}\otimes\boldsymbol{I}_{N_T})$, where $\bar{\boldsymbol{H}}_{SI}$ is a deterministic matrix, L is the Rician factor, $\otimes$ denotes the Kronecker product and σ_{SI}^2 is introduced to parameterize the capability of a certain SI cancellation design.

We compare four optimization algorithms.

- Algorithm 1: Only power but no beamforming is considered (Refer to Algorithm 1)
- Algorithm 2: All power and transmit and receive beamforming are considered (Refer to Sect. 4.3.5 and Fig. 4.3)
- Algorithm 2(sub1): Power and receive beamforming is optimized (transmit beamforming strategy used is Maximum Ratio Transmitting (MRT))
- Algorithm 2(sub2) : Power and transmit beamforming is optimized (receive beamforming strategy used is Maximum Ratio Combining (MRC))

We plot the evolution of the max-min weighted SINR τ in the DL against the iteration number for these four algorithms in Fig. 4.4. Firstly, the SINR is monotonically increasing against the iteration number. Secondly, the maximum transmission power P_B and SI attenuation σ_{SI}^2 do not affect the convergence rate of τ at all. Thirdly, when beamforming optimizations are considered, the SINR values will improve significantly but it will take more iterations to converge. We also verify

that the average number of random initialization of $\mathbb{W}$ and $\mathbb{V}$ is less than 20 times, which is acceptable compared to the iteration number of the proposed Algorithm 2.

Next, we investigate the system performance and benefits of jointly optimizing the power and transmit and receive beamforming. Fig. 4.5 plots τ versus the base station transmission power. We can observe that among all algorithms, Algorithm II, i.e., jointly optimizing the transmission power and transmit and receive beamforming, will result in the best performance.

For a FD system, it is necessary to evaluate the impact of SI on the system performance. We plot τ versus the SI attenuation σ_{SI}^2 in Fig. 4.6. We can see that when SI attenuation is high, e.g., $\sigma_{SI}^2 \leq -30$dB the performance gain of our proposed algorithm (Algorithm II) is notable. However, when the SI attenuation is very low, e.g., $\sigma_{SI}^2 \geq -20$dB, the performance of all the algorithm is very limited. The main reason is that in the low SI attenuation region, the SI at the BS is relatively large. Thus, the transmit power at the BS has to be reduced in order to ensure that the UL SINR requirements can be satisfied. As a result, τ becomes smaller. Effective SI cancellation therefore plays a very important role here.

Fig. 4.7 shows the relationship between τ and the UL SINR requirements γ. As γ increases, τ decreases. Our proposed algorithm (Algorithm II) is shown to have the best performance under all conditions. Thus, the effectiveness of our proposed algorithm is verified.

4.5 Summary

In this chapter, we have investigated a MIMO FD multi-user cellular system. We have formulated the weighted max-min DL SINR problem with additional UL SINR constraints. Joint optimization of the base station transmit power, UL transmit power, and base station transmit and receive beamforming is required. We have derived the network duality of the optimization problem consisting of multiple UL SINR constraints and a single power constraint. With the network duality property, we are able to break down the multiple-power-and-multiple-SINR-constraint problem into many single-power-and-multiple-SINR constraint sub-problems. As a result, we can solve the multiple-power-and-multiple-SINR constraint problem by using Perron–Frobenius theory and subgradient method jointly. Simulation results show that our proposed algorithm possesses fast convergence rate and leads to a better performance compared to other optimization mechanisms. Finally, our proposed algorithm can be easily extended to solve other max-min optimization problems with arbitrary weight power constraints (e.g., weights can be negative).

Appendix 4.A Proof of Lemma 4.1

Proof. We prove Lemma 1 by contradiction. Referring to (4.8), we can observe that when all other parameters are fixed, $\frac{\mathrm{SINR}_{k_d}^{\mathrm{DL}}(\mathbf{p})}{\beta_{k_d}}$ is (i) an increasing function of p_{k_d} $\forall k_d \in \mathcal{K}_d$; (ii) a decreasing function of $p_{k'_d}$ if $k'_d \neq k_d$ and $k'_d \in \mathcal{K}_d$; and (iii) a decreasing function of p_{k_u} $\forall k_u \in \mathcal{K}_u$. Referring to (4.9), we can also see that when all other parameters are fixed, $\mathrm{SINR}_{k_u}^{\mathrm{UL}}(\mathbf{p})$ is (iv) a decreasing function of p_{k_d} $\forall k_d \in \mathcal{K}_d$; and (v) an increasing function of p_{k_u} $\forall k_u \in \mathcal{K}_u$.

We also denote $\hat{\tau}^i$ as the optimal solution and $\hat{\mathbf{p}}^i$ as the optimal power vector. Then, we have

$$\hat{\tau}^i \leq \frac{\mathrm{SINR}_{k_d}^{\mathrm{DL}}(\hat{\mathbf{p}}^i)}{\beta_{k_d}} \quad \forall k_d \in \mathcal{K}_d. \tag{4.97}$$

Moreover, there must exist at least one $\hat{k}_d \in \mathcal{K}_d$ such that $\hat{\tau}^i = \frac{\mathrm{SINR}_{\hat{k}_d}^{\mathrm{DL}}(\hat{\mathbf{p}}^i)}{\beta_{\hat{k}_d}}$. Assuming that (4.97) is satisfied with at least one strict inequality, i.e., there exists a $k'_d \in \mathcal{K}_d$ such that $\hat{\tau}^i < \frac{\mathrm{SINR}_{k'_d}^{\mathrm{DL}}(\hat{\mathbf{p}}^i)}{\beta_{k'_d}}$. Due to (i) above, we can continue maintaining the strict inequality if we reduce only very slightly the transmit power corresponding to k'_d, i.e., $p_{k'_d}$. Moreover, when $p_{k'_d}$ is reduced,

1. $\mathrm{SINR}_{k_u}^{\mathrm{UL}}(\hat{\mathbf{p}}^i)$ increases due to (iv) and hence (4.13c) is still satisfied;
2. $\mathbf{t}_i^T \hat{\mathbf{p}}^i$ decreases and hence (4.13d) is still satisfied;
3. $\frac{\mathrm{SINR}_{k_d}^{\mathrm{DL}}(\hat{\mathbf{p}}^i)}{\beta_{k_d}}$ increases for all other $k_d \neq k'_d$ due to (ii) and hence (4.13b) is still satisfied.

In other words, reducing $p_{k'_d}$ slightly is also a feasible solution to the problem $\mathcal{T}^i$ in (4.13a). However, as indicated in Item 3) above, $\frac{\mathrm{SINR}_{k_d}^{\mathrm{DL}}(\hat{\mathbf{p}}^i)}{\beta_{k_d}}$ increases for all other $k_d \neq k'_d$ and hence the new $\frac{\mathrm{SINR}_{\hat{k}_d}^{\mathrm{DL}}(\hat{\mathbf{p}}^i)}{\beta_{\hat{k}_d}}$ is strictly larger than $\hat{\tau}^i$. It means that $\hat{\tau}^i$ is not the optimal solution which contradicts to our assumption. Hence for the optimal solution, there does not exist any strict inequality in (4.97) and

$$\hat{\tau}^i = \frac{\mathrm{SINR}_{k_d}^{\mathrm{DL}}(\hat{\mathbf{p}}^i)}{\beta_{k_d}} \quad \forall k_d \in \mathcal{K}_d. \tag{4.98}$$

Next, we assume that the constraint in (4.13c) is not satisfied with equality for some $k'_u \in K_u$, i.e., $\mathrm{SINR}_{k'_u}^{\mathrm{UL}}(\hat{\mathbf{p}}^i) > \beta_{k'_u}$. Due to (v) above, we can reduce slightly

the power corresponding to k'_u, i.e., $p_{k'_u}$, to maintain the strict inequality. Moreover, when $p_{k'_u}$ is reduced,

4. $\frac{\text{SINR}_{k_d}^{\text{DL}}(\hat{\mathbf{p}}^i)}{\beta_{k_d}}$ increases for all $k_d \in K_d$ due to (ii) and hence (4.13b) is still satisfied;

5. $\mathbf{t}_i^T \hat{\mathbf{p}}^i$ decreases and hence (4.13d) is still satisfied.

In other words, reducing $p_{k'_u}$ slightly is also a feasible solution to the problem $\mathcal{T}^i$ in (4.13a). However, as indicated in Item 4) above, $\frac{\text{SINR}_{k_d}^{\text{DL}}(\hat{\mathbf{p}}^i)}{\beta_{k_d}}$ increases for all $k_d \in K_d$ and they become strictly larger than $\hat{\tau}^i$. It means that $\hat{\tau}^i$ is not the optimal solution which contradicts to our assumption. Hence for the optimal solution, there does not exist any strict inequality in (4.13c) and

$$\text{SINR}_{k_u}^{\text{UL}}(\hat{\mathbf{p}}^i) = \beta_{k_u} \quad \forall k_u \in K_u. \tag{4.99}$$

Finally, we consider the constraint in (4.13d). Using (4.6) and assuming $\alpha > 1$, we have

$$\begin{aligned}
\text{SINR}_k(\alpha\mathbf{p}) &= \frac{\alpha p_k G_{kk}}{\left(\sum_{l\in\mathcal{K}, l\neq k} \alpha p_l G_{kl}\right) + n_k} \quad k \in \mathcal{K} \\
&> \frac{\alpha p_k G_{kk}}{\left(\sum_{l\in\mathcal{K}, l\neq k} \alpha p_l G_{kl}\right) + \alpha n_k} \\
&= \frac{p_k G_{kk}}{\left(\sum_{l\in\mathcal{K}, l\neq k} p_l G_{kl}\right) + n_k} \\
&= \text{SINR}_k(\mathbf{p}).
\end{aligned} \tag{4.100}$$

Assuming that (4.13d) is satisfied with strict inequality, i.e. $\mathbf{t}_i^T \hat{\mathbf{p}}^i < P_i$, we can increase $\hat{\mathbf{p}}^i$ with the factor $\alpha > 1$ such that $\mathbf{t}_i^T(\alpha\hat{\mathbf{p}}^i) = P_i$. Moreover, (4.100) has

shown that $\mathrm{SINR}_k(\alpha\mathbf{p})$ is an increasing function of $\mathbf{p}$. Therefore, when $\hat{\mathbf{p}}^i$ is increased by the factor $\alpha > 1$, $\frac{\mathrm{SINR}_{k_d}^{\mathrm{DL}}(\hat{\mathbf{p}}^i)}{\beta_{k_d}}$ $(\forall k_d \in \mathcal{K}_d)$ in (4.13b) and $\mathrm{SINR}_{k_u}^{\mathrm{UL}}(\hat{\mathbf{p}}^i)$ $(\forall k_u \in \mathcal{K}_u)$ in (4.13c) are increased and hence both (4.13b) and (4.13c) are still satisfied. Since $\frac{\mathrm{SINR}_{k_d}^{\mathrm{DL}}(\hat{\mathbf{p}}^i)}{\beta_{k_d}}$ is increased for all $k_d \in \mathcal{K}_d$, $\hat{\tau}^i$ is no longer the optimal solution. This contradicts to our assumption. Thus, the constraint in (4.13d) must be satisfied with strict equality, i.e., $\mathbf{t}_i^T\hat{\mathbf{p}}^i = P_i$. □

Appendix 4.B Proof of Theorem 4.1

Proof. We transform the problem $\mathcal{T}$ in (4.11a)–(4.11c) into epigraph form, i.e.,

$$\mathcal{T}: \max_{\tau,\mathbf{p}} \quad \tau \tag{4.101a}$$

$$s.t. \quad \tau \le \frac{\mathrm{SINR}_{k_d}^{\mathrm{DL}}(\mathbf{p})}{\beta_{k_d}}, \quad \forall k_d \in \mathcal{K}_d \tag{4.101b}$$

$$\mathrm{SINR}_{k_u}^{\mathrm{UL}}(\mathbf{p}) \ge \beta_{k_u}, \quad \forall k_u \in \mathcal{K}_u \tag{4.101c}$$

$$\mathbf{t}_i^T\mathbf{p} \le P_i, \quad \mathbf{p} \ge \mathbf{0}, \quad \forall i = 0, 1, \ldots, K_u. \tag{4.101d}$$

We denote the optimal solution and power vector by $\hat{\tau}$ and $\hat{\mathbf{p}}$, respectively. Then, $\hat{\tau}$ and $\hat{\mathbf{p}}$ must satisfy (4.13b)–(4.13d) for all $i = 0, 1, \ldots, K_u$. Using arguments similar to those in proving Lemma 4.1, we can prove that under the optimal solutions, (i) the constraints (4.101b) and (4.101c) are satisfied with equality and (ii) there exists an $s \in \{0, 1, \ldots, K_u\}$ such that $\mathbf{t}_s^T\hat{\mathbf{p}} = P_s$.[3]

Again, for the sub-problem $\mathcal{T}^i$ in (4.13a), we let $\hat{\mathbf{p}}^i$ be the unique solution and

[3]If $\mathbf{t}_i^T\hat{\mathbf{p}} < P_i$ for all $i = 0, 1, \ldots, K_u$, we can always increase $\hat{\mathbf{p}}$ by a factor of $\alpha > 1$ such that $\mathbf{t}_s^T\hat{\mathbf{p}} = P_s$ for some s and $\mathbf{t}_i^T\hat{\mathbf{p}} < P_i$ for all $i \ne s$.

$\hat{\tau}^i$ be the optimal value. From the definition of the sub-problem, we can further conclude that $\hat{\mathbf{p}} = \hat{\mathbf{p}}^s$ and $\hat{\tau} = \hat{\tau}^s$. To determine the value of s, we consider $i \in \{0, 1, \ldots, K_u\}$ where $i \neq s$. Since $i \neq s$, we have $\mathbf{t}_i^T \hat{\mathbf{p}} < P_i$ and hence $\hat{\mathbf{p}}$ is not the optimal power vector of $\mathcal{T}^i$. Therefore the corresponding τ, i.e., $\hat{\tau} = \frac{\mathrm{SINR}_{k_d}^{\mathrm{DL}}(\mathbf{p})}{\beta_{k_d}}$ $(\forall k_d \in \mathcal{K}_d)$, is not the optimal value of $\mathcal{T}^i$ and hence must be smaller than $\hat{\tau}^i$. Combining all the aforementioned arguments, we have $\hat{\tau}^s = \hat{\tau} < \hat{\tau}^i$ for all $i \neq s$ and the proof is complete. □

Appendix 4.C Proof of Lemma 4.2

Proof. We first make note of the fact that the matrices/vectors $\mathbf{B}$, $\mathbf{F}$, $\hat{\mathbf{p}}$, $\mathbf{n}$ and $\mathbf{t}$ and their components are non-negative. Hence their products such as $\mathbf{B}_u\mathbf{F}_{uu}$ are non-negative.

If $\rho(\mathbf{B}_u\mathbf{F}_{uu}) < 1$, $\lim_{j\to\infty}(\mathbf{B}_u\mathbf{F}_{uu})^j = \mathbf{0}$ and therefore $(\mathbf{I} - \mathbf{B}_u\mathbf{F}_{uu})$ is a non-singular matrix [113]. In addition, by using the Neumann series $(\mathbf{I} - \mathbf{B}_u\mathbf{F}_{uu})^{-1} = \sum_{j=0}^{\infty}(\mathbf{B}_u\mathbf{F}_{uu})^j$, we can conclude that $(\mathbf{I}-\mathbf{B}_u\mathbf{F}_{uu})^{-1}$ is a non-negative matrix because $\mathbf{B}_u\mathbf{F}_{uu}$ is non-negative [113]. When $(\mathbf{I} - \mathbf{B}_u\mathbf{F}_{uu})^{-1}$ is non-negative, the matrix $\mathbf{E}$ in (4.29) and the vector $\mathbf{e}$ in (4.30) and the vector $\mathbf{g}_i$ in (4.33) are also non-negative because all other matrices in the equations are non-negative. Moreover, if (4.39) is satisfied, P_i' in (4.32) becomes positive. Therefore, all terms in $\boldsymbol{\Upsilon}^i$ in (4.37) are non-negative and the conditions (4.38) and (4.39) are sufficient.

If $\boldsymbol{\Upsilon}^i$ is non-negative, $\mathbf{E}$, $\mathbf{e}$, $\frac{1}{P_i'}\mathbf{g}_i\mathbf{E}$ and $\frac{1}{P_i'}\mathbf{g}_i\mathbf{e}$ are non-negative. Based on (4.29) and (4.30), $(\mathbf{I} - \mathbf{B}_u\mathbf{F}_{uu})$ must be a non-singular matrix. By using the Neumann series $(\mathbf{I} - \mathbf{B}_u\mathbf{F}_{uu})^{-1} = \sum_{j=0}^{\infty}(\mathbf{B}_u\mathbf{F}_{uu})^j$, we can conclude that $\rho(\mathbf{B}_u\mathbf{F}_{uu}) < 1$ and

$(\mathbf{I}-\mathbf{B}_u\mathbf{F}_{uu})^{-1}$ is a non-negative matrix because $\mathbf{B}_u\mathbf{F}_{uu}$ is non-negative [113]. Based on (4.33), $\mathbf{g}_i$ is also non-negative and hence P_i' in $\frac{1}{P_i'}\mathbf{g}_i\mathbf{E}$ and $\frac{1}{P_i'}\mathbf{g}_i\mathbf{e}$ must be positive. When P_i' is positive, (4.32) shows that $P_i > \mathbf{t}_{i,u}^T(\mathbf{I}-\mathbf{B}_u\mathbf{F}_{uu})^{-1}\mathbf{B}_u\mathbf{n}_u$. The necessary conditions are therefore proved. □

Appendix 4.D Proof of Corollary 4.1

Proof. First using similar arguments as in the proof of Lemma 4.1, we have

$$\mathcal{T}(\boldsymbol{\theta}) = \frac{\mathrm{SINR}_{k_d}^{\mathrm{DL}}(\hat{\mathbf{p}})}{\beta_{k_d}}, \quad \forall k_d \in \mathcal{K}_d \tag{4.102a}$$

$$\mathrm{SINR}_{k_u}^{\mathrm{UL}}(\hat{\mathbf{p}}) = \beta_{k_u}, \qquad \forall k_u \in \mathcal{K}_u \tag{4.102b}$$

$$\sum\nolimits_i \theta_i \mathbf{t}_i^T \hat{\mathbf{p}} = \sum\nolimits_i \theta_i P_i \tag{4.102c}$$

where $\hat{\mathbf{p}}$ is the optimal power vector under $\mathcal{T}(\boldsymbol{\theta})$.

Next, we prove the following inequality.

$$\min\{\mathcal{T}(\boldsymbol{\theta}_1), \mathcal{T}(\boldsymbol{\theta}_2)\} \le \mathcal{T}(\lambda\boldsymbol{\theta}_1 + (1-\lambda)\boldsymbol{\theta}_2), \qquad 0 \le \lambda \le 1 \tag{4.103}$$

Let $\mathbf{p}^*$ denote the optimal power vector corresponding to $\mathcal{T}(\lambda\boldsymbol{\theta}_1 + (1-\lambda)\boldsymbol{\theta}_2)$. Ap-

plying (4.102a) to (4.102c), we obtain

$$\mathcal{T}(\lambda\boldsymbol{\theta}_1 + (1-\lambda)\boldsymbol{\theta}_2) = \frac{\mathrm{SINR}_{k_d}^{\mathrm{DL}}(\mathbf{p}^*)}{\beta_{k_d}}, \quad \forall k_d \in \mathcal{K}_d \tag{4.104a}$$

$$\mathrm{SINR}_{k_u}^{\mathrm{UL}}(\mathbf{p}^*) = \beta_{k_u}, \qquad \forall k_u \in \mathcal{K}_u \tag{4.104b}$$

$$\begin{aligned} &\textstyle\sum_i \left(\lambda\theta_{1,i} + (1-\lambda)\theta_{2,i}\right)\mathbf{t}_i^T\mathbf{p}^* = \sum_i \left(\lambda\theta_{1,i} + (1-\lambda)\theta_{2,i}\right)P_i \\ \Rightarrow\ &\lambda\left(\textstyle\sum_i \theta_{1,i}\mathbf{t}_i^T\mathbf{p}^*\right) + (1-\lambda)\left(\sum_i \theta_{2,i}\mathbf{t}_i^T\mathbf{p}^*\right) = \lambda\left(\sum_i \theta_{1,i}P_i\right) + (1-\lambda)\left(\sum_i \theta_{2,i}P_i\right). \end{aligned} \tag{4.104c}$$

From (4.104c), one of the following

$$\textstyle\sum_i \theta_{1,i}\mathbf{t}_i^T\mathbf{p}^* \le \sum_i \theta_{1,i}P_i \tag{4.105}$$

$$\textstyle\sum_i \theta_{2,i}\mathbf{t}_i^T\mathbf{p}^* \le \sum_i \theta_{2,i}P_i \tag{4.106}$$

must hold true. Without loss of generality, suppose (4.105) is true and hence $\mathbf{p}^*$ is a potential solution to $\mathcal{T}(\boldsymbol{\theta}_1)$.

Case I: $\sum_i \theta_{1,i}\mathbf{t}_i^T\mathbf{p}^* = \sum_i \theta_{1,i}P_i$

Given

$$\textstyle\sum_i \theta_{1,i}\mathbf{t}_i^T\mathbf{p}^* = \sum_i \theta_{1,i}P_i, \tag{4.107}$$

we can readily prove that

$$\textstyle\sum_i \theta_{2,i}\mathbf{t}_i^T\mathbf{p}^* = \sum_i \theta_{2,i}P_i \tag{4.108}$$

based on (4.104c). According to the Perron-Frobenius theory [55], combining (4.107),

(4.104b) and the fact that $\frac{\mathrm{SINR}_{k_d}^{\mathrm{DL}}(\mathbf{p}^*)}{\beta_{k_d}}$ is a constant for all $k_d \in \mathcal{K}_d$ (from (4.104a)), we can conclude that $\mathbf{p}^*$ is the unique solution for (4.102a) to (4.102c) for $\boldsymbol{\theta} = \boldsymbol{\theta}_1$, which also indicate that $\mathbf{p}^*$ is the optimal power vector for $\mathcal{T}(\boldsymbol{\theta}_1)$. Therefore,

$$\mathcal{T}(\boldsymbol{\theta}_1) = \frac{\mathrm{SINR}_{k_d}^{\mathrm{DL}}(\mathbf{p}^*)}{\beta_{k_d}}, \quad \forall k_d \in \mathcal{K}_d. \tag{4.109}$$

With (4.108) and similar arguments, we can conclude that $\mathbf{p}^*$ is also the optimal power vector for $\mathcal{T}(\boldsymbol{\theta}_2)$, i.e.,

$$\mathcal{T}(\boldsymbol{\theta}_2) = \frac{\mathrm{SINR}_{k_d}^{\mathrm{DL}}(\mathbf{p}^*)}{\beta_{k_d}}, \quad \forall k_d \in \mathcal{K}_d. \tag{4.110}$$

Comparing (4.104a), (4.109) and (4.110), the inequality (4.103) is proved for Case I.

Case II: $\sum_i \theta_{1,i} \mathbf{t}_i^T \mathbf{p}^* < \sum_i \theta_{1,i} P_i$

Given

$$\sum\nolimits_i \theta_{1,i} \mathbf{t}_i^T \mathbf{p}^* < \sum\nolimits_i \theta_{1,i} P_i, \tag{4.111}$$

we can readily prove that

$$\sum\nolimits_i \theta_{2,i} \mathbf{t}_i^T \mathbf{p}^* > \sum\nolimits_i \theta_{2,i} P_i \tag{4.112}$$

based on (4.104c). Due to (4.112), $\mathbf{p}^*$ cannot be the optimal power vector of $\mathcal{T}(\boldsymbol{\theta}_2)$. (In fact, the strict inequality in (4.111) indicates that $\mathbf{p}^*$ cannot be the optimal power vector of $\mathcal{T}(\boldsymbol{\theta}_1)$ neither.) We define the optimal power vector of $\mathcal{T}(\boldsymbol{\theta}_2)$ as $\mathbf{p}^\dagger$.

Using (4.102c), we have

$$\mathcal{T}(\boldsymbol{\theta}_2) = \frac{\mathrm{SINR}_{k_d}^{\mathrm{DL}}(\mathbf{p}^\dagger)}{\beta_{k_d}}, \quad \forall k_d \in \mathcal{K}_d \tag{4.113a}$$

$$\mathrm{SINR}_{k_u}^{\mathrm{UL}}(\mathbf{p}^\dagger) = \beta_{k_u}, \qquad \forall k_u \in \mathcal{K}_u \tag{4.113b}$$

$$\sum\nolimits_i \theta_{2,i} \mathbf{t}_i^T \mathbf{p}^\dagger = \sum\nolimits_i \theta_{2,i} P_i. \tag{4.113c}$$

We further define

$$\alpha_k = \frac{p_k^\dagger}{p_k^*} \qquad \forall k \in \mathcal{K}, \tag{4.114}$$

$$\check{k} = \arg\min_{k \in \mathcal{K}} \alpha_k. \tag{4.115}$$

Assuming that $\alpha_{\check{k}} \geq 1$, then $\alpha_k \geq 1$ for all $k \in \mathcal{K}$ and

$$\sum\nolimits_i \theta_{2,i} \mathbf{t}_i^T \mathbf{p}^\dagger \geq \sum\nolimits_i \theta_{2,i} \mathbf{t}_i^T \mathbf{p}^* > \sum\nolimits_i \theta_{2,i} P_i \tag{4.116}$$

where the first inequality comes from (4.114) and the second one comes from (4.112). The outcome in (4.116) contradicts with the fact in (4.113c). Therefore, the assumption $\alpha_{\check{k}} \geq 1$ is not justified and we conclude that $\alpha_{\check{k}} < 1$.

Next, assuming that $\check{k} \in \mathcal{K}_u$, we have

$$\begin{aligned}
\mathrm{SINR}_{\check{k}}^{\mathrm{UL}}(\mathbf{p}^{\dagger}) &= \frac{p_{\check{k}}^{\dagger} G_{\check{k}\check{k}}}{\sum_{l\in\mathcal{K}, l\neq\check{k}} p_l^{\dagger} G_{\check{k}l} + n_{\check{k}}} \\
&= \frac{\alpha_{\check{k}} p_{\check{k}}^{*} G_{\check{k}\check{k}}}{\sum_{l\in\mathcal{K}, l\neq\check{k}} \alpha_l p_l^{*} G_{\check{k}l} + n_{\check{k}}} \\
&< \frac{\alpha_{\check{k}} p_{\check{k}}^{*} G_{\check{k}\check{k}}}{\alpha_{\check{k}} \sum_{l\in\mathcal{K}, l\neq\check{k}} p_l^{*} G_{\check{k}l} + n_{\check{k}}} \\
&< \frac{\alpha_{\check{k}} p_{\check{k}}^{*} G_{\check{k}\check{k}}}{\alpha_{\check{k}} \sum_{l\in\mathcal{K}, l\neq\check{k}} p_l^{*} G_{\check{k}l} + \alpha_{\check{k}} n_{\check{k}}} \\
&= \frac{p_{\check{k}}^{*} G_{\check{k}\check{k}}}{\sum_{l\in\mathcal{K}, l\neq\check{k}} p_l^{*} G_{\check{k}l} + n_{\check{k}}} \\
&= \mathrm{SINR}_{\check{k}}^{\mathrm{UL}}(\mathbf{p}^{*}) = \beta_{\check{k}}
\end{aligned} \tag{4.117}$$

where the second equality follows from (4.114), and the third and fourth strict inequalities follow from that fact that $\min_{k\in\mathcal{K}} \alpha_k = \alpha_{\check{k}} < 1$. However, the outcome in (4.117) contradicts with the fact in (4.113b). Therefore, the assumption $\check{k} \in \mathcal{K}_u$ is not justified and we conclude that $\check{k} \in \mathcal{K}_d$.

Since $\min_{k\in\mathcal{K}} \alpha_k = \alpha_{\check{k}} < 1$ and $\check{k} \in \mathcal{K}_d$, we have

$$\begin{aligned}
\mathcal{T}(\boldsymbol{\theta}_2) &= \frac{\mathrm{SINR}_{k_d}^{\mathrm{DL}}(\mathbf{p}^\dagger)}{\beta_{k_d}}, \quad \forall k_d \in \mathcal{K}_d \\
&= \frac{p_{\check{k}}^\dagger G_{\check{k}\check{k}}}{\sum_{l\in\mathcal{K},l\neq\check{k}} p_l^\dagger G_{\check{k}l} + n_{\check{k}}} \\
&= \frac{\alpha_{\check{k}} p_{\check{k}}^* G_{\check{k}\check{k}}}{\sum_{l\in\mathcal{K},l\neq\check{k}} \alpha_l p_l^* G_{\check{k}l} + n_{\check{k}}} \\
&< \frac{\alpha_{\check{k}} p_{\check{k}}^* G_{\check{k}\check{k}}}{\alpha_{\check{k}} \sum_{l\in\mathcal{K},l\neq\check{k}} p_l^* G_{\check{k}l} + n_{\check{k}}} \\
&< \frac{\alpha_{\check{k}} p_{\check{k}}^* G_{\check{k}\check{k}}}{\alpha_{\check{k}} \sum_{l\in\mathcal{K},l\neq\check{k}} p_l^* G_{\check{k}l} + \alpha_{\check{k}} n_{\check{k}}} \\
&= \frac{p_{\check{k}}^* G_{\check{k}\check{k}}}{\sum_{l\in\mathcal{K},l\neq\check{k}} p_l^* G_{\check{k}l} + n_{\check{k}}} \\
&= \frac{\mathrm{SINR}_{\check{k}}^{\mathrm{DL}}(\mathbf{p}^*)}{\beta_{\check{k}}} \\
&= \mathcal{T}(\lambda\boldsymbol{\theta}_1 + (1-\lambda)\boldsymbol{\theta}_2)
\end{aligned} \tag{4.118}$$

where the last two equalities follow from (4.104a). Therefore, we have proved (4.103). Further, we can easily extend (4.103) to the general case, i.e.,

$$\min_i\{\mathcal{T}(\boldsymbol{\theta}_i)\} \leq \mathcal{T}\left(\sum\nolimits_i \lambda_i\boldsymbol{\theta}_i\right); \quad 0 \leq \lambda_i \leq 1 \ \ \forall i \ \text{ and } \ \sum \lambda_i = 1. \tag{4.119}$$

Finally, we will prove that the optimal solution $\hat{\tau}$ of $\mathcal{T}$ equals $\min\{\mathcal{T}(\boldsymbol{\theta}) : \boldsymbol{\theta} \geq \mathbf{0}\}$. We define $\boldsymbol{\theta}_i$ as a unit vector of length K_u with a 1 in its i-th entry and 0 elsewhere. From Theorem 4.1, we have

$$\hat{\tau} \ = \ \min_{i=0,\ldots,K_u} \hat{\tau}^i = \min_{i=0,\ldots,K_u} \{\mathcal{T}(\boldsymbol{\theta}_i)\} \in \mathcal{T}(\boldsymbol{\theta}). \tag{4.120}$$

We also normalize θ_i in (4.102c) by defining $\lambda_i = \frac{\theta_i}{\sum \theta_i}$ and we rewrite (4.102c) as

$$\begin{aligned}
& \textstyle\sum_i \theta_i \mathbf{t}_i^T \hat{\mathbf{p}} && = \sum_i \theta_i P_i \\
\Rightarrow \quad & \tfrac{\sum_i \theta_i \mathbf{t}_i^T \hat{\mathbf{p}}}{\sum \theta_i} && = \frac{\sum_i \theta_i P_i}{\sum \theta_i} \\
\Rightarrow \quad & \textstyle\sum_i \left(\frac{\theta_i}{\sum \theta_i}\right) \mathbf{t}_i^T \hat{\mathbf{p}} && = \sum_i \left(\frac{\theta_i}{\sum \theta_i}\right) P_i \\
\Rightarrow \quad & \textstyle\sum_i \lambda_i \mathbf{t}_i^T \hat{\mathbf{p}} && = \sum_i \lambda_i P_i; \qquad 0 \le \lambda_i \le 1 \ \ \forall i \ \text{ and } \ \sum \lambda_i = 1. \quad (4.121)
\end{aligned}$$

The result in (4.121) indicates that $\mathcal{T}(\boldsymbol{\theta})$ and $\mathcal{T}(\boldsymbol{\lambda})$ are identical, i.e.,

$$\mathcal{T}(\boldsymbol{\theta}) = \mathcal{T}(\boldsymbol{\lambda}); \qquad \lambda_i = \frac{\theta_i}{\sum \theta_i} \forall i; \tag{4.122}$$

where $\boldsymbol{\lambda}$ is the normalized version of $\boldsymbol{\theta}$. Combining (4.119) and (4.122), we obtain

$$\mathcal{T}(\boldsymbol{\theta}) = \mathcal{T}(\boldsymbol{\lambda}) = \mathcal{T}\left(\textstyle\sum_i \lambda_i \boldsymbol{\theta}_i\right) \ge \min_i \{\mathcal{T}(\boldsymbol{\theta}_i)\}. \tag{4.123}$$

Together with (4.120), we can conclude

$$\hat{\tau} \ = \ \min_{i=0,\ldots,K_u} \{\mathcal{T}(\boldsymbol{\theta}_i)\} = \min\{\mathcal{T}(\boldsymbol{\theta}) : \boldsymbol{\theta} \ge \mathbf{0}\}. \tag{4.124}$$

□

Appendix 4.E Proof of Corollary 4.2

Proof. To prove that $\mathcal{T}(\boldsymbol{\theta})$ is a quasi-convex function w.r.t. $\boldsymbol{\theta}$, we need to show that

$$\mathcal{T}(\lambda\boldsymbol{\theta}_1 + (1-\lambda)\boldsymbol{\theta}_2) \leq \max\{\mathcal{T}(\boldsymbol{\theta}_1), \mathcal{T}(\boldsymbol{\theta}_2)\} \tag{4.125}$$

for arbitrary $\boldsymbol{\theta}_1$ and $\boldsymbol{\theta}_2$ and $0 < \lambda < 1$. Let $\mathbf{p}^*$ denote the optimal power vector corresponding to $\mathcal{T}(\lambda\boldsymbol{\theta}_1 + (1-\lambda)\boldsymbol{\theta}_2)$. Following the procedures shown in the proof of Corollary 4.1, one of the following

$$\sum\nolimits_i \theta_{1,i}\mathbf{t}_i^T\mathbf{p}^* \leq \sum\nolimits_i \theta_{1,i}P_i \tag{4.126}$$

$$\sum\nolimits_i \theta_{2,i}\mathbf{t}_i^T\mathbf{p}^* \leq \sum\nolimits_i \theta_{2,i}P_i \tag{4.127}$$

must hold true. Without loss of generality, suppose (4.126) is true and hence $\mathbf{p}^*$ is a potential solution to $\mathcal{T}(\boldsymbol{\theta}_1)$. We further define

$$\tilde{\mathbf{p}} = \left(\frac{\sum_i \theta_{1,i}P_i}{\sum_i \theta_{1,i}\mathbf{t}_i^T\mathbf{p}^*}\right)\mathbf{p}^* \geq \mathbf{p}^*. \tag{4.128}$$

In (4.100), we have proved that $\mathrm{SINR}_k(\mathbf{p})$ is an increasing function of $\mathbf{p}$. Therefore, $\tilde{\mathbf{p}}$ satisfies the SINR constraints and power constraints of $\mathcal{T}(\boldsymbol{\theta}_1)$ and is also a feasible solution to $\mathcal{T}(\boldsymbol{\theta}_1)$. As a result, we have

$$\begin{aligned}\mathcal{T}(\lambda\boldsymbol{\theta}_1 + (1-\lambda)\boldsymbol{\theta}_2) &= \frac{\mathrm{SINR}_{k_d}^{\mathrm{DL}}(\mathbf{p}^*)}{\beta_{k_d}} \quad \forall k_d \in \mathcal{K}_d \\ &\leq \frac{\mathrm{SINR}_{k_d}^{\mathrm{DL}}(\tilde{\mathbf{p}})}{\beta_{k_d}} \quad \forall k_d \in \mathcal{K}_d \\ &\leq \mathcal{T}(\boldsymbol{\theta}_1)\end{aligned} \tag{4.129}$$

where the first inequality follows from the fact $\frac{\mathrm{SINR}_{k_d}^{\mathrm{DL}}(\mathbf{p})}{\beta_{k_d}}$ is an increasing function of $\mathbf{p}$ and the second inequality follows from that $\tilde{\mathbf{p}}$ is a feasible solution to $\mathcal{T}(\boldsymbol{\theta}_1)$. Similarly, we can prove that $\mathcal{T}(\lambda\boldsymbol{\theta}_1 + (1-\lambda)\boldsymbol{\theta}_2) \leq \mathcal{T}(\boldsymbol{\theta}_2)$ if (4.127) is true. Thus, (4.125) is proved and hence $\mathcal{T}(\boldsymbol{\theta})$ is a quasi-convex function w.r.t. $\boldsymbol{\theta}$. □

Appendix 4.F Proof of Lemma 4.3

To reduce the number of symbols, we will not show the index "i" in the proof. We assume that the initial beamforming matrices $\mathbb{W}^{(0)}$ and $\mathbb{V}^{(0)}$ satisfy the required conditions in (4.38) and (4.39), i.e., $\boldsymbol{\Upsilon}(\mathbb{W}^{(0)}, \mathbb{V}^{(0)})$ in (4.37) is a nonnegative matrix.

In the primal domain, $\hat{\mathbf{p}}_d^{(1)} > \mathbf{0}$ is derived from **Result 1**. Then, by using (4.27), $\mathbf{p}_u^{(1)} > \mathbf{0}$ can be obtained. Based on (4.25), we also have

$$\hat{\mathbf{p}}_u^{(1)} = \mathbf{B}_u^{(0)}\mathbf{F}_{uu}^{(0)}\hat{\mathbf{p}}_u^{(1)} + \mathbf{B}_u^{(1)}\mathbf{n}_u + \mathbf{B}_u^{(0)}\mathbf{F}_{ud}^{(0)}\hat{\mathbf{p}}_d^{(1)}. \tag{4.130}$$

Then, the receive beamforming $\mathbb{V}^{(1)}$ is updated using (4.89). As a result,

$$\mathrm{SINR}_{k_u}^{\mathrm{UL}}(\mathbb{V}^{(1)}) \geq \mathrm{SINR}_{k_u}^{\mathrm{UL}}(\mathbb{V}^{(0)}), \quad \forall k_u \in \mathcal{K}_u. \tag{4.131}$$

Note that the matrices $\mathbf{B}$ and $\mathbf{F}$ and their components are updated as the receive beamforming is updated. Combining (4.130), (4.131) and the definition of $\mathrm{SINR}_{k_u}^{\mathrm{UL}}(\mathbb{V})$, we have

$$\hat{\mathbf{p}}_u^{(1)} \geq \mathbf{B}_u^{(1)}\mathbf{F}_{uu}^{(1)}\hat{\mathbf{p}}_u^{(1)} + \mathbf{B}_u^{(1)}\mathbf{n}_u + \mathbf{B}_u^{(1)}\mathbf{F}_{ud}^{(1)}\hat{\mathbf{p}}_d^{(1)}. \tag{4.132}$$

Note that $\mathbf{B}_u^{(1)}$, $\mathbf{F}_{uu}^{(1)}$, $\mathbf{n}_u$ and $\mathbf{F}_{ud}^{(1)}$ are positive while $\hat{\mathbf{p}}_u^{(1)}$ and $\hat{\mathbf{p}}_d^{(1)}$ are non-negative with at least one positive element. Therefore, we have

$$\begin{aligned}
& \hat{\mathbf{p}}_u^{(1)} && > \mathbf{B}_u^{(1)}\mathbf{F}_{uu}^{(1)}\hat{\mathbf{p}}_u^{(1)} \\
\Rightarrow \quad & \frac{\hat{\mathbf{p}}_u^{(1)}}{\left(\hat{\mathbf{p}}_u^{(1)}\right)^T\hat{\mathbf{p}}_u^{(1)}} && > \frac{\mathbf{B}_u^{(1)}\mathbf{F}_{uu}^{(1)}\hat{\mathbf{p}}_u^{(1)}}{\left(\hat{\mathbf{p}}_u^{(1)}\right)^T\hat{\mathbf{p}}_u^{(1)}} \\
\Rightarrow \quad & 1 && > \frac{\left(\hat{\mathbf{p}}_u^{(1)}\right)^T\mathbf{B}_u^{(1)}\mathbf{F}_{uu}^{(1)}\hat{\mathbf{p}}_u^{(1)}}{\left(\hat{\mathbf{p}}_u^{(1)}\right)^T\hat{\mathbf{p}}_u^{(1)}} \\
\Rightarrow \quad & 1 && > \rho(\mathbf{B}_u^{(1)}\mathbf{F}_{uu}^{(1)})
\end{aligned} \tag{4.133}$$

and the required condition in (4.38) is satisfied. From (4.132), we obtain

$$\begin{aligned}
\hat{\mathbf{p}}_u^{(1)} &> \mathbf{B}_u^{(1)}\mathbf{F}_{uu}^{(1)}\hat{\mathbf{p}}_u^{(1)} + \mathbf{B}_u^{(1)}\mathbf{n}_u \\
\Rightarrow \hat{\mathbf{p}}_u^{(1)} &> (\mathbf{I} - \mathbf{B}_u^{(1)}\mathbf{F}_{uu}^{(1)})^{-1}\mathbf{B}_u^{(1)}\mathbf{n}_u.
\end{aligned} \tag{4.134}$$

Combining (4.134) and (4.26), we have

$$P \geq \mathbf{t}_u^T\hat{\mathbf{p}}_u^{(1)} > \mathbf{t}_u^T(\mathbf{I} - \mathbf{B}_u^{(1)}\mathbf{F}_{uu}^{(1)})^{-1}\mathbf{B}_u^{(1)}\mathbf{n}_u. \tag{4.135}$$

and the required condition in (4.39) is therefore satisfied. Since both (4.38) and (4.39) are satisfied based on $\mathbb{W}^{(0)}$ and $\mathbb{V}^{(1)}$, the power vector $\hat{\mathbf{p}}$ in the primal domain and hence the dual power vector $\hat{\mathbf{q}}$ in the dual domain can be updated.

The fact that the dual power vector $\hat{\mathbf{q}}^{(1)}$ in the dual domain can be evaluated also means that (4.83) and (4.84) are satisfied based on $\mathbb{W}^{(0)}$ and $\mathbb{V}^{(1)}$. Having

evaluated $\hat{\mathbf{q}}_d^{(1)}$ and $\hat{\mathbf{q}}_u^{(1)}$ using **Result 3**, we can re-write (4.76) as

$$\hat{\mathbf{q}}_u^{(1)} = \mathbf{B}_u^{(1)} \mathbf{F}_{uu}^{T\ (1)} \hat{\mathbf{q}}_u^{(1)} + \mathbf{B}_u^{(1)} \mathbf{t}_{i,u} + \mathbf{B}_u^{(1)} \mathbf{F}_{du}^{T\ (1)} \hat{\mathbf{q}}_d^{(1)}. \tag{4.136}$$

Then, the transmit beamforming $\mathbb{W}^{(1)}$ in the dual domain is updated using (4.93). As a result,

$$\mathrm{SINR}_{k_d}(\mathbb{W}^{(1)}) \geq \mathrm{SINR}_{k_d}(\mathbb{W}^{(0)}), \quad \forall k_d \in \mathcal{K}_d. \tag{4.137}$$

Combining (4.136), (4.137) and the definition of $\mathrm{SINR}_{k_d}(\mathbb{W})$ and using similar procedures as above, we can readily proved that (4.83) and (4.84) are satisfied. Since both (4.83) and (4.84) are satisfied based on $\mathbb{W}^{(1)}$ and $\mathbb{V}^{(1)}$, the dual power vector $\hat{\mathbf{q}}$ in the dual domain and hence the power vector $\hat{\mathbf{p}}$ in the primal domain can be updated.

The fact that the power vector $\hat{\mathbf{p}}^{(2)}$ in the primal domain can be evaluated again means that (4.38) and (4.39) are satisfied based on $\mathbb{W}^{(1)}$ and $\mathbb{V}^{(1)}$. We can therefore conclude that if the initial beamforming matrices $\mathbb{W}^{(0)}$ and $\mathbb{V}^{(0)}$ satisfy the required conditions in (4.38) and (4.39), the iterative beamforming matrices derived from our proposed algorithm will always satisfy the same conditions.

Appendix 4.G Proof of Lemma 4.5

where (a) is derived from the definition of subgradient method, (b) is from the network duality, (c) is from (4.89), (d) is from the network duality, (e) is from (4.93) and (f) is from the fact that the problem in (4.101a) is optimally solved with fixed beamforming under a single power constraint. Then, we readily have Lemma 4.5.

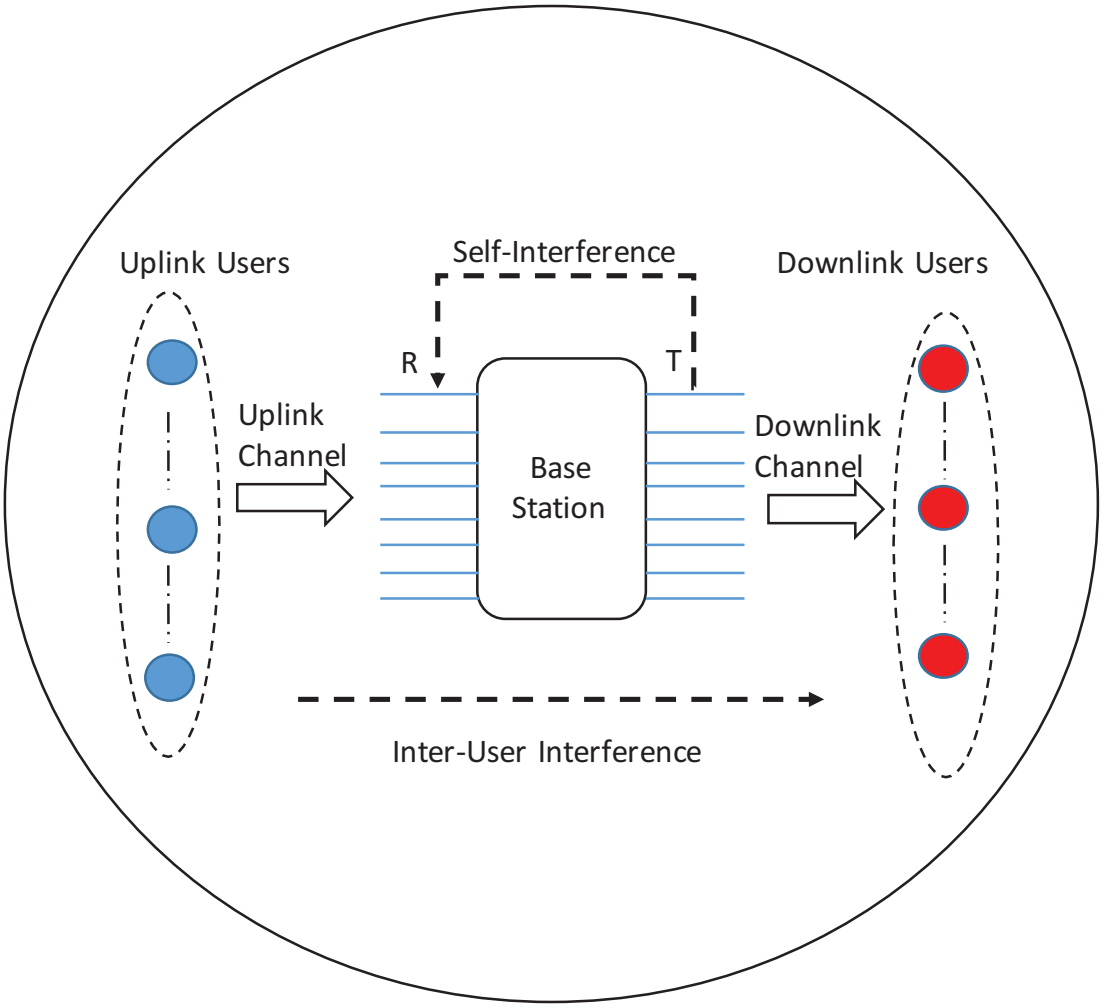

Figure 4.1: A single-cell MIMO system model with FD BS.

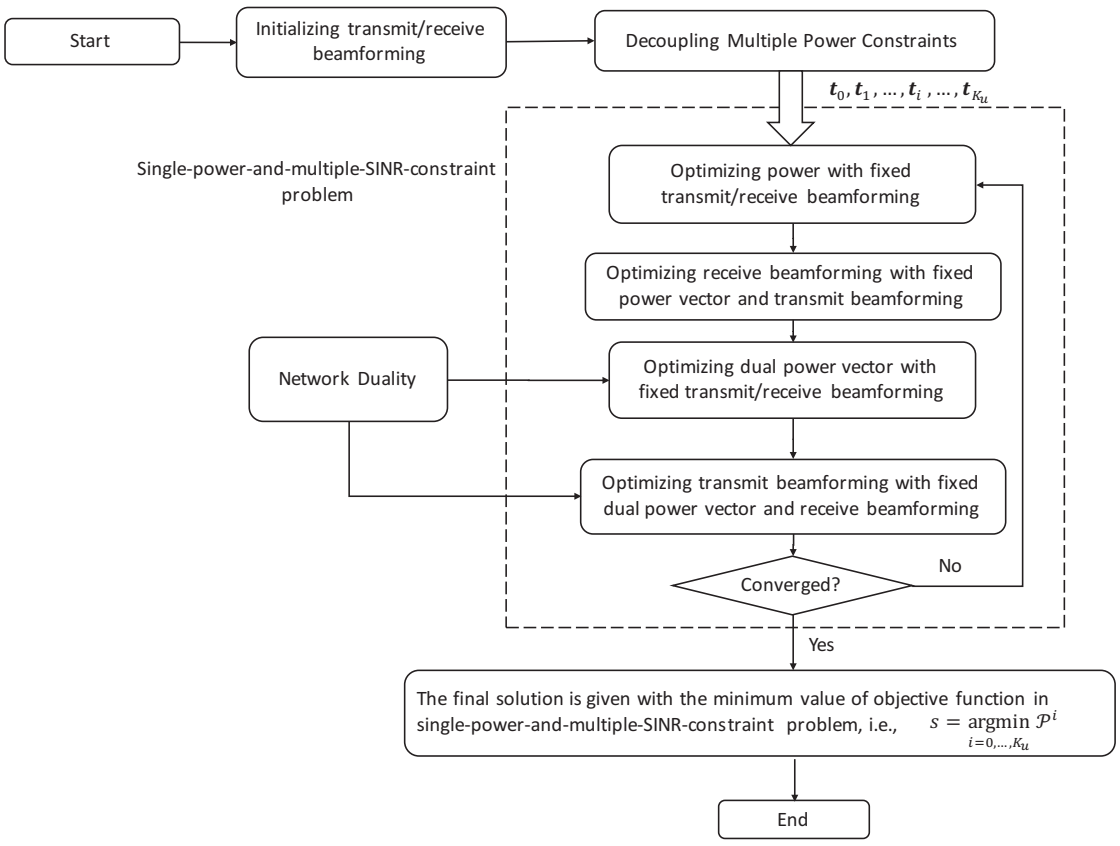

Figure 4.2: The flowchart for joint power and transmit/receive beamforming optimization by considering the power constraints individually.

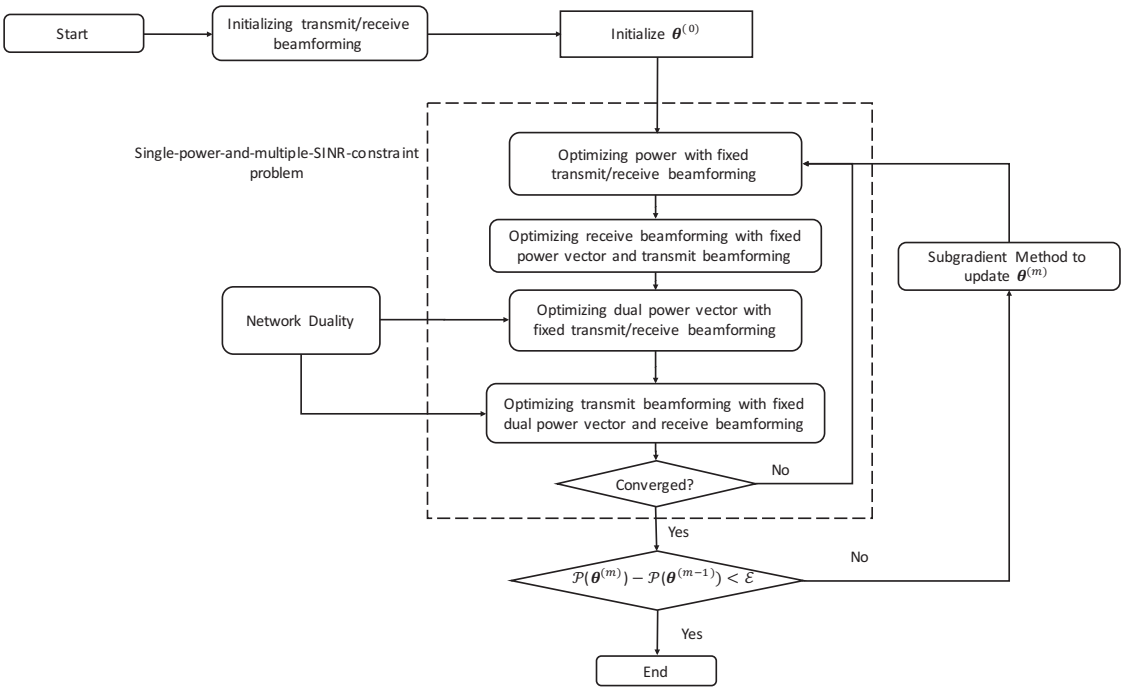

Figure 4.3: The flowchart for joint power and transmit/receive beamforming optimization by subgradient projection-based method.

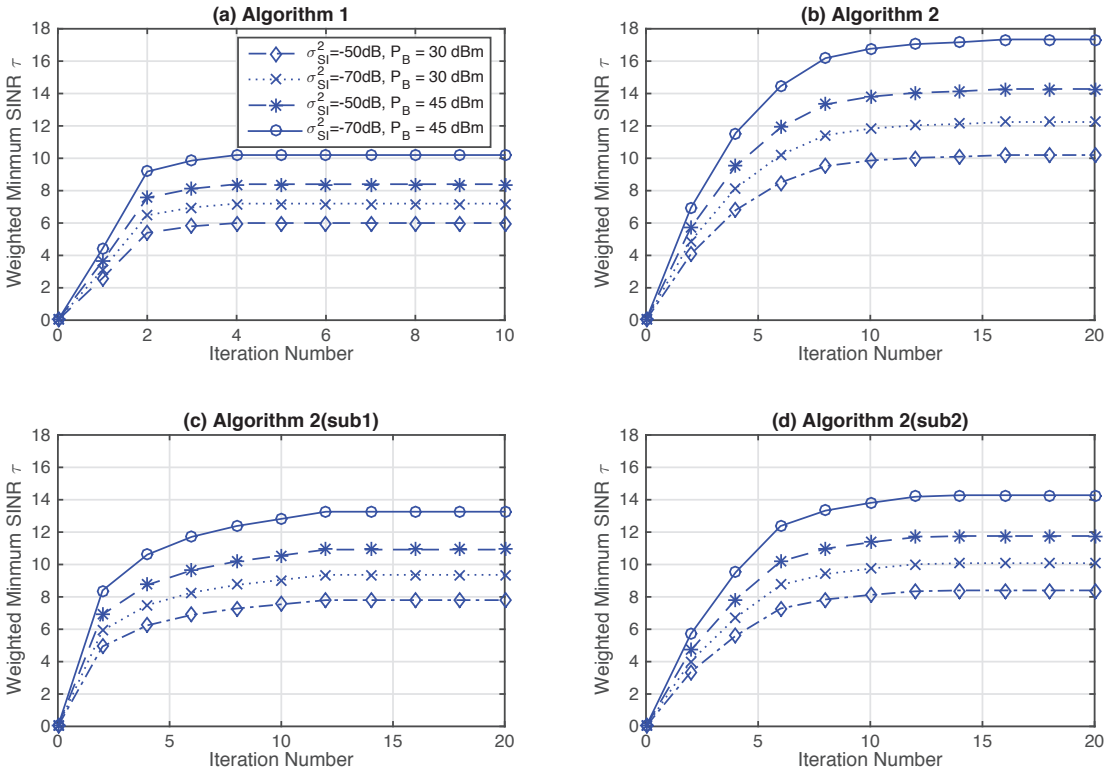

Figure 4.4: Convergence of τ against the iteration number for the four algorithms. Different maximum BS transmit power P_B and SI attenuation σ_{SI}^2 have been considered. The UL SINR requirement is $\gamma = 5$dB.

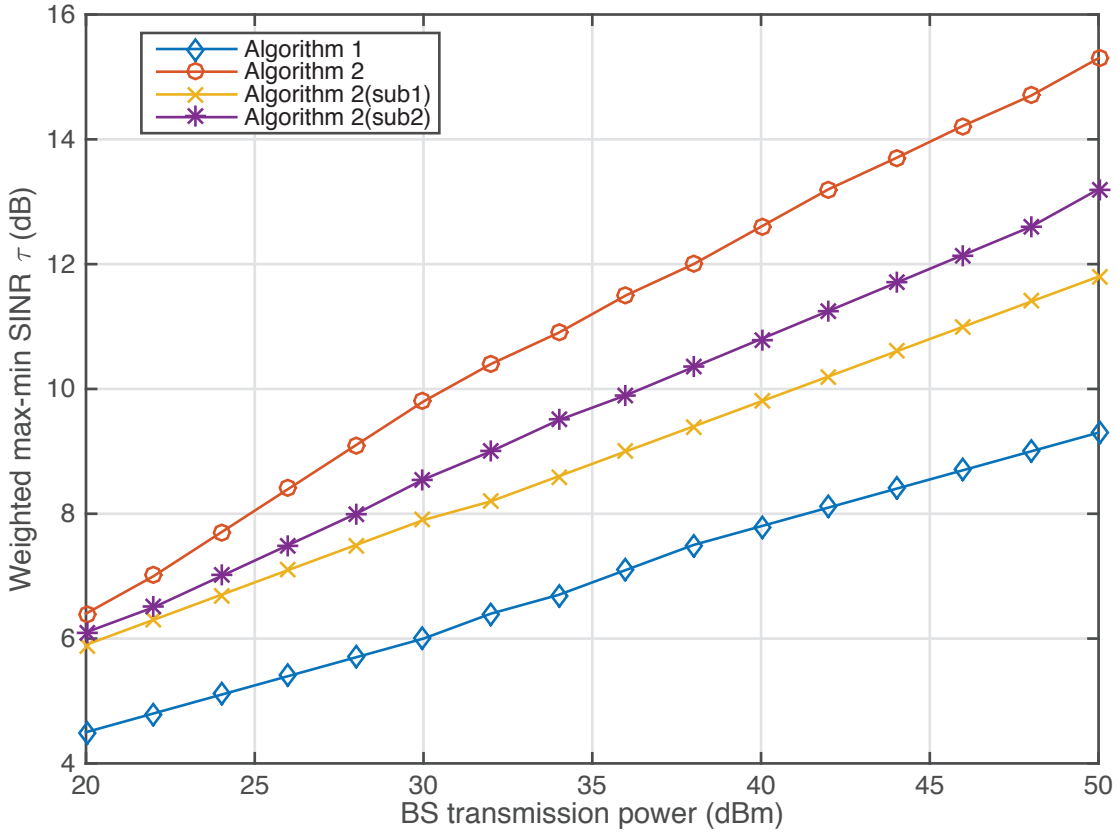

Figure 4.5: Weighted max-min DL SINR τ versus base station transmission power. The UL SINR requirements $\gamma = 5$dB and $\sigma_{SI}^2 = -50dB$.

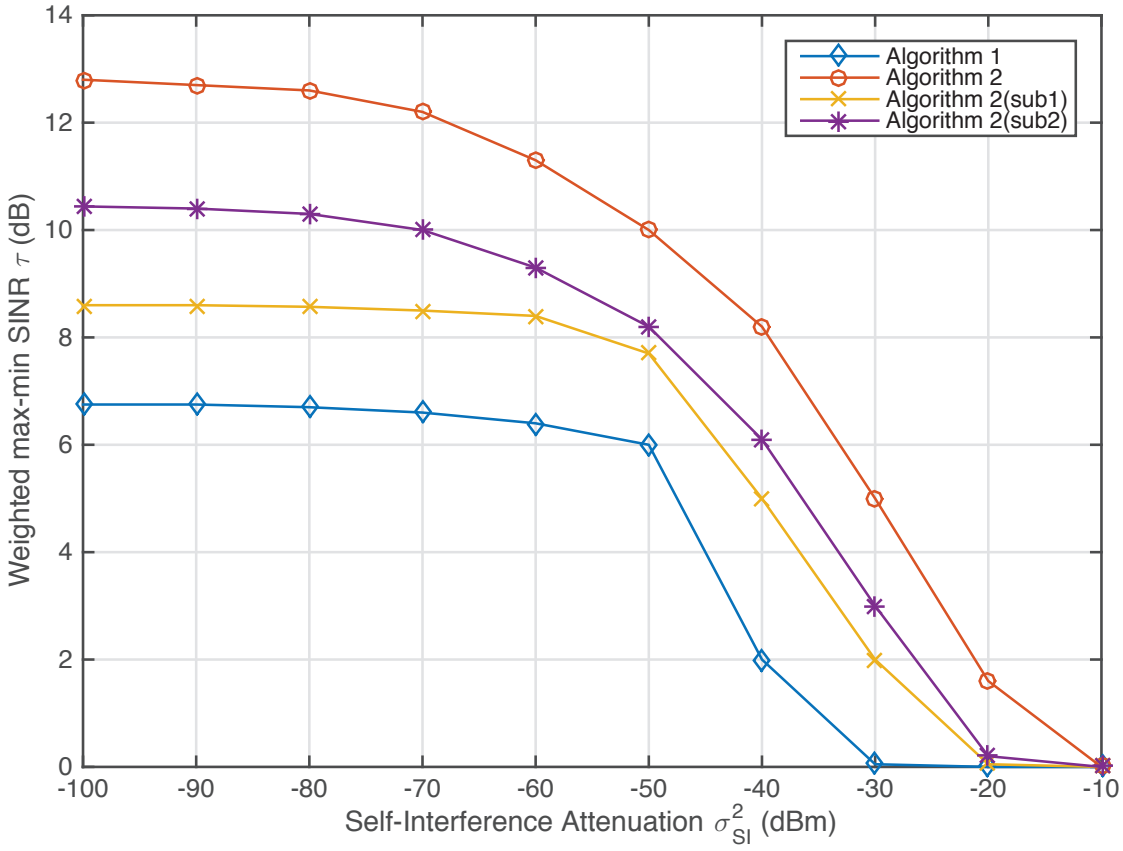

Figure 4.6: Weighted max-min DL SINR τ versus SI attenuation σ^2_{SI}. The UL SINR requirements $\gamma = 5$dB and the maximum base station transmit power $P_B = 30$dBm.

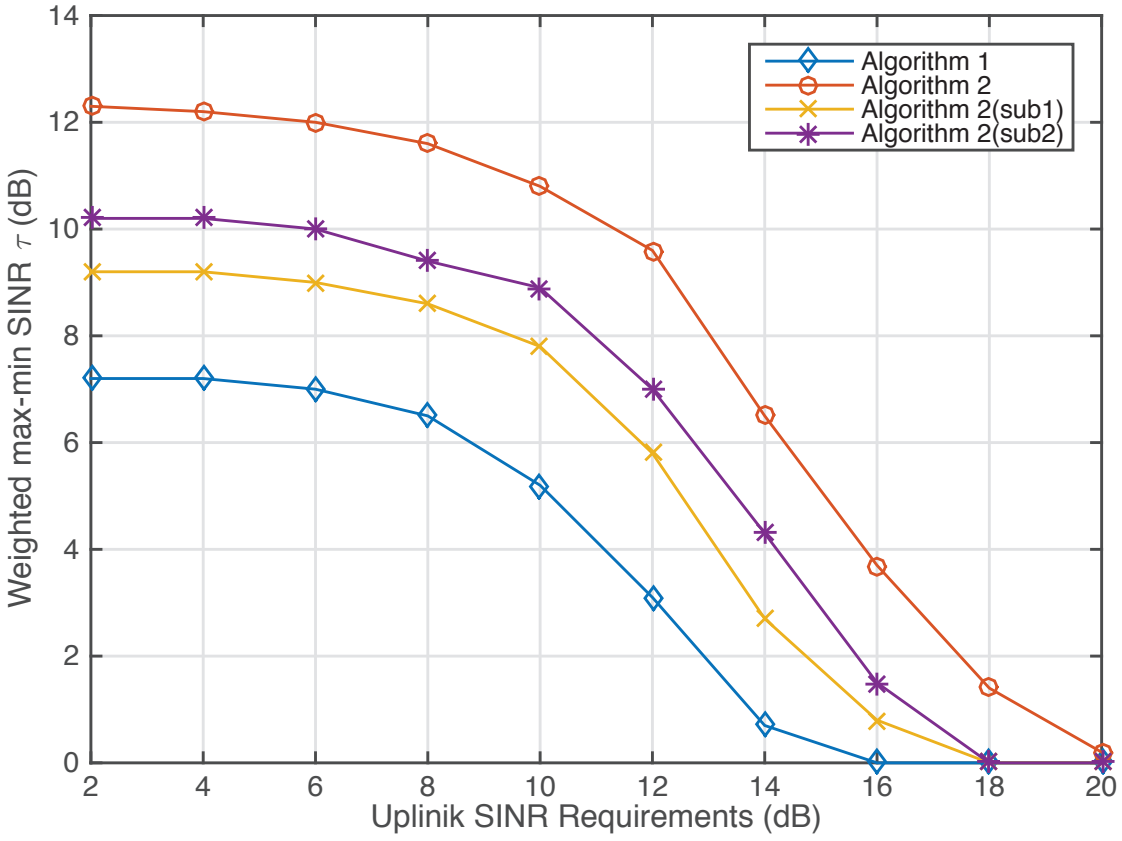

Figure 4.7: Weighted max-min DL SINR τ against UL SINR requirements γ. The maximum BS transmit power $P_B = 30$ dB and SI attenuation $\sigma_{SI}^2 = -70$ dB.

Chapter 5

Energy Efficiency Optimization in Full-Duplex Relay Systems

In this chapter, a FD relay system, in which a relay helps information delivery from the source to the destination in FD manner, is considered. The decode-and-forward relaying protocol is adopted since the relay has to decode the signals in order to perform self-interference cancellation. First, an optimization problem is formulated to maximize the energy efficiency (EE) in the FD relay system. The optimization problem is non-trivial and cannot be solved by conventional fractional programming methods, such as the Dinbelbach's method [114]. Then, the optimization problem is converted into an equivalent problem that can be further decomposed into two subproblems. The first subproblem can be solved by the Dinbelbach's method directly. The second subproblem is not quasi-concave because of the non-convex constraint, which cannot be solved by the Dinbelbach's method directly. An effective algorithm called sequential parametric convex approximation (SPCA) [87] is utilized to iter-

atively approach the optimum value at each iteration of the Dinbelbach's method. The joint algorithm is called SPCA-Dinbelbach.

5.1 System Model

We consider a three-node cooperative communication system in which the source S communicates with the destination D via a relay R, as shown in Fig. 5.1. The source and destination are equipped with a single antenna, while the relay is equipped with one receiving antenna and one transmitting antenna (can receive and transmit signals simultaneously). Let $x_s(t)$ and $x_r(t)$ denote the signals transmitted from S and from the transmitting antenna of R at the time instant t, respectively, where the average powers of transmitted symbols equal to 1, i.e., $E[x_s(t)'x_s(t)] = E[x_r(t)'x_r(t)] = 1$. Let H_{sr} denote the channel coefficient of the link between the source S and the relay R, H_{sd} denote the channel coefficient of the link between the source S and the destination D, and H_{rd} denote the channel coefficient of the link between the relay R and the destination D. The transmission powers of the source S and the relay R are denoted as P_s and P_r, respectively. Then, the received signals at the receiving antenna of R and D, denoted by $y_r(t)$ and $y_d(t)$ respectively, can be written as

$$y_r(t) = \sqrt{P_s}H_{sr}x_s(t) + \sqrt{P_r}H_{rr}x_r(t) + n_r(t), \tag{5.1}$$

$$y_d(t) = \sqrt{P_r}H_{rd}x_r(t) + \sqrt{P_s}H_{sd}x_s(t) + n_d(t), \tag{5.2}$$

where $n_r(t)$ and $n_d(t)$ are the additive white Gaussian noises at the relay R and the destination D, respectively, and follow $\mathcal{CN}(0, \sigma_z^2)$. It is assumed that the channel coefficient between node i and node j is $H_{ij} \sim \mathcal{CN}(0, \Omega_{i,j})$. Here $\Omega_{i,j}$ is determined

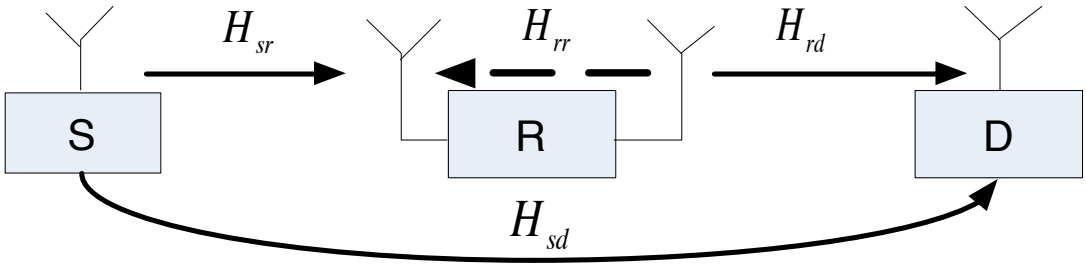

Figure 5.1: A full-duplex relay system. Solid lines denote information transmission and the dashed line denotes self-interference.

by the path-loss, i.e., $\Omega_{i,j} = (d_0/d_{ij})^m$, where m is the path-loss exponent, d_{ij} is the distance between node i and node j, and d_0 is the reference distance. The self-interference channel coefficient H_{rr} is modeled as $\sqrt{\beta}H_{SI}$, where β is the self-interference attenuation and $H_{SI} \sim \mathcal{CN}(0,1)$[1]. The effective channel gains are then defined as $G_{ij} = |H_{ij}|^2/\sigma_z^2$, $i \in \{s,r\}$, and $j \in \{r,d\}$.

The decode-and-forward relaying protocol is adopted at the relay[2]. Then, the achievable rate is given by [115, eq.7]

$$R_{\mathrm{DF}}(P_s, P_r) = \min\{R_{\mathrm{DF},1}(P_s, P_r), R_{\mathrm{DF},2}(P_s, P_r)\} \tag{5.3}$$

[1]Before analog domain cancellation, the self-interference channel has a strong line-of-sight component. So it can be modeled as a Ricean distribution with a large K-factor. It is shown experimentally in [10] that after applying a sufficiently large analog domain cancellation, the strong line-of-sight component is attenuated, resulting in a Ricean distribution with a small K-factor or a Rayleigh distribution.

[2]The decode-and-forward relaying protocol is adopted because the relay has to decode the signals in order to perform self-interference digital cancellation.

where $R_{\mathrm{DF},1}(P_s, P_r)$ and $R_{\mathrm{DF},2}(P_s, P_r)$ are defined as

$$R_{\mathrm{DF},1}(P_s, P_r) = \log_2(1 + \frac{P_s G_{sr}}{1 + \beta P_r G_{rr}}), \tag{5.4}$$

$$R_{\mathrm{DF},2}(P_s, P_r) = \log_2(1 + P_s G_{sd} + P_r G_{rd}). \tag{5.5}$$

However, if $G_{sd} \geq G_{sr}$, the achievable rate in (5.3) boils down to the rate of the direct transmission between the source and the destination, which is given by

$$R_{\mathrm{D}}(P_s) = \log_2(1 + P_s G_{sd}). \tag{5.6}$$

Hence, the overall achievable rate can be re-written as:

$$R(P_s, P_r) = \max\{R_{\mathrm{DF}}(P_s, P_r), R_{\mathrm{D}}(P_s)\}. \tag{5.7}$$

The EE of the FD relay system is studied, and is defined as

$$U_{\mathrm{eff}} = R(P_s, P_r)/P_T(P_s, P_r) \quad [\mathrm{bits/Joule}], \tag{5.8}$$

where the total power consumption P_T is calculated by

$$P_T(P_s, P_r) = P_s + P_r + P_c. \tag{5.9}$$

In (5.9), P_c denotes the energy consumed by the circuitry of the whole relay system, and is assumed to be constant. Assuming that the total power constraint of the source and relay is given by $P_s + P_r \leq P_{max}$, the optimal transmission powers P_s and P_r will be obtained by solving

Optimization Problem (P1)

$$\begin{aligned} \max_{P_s,P_r} \quad & U_{\text{eff}}(P_s, P_r) \\ \text{s.t.} \quad & C1 : P_s + P_r \leq P_{max}, \\ & C2 : P_s, P_r \geq 0. \end{aligned} \tag{5.10}$$

5.2 Algorithm

In this section, firstly the optimization problem **P1** will be transformed into an equivalent problem which can be further decomposed into two subproblems. Then, the subproblems will be solved one by one. In the optimization problem **P1**, the variables to be optimized are P_s and P_r. The objective function is a nonlinear fractional function, in which the numerator is a max-min function. Thus, this problem is very difficult to solve directly. Then, the optimization problem **P1** will be transformed into a simpler and equivalent problem, which can be solved. Note that assuming all the channel state informations are perfectly known at the source, the source does the optimization procedure in a centralized way, and then transmits the value of optimized power to the relay.

Lemma 5.1. *The solution to the optimization problem* **P1** *is equivalent to the solution to the optimization problem* **P2***, as described bellow.* ***Equivalent Optimization Problem (P2)***

$$\boldsymbol{P2.1}: \max_{P_s} \quad R_{\mathrm{D}}(P_s)/P_T(P_s,0) \tag{5.11}$$

$$\text{s.t.} \quad 0 \le P_s \le P_{max};$$

$$\boldsymbol{P2.2}: \max_{P_s,P_r} \quad R_{\mathrm{DF},2}(P_s,P_r)/P_T(P_s,P_r) \tag{5.12}$$

$$\text{s.t.} \quad P_s + P_r \le P_{max}, \tag{5.13}$$

$$P_s, P_r \ge 0, \tag{5.14}$$

$$R_{\mathrm{DF},1}(P_s,P_r) \ge R_{\mathrm{DF},2}(P_s,P_r), \tag{5.15}$$

where $R_{\mathrm{DF},1}(P_s,P_r)$*,* $R_{\mathrm{DF},2}(P_s,P_r)$*, and* $R_{\mathrm{D}}(P_s)$ *are defined in (5.4), (5.5), and (5.6), respectively. If* $G_{sd} \ge G_{sr}$*, solve the subproblem* **P2.1***; otherwise, solve the subproblem* **P2.2**.

Proof. Please refer to the Appendix 5.A. □

5.2.1 Solution to Problem P2.1

It is not hard to prove that the objective function of the problem **P2.1** is a quasi-concave function with respect to P_s, and the constraint is affine. Thus, we can directly use the traditional Dinkelbach's method to solve the problem seen in Algorithm 1. The detail of the Dinkelbach's method is given in the Appendix 2. It is worth to mention that at step 5 of Algorithm 1, we can derive a closed-form solution in each iteration. As follows, by applying the Karush-Kuhn-Tucker (KKT)

Algorithm 1 Dinkelbach's Method

1: Set $I_{\max}$ (maximum number of iterations),
$\epsilon_o > 0$ (convergence tolerance),
2: $q_1 = 0$ and $q_0 = 1$.
3: $i \leftarrow 1$.
4: **while** $q_i - q_{i-1} > \epsilon_o$ and $i < I_{\max}$ **do**
5: Solve $\max_{P_s}\{F(q_i) = R(P_s) - q_i P_T(P_s)\}$ subject to $0 \leq P_s \leq P_{max}$ to obtain the optimal solution P_s.
6: $q_i \leftarrow R(P_s)/P_T(P_s)$.
7: $i \leftarrow i + 1$.
8: **end while**
9: **return**

conditions [89], it can be obtained that

$$P_s = \left[\frac{1}{q_i} - \frac{1}{G_{sd}}\right]_0^{P_{max}} \tag{5.16}$$

where $[*]_0^{P_{max}} = \min(P_{max}, \max(0, *))$ is the box constraint.

5.2.2 Solution to Problem P2.2

Due to the non-convex constraint (5.15) , the problem **P2.2** is not a quasi-concave problem. It is not possible to use the traditional Dinkelbach's method because that convex optimization algorithm is not valid at step 5 of the Dinkelbach's Method in Algorithm 1. Specifically, the constraint (5.15) in the problem **P2.2** is extended as

$$\alpha_1 P_s + \alpha_2 P_r + \alpha_3 P_r P_s + \alpha_4 P_r^2 \leq 0, \tag{5.17}$$

where $\alpha_1 = G_{sd} - G_{sr}$, $\alpha_2 = G_{rd}$, $\alpha_3 = \beta G_{sd} G_{rr}$, and $\alpha_4 = \beta G_{sd} G_{rr}$.

Note that (5.17) is obviously a non-convex function. To deal with the non-

convex constraint, a SPCA method is utilized to iteratively solve the problem. Herein, we give the key lemma for the SPCA method.

Lemma 5.2. *Considering an optimization problem with non-convex constraint $g(\boldsymbol{x})$. If the function $G(\boldsymbol{x}, \lambda)$ have the following properties: i) for any $\boldsymbol{x}$, $g(\boldsymbol{x}) \leq G(\boldsymbol{x}, \lambda), \lambda > 0$; ii) for a given feasible point $\boldsymbol{x_0}$, there exists a $\lambda = \psi(\boldsymbol{x_0})$ satisfying $g(\boldsymbol{x}) = G(\boldsymbol{x}, \lambda)$ and $\nabla g(\boldsymbol{x}) = \nabla G(\boldsymbol{x}, \lambda)$, then $G(\boldsymbol{x}, \lambda)$ can replace $\lambda^{(l)}$ by $\psi(\boldsymbol{x}^{(l-1)})$ such that the relaxed problem with convex constraint $G(\boldsymbol{x}, \lambda)$ is solved iteratively until convergence. The iterative solution would finally converge to a KKT point.*

Proof. see [87]. □

It is observed in the constraint (5.15) that the unique effective part for non-convexity is $P_s P_r$. Thus, one only need to find a convex upper-bound to approach $P_s P_r$ iteratively. To do this, the following function is defined:

$$G([P_s, P_r], \lambda) = \frac{1}{2\lambda} P_s^2 + \frac{\lambda}{2} P_r^2, \tag{5.18}$$

which is a convex function used to over-estimate $P_r P_s$. Additionally, $\lambda^{(l+1)}$ is updated by $P_s^{(l)}/P_r^{(l)}$ iteratively. It is very easy to verify that the function $G([P_s, P_r], \lambda)$ satisfies **Lemma 3** (see Page 5).

Replacing $P_r P_s$ in (5.17) by $G([P_s, P_r], \lambda)$, the relaxed constraint is expressed as

$$\alpha_1 P_s + \alpha_2 P_r + \frac{\alpha_3}{2\lambda} P_s^2 + \frac{\alpha_3 \lambda}{2} P_r^2 + \alpha_4 P_r^2 \leq 0, \tag{5.19}$$

which can be proved as a convex constraint by the Hessian function [89].

The proposed SPCA-Dinkelbach algorithm is depicted as **Algorithm 2**. The

Algorithm 2 SPCA-Dinkelbach Algorithm

Set $I_{\max}^0$ (maximum number of outer iterations),
    $\epsilon_o > 0$ (convergence tolerance of outer iterations),
Set $I_{\max}^l$ (maximum number of inner iterations),
    $\epsilon_l > 0$ (convergence tolerance of inner iterations),
$q_1 = 0$ and $q_0 = 1$,
$\lambda^{(1)} = 0$ and $\lambda^{(0)} = 1$.
$i \leftarrow 1$.
while $q_i - q_{i-1} > \epsilon_o$ and $i < I_{\max}$ **do**
  while $|\lambda^{(l)} - \lambda^{(l-1)}| > \epsilon_l$ and $l < I_{\max}^l$ **do**
    Using the standard convex optimization (e.g., interior-point method) to solve the problem
    $\max_{P_s, P_r} F(q_i) = R_{\mathrm{DF},2}(P_s, P_r) - q_i P_T(P_s, P_r)$,
    s.t. (5.13), (5.14), and (5.19).
    Obtain the optimal transmission powers $P_s^{(l)}$ and $P_r^{(l)}$.
    $\lambda^{(l+1)} \leftarrow P_s^{(l)} / P_r^{(l)}$.
    $l \leftarrow l + 1$.
  end while
  $q_i \leftarrow R(P_s^{(l-1)}, P_r^{(l-1)}) / P_T(P_s^{(l-1)}, P_r^{(l-1)})$.
  $i \leftarrow i + 1$.
end while
return

algorithm is a dual iterative algorithm, in which the outer iteration is based on the Dinkelbach method and the inner iteration is based on SPCA. Although SPCA is converged to a solution satisfying the KKT conditions (i.e., local optimum is achieved), we find through extensive numerical simulations that the solution is in fact the global optimum. However, the global optimum cannot be derived theoretically so far.

5.3 Simulation Results

This section presents the results of applying the proposed SPCA-Dinkelbach algorithm to the FD relay system. The reference distance is $D_0 = 1$ m. The distance between the source and the destination is 10 m, and the relay is at the mid-point of the line connecting the source and the destination. The path-loss exponent is $m = 3$ and the noise power is $\sigma_z^2 = 10^{-6}$. The power consumption of circuitry is $P_c = 20$ dBm [116]. The convergence tolerance ϵ_o and ϵ_l are set as $\epsilon = 10^{-5}$. The results are retrieved by averaging over 1000 different channel realizations. We assume that the optimization process would be finished within one channel realization such that adaptive power can be optimally assigned from the source to the relay.

5.3.1 Convergence of the Proposed Algorithm

Fig. 5.2 illustrates the convergence behavior of the proposed SPCA-Dinkelbach algorithm. As seen in Fig. 5.2, the proposed algorithm converges to the optimal value within five outer iterations. We also study the number of inner iterations required during the second outer iteration. We find that the SPCA method converges within five inner iterations. The result demonstrates that the proposed algorithm indeed obtains the global optimal solution, even though the SPCA method only reaches the KKT conditions theoretically. We also find that the convergence speed is not highly related to β (the self-interference attenuation factor) in both inner and outer iterations. It is trivial to obtain that the computational complexity of the exhaustive search algorithm is proportional to $1/\epsilon = 10^5$. It is hard to derive the computational complexity of the SPCA-Dinkelbach method directly. However, based on the sim-

ulation results seen in Fig. 5.2, we can see that the maximal number of iterations of the outer iteration and the inner iteration in the SPCA-Dinkelbach method are both fixed as 4. In addition, the computational complexity of interior-point method to solve the convex problem in step 8 of algorithm 2 is $n^{3.5}\log(1/\epsilon)$ [89], in which n represents the number of optimized variables. To sum up, in this our optimization problem, the approximate computational complexity is $4 * 4 * 2^{3.5}\log(1/\epsilon) = 905$ which is much lower than that of exhaustive search algorithm.

5.3.2 Effects of P_{max} and β on Average EE

Fig. 5.3 illustrates the average EE against P_{max} for EE-maximization and rate-maximization schemes with different β. The EE-maximization scheme is implemented by our proposed SPCA-Dinkelbach algorithm. It can be observed in Fig. 5.3 that the average EE increases upon increasing P_{max}, and remains unchanged when P_{max} reaches a certain threshold. Specifically, when P_{max} is larger than 25 dBm, the average EE no longer increases under our simulation settings. It can be also obtained that the average EE increases as β decreases. When β equals -70 dBm and -90 dBm, the average EE under the settings are nearly the same. It implies that when β is very low and the total power is high (in our simulation $\beta = -70$ dB and $P_{max} = 25$ dBm), the optimal average EE does not change. In order to further exploit the performance improvement of EE-maximization scheme, we consider the rate-maximization scheme as a comparison. The rate-maximisation scheme is achieved by the similar procedure in Algorithm 2 except for choosing $q_i = 0$, which means that the outer iteration of **Algorithm 2** is not needed. In the rate-maximization scheme, when P_{max} increases, the average EE first increases and then

decreases. As the metric is average EE, the EE-maximization scheme is always better than or equal to the rate-maximization scheme. Interestingly, at low P_{max}, the results are the same except for $\beta = -10$ dB. The reason is that at low P_{max}, the total power constraint is always satisfied with equality, i.e., the source and relay would utilize the total power. Then, according to the expression of energy consumption in (5.9), the consumed power is always constant, i.e., $P_{max} + P_c$, which is also verified by our simulations. Due to the limited space, the corresponding simulation results are not given. Thus, we can conclude that the average EE of the EE-maximization scheme is equivalent to that of rate-maximization scheme.

5.3.3 Effects of P_{max} and β on Average Achievable Rate

We then compare the EE-maximization scheme with the rate-maximization scheme for the performance metrics of EE and achievable rate. In Fig. 5.4, it is obvious that the rate-maximization scheme can have better achievable rate than the EE-maximization scheme. As a sequel, The EE-maximization scheme has a performance degradation in terms of rate. Besides, it can be obtain that the EE-maximization scheme keeps constant achievable rate in high SNR region, specifically when the SNR is larger than 25dB. Combining with the results in Fig. 5.3, we can conclude that when the maximal total transmit power is increased, the actual total transmit power will be firstly increased and then fixed, which is similar as the performance metric of EE. Interestingly, we find that the achievable rate in $\beta = -10dB$ and $\beta = -30dB$ are almost the same while the EE in $\beta = -30dB$ is larger than that in $\beta = -10dB$. This fact explains that the higher the self-interference is, the more power would be consumed. However, when the self-interference is very low, i.e.,

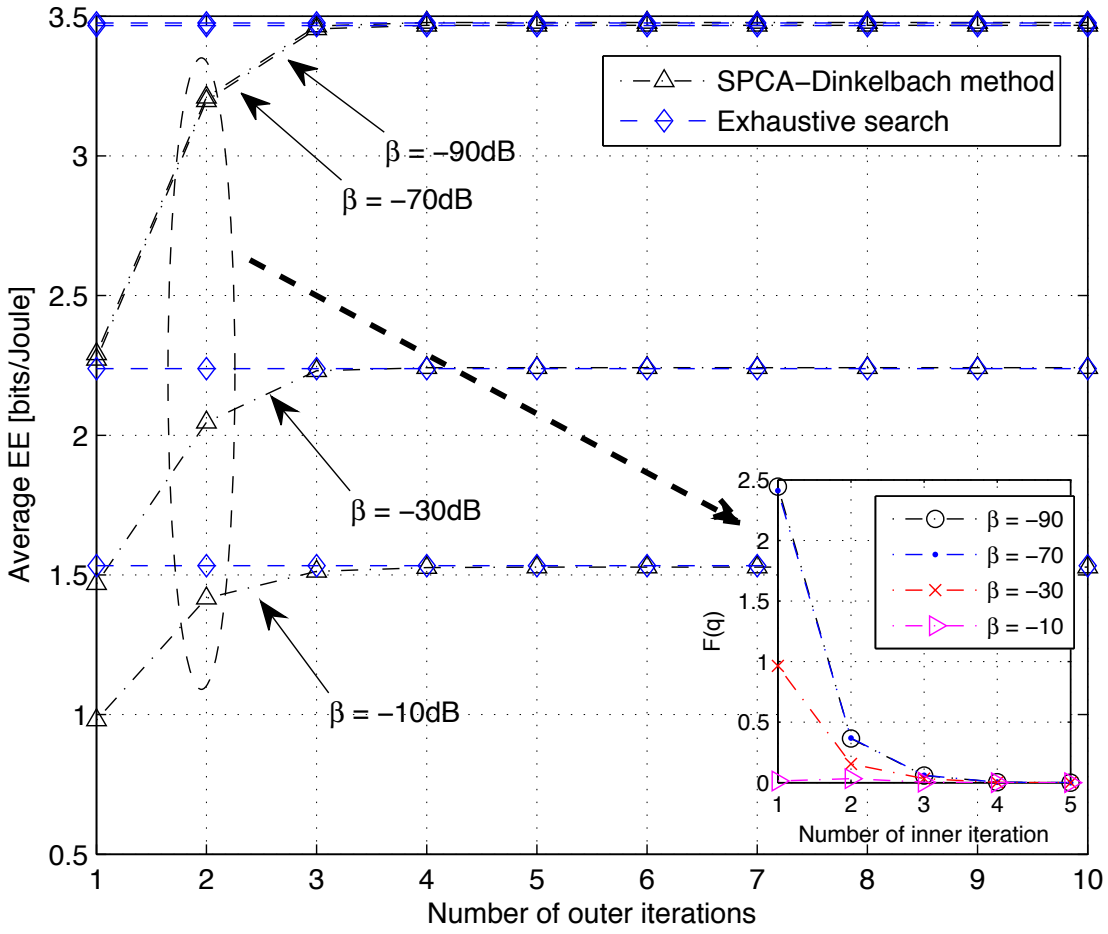

Figure 5.2: Convergence of the SPCA-Dinkelbach algorithm ($P_{max} = 30$ dBm).

$\beta = -70dB$ and $\beta = -90dB$, the performance of achievable rate and EE are nearly the same.

5.4 Summary

In this chapter, energy efficiency of a full-duplex relay system under the total power constraint and fixed circuitry power consumption has been studied. The formulated optimization problem is transformed into an equivalent problem which is decom-

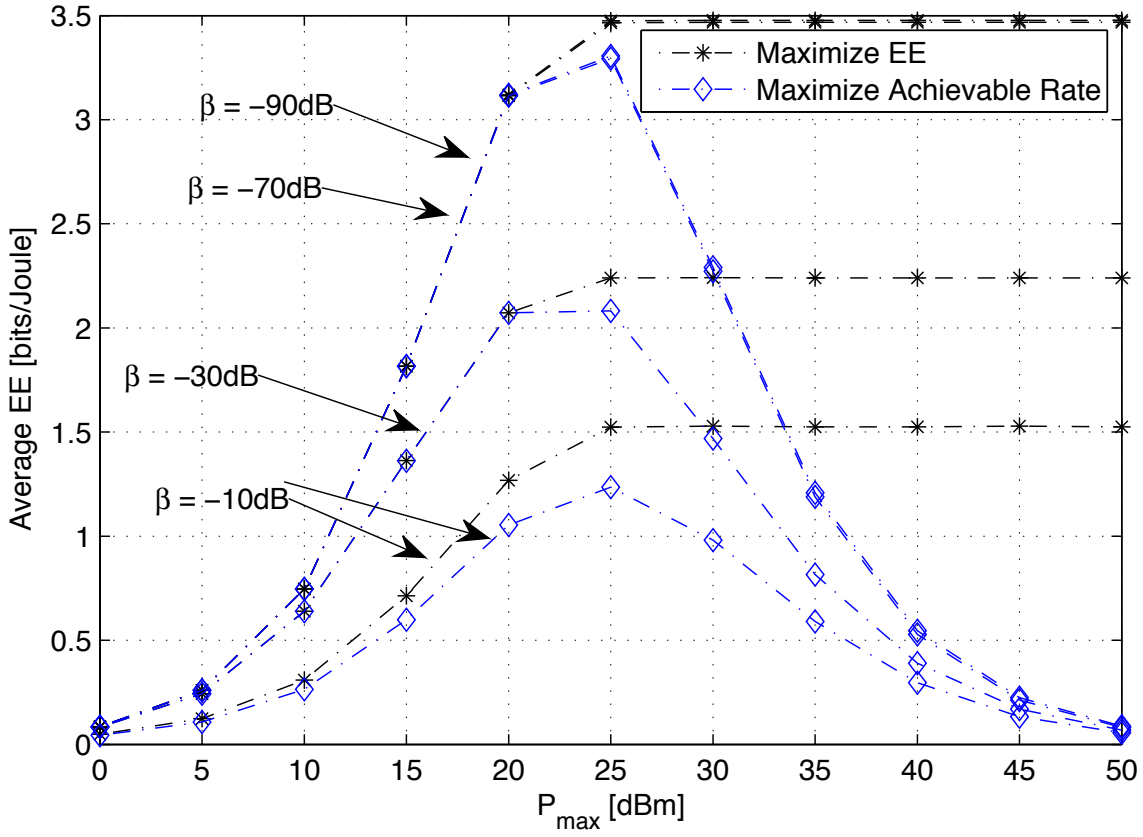

Figure 5.3: Average EE against P_{max} for the scheme of maximizing EE and maximizing achievable rate under different settings of β.

posed into two subproblems. The first subproblem is solved by the traditional Dinbelbach's method. Then, a dual iterative algorithm called SPCA-Dinbelbach method is used to solve the second subproblem. Simulation results show that the proposed algorithm can converge to the global optimum at different levels of self-interference.

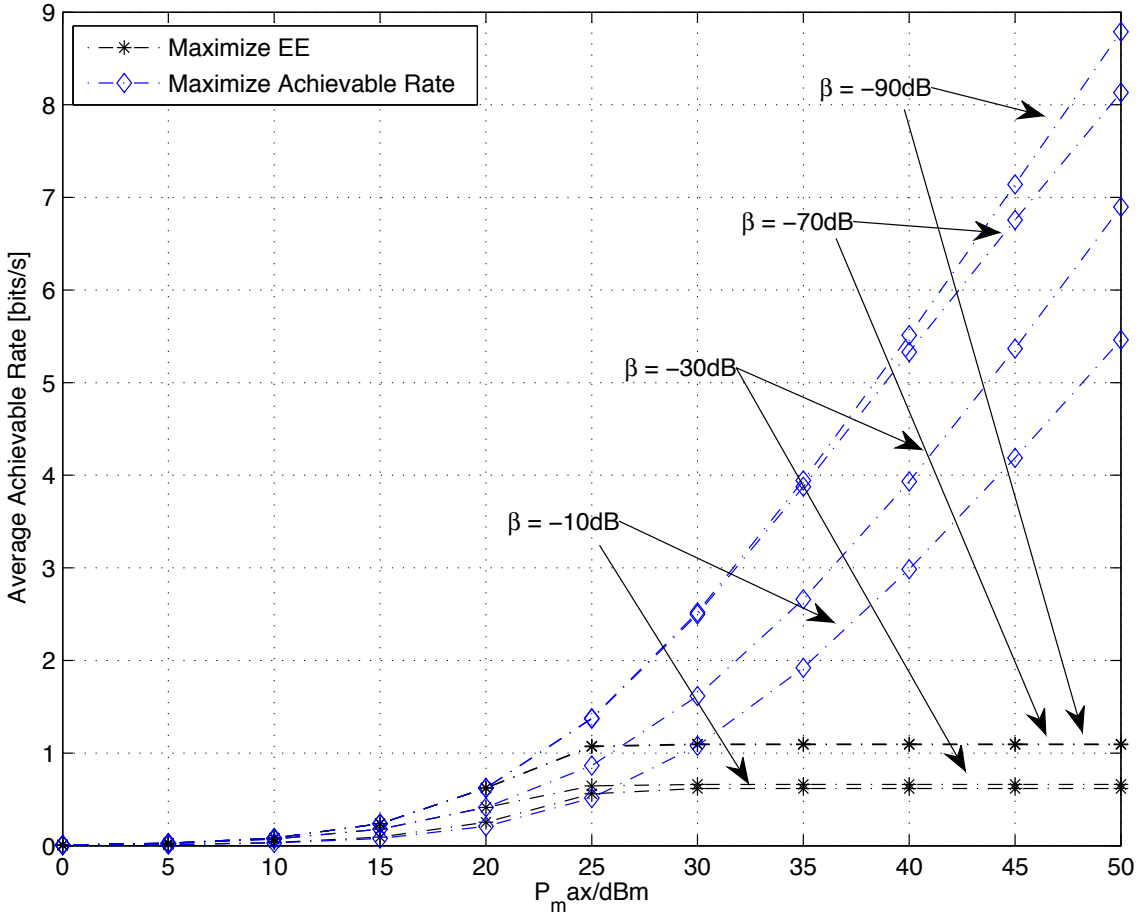

Figure 5.4: Average achievable rate against P_{max} for the scheme of maximizing EE and maximizing achievable rate under different settings of β.

Appendix 5.A Lemma 5.1

It is straightforward that if $G_{sd} \geq G_{sr}$, $R(P_s, P_r) = R_{\mathrm{D}}(P_s)$ according to (5.7). Thus, the problem can be simplified to

$$U_{\mathrm{eff}} = \frac{R_{\mathrm{D}}(P_s)}{P_T(P_s, P_r)} = \frac{R_{\mathrm{D}}(P_s)}{P_T(P_s, 0)}. \tag{5.20}$$

As a result, we need to solve P2.1 when $G_{sd} \geq G_{sr}$.

When $G_{sd} < G_{sr}$, we have

$$\begin{aligned} U_{\text{eff}} &= \frac{R_{\text{DF}}(P_s)}{P_T(P_s, P_r)} \\ &= \frac{\min\{R_{\text{DF},1}(P_s, P_r), R_{\text{DF},2}(P_s, P_r)\}}{P_T(P_s, P_r)}. \end{aligned} \tag{5.21}$$

We firstly give some lemmas before proving P2.2 which are obvious.

Lemma 5.3. *$R_{\text{DF},1}(P_s, P_r)$ is an increasing function with respect to (w.r.t.) P_s, and a decreasing function w.r.t. P_r.*

Lemma 5.4. *i) $P_T(P_s, P_r)$ is an increasing function w.r.t. P_s and P_r; ii) $P_T(P_s, P_r)$ is also a linear function w.r.t. P_s, P_r.*

We are now ready to prove P2.2.

Proof of P2.2: We prove it by self-contradiction. For the sake of notational simplicity, we define the constraint set as $\mathcal{F}$. We assume that $\{P_s^*, P_r^*\} \in \mathcal{F}$ as the optimal policy with the following constraint:

$$R_{\text{DF},1}(P_s^*, P_r^*) < R_{\text{DF},2}(P_s^*, P_r^*). \tag{5.22}$$

The optimal energy efficiency U_{eff}^* is therefore expressed as

$$\begin{aligned} U_{\text{eff}}^* &= \frac{\min\{R_{\text{DF},1}(P_s^*, P_r^*), R_{\text{DF},2}(P_s^*, P_r^*)\}}{P_T(P_s^*, P_r^*)} \\ &= \frac{R_{\text{DF},1}(P_s^*, P_r^*)}{P_T(P_s^*, P_r^*)}. \end{aligned} \tag{5.23}$$

According to Lemma 2 and 3, $R_{\text{DF},1}(P_s^*, P_r^*)$ is a decreasing function of P_r^* and $P_T(P_s^*, P_r^*)$ is an increasing function of P_r^*. Consequently, based on (5.23), U_{eff}^*

should be optimal when $P_r^* = 0$. Substituting $P_r^* = 0$ into (5.4) and (5.5) gives

$$R_{\mathrm{DF},1}(P_s^*, P_r^*) = \log_2(1 + P_s^* G_{sr}), \tag{5.24}$$

$$R_{\mathrm{DF},2}(P_s^*, P_r^*) = \log_2(1 + P_s^* G_{sd}). \tag{5.25}$$

Since it is given that $G_{sd} < G_{sr}$, the above results indicate $R_{\mathrm{DF},1}(P_s^*, P_r^*) > R_{\mathrm{DF},2}(P_s^*, P_r^*)$, which is contradictory to our assumption in (5.22). In conclusion, under any P_r^* in the optimal solution, $R_{\mathrm{DF},1}$ is larger than $R_{\mathrm{DF},2}$. Therefore, we prove that P2 is equivalent to P1.

Appendix 5.B Dinkelbach's Method

Consider a fractional programming problem

$$\begin{aligned} \max_{\boldsymbol{x} \in \mathcal{S}_0} \quad & R(\boldsymbol{x})/P_T(\boldsymbol{x}) \\ \text{s.t.} \quad & \boldsymbol{g}(\boldsymbol{x}) \leq 0. \end{aligned} \tag{5.26}$$

This problem is formed by denoting the objective function value as q so that a subtractive form of the objective function can be written as

$$F(q) = \max\{R(\boldsymbol{x}) - qP_T(\boldsymbol{x}))|\boldsymbol{g}(\boldsymbol{x}) \leq 0\}, q \in \mathbb{R}. \tag{5.27}$$

Additionally, it requires that $P_T(\boldsymbol{x}) > 0$ for all $\boldsymbol{x} \in \mathcal{S}$ where $\mathcal{S}$ is the feasible set of $\boldsymbol{x}$. Then, the function $F(q)$ has a series of important properties which are given in [114]. Explicitly, the solution to $F(q^*)$ is equivalent to the solution to the fractional programming problem (5.26). Dinkelbach has proposed an iterative method to find

increasing q values, which are feasible, by solving the parameterized problem of $\max_{\boldsymbol{x}}\{R(\boldsymbol{x} - q_{i-1}P_T(\boldsymbol{x}))\}$ at each iteration. Hence, it can be shown that the method produces an increasing sequence of q values, which converges to the optimal value $F(q^*) = 0$. Each iteration corresponds to solving $\max_{\boldsymbol{x}}\{R(\boldsymbol{x}) - q_{i-1}P_T(\boldsymbol{x})\}$, where q_{i-1} is a given value of the parameter q, to obtain the optimum value $\boldsymbol{x}^*$ at the ith iteration of the Dinkelbach's method. For more details and the proof of convergence, please refer to [114].

Chapter 6

Conclusions and Future Directions

6.1 Conclusions

To wireless communication engineers and scientists, the challenge of developing faster communication systems is not to increase the transmission rates of the point-to-point channels of a network anymore, but to increase the overall throughput of the network by guiding the information streams within the network efficiently. By considering full-duplex, the wireless networks would have a huge improvement compared with the half-duplex networks.

In this thesis, we have investigated full-duplex MIMO/OFDMA multi-user systems. Specifically, we have provided an optimization framework for the resource allocation problem of full-duplex multi-user OFDMA cellular systems with one full-duplex base station communicating with multiple half-duplex users in a bidirectional way. Simulation results show that when self-interference is low, uplink and downlink user-pairing can provide significant improvement on the system sum-rate compared

to the conventional unidirectional half-duplex transmission. In addition, by considering two different network deployments, i.e., urban macro cell scenario and small cell scenario, we show that the improvement of full-duplex transmission over half-duplex transmission highly depends on the channel parameters.

We have further investigated the joint optimization problem of transmission mode selection, subcarrier assignment, relay selection, subcarrier-pairing as well as power allocation in the DL of a cooperative OFDMA system. Simulation results show that our proposed algorithm can significantly enhance the overall system throughput compared to previous works.

Furthermore, we have exploited the potential performance gain of full-duplex multi-user MIMO system. We have investigated the max-min weighted SINR problem in a full-duplex multi-user MIMO system, where each user is equipped with a single antenna. We have considered a practical scenario in which the downlink minimum weighted SINR is maximized under some target SINR constraints for uplink users. Simulation results show that our proposed algorithm has a fast convergence rate and leads to a better performance compared to other optimization techniques that do not jointly considered all parameters.

Finally, we have proposed an optimization method for the energy efficiency of full-duplex relaying systems. Simulation results show that the proposed algorithm can converge to the global optimum very quickly.

6.2 Future Directions

In the following, we propose some possible future research directions.

- The average sum-rate [49, 97, 117] and goodput [100, 101] have been selected as the performance metrics in full-duplex multi-user OFDMA cellular systems. In the future, other constraints such as rate and usage fairness can be considered in the system model. Outage probability and diversity gain with appropriate user-selection can also be evaluated in a full-duplex multiuser cellular system.

- Full-duplex transmission mode without subcarrier-pairing in multi-user OFDMA cooperative relaying systems has been investigated here. It is worth investigating systems in which subcarrier-pairing is considered. While the problem becomes much more complicated, the solution should provide an enhanced throughput.

- As IC design and antenna technology advance, equipping multiple antennas in mobile devices will soon become more practical. Thus, extending our optimization frameworks to users with multiple antennas will be of great interest to the research community and industry.

- Full-duplex technology can be applied to both relays and base station. Therefore, the study of full-duplex base station together with full-duplex relaying in a cooperative network should be pursued in the future.

Bibliography

[1] T. Cover and A. E. Gamal, "Capacity theorems for the relay channel," *IEEE Transactions on Information Theory*, vol. 25, no. 5, pp. 572–584, Sep. 1979.

[2] J.-G. Kim, S. Ko, S. Jeon, J.-W. Park, and S. Hong, "Balanced topology to cancel Tx leakage in CW radar," *IEEE Microwave and Wireless Components Letters*, vol. 14, no. 9, pp. 443–445, Spe. 2004.

[3] C.-Y. Kim, J.-G. Kim, and S. Hong, "A quadrature radar topology with Tx leakage canceller for 24-GHz radar applications," *IEEE Transactions on Microwave Theory and Techniques*, vol. 55, no. 7, pp. 1438–1444, July 2007.

[4] D. Bliss, P. Parker, and A. Margetts, "Simultaneous transmission and reception for improved wireless network performance," in *IEEE/SP 14th Workshop on Statistical Signal Processing.* IEEE, Aug. 2007, pp. 478–482.

[5] T. Riihonen, S. Werner, and R. Wichman, "Spatial loop interference suppression in full-duplex MIMO relays," in *Signals, Systems and Computers, 2009 Conference Record of the Forty-Third Asilomar Conference on.* IEEE, Nov 2009, pp. 1508–1512.

[6] T. Riihonen, S. Werner, R. Wichman, and Z. Eduardo, "On the feasibility of full-duplex relaying in the presence of loop interference," in *IEEE 10th Workshop on Signal Processing Advances in Wireless Communications.* Perugia, Italy, June 2009, pp. 275–279.

[7] T. Riihonen, S. Werner, and R. Wichman, "Residual self-interference in full-duplex MIMO relays after null-space projection and cancellation," in *2010*

Conference Record of the Forty Fourth Asilomar Conference on Signals, Systems and Computers (ASILOMAR), IEEE. Pacific Grove , USA, Nov 2010, pp. 653–657.

[8] J. I. Choi, M. Jain, K. Srinivasan, P. Levis, and S. Katti, "Achieving single channel, full duplex wireless communication," in *Proceedings of the 16th annual international conference on Mobile computing and networking (Mobicom'10)*. New York, USA, Sep. 2010, pp. 1–12.

[9] M. Duarte and A. Sabharwal, "Full-duplex wireless communications using off-the-shelf radios: Feasibility and first results," in *2010 Conference Record of the Forty Fourth Asilomar Conference on Signals, Systems and Computers (ASILOMAR)*. Pacific Grove, USA, Nov. 2010, pp. 1558–1562.

[10] M. Duarte, C. Dick, and A. Sabharwal, "Experiment-driven characterization of full-duplex wireless systems," *IEEE Transactions on Wireless Communications*, vol. 11, no. 12, pp. 4296–4307, Dec. 2011.

[11] M. Jain, J. I. Choi, T. Kim, D. Bharadia, S. Seth, K. Srinivasan, P. Levis, S. Katti, and P. Sinha, "Practical, real-time, full duplex wireless," in *Proceedings of the 17th annual international conference on Mobile computing and networking (Mobicom'11)*. New York, USA, Sep. 2011, pp. 301–312.

[12] M. Duarte, A. Sabharwal, V. Aggarwal, R. Jana, K. Ramakrishnan, C. W. Rice, and N. Shankaranarayanan, "Design and characterization of a full-duplex multi-antenna system for WiFi networks," *IEEE Transactions on Vehicular Technology*, vol. 63, no. 3, pp. 1160–1177, March 2014.

[13] D. Bharadia, E. McMilin, and S. Katti, "Full duplex radios," in *Proceedings of the ACM SIGCOMM 2013 (SIGCOMM'13)*, 2013, pp. 375–386.

[14] E. Everett, A. Sahai, and A. Sabharwal, "Passive self-interference suppression for full-duplex infrastructure nodes," *IEEE Transaction on Wireless Communications*, vol. 13, no. 2, pp. 680–694, Feb. 2014.

[15] T. Riihonen, S. Werner, and R. Wichman, "Mitigation of loopback self-interference in full-duplex MIMO relays," *IEEE Transactions on Signal Processing*, vol. 59, no. 12, pp. 5983–5993, Dec. 2011.

[16] B. P. Day, A. R. Margetts, D. W. Bliss, and P. Schniter, "Full-duplex MIMO relaying: Achievable rates under limited dynamic range," *IEEE Journal on Selected Areas in Communications*, vol. 30, no. 8, pp. 1541–1553, Sep. 2012.

[17] M. Duarte, A. Sabharwal, V. Aggarwal, R. Jana, K. Ramakrishnan, C. Rice, and N. Shankaranarayanan, "Design and characterization of a full-duplex multi-antenna system for wifi networks," *IEEE transaction on Vehichle Technology*, submitted for publication, Oct.2012. [Available Online: preprint arXiv:1210.1639.

[18] T. Riihonen, S. Werner, and R. Wichman, "Mitigation of loopback self-interference in full-duplex mimo relays," *IEEE Transactions on Signal Processing*, vol. 59, no. 12, pp. 5983–5993, Dec. 2011.

[19] B. Chun and H. Park, "A spatial-domain joint-nulling method of self-interference in full-duplex relays," *IEEE Communications Letters*, vol. 16, no. 4, pp. 436–438, Apr. 2012.

[20] S. Kandukuri and S. Boyd, "Optimal power control in interference-limited fading wireless channels with outage-probability specifications," *IEEE Transactions on Wireless Communications*, vol. 1, no. 1, pp. 46–55, Aug. 2002.

[21] A. J. Goldsmith and S.-G. Chua, "Variable-rate variable-power MQAM for fading channels," *IEEE Transactions on Communications*, vol. 45, no. 10, pp. 1218–1230, Aug. 1997.

[22] C. U. Saraydar, N. B. Mandayam, and D. J. Goodman, "Efficient power control via pricing in wireless data networks," *IEEE Transactions on Communications*, vol. 50, no. 2, pp. 291–303, Aug. 2002.

[23] T. S. Rappaport, *Wireless Communications: Principles and Practice*. Prentice Hall, 1996, vol. 2.

[24] E. Yaacoub, A. M. El-Hajj, and Z. Dawy, "Uplink ofdma resource allocation with discrete rates: optimal solution and suboptimal implementation," *Transactions on Emerging Telecommunications Technologies*, vol. 23, no. 2, pp. 148–162, Mar 2012.

[25] N. U. Hassan and M. Assaad, "Downlink beamforming and resource allocation in multicell miso-ofdma systems," *Transactions on Emerging Telecommunications Technologies*, vol. 25, no. 2, pp. 173–182, Feb 2014.

[26] Z. Li, H. Wang, Z. Pan, N. Liu, and X. You, "Heterogenous qos-guaranteed load balancing in 3gpp lte multicell fractional frequency reuse network," *Transactions on Emerging Telecommunications Technologies*, vol. 25, no. 12, pp. 1169–1183, Feb 2014.

[27] D. Xu and Q. Li, "Resource allocation for outage probability minimisation in cognitive radio multicast networks," *Transactions on Emerging Telecommunications Technologies*, vol. 1, no. 1, pp. 1–12, Jan. 2014.

[28] M. Pischella and D. Le Ruyet, "Adaptive resource allocation and decoding strategy for underlay multi-carrier cooperative cognitive radio systems," *Transactions on Emerging Telecommunications Technologies*, vol. 24, no. 7-8, pp. 748–761, Nov 2013.

[29] T. Riihonen, R. Wichman, and S. Werner, "Evaluation of ofdm (a) relaying protocols: capacity analysis in infrastructure framework," *IEEE Transactions on Vehicular Technology*, vol. 61, no. 1, pp. 360–374, Nov. 2012.

[30] T. C.-Y. Ng and W. Yu, "Joint optimization of relay strategies and resource allocations in cooperative cellular networks," *IEEE Journal on Selected Areas in Communications*, vol. 25, no. 2, pp. 328–339, Feb. 2007.

[31] L. Weng and R. D. Murch, "Cooperation strategies and resource allocations in multiuser OFDMA systems," *IEEE Transactions on Vehicular Technology*, vol. 58, no. 5, pp. 2331–2342, Nov. 2009.

[32] D. W. K. Ng and R. Schober, "Cross-layer scheduling for OFDMA amplify-and-forward relay networks," *IEEE Transactions on Vehicular Technology*, vol. 59, no. 3, pp. 1443–1458, Dec. 2010.

[33] Z. Han, T. Himsoon, W. P. Siriwongpairat, and K. R. Liu, "Resource allocation for multiuser cooperative OFDM networks: Who helps whom and how to cooperate," *IEEE Transactions on Vehicular Technology*, vol. 58, no. 5, pp. 2378–2391, Aug. 2009.

[34] X. Zhang, X. Tao, Y. Li, N. Ge, and J. Lu, "On relay selection and subcarrier assignment for multi-user cooperative OFDMA networks with QoS guarantees," *IEEE Transactions on Vehicular Technology*, vol. 63, no. 9, pp. 4704 – 4717, Apr. 2014.

[35] D. W. K. Ng, E. S. Lo, and R. Schober, "Dynamic resource allocation in MIMO-OFDMA systems with full-duplex and hybrid relaying," *IEEE Transactions on Communications*, vol. 60, no. 5, pp. 1291–1304, Apr. 2012.

[36] T. Wang and L. Vandendorpe, "WSR maximized resource allocation in multiple df relays aided OFDMA downlink transmission," *IEEE Transactions on Signal Processing*, vol. 59, no. 8, pp. 3964–3976, May 2011.

[37] M. Tao and Y. Liu, "A network flow approach to throughput maximization in cooperative OFDMA networks," *IEEE Transactions on Wireless Communications*, vol. 12, no. 3, pp. 1138–1148, Mar. 2013.

[38] W. Dang, M. Tao, H. Mu, and J. Huang, "Subcarrier-pair based resource allocation for cooperative multi-relay OFDM systems," *IEEE Transactions on Wireless Communications*, vol. 9, no. 5, pp. 1640–1649, May 2010.

[39] M. Hajiaghayi, M. Dong, and B. Liang, "Optimal channel assignment and power allocation for dual-hop multi-channel multi-user relaying," in *2011 Proceedings IEEE INFOCOM*. Shanghai, 2011, pp. 76–80.

[40] Y. Liu, M. Tao, B. Li, and H. Shen, "Optimization framework and graph-based approach for relay-assisted bidirectional OFDMA cellular networks,"

IEEE Transactions on Wireless Communications, vol. 9, no. 11, pp. 3490–3500, Oct. 2010.

[41] Y. Liu and M. Tao, "Optimal channel and relay assignment in OFDM-based multi-relay multi-pair two-way communication networks," *IEEE Transactions on Communications*, vol. 60, no. 2, pp. 317–321, Nov. 2012.

[42] T. Wang, F. Glineur, J. Louveaux, and L. Vandendorpe, "Weighted sum rate maximization for downlink OFDMA with subcarrier-pair based opportunistic DF relaying," *IEEE Transactions on Signal Processing*, vol. 61, no. 10, pp. 2512–2524, May 2013.

[43] C.-N. Hsu, H.-J. Su, and P.-H. Lin, "Joint subcarrier pairing and power allocation for OFDM transmission with decode-and-forward relaying," *IEEE Transactions on Signal Processing*, vol. 59, no. 1, pp. 399–414, Sep 2011.

[44] H. Zhang, Y. Liu, and M. Tao, "Resource allocation with subcarrier pairing in OFDMA two-way relay networks," *IEEE Wireless Communications Letters*, vol. 1, no. 2, pp. 61–64, Jan. 2012.

[45] T. Cover and A. E. Gamal, "Capacity theorems for the relay channel," *IEEE Transactions on Information Theory*, vol. 25, no. 5, pp. 572–584, Sep. 1979.

[46] T. Riihonen, S. Werner, and R. Wichman, "Hybrid full-duplex/half-duplex relaying with transmit power adaptation," *IEEE Transactions on Wireless Communications*, vol. 10, no. 9, pp. 3074–3085, Sep. 2011.

[47] D. Bharadia and S. Katti, "Fastforward: fast and constructive full duplex relays," in *Proceedings of the 2014 ACM conference on SIGCOMM*. New York, USA, Oct. 2014, pp. 199–210.

[48] A. Sabharwal, P. Schniter, D. Guo, D. W. Bliss, S. Rangarajan, and R. Wichman, "In-band full-duplex wireless: Challenges and opportunities," *IEEE Journal on Selected Areas in Communications*, vol. 32, no. 6, pp. 1637–1652, June 2014.

[49] D. Nguyen, L.-N. Tran, P. Pirinen, and M. Latva-aho, "Precoding for full duplex multiuser MIMO systems: Spectral and energy efficiency maximization," *IEEE Transactions on Signal Processing*, vol. 61, no. 16, pp. 4038–4050, Aug. 2013.

[50] D. Nguyen, L. Tran, P. Pirinen, and M. Latva-aho, "On the spectral efficiency of full-duplex small cell wireless systems," *IEEE Transactions on Wireless Communications*, vol. 13, no. 9, pp. 4896–4910, Sep. 2014.

[51] W. Yang and G. Xu, "Optimal downlink power assignment for smart antenna systems," in *Proceedings of the 1998 IEEE International Conference on Acoustics, Speech and Signal Processing*, vol. 6. Seattle, WA, 1998, pp. 3337–3340.

[52] P. Lancaster and M. Tismenetsky, *The theory of matrices: with applications*. Academic press, 1985.

[53] M. Bengtsson and B. Ottersten, *Optimal and suboptimal transmit beamforming*. L. C. Godara, Ed. Boca Raton, FL: CRC Press, 2001.

[54] J.-H. Chang, L. Tassiulas, and F. Rashid-Farrokhi, "Joint transmitter receiver diversity for efficient space division multiaccess," *IEEE Transactions on Wireless Communications*, vol. 1, no. 1, pp. 16–27, Jan. 2002.

[55] M. Schubert and H. Boche, "Solution of the multiuser downlink beamforming problem with individual SINR constraints," *IEEE Transactions on Vehicular Technology*, vol. 53, no. 1, pp. 18–28, Jan. 2004.

[56] A. Wiesel, Y. C. Eldar, and S. Shamai, "Linear precoding via conic optimization for fixed MIMO receivers," *IEEE Transactions on Signal Processing*, vol. 54, no. 1, pp. 161–176, Jan. 2006.

[57] D. Wajcer, S. Shamai, and A. Wiesel, "On superposition coding and beamforming for the multi-antenna Gaussian broadcast channel," in *Information Theory and Applications Workshop*. San Diego, CA, 2006.

[58] H. T. Do and S.-Y. Chung, "Linear beamforming and superposition coding with common information for the Gaussian MIMO broadcast channel," *IEEE Transactions on Communications*, vol. 57, no. 8, pp. 2484–2494, Aug. 2009.

[59] C. W. Tan, M. Chiang, and R. Srikant, "Maximizing sum rate and minimizing MSE on multiuser downlink: Optimality, fast algorithms and equivalence via max-min SINR," *IEEE Transactions on Signal Processing*, vol. 59, no. 12, pp. 6127–6143, Dec. 2011.

[60] D. W. Cai, T. Q. Quek, and C. W. Tan, "A unified analysis of max-min weighted SINR for MIMO downlink system," *IEEE Transactions on Signal Processing*, vol. 59, no. 8, pp. 3850–3862, Aug. 2011.

[61] U. Krause, "Concave Perron–Frobenius theory and applications," *Nonlinear Analysis: Theory, Methods & Applications*, vol. 47, no. 3, pp. 1457–1466, Aug. 2001.

[62] V. D. Blondel, L. Ninove, and P. Van Dooren, "An affine eigenvalue problem on the nonnegative orthant," *Linear Algebra and its Applications*, vol. 404, pp. 69–84, July 2005.

[63] Y. Huang, G. Zheng, M. Bengtsson, K.-K. Wong, L. Yang, and B. Ottersten, "Distributed multicell beamforming with limited intercell coordination," *IEEE Transactions on Signal Processing*, vol. 59, no. 2, pp. 728–738, Feb. 2011.

[64] ——, "Distributed multicell beamforming design approaching Pareto boundary with max-min fairness," *IEEE Transactions on Wireless Communications*, vol. 11, no. 8, pp. 2921–2933, Aug. 2012.

[65] A. Tajer, N. Prasad, and X. Wang, "Robust linear precoder design for multi-cell downlink transmission," *IEEE Transactions on Signal Processing*, vol. 59, no. 1, pp. 235–251, Jan. 2011.

[66] S. He, Y. Huang, L. Yang, A. Nallanathan, and P. Liu, "A multi-cell beamforming design by uplink-downlink max-min SINR duality," *IEEE Transactions on Wireless Communications*, vol. 11, no. 8, pp. 2858–2867, Aug. 2012.

[67] L. Zhang, Y.-C. Liang, and Y. Xin, "Joint beamforming and power allocation for multiple access channels in cognitive radio networks," *IEEE Journal on Selected Areas in Communications*, vol. 26, no. 1, pp. 38–51, Jan. 2008.

[68] L. Zhang, R. Zhang, Y.-C. Liang, Y. Xin, and H. V. Poor, "On Gaussian MIMO BC-MAC duality with multiple transmit covariance constraints," *IEEE Transactions on Information Theory*, vol. 58, no. 4, pp. 2064–2078, Apr. 2012.

[69] D. W. Cai, T. Q. Quek, C. W. Tan, and S. H. Low, "Max-min SINR coordinated multipoint downlink transmission duality and algorithms," *IEEE Transactions on Signal Processing*, vol. 60, no. 10, pp. 5384–5395, Oct. 2012.

[70] C. Isheden, Z. Chong, E. Jorswieck, and G. Fettweis, "Framework for link-level energy efficiency optimization with informed transmitter," *IEEE Transactions on Wireless Communications*, vol. 11, no. 8, pp. 2946–2957, Aug. 2012.

[71] K. T. K. Cheung, S. Yang, and L. Hanzo, "Achieving maximum energy-efficiency in multi-relay ofdma cellular networks: a fractional programming approach," *IEEE Transactions on Communications*, vol. 61, no. 7, pp. 2746–2757, July 2013.

[72] A. K. Karmokar and A. Anpalagan, "Energy-efficient cross-layer design of dynamic rate and power allocation techniques for cognitive green radio networks," *Transactions on Emerging Telecommunications Technologies*, vol. 24, no. 7-8, pp. 762–776, October 2013.

[73] X. Tang, J. Pu, Y. Gao, Z. Xiong, and Y. Weng, "Energy-efficient multicast routing scheme for wireless sensor networks," *Transactions on Emerging Telecommunications Technologies*, vol. PP, no. 99, p. DOI: 10.1002/ett.2661, May 2013.

[74] M. Ashraf and S. Sohaib, "Energy-efficient delay tolerant space time codes for asynchronous cooperative communications," *Transactions on Emerging Telecommunications Technologies*, vol. PP, no. 99, p. DOI: 10.1002/ett.2781, January 2014.

[75] P. Reviriego, J. A. Maestro, J. A. Hernández, and D. Larrabeiti, "Study of the potential energy savings in ethernet by combining energy efficient ethernet and adaptive link rate," *Transactions on Emerging Telecommunications Technologies*, vol. 23, no. 3, pp. 227–233, October 2012.

[76] W. Ejaz, G. A. Shah, N. ul Hasan, and H. S. Kim, "Energy and throughput efficient cooperative spectrum sensing in cognitive radio sensor networks," *Transactions on Emerging Telecommunications Technologies*, vol. PP, no. 99, p. DOI: 10.1002/ett.2803, March 2014.

[77] C. Li, J. M. Cioffi, and L. Yang, "Optimal energy efficient joint power allocation for two-hop single-antenna relaying systems," *Transactions on Emerging Telecommunications Technologies*, vol. 25, no. 7, pp. 745–751, June 2014.

[78] M. Naeem, K. Illanko, A. K. Karmokar, A. Anpalagan, and M. Jaseemuddin, "Power allocation in decode and forward relaying for green cooperative cognitive radio systems," in *Wireless Communications and Networking Conference (WCNC), 2013 IEEE*. IEEE, 2013, pp. 3806–3810.

[79] K. T. K. Cheung, S. Yang, and L. Hanzo, "Maximizing energy-efficiency in multi-relay ofdma cellular networks," *arXiv preprint 1401.6083*, vol. PP, no. 99, p. 1, 2013.

[80] C. Li, F. Sun, J. Cioffi, and L. Yang, "Energy efficient mimo relay transmissions via joint power allocations," *IEEE Transactions on Circuits and Systems II: Express Briefs*, vol. 61, no. 7, pp. 531–535, July 2011.

[81] A. Zafar, R. M. Radaydeh, Y. Chen, and M.-S. Alouini, "Energy-efficient power allocation for fixed-gain amplify-and-forward relay networks with partial channel state information," *IEEE Wireless Communications Letters*, vol. 1, no. 6, pp. 553–556, December 2012.

[82] Y. Jing and H. Jafarkhani, "Single and multiple relay selection schemes and their achievable diversity orders," *IEEE Transactions on Wireless Communications*, vol. 8, no. 3, pp. 1414–1423, March 2009.

[83] S. Atapattu, Y. Jing, H. Jiang, and C. Tellambura, "Relay selection and performance analysis in multiple-user networks," *IEEE Journal on Selected Areas in Communications*, vol. 31, no. 8, pp. 1517–1529, August 2013.

[84] M. Chiang, C. W. Tan, D. P. Palomar, D. O'Neill, and D. Julian, "Power control by geometric programming," *IEEE Transactions on Wireless Communications*, vol. 6, no. 7, pp. 2640–2651, July 2007.

[85] L. P. Qian, Y. J. A. Zhang, and J. Huang, "MAPEL: Achieving global optimality for a non-convex wireless power control problem," *IEEE Transactions on Wireless Communications*, vol. 8, no. 3, pp. 1553–1563, Mar. 2009.

[86] W. Yu and R. Lui, "Dual methods for nonconvex spectrum optimization of multicarrier systems," *IEEE Transactions on Communications*, vol. 54, no. 7, pp. 1310–1322, July 2006.

[87] A. Beck, A. Ben-Tal, and L. Tetruashvili, "A sequential parametric convex approximation method with applications to nonconvex truss topology design problems," *Journal of Global Optimization*, vol. 47, no. 1, pp. 29–51, May 2010.

[88] C. Y. Wong, R. S. Cheng, K. B. Lataief, and R. D. Murch, "Multiuser OFDM with adaptive subcarrier, bit, and power allocation," *IEEE Journal on Selected Areas in Communications*, vol. 17, no. 10, pp. 1747–1758, Oct. 1999.

[89] S. P. Boyd and L. Vandenberghe, *Convex Optimization*. Cambridge university press, 2004.

[90] N. Z. Shor, K. C. Kiwiel, and A. Ruszcaynski, *Minimization methods for non-differentiable functions*. New York: Springer, 1985.

[91] D. P. Palomar and M. Chiang, "A tutorial on decomposition methods for network utility maximization," *IEEE Journal on Selected Areas in Communications*, vol. 24, no. 8, pp. 1439–1451, Aug. 2006.

[92] R. Zhang and S. Cui, "Cooperative interference management with MISO beamforming," *IEEE Transactions on Signal Processing*, vol. 58, no. 10, pp. 5450–5458, Oct. 2010.

[93] W.-L. Li, Y. Zhang, A.-C. So, and M. Z. Win, "Slow adaptive OFDMA systems through chance constrained programming," *IEEE Transactions on Signal Processing*, vol. 58, no. 7, pp. 3858–3869, July 2010.

[94] A.-C. So and Y. J. Zhang, "Distributionally robust slow adaptive OFDMA with soft qos via linear programming," *IEEE Journal on Selected Areas in Communications*, vol. 31, no. 5, pp. 947–958, May 2013.

[95] T. R. Sector, "TR 36.814-further advancements for E-UTRA: Physical layer aspects (release 9)," in *3rd Generation Partnership Project Tech. Rep.* TSGRA Network, 2010.

[96] I. Sector, "Guidelines for evaluation of radio transmission technologies for IMT-2000," in *International Telecommunication Union.* ITU-R.M Recommendation, 1997.

[97] D. Nguyen, L.-N. Tran, P. Pirinen, and M. Latva-Aho, "On the spectral efficiency of full-duplex small cell wireless systems," *IEEE Transactions on Wireless Communications*, vol. 13, no. 9, pp. 4896–4910, July 2014.

[98] Y. J. Zhang and K. B. Letaief, "Multiuser adaptive subcarrier-and-bit allocation with adaptive cell selection for OFDM systems," *IEEE Transactions on Wireless Communications*, vol. 3, no. 5, pp. 1566–1575, Sep. 2004.

[99] J. Huang, V. G. Subramanian, R. Agrawal, and R. Berry, "Joint scheduling and resource allocation in uplink OFDM systems for broadband wireless access networks," *IEEE Journal on Selected Areas in Communications*, vol. 27, no. 2, pp. 226–234, Feb. 2009.

[100] V. K. Lau, W. K. Ng, and D. S. W. Hui, "Asymptotic tradeoff between cross-layer goodput gain and outage diversity in OFDMA systems with slow fading and delayed CSIT," *IEEE Transactions on Wireless Communications*, vol. 7, no. 7, pp. 2732–2739, July 2008.

[101] Y. Huang and B. D. Rao, "Performance analysis of heterogeneous feedback design in an OFDMA downlink with partial and imperfect feedback," *IEEE Transactions on Signal Processing*, vol. 61, no. 4, pp. 1033–1046, Nov. 2013.

[102] I. Krikidis, H. A. Suraweera, P. J. Smith, and C. Yuen, "Full-duplex relay selection for amplify-and-forward cooperative networks," *IEEE Transactions on Wireless Communications*, vol. 11, no. 12, pp. 4381–4393, Dec. 2012.

[103] D. Bharadia and S. Katti, "Full duplex MIMO radios," in *Proceedings of the 11th USENIX Conference on Networked Systems Design and Implementation*. Berkeley, USA, 2014, pp. 359–372.

[104] S. Sesia, I. Toufik, and M. Baker, *LTE: the UMTS Long Term Evolution*. Wiley Online Library, 2009.

[105] L. Nuaymi, *: Technology for Broadband Wireless Access*. John Wiley & Sons, 2007.

[106] N. Ferdinand, M. Nokleby, and B. Aazhang, "Low-density lattice codes for full-duplex relay channels," *IEEE Transactions on Wireless Communications*, vol. 14, no. 4, pp. 2309–2321, April 2015.

[107] G. Kramer, M. Gastpar, and P. Gupta, "Cooperative strategies and capacity theorems for relay networks," *IEEE Transactions on Information Theory*, vol. 51, no. 9, pp. 3037–3063, Aug. 2005.

[108] C. T. Ng and H. Huang, "Linear precoding in cooperative mimo cellular networks with limited coordination clusters," *IEEE Journal on Selected Areas in Communications*, vol. 28, no. 9, pp. 1446–1454, Dec 2010.

[109] D. W. K. Ng, E. S. Lo, and R. Schober, "Energy-efficient resource allocation in multi-cell OFDMA systems with limited backhaul capacity," *IEEE Transactions on Wireless Communications*, vol. 11, no. 10, pp. 3618–3631, Sep. 2012.

[110] D. B. West *et al.*, *Introduction to graph theory*. Prentice hall Upper Saddle River, 2001, vol. 2.

[111] H. W. Kuhn, "The Hungarian method for the assignment problem," *Naval research logistics quarterly*, vol. 2, no. 1-2, pp. 83–97, Mar. 1955.

[112] T. Wang and L. Vandendorpe, "Sum rate maximized resource allocation in multiple DF relays aided OFDM transmission," *IEEE Journal on Selected Areas in Communications*, vol. 29, no. 8, pp. 1559–1571, 2011.

[113] C. D. Meyer, *Matrix analysis and applied linear algebra*. Siam, 2000, vol. 2.

[114] W. Dinkelbach, "On nonlinear fractional programming," *Management Science*, vol. 13, no. 7, pp. 492–498, Mar. 1967.

[115] A. Host-Madsen and J. Zhang, "Capacity bounds and power allocation for wireless relay channels," *IEEE Transactions on Information Theory*, vol. 51, no. 6, pp. 2020–2040, June 2005.

[116] G. Auer, V. Giannini, C. Desset, I. Godor, P. Skillermark, M. Olsson, M. A. Imran, D. Sabella, M. J. Gonzalez, O. Blume *et al.*, "How much energy is needed to run a wireless network?" *IEEE Wireless Communications*, vol. 18, no. 5, pp. 40–49, Oct. 2011.

[117] S. Huberman and T. Le-Ngoc, "MIMO full-duplex precoding: A joint beamforming and self-interference cancellation structure," *IEEE Transactions on Wireless Communications*, vol. 14, no. 4, pp. 2205–2217, Apr. 2015.